Funktionale Analyse des Phytosulfokin Rezeptors 1 aus *Arabidopsis thaliana*

Dissertation

zur Erlangung des Doktorgrades der
Mathematisch-Naturwissenschaftlichen Fakultät
der Christian-Albrechts-Universität
zu Kiel

vorgelegt von
Jens Hartmann
aus Hannover

Kiel
2014

Erste Gutachterin: Prof. Dr. Margret Sauter

Zweite Gutachterin: Prof. Dr. Karin Krupinska

Tag der mündlichen Prüfung: 02.06.2014

Zum Druck genehmigt: 02.06.2014

Abkürzungsverzeichnis

ACR4	*Arabidopsis Crinkly 4*
ATP	Adenosintriphosphat
BAK1	*BRI1-associated Receptor Kinase 1*
BES1	*BRI1 EMS Suppressor 1*
BiFC	Bimolekulare Fluoreszenzkomplementation
BIN2	*Brassinosteroid-Insensitive 2*
BKI1	*BRI1 Kinase Inhibitor 1*
BL	Brassinosteroid 24-Epibrassinolid
bp	Basenpaare
BRI1	*Brassinosteroid Insensitive 1*
BRL	*BRI1-like*
BSK	*BR Signaling Kinase*
BSU1	*BRI1 Suppressor 1*
BZ	Brassinazol
BZR1	*Brassinazole Resistant 1*
CaM	Calmodulin
CaMBD	CaM-Bindungsdomäne
CaMK	*CaM-dependent Protein Kinase*
cDNA	Komplementäre DNA (*copy-DNA*)
CDK	*Cyclin-dependent Kinase*
cGMP	Cyklisches Guanosinmonophosphat
CLE	*Clavata/Embryo Surrounding Region*
CLSM	Konfokales Laser Scanning Mikroskop
CLV	Clavata
CNGC	*Cyclic Nucleotide-gated Channel*
CRN	Coryne
DET2	*DE-ETIOLATED2*
DNA	Desoxyribonukleinsäure

DWF	*DWARF*
et al.	und andere (*et alii*)
FLS2	*Flagellin Insensitive 2*
GFP	Grün Fluoreszierendes Protein
GL2	Glabra 2
GLU	Glutamat
GSK3	*Glycogen Synthase Kinase 3*
GTP	Guanosintriphosphat
HEC1	Hecate 1
HEPES	Hydroxyethylpiperazin-Ethansulfonsäure-Puffer
kDA	Kilodalton
LB	Medium für die Anzucht von Bakterien (*Lysogeny Broth*)
LC-ESI-MS/MS	Flüssigchromatographie-Tandem-Massenspektrometrie
LRR	Leuzin-reiche Wiederholungssequenz (*Leucine-rich Repeat*)
Lys	Lysin
MAPK	*Mitogen-activated Protein Kinase*
MLCK	*Myosin Light Chain Kinase*
mRNA	Boten RNA (*Messenger RNA*)
MS	Nährmedium nach Murashige und Skoog
NaCl	Natriumchlorid
NaOH	Natriumhydroxid
PAPS	3´-Phosphoadenosin 5´-Phosphosulfat
PCR	Polymerasekettenreaktion (*Polymerase Chain Reaction*)
PEPR1	*Plant Elicitor Peptide Receptor 1*
Pfu	*Pyrococcus furiosus*
PLT	Plethora
POL	Poltergeist
PP2A	Protein Phosphatase 2A
PSK	Phytosulfokin

PSKR	Phytosulfokin Rezeptor
PSY1	*Plant Peptide Containing Sulfated Tyrosine 1*
qPCR	Quantitative Real Time PCR
RALF	*Rapid Alkalinization Factor*
RAM	Wurzelapikalmeristem
RGF	*Root Meristem Growth Factor*
RK	Rezeptorkinase
RNA	Ribonukleinsäure
RPK2	*Receptor-like Protein Kinase 2*
rpm	Umdrehungen pro Minute (*revolutions per minute*)
RT	Raumtemperatur
RT-PCR	Reverse Transkriptions-PCR
SAM	Sprossapikalmeristem
SBT	Subtilisin Serin Protease
SCR	*Scarecrow*
SDS	Natriumdodecylsulfat
Ser	Serin
SERK	*Somatic Embryogenesis Receptor-like Kinase*
SOT	Sulfotransferase
Taq	*Thermus aquaticus*
T-DNA	Transfer-DNA
Thr	Threonin
TPST	Tyrosylprotein Sulfotransferase
Trp	Tryptophan
Tyr	Tyrosin
v/v	Volumen/Volumen (*volume per volume*)
w/v	Gewicht/Volumen (*weight per volume*)
WT	Wildtyp
WOX5	*Wuschel-related Homeobox 5*
WUS	*Wuschel*

Inhaltsverzeichnis

Zusammenfassung

Der Peptidwachstumsfaktor Phytosulfokin (PSK) wird in *Arabidopsis thaliana* von zwei Plasmamembran-lokalisierten Rezeptoren, PSKR1 und PSKR2, perzipiert, die zur Klasse der Leuzin-reichen Rezeptorkinasen gehören. In dieser Arbeit wurde insbesondere PSKR1 aus Arabidopsis funktional analysiert. Die Überexpression von *PSKR1* und *PSKR2* im Wildtyp führte zu einer Steigerung des Wurzel- und Hypokotylwachstums, was zeigt, dass die Abundanz der PSK-Rezeptoren das Wachstum limitiert. Die Expression von *PSKR1* in der Epidermis über den Promotor *CER6* im *pskr1-3 pskr2-1* (*r1r2*) Hintergrund zeigte, dass die Perzeption von PSK in der Epidermis ausreicht, um das Wachstum nicht nur der äußeren, sondern auch der inneren Zellschichten anzuregen. Darüber hinaus förderte die Expression von *PSKR1* über den Atrichoblasten-spezifischen Promotor *GL2* in *r1r2* nicht nur bei den Atrichoblasten, sondern auch bei Trichoblasten das Wachstum. Die Expression von *PSKR1* in einem Zelltyp der Wurzelepidermis reicht also aus, das Wachstum des gesamten Organs zu fördern. PSK fungiert damit als nicht-zellautonomer Wachstumsfaktor. Über bioinformatische Analysen wurde bei PSKR1 eine Calmodulin (CaM)-Bindungsdomäne identifiziert und durch den Austausch des konservierten Tryptophans W831 gegen ein hydrophiles Serin funktional untersucht. Die Expression der in der CaM-Bindungsdomäne mutierten Rezeptorvariante in *r1r2* führte zu einer Verstärkung des *r1r2* Phänotyps mit reduziertem Wurzel- und Sprosswachstum. Der Austausch des konservierten Lysins K762 gegen ein negativ geladenes Glutamat führte bei dem ektopisch exprimierten cytoplasmatischen Teil von PSKR1 *in vitro* zu einem Verlust der Kinaseaktivität. Die Expression von Kinase-inaktivem PSKR1 in *r1r2* resultierte in einem reduzierten Wurzel- und Sprosswachstum. Damit wurde gezeigt, dass sowohl die Kinaseaktivität von PSKR1, als auch die Bindung von CaM an den Rezeptor essentiell für die wachstumsfördernde Wirkung von PSK *in planta* sind. Um die Regulation des Rezeptors über Phosphorylierung zu untersuchen, wurden in einer Kooperation Phosphorylierungsstellen von PSKR1 kartiert. Gerichtete phosphoablative Mutationen von nachgewiesenen Phosphorylierungsstellen zeigten, dass drei konservierte Threonine und ein Serin (T890, S893, T894 und T899) in der Aktivierungsschleife von PSKR1 essentiell für die Kinaseaktivität *in vitro* sowie für die Funktion des Rezeptors *in planta* sind. Die Expression einer Rezeptorvariante in *r1r2*,

bei der T890, S893, T894 und T899 zu Alanin mutiert wurden, resultierte in einer Hemmung des Wurzelwachstums im Vergleich zum Wildtyp und auch im Vergleich zu *r1r2* Keimlingen.

Summary

In *Arabidopsis thaliana*, the peptide growth factor phytosulfokine (PSK) is perceived by two plasma membrane-localized receptors termed PSKR1 and PSKR2 that belong to the leucine-rich repeat class of receptor kinases. In this study functional analysis in particular of PSKR1 from Arabidopsis was performed. Overexpression of *PSKR1* and *PSKR2* in the wild type resulted in promotion of root and hypocotyl growth showing that abundance of PSK receptors limits growth. Epidermis-specific expression of *PSKR1* in the *pskr1-3 pskr2-1* (*r1r2*) background driven by the *CER6* promoter showed that perception of PSK in the epidermis is sufficient to stimulate growth not only of the outer but also of the inner cell layers. Furthermore, expression of *PSKR1* driven by the atrichoblast-specific promoter *GL2* in *r1r2* promoted growth not only of atrichoblast cells but also of root hair-forming trichoblasts. Hence, expression of *PSKR1* in one cell type of the epidermis is sufficient to stimulate whole-organ growth indicating that PSK acts as a non-cell autonomous growth factor *in planta*. Bioinformatic analysis identified a calmodulin (CaM)-binding site in PSKR1. Replacement of the conserved tryptophan W831 in the CaM binding site by a hydrophilic serine resulted in loss of CaM binding. Expression of the CaM binding site mutated receptor variant in *r1r2* enhanced the *r1r2* phenotype with reduced root and shoot growth. Replacement of the conserved lysine K762 by a negatively charged glutamate caused loss of *in vitro* kinase activity of the ectopically expressed cytoplasmic protein portion of PSKR1. Expression of the kinase-inactive PSKR1 (K762E) in *r1r2* resulted in reduced root and shoot growth. Hence, both, PSKR1 kinase activity and CaM binding to the receptor are essential for the growth promoting effect of PSK *in planta*. To study the regulation of the receptor by phosphorylation, a phosphosite mapping of PSKR1 was performed in collaboration. Subsequent functional analysis of identified phosphorylation sites by site-directed mutagenesis demonstrated that three conserved threonines and one serine (T890, S893, T894 and T899) located in the activation loop of PSKR1 are required for *in vitro* PSKR1 kinase activity and for receptor function *in planta*. Expression of the receptor variant PSKR1(T890A S893A T894A T899A) in which these phosphorylation sites were replaced by alanine in the *r1r2* background resulted in reduced root growth compared to both wild type and *r1r2* seedlings indicating that PSKR1 is subject to regulation by phosphorylation.

Einleitung

Verschiedene Signalwege in der Pflanze

Die Zellen innerhalb eines eukaryotischen Organismus müssen über kurze und lange Distanzen miteinander kommunizieren. Hierbei spielt insbesondere bei Höheren Pflanzen interzelluläre Kommunikation eine wichtige Rolle (Gallagher und Benfey, 2005; Wang und Fiers, 2010). Pflanzen sind als immobile Organismen auf die Fähigkeiten angewiesen, ihr Wachstum und ihre Entwicklung mit äußeren Umweltbedingungen zu koordinieren. Die mit der Umwelt in Kontakt stehenden Zellen müssen äußere Reize wahrnehmen und zu anderen Zellen und Organen weiterleiten. Die Komplexität der Kommunikation von Zelle zu Zelle wird dadurch erhöht, dass die Position der einzelnen Pflanzenzellen über starre Zellwände festgelegt ist. Dies könnte in der Evolution verschiedener Mechanismen die treibende Kraft einer interzellulären Kommunikation gewesen sein, welche das Wachstum und die Entwicklung einer Pflanze steuern. Aufgrund der Zellwände gibt es für Pflanzen zwei Wege für einen interzellulären Transport: Zum einen können beim apoplastischen Transport Signale durch den Raum zwischen Zellwand und Plasmamembran weitergeleitet werden. Zum anderen erfolgt eine direkte Signalweiterleitung zwischen Zellen über Plasmodesmen und stellt einen symplastischen Transport dar.

Die ober- und unterirdischen Organe einer Pflanze werden durch zwei verschiedene Stammzellpopulationen, die Meristeme, gebildet. Jedes Meristem besteht aus sogenannten Nischenzellen, welche im Spross das organisierende Zentrum und in der Wurzel das ruhende Zentrum bilden (Abbildung 1). Beide Zentren sind umgeben von Stammzellen, welche die kontinuierliche Bildung neuen Gewebes und verschiedener Organe unterstützen (Scheres, 2007). Die Bildung dieser Gewebe und Organe erfordert genau abgestimmte Zellteilungen und die Aneignung korrekter Zellidentitäten (Scheres und Benfey, 1999). In Pflanzen hängt die Bestimmung über das Zellschicksal hauptsächlich von der Lage der jeweiligen Zelle ab und lässt sich daher auch durch eine experimentelle Veränderung der Zellposition verändern (van den Berg et al., 1995; Berger et al., 1998; Scheres, 2007).

Die Analyse chimärer Pflanzen hat das Wissen über die Organisation der Zellabstammung und über die Kommunikation zwischen Zellschichten enorm bereichert (Stewart und Burk, 1970; Szymkowiak und Sussex, 1996; Marcotrigiano, 2001). In Höheren Pflanzen stammen die Organe des Sprosses von drei klonal verschiedenen Zellschichten ab, welche sich im Sprossmeristem befinden: Die äußerste Schicht ist die L1-Schicht, die Zellen unmittelbar darunter bilden die L2-Schicht und die inneren Gewebe definieren die L3-Schicht (Satina et al., 1940; Abbildung 1B). Zellen der L1-Schicht bilden die Epidermis und damit die Grenzschicht zwischen Spross und Umwelt, aus der L2-Schicht gehen photosynthetisch aktive Zellen hervor und das Leitgewebe wird aus Zellen der L3-Schicht gebildet (Stewart und Burk, 1970).

Die inneren Zellschichten eines wachsenden Stängels strecken sich nach der Trennung von der äußeren Epidermis (Peters und Tomos, 1996). Die Epidermis hingegen kontrahiert, da die verschiedenen Zellschichten unter differenziellen Spannungen stehen. Es wurde in zahlreichen Studien die Hypothese aufgestellt, dass die expandierenden, dünnwandigen Zellen der inneren Zellschichten die treibende Kraft für das Stängel- beziehungsweise Hypokotylwachstum darstellen (Kutschera, 1992; Niklas und Paolillo, 1997; Kutschera und Niklas, 2007; Kutschera, 2008; Savaldi-Goldstein et al., 2007). Nach dieser Hypothese bestimmt die durch dicke Zellwände charakterisierte Epidermisschicht die Wachstumsrate von Stängeln und Hypokotylen. Des Weiteren konnte gezeigt werden, dass die Epidermis durch eine gesteigerte Expansion ihrer Zellen Zellteilungsdefekte kompensieren kann (Serralbo et al., 2006; Bemis und Torii, 2007). Bemis und Torii (2007) wiesen nach, dass die Epidermis nicht die Zellteilungsrate in den inneren Zellschichten kontrolliert. Die durch eine L1-spezifische Expression des *CYCLIN-DEPENDENT KINASE* (*CDK*)-Gens *ICK1* unterdrückte epidermale Zellteilung konnte durch die inneren Zellschichten teilweise behoben werden (Bemis und Torii, 2007). Nach Serralbo et al. (2006) ist an diesem Prozess vermutlich eine Bewegung von Regulatoren des Zellzyklus zwischen den verschiedenen Zellschichten beteiligt. Die reduzierte epidermale Zellteilung schränkte zudem in den inneren Zellschichten die Zellexpansion ein. Dies wurde dadurch kompensiert, dass sich in der L2-Schicht Zellen mit kleinerem Volumen bildeten (Serralbo et al., 2006). Insgesamt lassen die bisherigen Studien darauf schließen, dass die Epidermis die Wachstums-limitierende

Zellschicht darstellt. Vermutlich tragen sowohl mechanische, als auch chemische Signale zu einer Kommunikation zwischen den Zellschichten bei, um koordiniertes Wachstum zu gewährleisten.

In der Wurzel der Modellpflanze *Arabidopsis thaliana* sind alle Zellschichten in einem einfachen polysymmetrischen Muster klonaler Zellreihen angeordnet (Stahl und Simon, 2010; Abbildung 1C). Das Wurzelmeristem lässt sich in drei Hauptregionen einteilen: Die meristematische Zone, die Elongationszone und die Differenzierungszone. Die meristematische Zone enthält die Stammzellnische, in der sich kaum teilende Zellen des ruhenden Zentrums befinden (Wang et al., 2005a). Diese Zellen inhibieren über nicht-zellautonome Signale die Differenzierung der umliegenden Stammzellen (van den Berg et al., 1997).

Die Mechanismen einer Signalweiterleitung, welche die Entwicklung einer Pflanze steuern, beinhalten Effektoren für eine Kommunikation über große Distanzen (Abbildung 1A). Dazu gehören beispielsweise Phytohormone (De Smet und Jürgens, 2007; Lau et al., 2008). Hingegen stellen mobile Transkriptionsfaktoren, nichtkodierende RNAs und kleine mobile Peptide Effektoren für eine lokale Kommunikation innerhalb eines Organs zwischen benachbarten Zellen dar (Abbildung 1B, C) (Kurata et al., 2005; Butenko et al., 2009; Busch und Benfey, 2010; Van Norman et al., 2011).

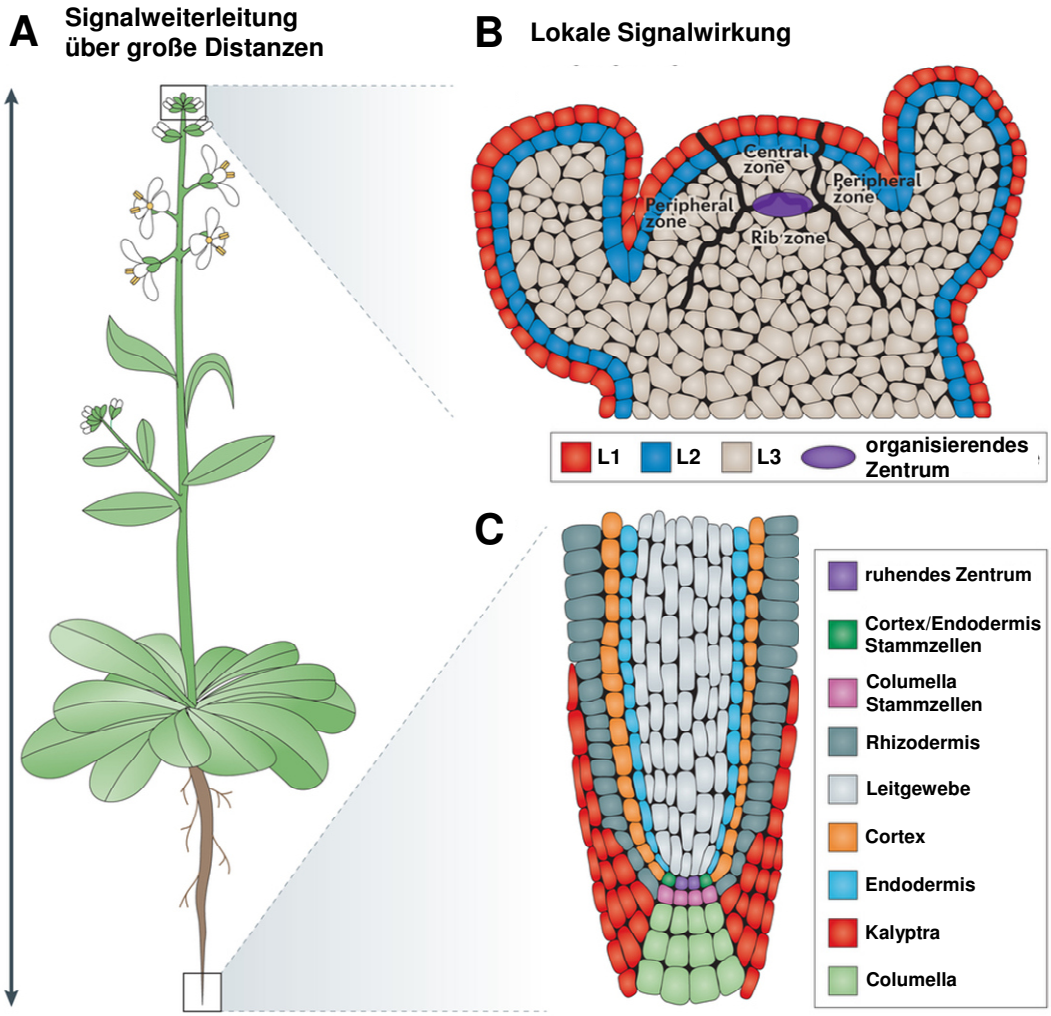

Abbildung 1: Schematische Darstellung der Meristeme in *Arabidopsis thaliana* und mögliche Signalwege. In Arabidopsis gibt es zwei verschiedene Arten der Signalweiterleitung: Effektoren wie beispielsweise Phytohormone steuern die Kommunikation über große Distanzen, wie zwischen Spross und Wurzel (A). Unter anderem vermitteln kleine mobile Peptide die interzelluläre Kommunikation innerhalb eines Organs (B, C). Die Gewebe und Organe in Arabidopsis werden von zwei verschiedenen Meristemen gebildet, wobei sich eines am äußersten Ende der Sprossspitze (SAM) (B) und das andere in der Wurzelspitze (RAM) (C) befindet. Jedes Meristem besteht aus Stamm- und sogenannten Nischenzellen, letztere bilden im Spross das organisierende Zentrum und in der Wurzel das ruhende Zentrum. SAM und RAM zeichnen sich durch eine individuelle Organisation aus: Das SAM enthält drei verschiedene Zellschichten (L1, L2 und L3) und die zentrale Zone ("*central zone*"), innerhalb derer sich die eigentlichen Stammzellen befinden (B). Die Stammzellen in der zentralen Zone geben durch Teilung Zellen zur Differenzierung an die periphere Zone ("*peripheral zone*") des Meristems ab. Unterhalb der zentralen Zone befindet sich die Rippenzone ("*rib zone*"), welche hauptsächlich zum Sprosswachstum beiträgt. Das organisierende Zentrum des SAM ist an der Verbindungsstelle von zentraler, peripherer und der Rippenzone lokalisiert und fungiert in der Aufrechterhaltung der Spross-Stammzellen. (C) Das ruhende Zentrum im RAM ist umgeben von Stammzellen, welche in der Wurzel ein oder zwei Zelltypen bilden. Aus den Stammzellen oberhalb und unterhalb des ruhenden Zentrums gehen Leitgewebe beziehungsweise Columella-Zellen hervor. Die Rhizodermis und Kalyptra werden wie Cortex und Endodermis aus der gleichen Stammzelle gebildet (verändert nach Sparks et al., 2013).

Peptide mit Signalwirkung steuern Wachstums-, Differenzierungs- und Entwicklungsprozesse in Pflanzen

Genetische und biochemische Analysen haben gezeigt, dass Peptide eine wichtige Rolle bei der interzellulären Kommunikation in Pflanzen spielen. In Arabidopsis gibt es über 900 putative Gene, welche für sekretierte Peptide kodieren (Matsubayashi, 2011). Peptide sind an der Regulation diverser physiologischer Prozesse, wie Pollen-, Stomata-, und Meristementwicklung, Organabszission und Wurzelwachstum, sowie an Abwehrmechanismen gegen Pathogene beteiligt (Matsubayashi, 2011; Matsubayashi und Sakagami, 2006). Nach Murphy et al. (2012) sind Peptide in der Regel kleiner als etwa 120 Aminosäuren und liegen oft in sehr niedrigen physiologischen Konzentrationen im nanomolaren Bereich vor. Sekretierte Peptide lassen sich in zwei Gruppen einteilen: Peptide der Gruppe 1, welche komplexe post-translationale Modifikationen gefolgt von proteolytischen Prozessierungen durchlaufen und Kandidaten der Gruppe 2, welche mehrere innermolekulare Disulfidbrücken aufweisen (Matsubayashi, 2012). Hinsichtlich der Peptide beider Gruppen wird vermutet, dass diese durch den Apoplast diffundieren und an Ziel-Rezeptoren der gleichen sowie benachbarter Zellen binden (Hirakawa et al., 2008).

Bisher wurden drei Arten post-translationaler Modifikationen von Peptiden beschrieben: Sulfatierung, Hydroxylierung und Arabinosylierung (Matsubayashi, 2011). Gene der Peptide aus Gruppe 1 und viele derer aus Gruppe 2 kodieren für Proteine, welche länger als die aktiven Peptide sind. Die aktiven Peptide werden durch proteolytische Prozessierungen freigesetzt. Hier sind Enzyme aus der Subtilase-Gruppe von Serin-Proteasen beteiligt (Ni und Clark 2006; Srivastava et al., 2008; Ni et al., 2011).

Ryan (1974) hat das erste pflanzliche Peptid, das Systemin (TomSys), in der Tomate identifiziert. Es konnte gezeigt werden, dass die Applikation von Extrakten verwundeter Tomatenblätter bei jungen Tomatenpflanzen die Bildung der Proteinaseinhibitoren I und II induzierte. Über die Aufreinigung des Peptids aus den Blattextrakten der Tomate und durch die Verwendung eines synthetischen Peptids konnte ein 18 Aminosäuren langes Polypeptid als aktiver Bestandteil identifiziert werden (Ryan, 1974; Pearce et al., 1991). Aufgrund einer TomSys-vermittelten Alkalisierung des Mediums von Suspensionskulturen wurde vermutet, dass andere

aktive Peptide einen ähnlichen Effekt bewirken könnten (Meindl et al., 1998; Schaller und Oecking, 1999; Pearce et al., 2001). Nach der Entdeckung des TomSys wurden durch die Verwendung eines Alkalisierungsassays in Extrakten verwundeter Tabakblätter zwei Peptide gefunden, welche aber keine Sequenz-Ähnlichkeit mit TomSys aufwiesen (Ryan und Pearce, 2003). Beide identifizierten Hydroxyprolin-reichen Peptide, das Tabak Systemin I (TobHypSysI) und TobHypSysII, zeigten aber eine ähnliche Wirkungsweise wie das TomSys. Durch die Verwendung des Alkalisierungsassays konnte in Tabak auch ein *RAPID ALKALINIZATION FACTOR* (RALF) identifiziert werden. Im Gegensatz zu den Systeminen ist RALF nicht an der Reaktion auf Verwundung beteiligt (Pearce et al., 2001). RALF aus Tabak ist ein 49 Aminosäuren langes sekretiertes Peptid, welches aus einem 115 Aminosäuren langen Vorläuferpeptid gebildet wird (Bedinger et al., 2010). In Arabidopsis kodieren 34 Gene für RALFs und *RALF-LIKE* (RALFL) Peptide (Pearce et al., 2001; Olsen et al., 2002; Bedinger et al., 2010; Cao und Shi, 2012). Die Applikation von RALFs und RALFLs bewirkt im Vergleich zu Systemin eine schnellere Alkalisierung des Mediums, welches die Suspensionskultur umgibt (Pearce et al., 2001; Ryan et al., 2002; Bedinger et al., 2010; Covey et al., 2010). Das RALF Peptid inhibiert das Wurzelwachstum und die Wurzelhaarbildung von Arabidopsis-Keimlingen, welche in Medium angezogen werden, das synthetisches RALF enthält (Pearce et al., 2001; Bedinger et al., 2010). Eine Überexpression von AtRALF1 beziehungsweise AtRALF23 führt zu einem Zwergenwuchs-Phänotyp (Matos et al., 2008; Srivastava et al., 2009). Vermutlich haben RALFs und RALFLs eine Auswirkung auf das Wachstum, indem sie die Zellexpansion kontrollieren (Bergonci et al., 2014). Bergonci et al. (2014) konnten zeigen, dass eine Überexpression von AtRALF1 durch eine Reduzierung der Zellgröße zu kürzeren Wurzeln und Hypokotylen führt. Nach Bedinger et al. (2010) werden bei der Signalweiterleitung von RALF *MITOGEN-ACTIVATED PROTEIN KINASEs* (MAPKs) aktiviert. Als die erste Reaktion auf eine AtRALF1-Applikation konnte ein signifikanter Anstieg der cytoplasmatischen Ca^{2+}-Konzentration gemessen werden (Haruta et al., 2008).

Bei der Sprossentwicklung stellt das Peptid CLAVATA3 (CLV3), wie in Abbildung 2A gezeigt, einen wichtigen Regulator der Stammzellnische dar (Fletcher et al., 1999; Kondo et al., 2006). *CLV3* kodiert für ein 96 Aminosäuren langes Peptid, welches post-translational modifiziert und proteolytisch prozessiert wird. CLV3 gehört zur Familie der *CLV3/EMBRYO SURROUNDING REGION (ESR)-RELATED* (CLE) Peptide, welche in Arabidopsis aus 32 Mitgliedern besteht (Jun et al., 2010). CLV3 interagiert mit drei membranständigen Rezeptorkomplexen: CLAVATA1 (CLV1) Homodimeren, CLAVATA2 (CLV2)-CORYNE (CRN) Heterodimeren und *RECEPTOR-LIKE PROTEIN KINASE 2* (RPK2) Homodimeren (Clark et al., 1997; Jeong et al., 1999; Müller et al., 2008; Guo et al., 2010). Es konnte gezeigt werden, dass CLV3 extrazellulär direkt an das CLV1 Rezeptorprotein bindet (Fletcher und Meyerowitz, 2000; Ogawa et al., 2008; Bleckmann et al., 2010). Bemerkenswerterweise interagiert arabinosyliertes CLV3 stärker mit CLV1 als das Peptid ohne diese Modifizierung (Ohyama et al., 2009). CLV2 bildet mit CRN einen Rezeptor-ähnlichen Proteinkomplex, wobei CRN CLV2 für eine Lokalisation an der Plasmamembran benötigt (Bleckmann et al., 2010; Guo et al., 2010; Nimchuk et al., 2011). Es lässt sich vermuten, dass der CLV2-CRN Komplex in den CLV3 Signalweg involviert ist. RPK2 stellt einen dritten, unabhängigen CLV3 Signalweg dar (Kinoshita et al., 2010). CLV3 fördert die Differenzierung von Stammzellen im Spross-Apikalmeristem (SAM) (Fletcher et al., 1999; Abbildung 2A). Die Signaltransduktion nach der Bindung von CLV3 an einen Rezeptorkomplex führt zu einer Einschränkung der Expression von *WUSCHEL*, einem Homeodomänen-Transkriptionsfaktor (Schoof et al., 2000). Genetische und biochemische Studien zeigten, dass die Proteinphosphatasen POLTERGEIST (POL) und *POLTERGEIST-LIKE1* (PLL1) als Zwischenglieder in der Signalkette zwischen CLV3-Perzeption und *WUSCHEL*-Regulation fungieren (Williams et al., 1997; Trotochaud et al., 1999; Yu et al., 2000; Song et al., 2006). WUSCHEL fördert die Stammzell-Identität in einer nicht-zellautonomen Weise (Laux et al., 1996; Mayer et al., 1998; Brand et al., 2000). Bei Abnahme der Anzahl an Stammzellen wird die Expression von *CLV3* reduziert. Dies führt zu einer Erhöhung der *WUSCHEL*-Expression und der Teilung von Stammzellen. Bei Zunahme der Stammzellen erhöht sich über einen rückgekoppelten Signalweg die *CLV3*-Expression bei gleichzeitiger Herunterregulierung der *WUSCHEL*-Expression. Dies führt zu einer geringeren Teilungsrate von Stammzellen (Brand et al., 2000; Schoof et al., 2000; Müller et al.,

2006; Yadav et al., 2011). Schuster et al. (2014) konnten darüber hinaus zeigen, dass der bHLH Transkriptionsfaktor *HECATE1* (HEC1) die Expression von *WUSCHEL* und *CLV3* unterdrückt. HEC1 trägt durch eine Förderung der Proliferation von Stammzellen zur Funktion des SAM bei. Das Gleichgewicht zwischen Zellteilung und Differenzierung von Stammzellen im Sprossmeristem wird daher über den CLV3 Signalweg reguliert.

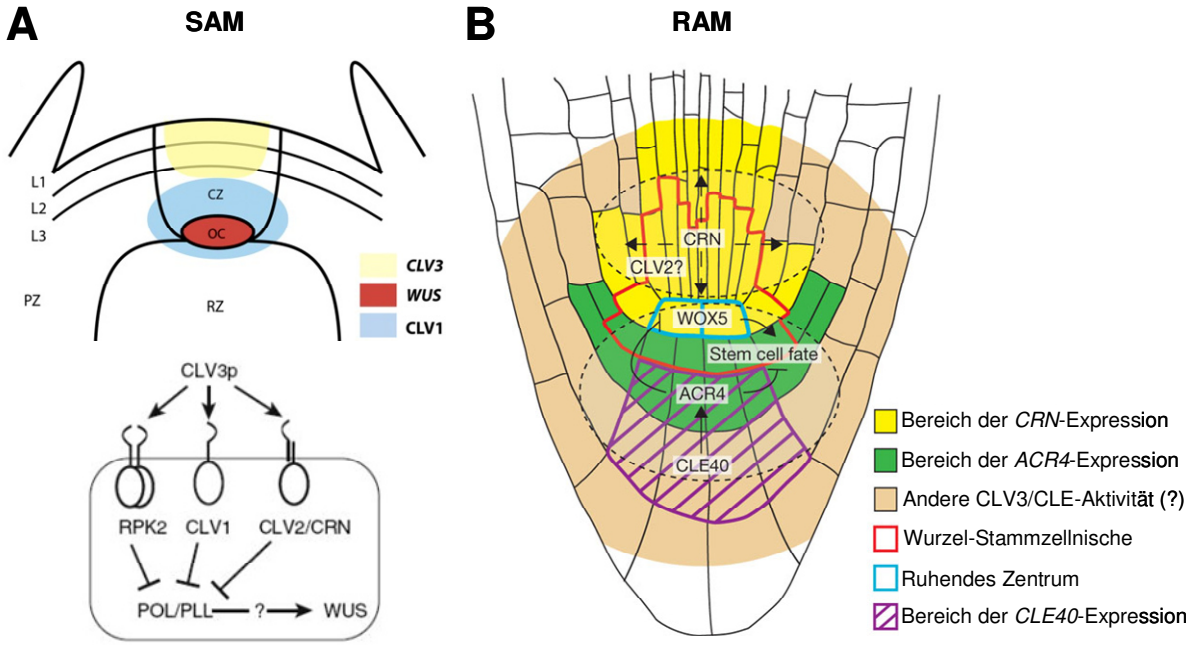

Abbildung 2: Modelle für die CLE-abhängige Aufrechterhaltung von Stammzellen im Spross- und Wurzelapikalmeristem (SAM, RAM). (A) Innerhalb der zentralen Zone (CZ) des SAM wird der mobile Transkriptionsfaktor *WUSCHEL* (*WUS*) im organisierenden Zentrum (OZ) exprimiert (rot) und wandert in die L1- und L2-Schicht, um die *CLV3*-Expression (gelb) in den Stammzellen zu fördern. CLV3 wiederum wandert in die L3-Schicht, um an die Rezeptorkomplexe CLV1 (blau), CLV2-CRN und RPK2 zu binden und so über eine POL/PLL-Hemmung die *WUS*-Expression zu unterdrücken. (B) Im RAM wird *CLE40*, ein Homolog von *CLV3*, in den Columella-Zellen unterhalb des ruhenden Zentrums exprimiert. CLE40 bindet an den Rezeptor ACR4, um die Expression von *WUSCHEL-RELATED HOMEOBOX5* (*WOX5*) im ruhenden Zentrum einzuschränken, WOX5 wiederum wird für die Aufrechterhaltung der Columella-Stammzellen benötigt. Neben *CLE40* und *ACR4* werden einige andere *CLEs* und Rezeptoren im RAM exprimiert, dies deutet auf das Vorhandensein eines komplexen CLE-Signalnetzwerks hin. Die Rolle von CRN ist derzeit unbekannt, möglicherweise fungiert CRN zusammen mit CLV2 in der Aufrechterhaltung des Wurzelmeristems. Die gepunkteten Ellipsen deuten den CLE40/ACR4-Signalweg beziehungsweise einen unabhängigen, möglichen Signalweg über CLV2/CRN an (verändert nach De Smet et al., 2009; Katsir et al., 2011; Murphy et al., 2012).

Im Wurzel-Apikalmeristem (RAM) wurde ein Signalweg gefunden, welcher dem CLV3 Signalweg ähnlich ist (Abbildung 2B): Hier perzipiert das Rezeptorprotein *ARABIDOPSIS CRINKLY4* (ACR4) das CLE40 Peptid, welches an der Differenzierung von Columella-Stammzellen mitwirkt (Hobe et al., 2003; De Smet et al., 2008; Stahl et al., 2009). Bemerkenswerterweise konnten Stahl et al. (2013) in diesem Zusammenhang zeigen, dass CLV1 im Wurzelmeristem als Korezeptor von ACR4 fungieren könnte, was auf einen evolutionär konservierten Mechanismus in der Aufrechterhaltung meristematischer Aktivität hindeutet. Differenzierende Columella-Zellen exprimieren sowohl *ACR4* als auch *CLE40*. Über eine Regulierung der *WUSCHEL-RELATED HOMEOBOX5* (*WOX5*) Expression erhalten ACR4 und CLE40 die Größe der Wurzel-Stammzellnische aufrecht, indem sie die Anzahl an Columella-Ausgangszellen kontrollieren (Haecker et al., 2004; Stahl et al., 2009).

Matsuzaki et al. (2010) identifizierten eine weitere Peptid-Familie, deren Mitglieder ebenfalls an der Aufrechterhaltung des Wurzelmeristems beteiligt sind: Die CLE-ähnlichen (CLEL) Peptide, auch bekannt als *Root Meristem Growth Factors* (RGFs), wurden anhand ihrer post-translationalen Modifikationen identifiziert. Die einzige Gemeinsamkeit zwischen CLEs und CLEL Peptiden besteht in einer ähnlichen Peptid-Struktur (Meng et al., 2012). Obwohl die beschriebenen Signalwege im SAM und RAM in ihrer Funktionsweise auffallend ähnlich sind, gibt es einen entscheidenden Unterschied: Im SAM wird die Größe der Stammzellnische durch Signale von den Stammzellen reguliert, wohingegen im RAM die Signale von differenzierenden Columella-Zellen stammen.

Die Tyrosin-Sulfatierung als bedeutende post-translationale Modifikation von Peptiden

Die Sulfatierung von Tyrosinen stellt bei den meisten Eukaryoten eine post-translationale Modifikation von Proteinen und Peptiden dar, welche über den sekretorischen Weg synthetisiert werden. Diese Modifikation wird durch ein spezifisches Enzym, die Tyrosylprotein-Sulfotransferase (TPST) vermittelt. Die TPST katalysiert den Transfer eines Sulfats von 3'-Phosphoadenosin 5'-Phosphosulfat (PAPS) zur Phenolgruppe des Tyrosins (Huttner, 1982; Moore, 2003). Bislang wurde das Erkennungs-Motiv für die Tyrosin-Sulfatierung von Peptiden nicht aufgeklärt. Es konnte aber gezeigt werden, dass ein Asparaginsäure-Rest N-terminal von einem

Tyrosin die minimale Voraussetzung für eine Tyrosin-Sulfatierung in Pflanzen darstellt. Mehrere saure Aminosäuren in der Nähe vom Tyrosin führen zu einer signifikanten Erhöhung der Sulfatierung (Hanai et al., 2000a). In Pro- und Eukaryoten gibt es noch weitere Sulfotransferasen (SOTs), die ebenfalls eine Sulfatgruppe von PAPS auf eine Hydroxylgruppe verschiedenster Substrate übertragen (Klein und Papenbrock, 2004; Klein et al., 2006). Die Funktionen der SOTs sind vielfältig, in Pflanzen spielen sie vermutlich eine Rolle beim Wachstum, der Entwicklung und der Anpassung an Stress. Nach Klein und Papenbrock (2004) konnten in Arabidopsis 18 Gene identifiziert werden, die für SOT Proteine kodieren.

Die TPST aus Arabidopsis (AtTPST) ist ein Transmembran-Protein, welches 62 kDa groß und im Golgi-Apparat lokalisiert ist (Komori et al., 2009). Die AtTPST wird in der gesamten Pflanze exprimiert, wobei sich die höchste Expression im RAM zeigt. Bemerkenswerterweise weist die AtTPST keine Sequenzähnlichkeit mit tierischen TPSTs auf, obwohl in beiden Fällen der identische Sulfat-Transfer mit PAPS als Kosubstrat katalysiert wird. Darüber hinaus ist die AtTPST ein TypI Transmembran-Protein, welches eine C-terminale Transmembrandomäne aufweist. Im Gegensatz dazu stellen tierische TPSTs TypII Transmembran-Proteine dar, hier befindet sich die Transmembrandomäne in der Nähe des N-Terminus (Beisswanger et al., 1998; Ouyang et al., 1998; Moore, 2003). Dies lässt darauf schließen, dass im Laufe der Evolution Pflanzen und Tiere unabhängig voneinander Enzyme für Tyrosin-Sulfatierungen hervorgebracht haben. Die AtTPST wird durch ein Gen kodiert. Die *tpst-1 Knockout* Mutante zeigt eine deutliche Zwergwüchsigkeit (Komori et al., 2009). Des Weiteren weisen *tpst-1* Pflanzen und Keimlinge eine reduzierte Anzahl an Blüten und Schoten, hellgrüne Blätter, eine frühe Seneszenz, ein kleineres Wurzelapikalmeristem und stark verkürzte Wurzeln auf (Komori et al., 2009; Zhou et al., 2010; Matsuzaki et al., 2010).

Bisher wurden drei Tyrosin-sulfatierte Peptide in Pflanzen gefunden: Phytosulfokin (PSK) (Abbildung 3A) (Matsubayashi und Sakagami, 1996), *Plant Peptide Containing Sulfated Tyrosine 1* (PSY1) (Amano et al, 2007) und die bereits oben erwähnten RGFs (Matsuzaki et al., 2010). Alle drei Arten Tyrosin-sulfatierter Peptide sind essentiell für das Wurzelwachstum in Arabidopsis (Komori et al., 2009; Matsuzaki et al., 2010).

Identifizierung und Wirkungsweisen der Tyrosin-sulfatierten Peptide PSK, PSY1 und RGF1

Um das Zellwachstum von Protoplasten verschiedener Pflanzenarten in einer Zellkultur geringer Dichte zu fördern, wurden spezielle Kulturtechniken, wie beispielsweise sogenannte „Ziehkulturen“, herangezogen (Raveh et al., 1973; Bellincampi und Morpurgo, 1987; Birnberg et al., 1988). Dazu wurden die Zielzellen geringer Dichte in räumlicher Nähe, aber getrennt von „Ziehzellen“ hoher Dichte angezogen. Es entstand die Theorie, dass eine interzelluläre Kommunikation, welche auf ein chemisches Signal zurückzuführen ist, am Zellwachstum beteiligt ist. Dieses Signal wird von den „Ziehzellen“ selbst produziert, ins Medium sekretiert und fördert die Proliferation von Zellen niedriger Dichte (Bellincampi und Morpurgo, 1987; Birnberg et al., 1988). In Suspensionskulturen von Maiszellen wurde dieses Signal, auch bekannt als konditionierender Faktor, als stark hydrophiles und neutrales Molekül identifiziert (Birnberg et al., 1988). In Karotten-Zellkulturen zeigte das entsprechende Molekül ebenfalls einen hydrophilen Charakter und war relativ hitzestabil (Bellincampi und Morpurgo, 1987).

Durch die Verwendung eines entsprechenden Systems, bei dem Spargel-Mesophyllzellen genutzt wurden, um den konditionierenden Faktor zu finden, konnte ein sulfatiertes Pentapeptid (PSK) identifiziert werden (Matsubayashi und Sakagami 1996). PSK mit der Aminosäuresequenz Tyr(SO_3H)-Ile-Tyr(SO_3H)-Thr-Gln ist ein fünf Aminosäuren langes sekretiertes Peptid, welches zwei sulfatierte Tyrosine enthält (Abbildung 3A). PSK wirkt als autokrines Signal in Pflanzenzellen und fördert stark die Proliferation von Suspensionszellen in geringer Dichte (Matsubayashi und Sakagami 1996). PSK ist wasserlöslich, hitzestabil und bereits in nanomolaren Konzentrationen wirksam (Matsubayashi et al., 1996, 1997, 2002). PSK wurde mit der identischen Struktur auch in konditionierten Medien verschiedener Pflanzenarten wie *Oryza sativa* (Yang et al., 1999), *Zea mays* (Matsubayashi et al., 1997), *Zinnia elegans* (Matsubayashi et al., 1999), *Daucus carota* (Hanai et al., 2000b) und *Arabidopsis thaliana* (Yang et al., 2001) gefunden. Neben der Förderung der Proliferation von Suspensionszellen in geringer Dichte löst PSK in nanomolaren Konzentrationen die Differenzierung von Zinnien-Mesophyllzellen zu Tracheenelementen aus (Matsubayashi et al., 1999). Es fördert die somatische Embryogenese bei der Karotte (Kobayashi et al., 1999; Hanai et al., 2000b) und der

Sicheltanne (Igasaki et al., 2003). PSK stimuliert die Bildung von Adventivwurzeln bei der Gurke (Yamakawa et al., 1998) und hat bei Tabakpflanzen einen regulatorischen Effekt bei der Pollenkeimung (Chen et al., 2000). Han et al. (2014) zeigten, dass PSK bei der Baumwolle eine Verlängerung der Fasern fördert. Darüber hinaus wiesen Yamakawa et al. (1999) nach, dass hohe PSK-Konzentrationen bei gleichzeitig hohen Temperaturen das Wachstum und den Chlorophyll-Gehalt von Arabidopsis-Keimlingen förderten. Dies deutet darauf hin, dass PSK in der Vermittlung von Hitzestress-Toleranz in Pflanzen beteiligt sein könnte. Neuere Studien haben gezeigt, dass PSK abhängig von der verwendeten Konzentration das Wurzel- und Hypokotylwachstum bei Arabidopsis beziehungsweise Mais fördert (Kutschmar et al., 2009; Stührwohldt et al., 2011). Dieser Effekt war jeweils auf eine PSK-vermittelte Steigerung der Zellexpansion zurückzuführen.

Matsubayashi et al. (1996) isolierten aus dem konditionierten Medium von Spargel-Mesophyllzellen neben PSK auch eine C-terminal verkürzte Form, das disulfatierte Tetrapeptid PSK-β mit der Aminosäuresequenz Tyr(SO_3H)-Ile-Tyr(SO_3H)-Thr. Vermutlich stellt PSK-β ein Abbauprodukt von PSK dar, es besitzt weniger als 10% der mitogenen Aktivität von PSK (Matsubayashi et al., 1996; Matsubayashi und Sakagami 1996). Die Analyse weiterer PSK-Analoga zeigte, dass für die mitogene Aktivität von PSK die Sulfatierung von Tyr^1 und Tyr^2 unentbehrlich ist. Das komplett unsulfatierte Peptid zeigte eine Aktivität von weniger als 0,1% (Matsubayashi et al., 1996). Die Beseitigung der Sulfatierung an jeweils einem der beiden Tyrosine resultierte in einer mitogenen Aktivität von 0,6% (Tyr^1) und 4% (Tyr^2) (Matsubayashi et al., 1996). Das N-terminale disulfatierte Tripeptid stellt den aktiven Kern von PSK dar (Yamakawa et al., 1998; Yang et al., 2000).

PSK wird aus höhermolekularen etwa 80 Aminosäuren langen Präproproteinen (Abbildung 3B) gebildet und durchläuft wie PSY1 und die RGFs post-translationale Modifikationen und proteolytische Prozessierungen (Yang et al., 2000). Die Sulfatierung der beiden Tyrosine von PSK, katalysiert durch die TPST, ist essentiell für die biologische Aktivität des Peptids. Lorbiecke und Sauter (2002) konnten zeigen, dass das PSK durch die Sulfatierung stark hydrophil wird. Die erste Struktur eines 89 Aminosäuren langen PSK-Präproproteins, die aufgeklärt werden konnte, war aus Reis (Yang et al., 1999) und ist in Abbildung 3B gezeigt. OsPSK weist ein

hydrophobes Signalpeptid am N-Terminus auf, die PSK-Sequenz befindet sich nahe dem C-Terminus (Yang et al., 1999). Die für PSK-Präproproteine kodierenden Gene sind redundant über das Genom verteilt und wurden nach der Identifizierung in Reis auch in anderen Pflanzenarten gefunden (Yang et al., 1999; Yang et al., 2001; Lorbiecke und Sauter, 2002). In Arabidopsis kodieren fünf paraloge Gene für PSK-Präproproteine, welche in Kallusgewebe, Blättern, Wurzeln und Stängeln exprimiert werden (Matsubayashi et al., 2006). Neben der hochkonservierten PSK-Sequenz sind Regionen mit zahlreichen sauren und basischen Aminosäuren in der Mitte sowie am C-terminalen Ende charakteristisch für PSK-Präproproteine (Lorbiecke und Sauter, 2002; Abbildung 3B). Darüber hinaus wurden im Bereich der PSK-Sequenz weitere konservierte Aminosäuren identifiziert. Invariante Aminosäuren spiegeln sich in der als Signaturmotiv bezeichneten Konsensus-Sequenz $Cx_{(4-9)}$[E/D/Q]x$Cx_{(2)}RRx_{(3-4)}$AH[T/LA/]DYIYTQ wider, wobei variable Aminosäuren mit einem „x“ gekennzeichnet sind. Die PSK-Präproproteine weisen 8-10 Aminosäuren vor der PSK-Sequenz di-basische Reste auf, welche charakteristisch für Substratbindungsstellen von Subtilisin-ähnlichen Serin-Proteasen sind (Barr, 1991). Das Arabidopsis-Genom enthält 56 Gene, die für Subtilasen kodieren (Rautengarten et al., 2005). Srivastava et al. (2008) zeigten, dass in Arabidopsis die Subtilisin Serin-Protease AtSBT1.1 für die initiale proteolytische Prozessierung des Präproproteins PSK4 verantwortlich ist. Für andere Präproproteine konnte die proteolytische Spaltung noch nicht gezeigt werden. Die Prozessierungsstelle liegt N-terminal der PSK-Sequenz. Dies deutet darauf hin, dass die di-basischen Reste die initialen Prozessierungsstellen darstellen aber nicht in jedem Fall die Grenzen des reifen Peptids definieren. Es ist denkbar, dass in Pflanzen die proteolytische Prozessierung eine Reihe komplexer Schritte, wie beispielsweise das initiale Schneiden gefolgt von einem weiteren Verkürzen der Peptide, beinhaltet.

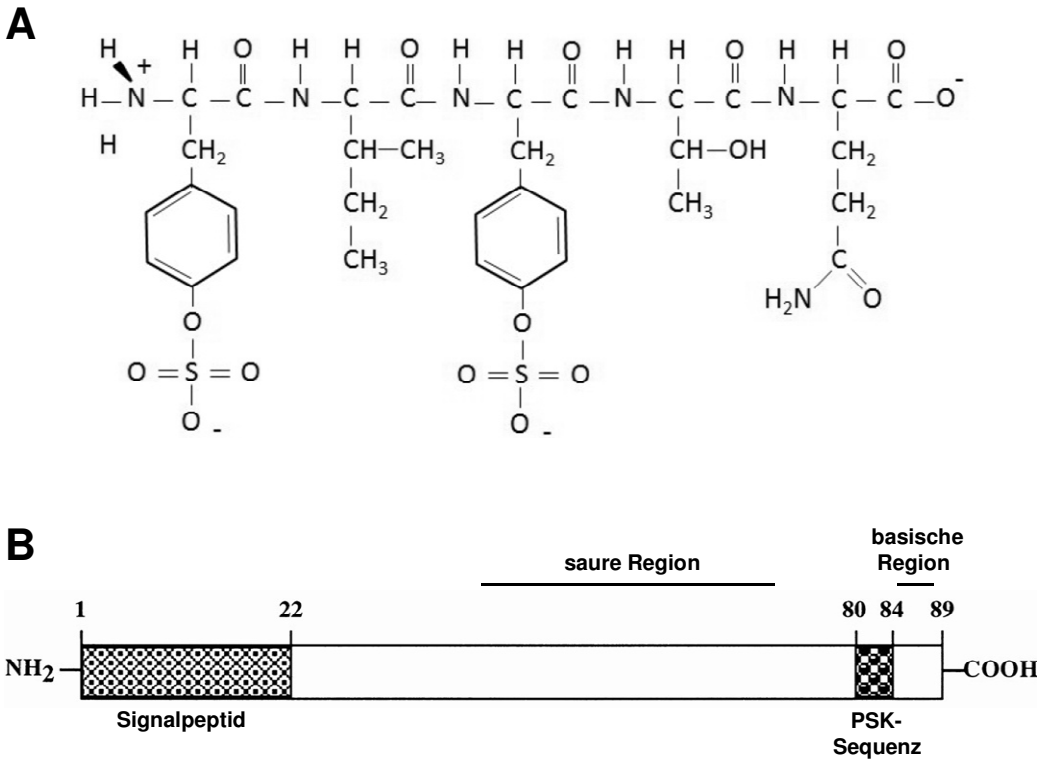

Abbildung 3: Strukturformel von PSK und schematische Darstellung des PSK-Präproproteins aus *Oryza sativa*. (A) Strukturformel des Pentapeptids PSK (Tyr(SO_3H)-Ile-Tyr(SO_3H)-Thr-Gln. Die lineare Darstellung zeigt die Aminosäuren des Peptids mit den beiden sulfatierten Tyrosin-Resten. (B) Schematische Darstellung des PSK-Präproproteins aus *Oryza sativa* (verändert nach Yang et al., 2000). Das PSK-Präproprotein aus Reis ist 89 Aminosäuren lang und weist ein 22 Aminosäuren langes hydrophobes Signalpeptid am N-Terminus auf. Die konservierte PSK-Sequenz befindet sich nahe dem C-Terminus. In der Mitte des Präproproteins befindet sich eine „saure Region" mit zahlreichen sauren Aminosäuren und am C-Terminus lassen sich vermehrt basische Aminosäuren in einer „basischen Region" finden (Lorbiecke und Sauter, 2002).

PSY1 konnte durch eine umfassende Analyse von Tyrosin-sulfatierten Peptiden in dem Medium einer Arabidopsis-Suspensionskultur identifiziert werden. PSY1 ist ein 18 Aminosäuren langes sekretiertes Glykopeptid, welches einen sulfatierten Tyrosin-Rest aufweist und aus einem 75 Aminosäuren langen Vorläuferpeptid proteolytisch freigesetzt wird (Amano et al., 2007). Zusätzlich zur Tyrosin-Sulfatierung weist PSY1 eine Prolin-Hydroxylierung und eine Hydroxyprolin-Arabinosylierung auf. Es konnte gezeigt werden, dass eine fehlende Sulfatierung des Tyrosins und eine fehlende Glykosylierung zu einem Verlust der PSY1-Aktivität führen (Amano et al., 2007). Das Expressionsmuster und die physiologische Aktivität von PSY1 und PSK sind ähnlich. Die beiden strukturell verschiedenen Tyrosin-sulfatierten Peptide PSY1 und PSK wirken während des Wachstums und der Entwicklung von Arabidopsis redundant an

der Zellproliferation, Zellexpansion und Wundheilung mit (Amano et al., 2007). PSY1 ist bereits in nanomolaren Konzentrationen wirksam und wird in verschiedenen Geweben von Arabidopsis exprimiert. Die Expression im SAM und in der Streckungszone der Wurzel ist am stärksten. Die Zugabe von PSK und PSY1 zu *tpst-1* Keimlingen förderte die Zellelongation wohingegen die meristematische Aktivität nicht wiederhergestellt wurde (Matsuzaki et al., 2010). Dies deutete darauf hin, dass andere Tyrosin-sulfatierte Peptide als PSK und PSY1 in der Aufrechterhaltung von Wurzel-Stammzellen und in der Regulation der meristematischen Aktivität involviert sind.

Über eine *in silico* Suche nach Genen, welche für sulfatierte Peptide kodieren, und durch die Verwendung synthetischer sulfatierter Peptide konnte RGF1 als ein Faktor identifiziert werden, welcher in der Aufrechterhaltung der Wurzel-Stammzellnische beteiligt ist (Matsuzaki et al., 2010). Die Zugabe von PSK, PSY1 und RGF1 zu *tpst-1* Keimlingen restaurierte vollständig den Wurzel-Phänotyp. RGF1 gehört zu der Familie von RGFs, welche funktionell redundante sulfatierte Peptide darstellen. In Arabidopsis gibt es insgesamt neun Gene, die für RGFs kodieren. Über eine post-translationale Tyrosin-Sulfatierung und proteolytische Prozessierung werden die 13 Aminosäuren langen RGFs aus etwa 100 Aminosäuren langen Vorläuferpeptiden gebildet. RGFs werden hauptsächlich in der Stammzellregion und der innersten Schicht der zentralen Columella-Zellen exprimiert und diffundieren durch den Apoplast in die meristematische Zone (Matsuzaki et al., 2010). RGFs regulieren das Wurzelwachstum, indem sie *PLETHORA* (PLT) Transkriptionsfaktoren stabilisieren. PLTs werden spezifisch im Wurzelmeristem exprimiert und für dessen Aufrechterhaltung benötigt (Aida et al., 2004; Galinha et al., 2007). Unabhängig davon konnte gezeigt werden, dass die Expression von PLT sowie die Lokalisation von Biosynthese- und Transporterproteinen des Phytohormons Auxin von AtTPST abhängt, möglicherweise weil dieses RGF1 sulfatiert (Zhou et al., 2010).

Die PSK Rezeptoren gehören zu der Unterfamilie der Rezeptorkinasen mit Leuzin-reichen Wiederholungssequenzen

Die Rezeptoren für Peptide mit Signalwirkung lassen sich in die Familien der Rezeptorkinasen (RK) und der Rezeptor-ähnlichen Kinasen (RLK) einteilen (Shiu und Bleecker, 2001). In Arabidopsis gibt es über 600 putative RLKs, wovon mehr als 66% transmembrane oder Membran-assoziierte Kinasen sind (Shiu und Bleecker, 2001, 2003; Torii, 2004). Die biologische Funktion der RLKs kann nach Shiu et al. (2004) in zwei Kategorien eingeteilt werden: Die erste Kategorie enthält Rezeptoren, die das Wachstum und die Entwicklung steuern. In Arabidopsis gehören hierzu beispielsweise: ERECTA, welches an der Form-Festlegung von Organen, die vom SAM abstammen, beteiligt ist (Torii et al., 1996), CLV1, der für die Aufrechterhaltung des Sprossmeristems verantwortlich ist (Clark et al., 1997) und *BRASSINOSTEROID INSENSITIVE 1* (BRI1), ein Regulator von Zellteilung, -wachstum und -differenzierung (Li und Chory, 1997; Clouse, 2011). Zu der zweiten Kategorie gehören RLKs, welche in die Interaktion zwischen Pflanze und Mikroorganismen sowie in Abwehrmechanismen involviert sind. Beispielsweise ist der *SYSTEMIN CELL-SURFACE RECEPTOR 160* (SR160) in der Tomate an der Systemin-Signalweiterleitung beteiligt (Scheer und Ryan, 2002), Xa21 vermittelt beim Reis Resistenz gegenüber Bakterien (Song et al., 1995) und *FLAGELLIN INSENSITIVE 2* (FLS2) stellt in Arabidopsis den Rezeptor für den bakteriellen Elicitor Flagellin dar (Gomez-Gomez und Boller, 2000). Für einen der beiden PSK-Rezeptoren, PSKR1 (Abbildung 4), konnte eine Beteiligung sowohl an der Kontrolle der Zellproliferation und der Zellexpansion, als auch an der Antwort gegenüber Pathogenen gezeigt werden (Matsubayashi et al., 2002, 2006; Kutschmar et al., 2009; Stührwohldt et al., 2011; Igarashi et al., 2012; Mosher et al., 2013; Shen und Diener, 2013).

Innerhalb der Familie der RKs bilden die Rezeptoren mit Leuzin-reichen Wiederholungssequenzen (LRR-RK) die größte Unterfamilie, welche in Arabidopsis aus über 200 Mitgliedern besteht (Yin et al., 2002; Dievart und Clark, 2003; Shiu et al., 2004). Die meisten Rezeptoren, welche kleine post-translational modifizierte Peptide binden, gehören zu dieser Unterfamilie. Die LRR-RKs werden aufgrund ihrer Ähnlichkeit innerhalb der cytoplasmatischen Kinasedomäne in 13 Untergruppen eingeteilt (Shiu und Bleecker, 2001). PSKR1 und CLV1 gehören zu der Untergruppe LRR X beziehungsweise LRR XI. RLKs können darüber hinaus auch anhand

konservierter Aminosäuren innerhalb der Kinasedomäne klassifiziert werden (Krupa et al., 2004). Die meisten RLKs weisen ein konserviertes Arginin (R) und ein invariantes Aspartat (D) in der Subdomäne VI vor der sogenannten Aktivierungsschleife auf. Bei manchen RLKs fehlt nach Dardick und Ronald (2006) das konservierte Arginin ("*non-RD kinases*") wohingegen bei wenigen die beiden konservierten Aminosäuren nicht zu finden sind ("*RD-minus kinases*"). Die Aktivierungsschleife dient als Kinase-Aktivator, indem sie die Effizienz des Phosphotransfers erhöht (Adams, 2003). Viele RD-Kinasen sind an der Regulation von Wachstum und Entwicklung beteiligt, wohingegen "*non-RD kinases*" mit Abwehrmechanismen in Verbindung gebracht werden (Dardick und Ronald, 2006). Vertreter der "*RD-minus kinases*" stellen beispielsweise die RLKs LePRK1 und LePRK2 aus der Tomate dar, welche an der Interaktion zwischen Pollen und Stempel beteiligt sind (Muschietti et al., 1998).

Proteine, welche Tritium- oder 35S-markiertes PSK binden, wurden zum ersten Mal in der mikrosomalen Fraktion von Reiszellen nachgewiesen (Matsubayashi et al., 1997; Matsubayashi und Sakagami, 1999). Darüber hinaus konnten Matsubayashi und Sakagami (2000) beim Reis 120 kDa und 160 kDa große Glykoproteine identifizieren, welche Tritium-markiertes PSK banden. Ein PSK-bindendes Rezeptorprotein wurde durch eine Solubilisierung mittels eines Detergens und anschließender Affinitätschromatographie mit einer PSK-Sepharose Säule aus mikrosomalen Fraktionen der Karotte aufgereinigt (Matsubayashi et al., 2002). Das identifizierte Protein stellte sich als 1021 Aminosäuren lange RK mit zahlreichen LRRs in der extrazellulären Domäne, einer einzelnen transmembranen Domäne und einer cytoplasmatischen Kinasedomäne heraus. Eine Überexpression dieser identifizierten RK in Karottenzellen bewirkte nach PSK-Applikation ein gesteigertes Kalluswachstum und eine erhebliche Zunahme an Bindungsstellen für Tritium-markiertes PSK (Matsubayashi et al., 2002). Dies ließ den Schluss zu, dass dieses als DcPSKR1 bezeichnete PSK-Rezeptorprotein und PSK als Rezeptor-Ligand Paar fungieren (Matsubayashi et al., 2002). Die entsprechende Bindungsstelle für den Liganden PSK wurde in DcPSKR1 über Deletionsstudien in der extrazellulären Region zwischen Glu^{503} und Lys^{517} innerhalb der von LRRs umgebenen sogenannten Inseldomäne identifiziert (Shinohara et al., 2007). In dieser Studie konnte gezeigt werden, dass die Inseldomäne von DcPSKR1 eine Bindungstasche bildet, welche

direkt mit PSK interagiert. Der PSK-Rezeptor aus der Karotte zeigt auf der Aminosäureebene eine hohe Übereinstimmung mit einer LRR-RK aus Arabidopsis. AtPSKR1 ist das entsprechende Orthologe von DcPSKR1 und kodiert für eine LRR-RK bestehend aus 1008 Aminosäuren, die zu 60% identisch zu DcPSKR1 sind (Matsubayashi et al., 2006). Das 150 kDa große AtPSKR1-Protein besteht aus einem N-terminalen Signalpeptid, insgesamt 21 hintereinander angeordneten extrazellulären LRRs, der zwischen der 17. und 18. LRR lokalisierten 36 Aminosäuren langen Inseldomäne, einer einzelnen transmembranen Domäne und einer cytoplasmatischen Serin/Threonin Kinasedomäne (Matsubayashi et al., 2006; Abbildung 4).

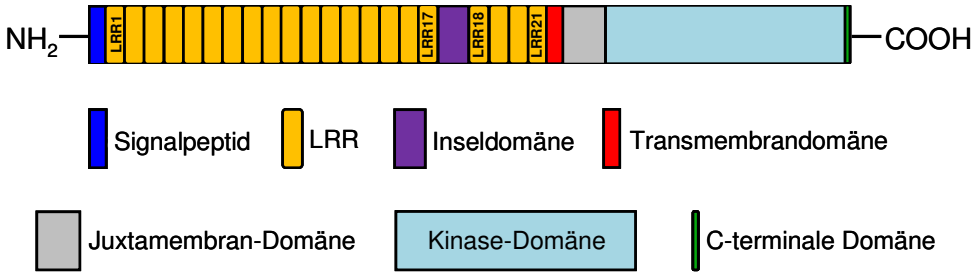

Abbildung 4: Schematische Darstellung der Rezeptorkinase AtPSKR1 mit Leuzin-reichen Wiederholungssequenzen (LRRs) aus Arabidopsis. Der Rezeptor für PSK gehört zu der Unterfamilie der LRR Rezeptorkinasen (LRR-RK). AtPSKR1 besteht aus einem N-terminalen Signalpeptid, einem extrazellulären Bereich mit insgesamt 21 LRRs, einer Transmembrandomäne und einer cytoplasmatischen Juxtamembran-, Kinase-, und C-terminalen Domäne. Zwischen der 17. und 18. LRR befindet sich die PSK-bindende Inseldomäne.

Die LRRs von AtPSKR1 werden flankiert von Cystein-reichen Domänen, wobei jede Domäne 2 Cystein-Reste enthält. Diese Cystein-Reste können an der Bildung von intra- und intermolekularen Disulfidbrücken beteiligt sein (Trotochaud et al., 1999; Dievart und Clark, 2003). Trotochaud et al. (1999) zeigten, dass die gepaarten Cystein-Reste an der Heterodimerisierung von CLV1 und CLV2 mitwirken. Die Aminosäuresequenzen der Inseldomäne sind zwischen DcPSKR1 und AtPSKR1 hoch konserviert. Eine in die Bindung des Liganden involvierte Inseldomäne konnte auch innerhalb der extrazellulären LRRs des Brassinosteroid-Rezeptors BRI1 identifiziert werden (Kinoshita et al., 2005). AtPSKR1 gehört, wie auch BRI1, *BRI1-LIKE 1* (BRL1), BRL2 und BRL3, zu der LRR-RKs Untergruppe LRR X (Shiu und

Bleecker, 2001; Caño-Delgado et al., 2004). Es konnte gezeigt werden, dass AtPSKR1 in Kallusgewebe, Blättern, Stängeln, Blüten und am stärksten in der Wurzelspitze exprimiert wird (Matsubayashi et al., 2006; Kutschmar et al., 2009). Keimlinge einer AtPSKR1 *Knockout* Mutante (*pskr1-1*) zeigten ein im Vergleich zum Wildtyp reduziertes Wurzelwachstum und bei *pskr1-1* Kalli setzte eine verfrühte Seneszenz bereits nach drei Wochen ein (Matsubayashi et al., 2006). Diese verfrühte Seneszenz konnte auch bei vier Wochen alten *pskr1-1* Pflanzen beobachtet werden. Bei einer Überexpression von AtPSKR1 (*AtPSKR1ox*) zeigten *AtPSKR1ox* Kalli und Pflanzen eine verzögerte Seneszenz.

Im Genom von Arabidopsis gibt es zwei homologe Gene zu *AtPSKR1*: *AtPSKR2* (At5g53890) und *AtPSY1R* (At1g72300). Beide Gene kodieren für LRR-RLKs, welche 48,6% beziehungsweise 43,6% Sequenzidentität mit AtPSKR1 aufweisen. Beide Gene enthalten kein Intron. Ihre Genprodukte weisen mit 1036 Aminosäuren für AtPSKR2 und 1095 Aminosäuren für AtPSY1R eine im Vergleich zu AtPSKR1 ähnliche Größe auf und besitzen extrazelluläre LRRs. Die Inseldomänen von AtPSKR2 und AtPSY1R sind 39 beziehungsweise 38 Aminosäuren lang, wobei es keine Ähnlichkeit zwischen AtPSKR1, AtPSKR2 und AtPSY1R gibt. AtPSKR2 interagiert mit PSK und ist an der Perzeption des Liganden beteiligt, zeigt aber im Vergleich zu AtPSKR1 eine geringere Aktivität (Amano et al., 2007). Keimlinge einer AtPSKR2 *Knockout* Mutante (*pskr2-1*) zeigten einen im Vergleich zu *pskr1-1* weniger stark ausgeprägten Wurzelphänotyp (Amano et al., 2007). AtPSY1R ist der Rezeptor des Tyrosin-sulfatierten Glykopeptids PSY1, perzipiert aber kein PSK. AtPSKR1 und AtPSKR2, aber nicht AtPSY1R, haben einen teilweise redundanten Effekt bei der Immunabwehr in Arabidopsis (Mosher et al., 2013). Die *pskr1/pskr2/psy1r* Dreifach-*Knockout* Mutante zeigte wie die *tpst-1 Knockout* Mutante eine erhöhte Resistenz gegenüber einer bakteriellen Infektion und gleichzeitig eine gesteigerte Anfälligkeit gegenüber einer Infektion mit *Alternaria brassicicola*. Eine PSK-Applikation bei der *tpst-1* Mutante bewirkte teilweise eine Restaurierung der mit der Pathogenabwehr verbundenen Phänotypen. Dies deutet auf einen direkten PSK-vermittelten Effekt bei der Abwehr bestimmter Pathogene hin (Mosher et al., 2013). Diese gesteigerte Anfälligkeit gegenüber bestimmten Pathogenen, welche über den Signalweg Tyrosin-sulfatierter Peptide vermittelt wird, konnten auch Shen und Diener (2013) durch eine Analyse von *pskr1*, *pskr2* und *psy1r Knockout* Mutanten bestätigen.

Brassinosteroide (BRs) zeigen, wie das disulfatierte Pentapeptid PSK, bei der Zellexpansion und darüber hinaus bei vielen Entwicklungs- und Wachstumsprozessen bedeutende Effekte (Clouse, 2011). In Arabidopsis werden BRs von den LRR-RLKs BRI1 und dessen Homologen BRL1 und BRL3 perzipiert (Li und Chory, 1997; Caño-Delgado et al., 2004). BRI1 weist insgesamt 25 extrazelluläre LRRs in Form einer Superhelix auf. Zwischen der 21. und 22. LRR befindet sich eine 70 Aminosäuren lange Inseldomäne, welche die BR-Bindungsstelle bildet (Kobe und Kajava, 2001; Hothorn et al., 2011; She et al., 2011). Es besteht eine hohe strukturelle Ähnlichkeit zwischen BRI1 und den PSK-Rezeptoren.

In Abwesenheit von BRs verhindert der negative Regulator *BRI1 KINASE INHIBITOR 1* (BKI1) eine Zusammenlagerung von BRI1 mit seinem Korezeptor *BRI1-ASSOCIATED RECEPTOR KINASE 1* (BAK1) und unterbindet dadurch die BRI1-Aktivität (Wang und Chory, 2006; Jaillais et al., 2011). In diesem Zustand ist die *BRASSINOSTEROID-INSENSITIVE 2* (BIN2), eine *GLYCOGEN SYNTHASE KINASE 3* (GSK3)/Shaggy-ähnliche Proteinkinase aktiv. Diese phosphoryliert die beiden Transkriptionsfaktoren *BRASSINAZOLE RESISTANT 1* (BZR1) und *BRI1 EMS SUPPRESSOR 1* (BES1) (Gampala et al., 2007). Dies führt zu einem Proteasomen-vermittelten Abbau der beiden Transkriptionsfaktoren beziehungsweise zu einem Zurückhalten von BZR1 und BES1 im Cytoplasma, wobei an diesem Prozess 14-3-3 Proteine beteiligt sind.

Nach der BR-Perzeption interagiert BRI1 mit BAK1 und durch sequenzielle Transphosphorylierungen aktivieren sich die beiden Rezeptoren gegenseitig (Wang et al., 2008). Im Anschluss aktiviert BRI1 durch Phosphorylierungen die *BR SIGNALING KINASES* BSK1, BSK2 und BSK3. Diese wiederum binden an die Protein-Phosphatase *BRI1 SUPPRESSOR 1* (BSU1), wodurch diese aktiviert wird (Tang et al., 2008). Über eine katalysierte Dephosphorylierung fungiert BSU1 als BIN2-Inhibitor und gleichzeitig werden die Transkriptionsfaktoren BES1 und BZR1 durch die PROTEIN PHOSPHATASE 2A (PP2A) dephosphoryliert (Mora-Garcia et al., 2004; Tang et al., 2011). Dadurch kommt es zu einer Anreicherung der aktiven Formen von BES1 und BZR1 im Zellkern, welche dort an die genomische DNA binden und die Expression von Zielgenen regulieren (He et al., 2005; Yin et al., 2005; Sun et al., 2010; Yu et al., 2011). Es konnte gezeigt werden, dass BRI1 außer BAK1

zahlreiche andere Substrate wie beispielsweise eine Protonen-ATPase (P-ATPase, AHA1) und die LRR-RLKs *BAK1-LIKE KINASE* (BKK), BAK7, *SOMATIC EMBRYOGENESIS RECEPTOR-LIKE KINASE 4* (SERK4) und SERK1 phosphoryliert (Caesar et al., 2011; Witthöft et al., 2011; Albrecht et al., 2008). Die direkte Interaktion zwischen BRI1 und der P-ATPase vermittelt eine schnelle, BR-induzierte Hyperpolarisation der Plasmamembran und eine Expansion der Zellwand (Caesar et al., 2011).

Zahlreiche unabhängige genetische Studien haben in Arabidopsis insgesamt über zwei Dutzend *bri1* Mutanten-Allele identifiziert, von denen die meisten einen extremen Zwergenwuchs-Phänotyp, eine veränderte Blattmorphologie, eine unnormale Entwicklung des Leitgewebes, eine verzögerte Blüte und Seneszenz sowie eine reduzierte männliche Fertilität zeigten (Clouse et al., 1996; Kauschmann et al., 1996; Li und Chory, 1997; Noguchi et al., 1999; Friedrichsen et al., 2000). Der Zwergenwuchs-Phänotyp der *bri1* Allele lässt sich auf eine verminderte Zellelongation und Zellteilung in Wurzeln, Sprossen und Blättern zurückführen (Gonzalez et al., 2010; González-García et al., 2011). BR-insensitive Mutanten konnten auch in anderen Pflanzenarten wie *Solanum lycopersicum* (Koka et al., 2000; Montoya et al., 2002), *Oryza sativa* (Yamamuro et al., 2000), *Hordeum vulgare* (Chono et al., 2003), *Gossypium hirsutum* (Sun et al., 2004), *Pisum sativum* (Nomura et al., 2003) und *Glycine max* (Wang et al., 2014) gefunden werden. Die meisten Mutationen der *bri1* Allele liegen gehäuft in der extrazellulären BRI1-Inseldomäne oder innerhalb der cytoplasmatischen Kinasedomäne. Dies deutet auf die essentielle Rolle der Liganden-Bindung und der Kinaseaktivität für die Funktion von BRI1 hin. Es konnte gezeigt werden, dass eine Überexpression von BAK1 den Phänotyp eines schwachen *bri1* Allels unterdrückt (Li et al., 2002; Nam und Li, 2004). Die *bak1 Knockout* Mutante ähnelte phänotypisch der schwachen *bri1* Mutante und die Überexpression einer Kinase-inaktiven BAK1-Variante rief einen starken Zwergenwuchs-Phänotyp hervor, der dem eines starken *bri1* Allels ähnlich war (Li et al., 2002). Li et al. (2002) führten dies auf einen sogenannten dominant-negativen Effekt der Kinase-inaktiven BAK1-Variante zurück. Genetische Studien mit *Knockout* Mutanten von BAK1, SERK3 und SERK4 bestätigten deren essentielle Rollen im BR-Signalweg und darüber hinaus auch in anderen Signalwegen (He et al., 2007; Albrecht et al., 2008). BAK1 fungiert auch als Korezeptor für einige Liganden-

bindende RLKs, welche in Abwehrmechanismen gegen Pathogene involviert sind (Chinchilla et al., 2007; Li, 2010). Die Beteiligung von BAK1 an verschiedenen Signalwegen vermittelt vermutlich deren gegenseitige Abstimmung zwischen Wachstum und Abwehrmechanismen (Albrecht et al., 2012; Belkhadir et al., 2012; Wang, 2012).

Das Ca^{2+}-bindende Sensorprotein Calmodulin (CaM) interagiert mit der CaM-Bindungsdomäne von Zielproteinen

In Pflanzen stellt Kalzium ein wichtiges Signalmolekül dar, wobei die Kalzium-vermittelte Signalübertragung bereits gut untersucht ist (McAinsh und Pittman, 2009; Clapham, 2007). Für Kalzium wurde eine Beteiligung an den Signalwegen für Auxin (Yang und Poovaiah, 2000), Gibberellinsäure (Chen et al., 1997), Cytokinin (Hahm und Saunders, 1991) sowie BRs (Du und Poovaiah, 2005; Oh et al., 2012; Zhao et al., 2013) gezeigt. Verschiedene biotische und abiotische Reize lösen in der Zelle durch die Aktivität von Membrankanälen und Transportern Kalziumsignale unterschiedlicher Stärke und Länge aus (Reddy, 2001; Bouché et al., 2005; Hepler, 2005; McAinsh und Pittman, 2009; DeFalco et al., 2010). Die veränderten Kalziumkonzentrationen werden von Proteinen, welche als Kalziumsensoren fungieren, erfasst und in Reaktionen umgewandelt (Day et al., 2002; Reddy und Reddy, 2004; Boonburapong und Buaboocha, 2007). Die Mehrzahl der Kalziumsensoren stellen Proteine dar, welche konservierte Kalzium-bindende *Helix-Loop-Helix*-Motive besitzen, die auch als EF-Hände bezeichnet werden (Day et al., 2002). Nach Day et al. (2002) gibt es in Arabidopsis etwa 250 putative Kalziumsensoren, die EF-Hände aufweisen. Calmoduline (CaMs), CaM-ähnliche Proteine (CMLs) und Calcineurin B-ähnliche Proteine (CBLs) gehören zu der Gruppe von Kalziumsensoren, die keine enzymatische Aktivität oder andere funktionale Domänen besitzen (McCormack et al., 2005; Luan, 2009; DeFalco et al., 2010). Diese Kalziumsensoren interagieren nach der Kalziumbindung mit Zielproteinen und regulieren dadurch deren Aktivitäten. In Arabidopsis werden insgesamt vier CaM-Isoformen durch sieben Gene, *CaM1*/*CaM4*, *CaM2*/*CaM3*/*CaM5*, *CaM6* und *CaM7*, kodiert (DeFalco et al., 2010). Außerdem kodieren in Arabidopsis 50 Gene für CMLs (McCormack und Braam, 2003). Es konnten in Pflanzen über 300 Proteine identifiziert werden, die mit CaMs und CMLs interagieren (Zhang und Lu, 2003; Bouché et al., 2005; Popescu et al., 2007). CaM Proteine zeigen eine differenzielle

Expression und verschiedene Affinitäten gegenüber Kalzium und ihren Zielproteinen (Reddy et al., 1999; McCormack et al., 2005; Popescu et al., 2007). CaMs sind auf der Aminosäureebene hoch konserviert. Sie bestehen aus zwei globulären Domänen, welche jeweils zwei EF-Hände aufweisen (Chin und Means, 2000). Jede EF-Hand bindet ein Kalziumion, so dass pro CaM insgesamt vier Kalziumionen gebunden werden können (Vogel, 1994; Crouch und Klee, 1980). Nach der Kalziumbindung werden nach innen gekehrte, hydrophobe Seitenketten von Aminosäuren der globulären Domänen des CaM nach außen gekehrt (Zhang et al., 1995; Ikura et al., 1992). Dies erlaubt die Interaktion der CaMs mit Zielproteinen, wobei die nach außen gekehrten hydrophoben Seitenketten die CaM-Bindungsdomäne (CaMBD) des jeweiligen Zielproteins umschließen. CaMBDs sind in der Regel 14 bis 26 Aminosäuren lang und neigen dazu, eine amphipathische α-Helix auszubilden (O'Neil und DeGrado, 1990; Rhoads und Friedberg, 1997; Ishida und Vogel, 2006; Rainaldi et al., 2007). Deren hydrophobe Seite bindet CaMs. Die Bedeutung hydrophober sogenannter Anker-Aminosäuren für die CaM-Bindung an die Zielproteine *MYOSIN LIGHT CHAIN KINASE* (MLCK), *CaM-DEPENDENT PROTEIN KINASE IIα* (CaMKII) und NtMKP1 wurde gezeigt (Ikura et al., 1992; Meador et al., 1992, 1993; Yamakawa et al., 2004). Diese Anker-Aminosäuren befanden sich jeweils in der Nähe des N- beziehungsweise C-Terminus der CaMBDs der Zielproteine. Kataoka et al. (1991) wiesen nach, dass verkürzte Peptide der CaMBD einer Ca^{2+}-ATPase humaner Erythrozyten, bei denen eine der endständigen hydrophoben Anker-Aminosäuren fehlte, eine reduzierte CaM-Bindung aufwiesen. Die hydrophobe Aminosäure Tryptophan (Trp) befindet sich häufig am N-Terminus von CaMBDs. Für das Trp wurde gezeigt, dass es stärker mit der C-terminalen Domäne des CaM interagiert (Ikura et al., 1992; Meador et al., 1993; Yamauchi et al., 2003). Dadurch wird die relative Orientierung des Zielproteins innerhalb des Kanals, welcher von den globulären Domänen des CaM gebildet wird, festgelegt. Nach Goldberg et al. (1996) ist die aromatische Seitenkette des N-terminalen Trp der CaMBD von CaMKI nach außen gerichtet. Masayuki und Nairn (1998) zeigten, dass der Austausch dieses Trp von CaMKI gegen ein hydrophiles Serin in einer signifikanten Reduzierung der CaM-Bindung an das Zielprotein resultierte. Nach Masayuki und Nairn (1998) stellt das Trp die primäre Stelle für eine CaM-Bindung an CaMKI dar.

Zielsetzung dieser Arbeit

Im Rahmen dieser Arbeit sollte der PSK Rezeptor PSKR1 aus *Arabidopsis thaliana* funktional analysiert werden. Ein Ziel war es, zu klären, ob die Menge an verfügbaren PSK-Rezeptoren das PSK-vermittelte Wachstum begrenzt. Darüber hinaus sollte untersucht werden, in welchem Gewebe PSK *in planta* wachstumsfördernd wirkt. Um die Regulation von PSKR1 zu analysieren, sollten zum einen Phosphorylierungsstellen des Rezeptors kartiert und exemplarisch über eine gerichtete Mutagenese funktional untersucht werden. Zum anderen sollte eine vorhergesagte Calmodulin-Bindungsstelle von PSKR1 überprüft und auf ihre mögliche Bedeutung für die *in planta* Rezeptorfunktion aufgeklärt werden.

Kapitel 1

Phytosulfokine control of growth occurs in the epidermis, is likely to be non-cell autonomous and is dependent on brassinosteroids

Die in diesem Kapitel vorgestellten Arbeiten, mit Ausnahme der Expressionsanalyse von *CER6:GUS* Keimlingen, der Ausmessung von Trichoblasten- und Atrichoblasten-Zelllängen und der pharmakologischen und genetischen Ansätze zur Untersuchung einer BR-abhängigen PSK-Wachstumsförderung wurden im Rahmen dieser Promotionsarbeit von mir durchgeführt.

the plant journal

SEB Society for Experimental Biology

The Plant Journal (2013) **73,** 579–590 doi: 10.1111/tpj.12056

Phytosulfokine control of growth occurs in the epidermis, is likely to be non-cell autonomous and is dependent on brassinosteroids

Jens Hartmann, Nils Stührwohldt, Renate I. Dahlke and Margret Sauter*

Entwicklungsbiologie und Physiologie der Pflanzen, Am Botanischen Garten 5, Kiel 24113, Germany

Received 13 April 2012; revised 2 October 2012; accepted 17 October 2012; published online 10 December 2012.
*For correspondence (e-mail msauter@bot.uni-kiel.de)

SUMMARY

Phytosulfokine (PSK) is a secreted disulfated pentapeptide that controls root and shoot growth. The ubiquitous expression of PSK precursor and of the LRR receptor kinase genes in Arabidopsis raised the question of whether PSK acts as an autocrine growth factor *in planta*. Expression of *PSKR1* under the control of tissue- and cell type-specific promoters in a receptor null background strongly suggests that PSK is a non-cell autonomous signal that controls growth through localized activity in the epidermis. *pskr1–3 pskr2–1* seedlings had shorter roots and hypocotyls than the wild type, whereas *35S: PSKR1* or *35S: PSKR2* seedlings were larger, indicating that receptor abundance limits growth *in planta*. The preferential expression of *PSKR1* in the epidermis of *CER6: PSKR1 pskr1–3 pskr2–1* seedlings was sufficient to promote wild-type growth. Moreover, in *GL2:PSKR1 pskr1–3 pskr2–1* seedlings that express *PSKR1* in atrichoblasts of the root epidermis, root growth was restored to wild-type levels. In *pskr1–3 pskr2–1* seedlings, trichoblasts and atrichoblasts were shorter than in the wild type. Trichoblasts of *GL2:PSKR1 pskr1–3 pskr2–1* seedlings, which are unable to sense PSK, nonetheless had acquired wild-type length, suggesting that PSK acts as a non-cell autonomous signal. Inhibition of brassinosteroid (BR) biosynthesis with brassinazole (BZ) caused a loss of responsiveness to PSK in wild-type, *tpst–1* (*tyrosylprotein sulfotransferase–1*), *PSKR1ox12* and *CER6:PSKR1 –3–1* seedlings, as did the genetic knock-out of BR synthesis in *det2–1* and of BR perception in *bri1–9*, suggesting that BR mediates PSK-dependent growth. Quantitative PCR analysis of BR-related genes in wild-type, *pskr1–3 pskr2–1*, *PSKR1ox* and *tpst–1* seedlings showed largely unchanged transcript levels of BR biosynthesis genes.

Keywords: *Arabidopsis thaliana*, brassinosteroid, elongation, epidermis, peptide growth factor, phytosulfokine.

INTRODUCTION

Multicellular plants grow and develop as an integrated unit with individual plant cells being glued together through their walls, rendering them immotile. Growth and development are therefore dependent on the coordinated proliferation and expansion of individual cells, and rely on cell–cell communication mediated by both chemical and mechanical signals. The autocrine growth factor phytosulfokine (PSK) is a 5–amino acid disulfated peptide of the sequence Tyr(SO_3H)-Ile-Tyr(SO_3H)-Thr-Gln. PSK is produced from preproproteins encoded by five genes in *Arabidopsis thaliana* that are expressed throughout the plant life cycle, suggesting that PSK plays a ubiquitous role in plant growth and development (Matsubayashi *et al.*, 1996; Yang *et al.*, 2000; Yang *et al.*, 2001; Lorbiecke and Sauter, 2002; Stührwohldt *et al.*, 2011). Post-translational sulfation of the PSK precursor proteins is required for peptide activity, and is catalyzed by the enzyme tyrosylprotein sulfotransferase (TPST) in the *cis*-Golgi (Komori *et al.*, 2009). Post-translational proteolytic processing of the PSK4 proprotein from Arabidopsis was shown to be catalyzed by a subtilisin serine protease in the apoplast, but other proteases are predicted to exist (Srivastava *et al.*, 2008). The active PSK peptide binds to plasma membrane-localized leucine-rich repeat (LRR) receptor kinases that are conserved in *Daucus carota* ssp. *sativus* (carrot; Matsubayashi *et al.*, 2002) and Arabidopsis (Matsubayashi *et al.*, 2006). Two PSK receptor genes, *PSKR1* and *PSKR2*, were identified in Arabidopsis.

PSK was first identified as a signal that promotes the proliferation of cells kept at a low density in *in vitro* cell cultures of both dicot and monocot plants (Matsubayashi

et al., 1996; Matsubayashi *et al.*, 1997; Hanai *et al.*, 2000; Yang *et al.*, 2000). Carrot cells overexpressing the receptor kinase showed enhanced proliferation after application of PSK (Matsubayashi *et al.*, 2002). *In planta*, PSK signaling participates in the control of root and shoot growth. Root growth and hypocotyl elongation are promoted by PSK, mainly through the signaling of cell elongation rather than cell division (Matsubayashi *et al.*, 2006; Kutschmar *et al.*, 2009; Stührwohldt *et al.*, 2011). Seedlings of the T–DNA insertion knock-out lines *pskr1–2* and *pskr1–3* had shorter roots and shorter hypocotyls, whereas *pskr2–1* seedlings had slightly shorter roots but wild-type (wt) hypocotyl lengths, indicating that root elongation was predominantly, and hypocotyl elongation was solely, controlled through PSKR1, with PSKR2 contributing to seedling growth control only to a minor degree. *PSKR1* was shown to be expressed in roots, hypocotyl, leaves, stem and flowers, and expression of *PSKR2* in hypocotyl was also reported (Kutschmar *et al.*, 2009; Stührwohldt *et al.*, 2011). *PSKR1:GUS* analysis indicated that the *PSKR1* promoter was active in all cell layers in the growth region of the root. Expression of *PSKR1* in the hypocotyl was very weak, as indicated by *PSKR1:GUS* analysis, and was not specific to defined cell layers. Hence expression analysis did not clarify whether PSK is active in defined tissues.

In higher plants, the shoot meristem gives rise to all above-ground organs and has an organized pattern: the shoot epidermis is derived from the L1 layer, the photosynthesizing cells of the sub-epidermis are produced from the L2 layer and cells comprising the ground tissues descend from L3 (Stewart and Burk, 1970; Szymkowiak and Sussex, 1996; Marcotrigiano, 2001). As the cells of the different layers are immotile because of the connecting cell walls, they are forced to grow together in a coordinated manner. When the inner layers of a growing stem are separated from the outer epidermis they rapidly extend, whereas the epidermis contracts because the different layers are under differential tension (Peters and Tomos, 1996). It was hypothesized that the dividing, expanding or turgid thin-walled cells of the inner layers are the driving force for stem and hypocotyl growth, whereas the expansion-limiting thick-walled epidermal cell layer determines the rate of growth (Kutschera, 1992, 2008; Niklas and Paolillo, 1997; Kutschera and Niklas, 2007; Savaldi-Goldstein *et al.*, 2007). Furthermore, it was shown that the epidermis can compensate for defects in cell division through excessive epidermal cell expansion (Serralbo *et al.*, 2006; Bemis and Torii, 2007). Cell division in the inner layers was not controlled by the epidermis (Bemis and Torii, 2007), but suppressed epidermal cell division through L1-specific expression of the CDK inhibitor ICK1 was partially rescued by the inner layers, presumably via intercellular movement of cell cycle regulators (Serralbo *et al.*, 2006). Nonetheless, reduced epidermal cell division put mechanical constraints on the cell expansion of the inner layers, which was compensated for in the L2 by generating smaller cells. Taken together, current findings support the idea that the epidermis is the growth-limiting cell layer, and that both biochemical signals as well as mechanical constraints contribute to interlayer communication to ensure coordinated growth.

The structure of a root is generated from a single layer of stem cells that surround the quiescent center, which produce the central cylinder including the pericycle, a surrounding endodermis, cortex and an epidermis that separates the root from its environment (Stahl and Simon, 2010). Likewise, root elongation depends upon the coordinated growth of cells in all layers, and hence on interlayer communication. Cell–cell communication can take place via the symplastic movement of signaling molecules or via extracellular diffusible signals. PSK is a soluble extracellular peptide proposed to participate in cell–cell communication. The expression patterns of *PSK* and *PSKR* genes suggest that receptor and ligand are ubiquitously present without specifying a specific function. In this study we asked to what extent PSK signaling controlled elongation growth by comparing signaling knock-out and overexpression mutants. We further investigated if PSK signaling of cell expansion was required in all tissues or if signaling in the epidermal cell layer, or even in defined epidermal cells, was sufficient to promote elongation growth. Our data support the view that root and shoot growth is dependent on PSK receptor abundance in the epidermis, and that PSK perception in a subset of epidermal cells is sufficient to drive PSK-dependent elongation growth.

RESULTS

The abundances of *PSKR1* and *PSKR2* limit seedling growth

To analyze if seedling growth in Arabidopsis was controlled at the level of PSK perception, we generated plants that overexpressed either *PSKR1* or *PSKR2*. To elevate the abundance of PSK receptors, the coding regions of the receptor genes *PSKR1* and *PSKR2* were put under the control of the constitutively overexpressing *35S* cauliflower mosaic virus promoter. RT-PCR analysis of *PSKR1* and *PSKR2* transcripts in two independent transgenic lines each revealed enhanced gene expression (Figures 1a and S1a). In order to study the effect of *PSKR1* overexpression on growth, wt seedlings and seedlings of *PSKR1ox12* and *PSKR1ox2* lines were grown on plates with half-strength MS medium in the presence or absence of 1 μM PSK (Figures 1 and 2) for comparison, wt seedlings and *pskr1–3* seedlings with a T–DNA insertion in the *PSKR1* gene that eliminates expression were raised on the same plates (Figure 1b). Hypocotyls of etiolated *PSKR1ox12* and *PSKR1ox2* seedlings were significantly longer than wt hypocotyls, indicating that the abundance of PSKR1 was

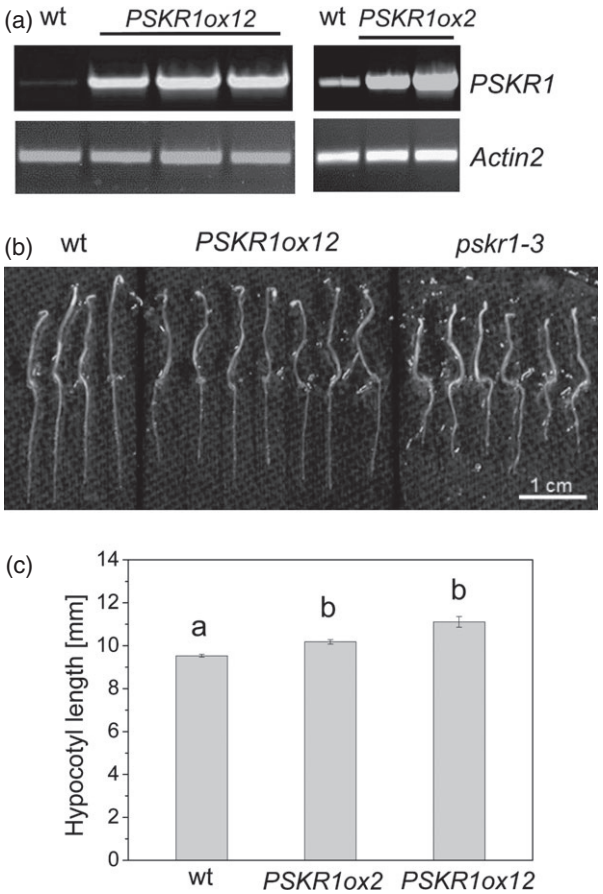

Figure 1. Overexpression of *PSKR1* promotes hypocotyl elongation.
(a) The expression of *PSKR1* was analyzed in leaves of 14–day-old wild-type (wt), *PSKR1ox12* and *PSKR1ox2* plants by RT-PCR. *Actin2* cDNA was amplified as a control for RNA input.
(b) Phenotypes of 5–day-old etiolated wt, *PSKR1ox12* and *pskr1–3* seedlings grown on half-strength MS medium.
(c) Average (± SE) hypocotyl lengths of 5–day-old etiolated seedlings were determined in two independent experiments with $n \geq 49$ seedlings analyzed per genotype. Different letters indicate significantly different values ($P < 0.001$, ANOVA, Tukey's test).

limiting hypocotyl elongation (Figure 1b,c). This conclusion was supported by the observation that *pskr1–3* hypocotyls were on average 29% shorter than wt (Stührwohldt *et al.*, 2011; Figure 1b).

The root elongation of light-grown seedling roots was also significantly enhanced by 35.9% in *PSKR1ox12* (Figure 2a,c) and by 23.3% in *PSKR1ox2* (Figure 2d), as compared with wt, and resulted in nearly twofold longer roots in *PSKR1ox12* as compared with *pskr1–3* seedlings (Figure 2a). The addition of 1 μM PSK resulted in even longer roots in wt and *PSKR1ox12* (Figure 2c), indicating that PSK-dependent root growth was limited both by the concentration of the ligand and at the level of receptor abundance. Growth promotion at the post-seedling stage by PSKR1 overexpression was observed in four-week-old *PSKR1ox12* plants, which had larger rosettes than the wt (Figure 2b).

PSKR2 was shown previously to have only a minor impact on root growth. *pskr2–1* seedling roots were slightly shorter than wt roots, compared with *pskr1–3* roots (Kutschmar *et al.*, 2009; Figure S1b). So far no functional differences were reported for the two receptor proteins, and differences in knock-out phenotypes may be a result of the differential abundance of the two receptors. In order to analyze whether *PSKR2* could promote root growth similarly to *PSKR1* when expressed at high levels, two independent *35S:PSKR2* lines were generated and analyzed (Figure S1a–f). Roots of light-grown *PSKR2ox1* and *PSKR2ox6* seedlings were significantly longer by 25 and 32.8%, respectively, as compared with the wt (Figure S1b, c), indicating that *PSKR2* can enhance root growth to a similar degree as *PSKR1* when expressed at high levels. Likewise, overexpression of *PSKR2* promoted hypocotyl elongation, as analyzed in etiolated seedlings (Figure S1e, f). The addition of PSK did not further promote root or hypocotyl growth in *PSKR2*-overexpressing lines, indicating that PSK was present at saturating levels, as described previously (Figure S1f; Stührwohldt *et al.*, 2011). *PSKR2*-overexpressing plants also had larger rosettes, indicating that PSK receptors control seedling and vegetative shoot growth (Figure S1d).

Hypocotyl and root growth are controlled by PSK signaling in the epidermis

The epidermis is considered as the growth-limiting tissue layer, and was shown previously to control brassinosteroid-dependent elongation growth in Arabidopsis seedlings (Savaldi-Goldstein *et al.*, 2007; Hacham *et al.*, 2010). We therefore asked whether PSK signaling of elongation growth in the epidermis was sufficient to promote growth. To answer this question, we expressed *PSKR1* under the control of the *CER6* promoter in the *pskr1–3 pskr2–1*, double-receptor knock-out mutant background. Based on expression data obtained from the Arabidopsis eFP browser database, *CER6* is active in the stem and leaf epidermis, but not in leaf mesophyll cells (http://bar.utoronto.ca/efp/cgi-bin/efpWeb.cgi; Winter *et al.*, 2007). The *pskr1–3 pskr2–1* mutant was generated by crossing *pskr1–3* and *pskr2–1* plants, and the homozygous double knock-out mutant was previously shown to be devoid of *PSKR1* and *PSKR2* transcripts (Kutschmar *et al.*, 2009). A 1.2–kb promoter fragment upstream of the ATG start codon of the epidermis-specific *CER6* gene was cloned in front of the *PSKR1* coding region, and the resulting expression vector was transformed into *pskr1–3 pskr2–1* plants. Three independent *CER6:PSKR1 pskr1–3 pskr2–1* transformants were analyzed and shown to express *PSKR1* to levels comparable with or slightly higher than those found in the wt (Figure 3a). Analysis of *CER6:GUS* plants showed GUS activity in cotyledons, in the hypocotyl and in the primary root tip of etiolated (Figure 3b,c)

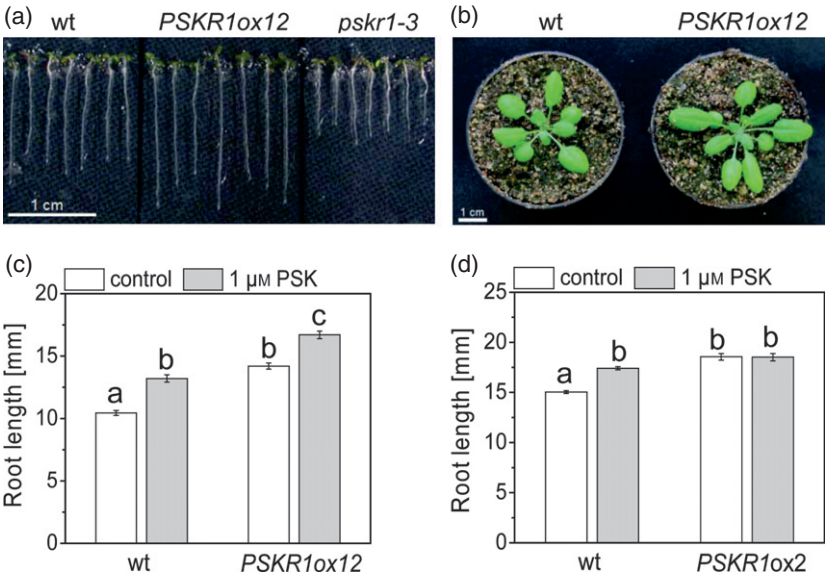

Figure 2. Overexpression of *PSKR1* promotes root growth.
(a) Phenotypes of 5–day-old de-etiolated wild-type (wt), *PSKR1ox12* and *pskr1–3* seedlings.
(b)Phenotypes of 4–week-old wt and *PSKR2ox12* plants.
(c)Average (±SE) root lengths of wt and *PSKR1ox12* seedlings.
(d)Average (±SE) root lengths of wt and *PSKR1ox2* seedlings. Root lengths were determined in two independent experiments with $n \geq 66$ seedlings analyzed per genotype and treatment. Different letters indicate significantly different values ($P < 0.001$, ANOVA, Tukey's test).

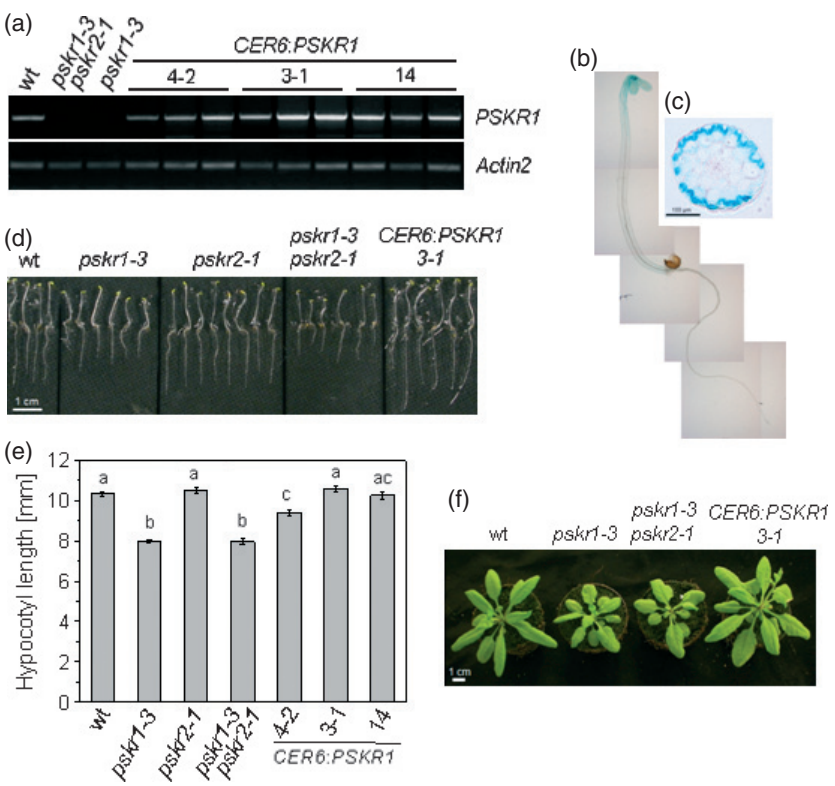

Figure 3. PSK perception in the epidermis promotes hypocotyl growth.
(a) Expression of *PSKR1* in leaves of 14–day-old wild-type (wt), *pskr1–3 pskr2–1* and *pskr1–3* plants, and in plants of *CER6:PSKR1 pskr1–3 pskr2–1* lines *4–2*, *3–1* and *14* (*CER6:PSKR1–4–2*, *CER6:PSKR1–3–1* and *CER6:PSKR1–14*) that express *PSKR1* under the control of the epidermis-specific *CER6* promoter in the double PSK receptor knock-out background. *Actin2* cDNA was amplified as a control for RNA input.
(b) β–Glucuronidase activity in a 5–day-old etiolated *CER6:GUS* seedling.
(c) Cross section through the upper third of the hypocotyl, 20 µm thick.
(d) Phenotypes of 5–day-old etiolated wt, *pskr1–3*, *pskr2–1*, *pskr1–3 pskr2–1* and *CER6:PSKR1 pskr1–3 pskr2–1* seedlings (*CER6:PSKR1–4–2*, *CER6:PSKR1–3–1* and *CER6:PSKR1–14*).
(e) Average (±SE) hypocotyl lengths of etiolated seedlings were determined in three independent experiments with at least 22 seedlings analyzed per genotype. Different letters indicate significantly different values ($P < 0.001$, ANOVA, Tukey's test).
(f) Phenotypes of 4–week-old soil-grown wt, *pskr1–3*, *pskr1–3 pskr2–1* and *CER6:PSKR1–3–1 pskr1–3 pskr2–1* plants.

and de-etiolated seedlings (Figure 4a–e). Cross-sections confirmed that GUS activity was localized preferentially in the epidermal cell layer of the hypocotyl, as reported previously (Millar *et al.*, 1999; Hooker *et al.*, 2002; Figures 3c and 4c).

Hypocotyl lengths were determined in 5–day-old etiolated seedlings of three independent *CER6:PSKR1 pskr1–3 pskr2–1* lines termed *4–2*, *3–1* and *14*, and compared with hypocotyls of wt, *pskr1–3*, *pskr2–1* and *pskr1–3 pskr2–1* seedlings (Figure 3d,e). Hypocotyls of *pskr1–3* and *pskr1–3 pskr2–1* seedlings were shorter than wt hypocotyls. Hypocotyls of the three independent *CER6:PSKR1 pskr1–3 pskr2–1* lines *4–2*, *3–1* and *14* displayed partially or fully restored hypocotyl elongation

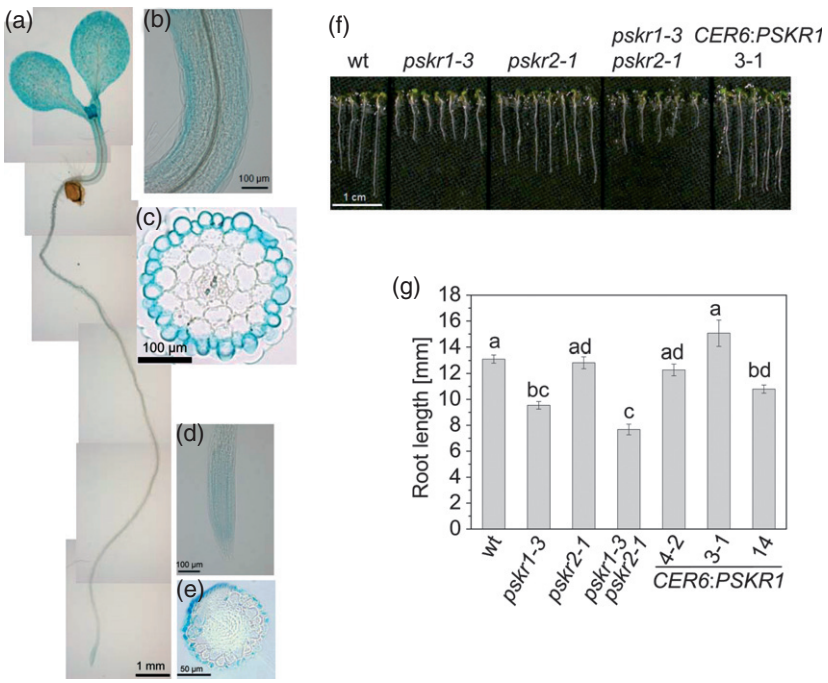

Figure 4. PSK perception in the epidermis promotes root growth.
(a–e) β-Glucuronidase activity was analyzed in 5-day-old de-etiolated *CER6:GUS* seedlings: (a) intact seedling; (b) middle of the hypocotyl; (c) cross section through the mid-hypocotyl; (d) root tip; (e) cross section through root tip.
(f) Phenotypes of 5-day-old de-etiolated wild-type (wt), *pskr1-3*, *pskr2-1*, *pskr1-3 pskr2-1* and *CER6:PSKR1 pskr1-3 pskr2-1* seedlings (*CER6:PSKR1-4-2*, *CER6:PSKR1-3-1* and *CER6:PSKR1-14*).
(g) Average (±SE) root lengths were determined for the lines indicated in three independent experiments, with at least 13 seedlings analyzed per genotype. Different letters indicate significantly different values ($P < 0.001$, ANOVA, Tukey's test).

(Figure 3e). Hypocotyls reached wt length in lines *3-1* and *14*, indicating that PSK perception in the epidermis was sufficient to mediate PSK-dependent hypocotyl growth. Analysis of 4-week-old, soil-grown plants showed that the rosette size of *CER6:PSKR1* plants was similar to wt, whereas shoots of *pskr1-3* and *pskr1-3 pskr2-1* knock-out mutants were smaller than wt or *CER6:PSKR1 pskr1-3 pskr2-1* plants (Figure 3f). Hence, shoot growth retardation in the PSK receptor knock-out background was restored by epidermal expression of *PSKR1*. Furthermore, epidermal perception of PSK restored wt growth not only in seedlings but also during plant maturation (Figure 3f).

When analyzing de-etiolated *CER6:GUS* seedlings we observed GUS activity in cotyledons, hypocotyl (Figure 4a–c) and in the growth region of the root tip (Figure 4d,e). As in the shoot, GUS expression in the root was detected in the epidermal cell layer (Figure 4e). In order to see whether epidermal *PSKR1* expression in the root was sufficient to restore the short-root phenotype of PSK receptor knock-out seedlings, we compared root lengths of *pskr1-3* and *pskr2-1* single knock-out and *pskr1-3 pskr2-1* double knock-out seedlings with *CER6:PSKR1 pskr1-3 pskr2-1* lines *4-2*, *3-1* and *14* (Figure 4f,g). The wt root length was fully restored in lines *4-2* and *3-1*, and was partially restored in line 14. These results support the view that perception of PSK in the epidermis is sufficient to promote hypocotyl and root growth. It is also possible that residual *CER6* promoter activity in tissues other than the epidermis contributed to growth promotion by PSKR1.

PSK promotes cell elongation in a non-cell-autonomous manner

The perception of PSK in the epidermis of either shoot or root appeared to be sufficient to drive elongation growth. In order to verify that PSKR1 activity in the epidermis was responsible for growth promotion, we next expressed *PSKR1* under the control of the *GLABRA2* (*GL2*) promoter in the *pskr1-3 pskr2-1* receptor knock-out background (Figure 5). The *GL2* promoter drives gene expression in atrichoblasts of the root epidermis and in cells of the lateral cap, but not in trichoblast cells or in other root cell types of the root, as shown previously by *in situ* RNA hybridization and a sensitive GFP reporter (Hung *et al.*, 1998; Lin and Schiefelbein, 2001; Hacham *et al.*, 2010). This highly preferential expression is visualized in *GL2:GUS* seedlings, which show GUS staining in defined cell files of the growth region at the root tip (Figure 5a,b). RT-PCR analysis of wt, *pskr1-3 pskr2-1* and *GL2:PSKR1 pskr1-3 pskr2-1* lines confirmed *PSKR1* expression in wt and *GL2:PSKR1 pskr3-1 pskr2-1* lines (Figure 5c). Root growth was subsequently analyzed in 5-day-old seedlings (Figure 5d,e). *GL2:PSKR1-1* roots reached wt lengths and seedling roots of *GL2:PSKR1-2* were significantly longer than wt roots, indicative of a PSKR overexpressor phenotype. The short-root phenotype of *pskr1-3 pskr2-1* was hence fully restored when PSK perception occurred in single cell files of the root epidermis. Atrichoblast-specific expression of *PSKR1* also partially restored wt growth in 4-week-old *GL2:PSKR1-1* plants (Figure 5f).

In order to analyze whether PSK signaling promoted elongation in the trichoblasts, which do not express a PSK

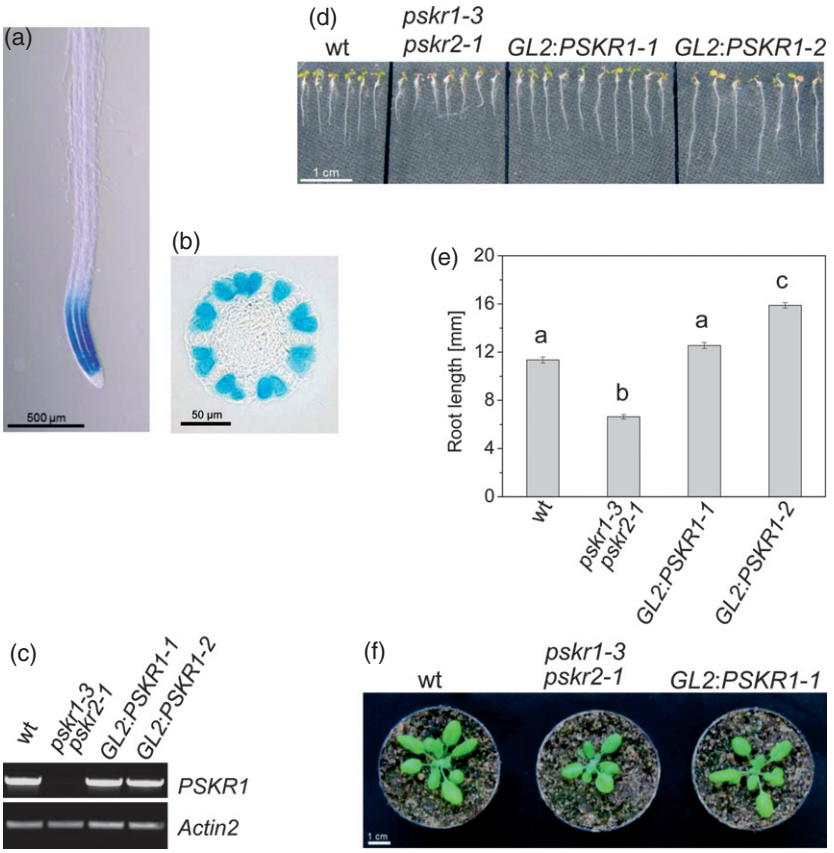

Figure 5. PSK perception in atrichoblasts of the epidermis promotes root growth.
(a, b) β–Glucuronidase activity was analyzed in 5–day-old de-etiolated *GL2:GUS* seedlings: (a) intact root; (b) cross section through root tip.
(c) Expression of *PSKR1* was analyzed in 5–day-old wild-type (wt), *pskr1–3 pskr2–1*, *GL2:PSKR1–1 pskr1–3 pskr2–1* (*GL2:PSKR1-1*) and *GL2:PSKR1–2 pskr1–3 pskr2–1* (*GL2:PSKR1–2*) seedlings by RT-PCR. *Actin2* cDNA was amplified as a control for RNA input.
(d) Phenotypes of 5–day-old de-etiolated wt, *pskr1–3 pskr2–1*, *GL2:PSKR1–1 pskr1–3 pskr2–1* and *GL2:PSKR1–2 pskr1–3 pskr2–1* seedlings.
(e) Average (±SE) root lengths were determined for the lines indicated in two independent experiments, with at least 93 seedlings analyzed per genotype. Different letters indicate significantly different values ($P < 0.001$, ANOVA, Tukey's test).
(f) Phenotypes of 4–week-old soil-grown wt, *pskr1–3 pskr2–1* and *GL2:PSKR1–1 pskr1–3 pskr2–1* plants.

receptor, we determined cell lengths in the growth region of wt, *pskr1–3 pskr2–1*, *GL2:PSKR1–1 pskr1–3 pskr2–1* and *CER6:PSKR1–3–1 pskr1–3 pskr2–1* roots (Figure 6). On average, mature atrichoblasts were longer than trichoblasts in all genotypes (Figure 6a). Both mature atrichoblast and trichoblast cells were significantly shorter in the PSK receptor double knock-out line *pskr1–3 pskr2–1* than in wt, and were comparable in length in wt, *GL2:PSKR1–1 pskr1–3 pskr2–1* and *CER6:PSKR1–3–1 pskr1–3 pskr2–1* roots, indicating that expression of PSKR1 in atrichoblasts was sufficient to drive cell elongation of trichoblast cells. A more detailed analysis revealed shorter trichoblast and atrichoblast cells in *pskr1–3 pskr2–1* roots not only at maturity but also during the elongation phase, and comparable cell length profiles in wt, *GL2:PSKR1–1 pskr1–3 pskr2–1* and *CER6:PSKR1–3–1 pskr1–3 pskr2–1* (Figure 6b). The cell length analyses thus support the view that a signal is transmitted in response to PSK from PSK perceiving atrichoblasts to promote elongation growth in PSK receptor-less trichoblasts.

PSK signaling of root growth requires brassinosteroid synthesis

Based on previous observations that brassinosteroid-dependent growth was driven by brassinosteroid (BR) perception or synthesis in the epidermis (Savaldi-Goldstein *et al.*, 2007), we hypothesized that PSK signaling of cell growth in the epidermis might be mediated by BR. To test this hypothesis, wt and *tpst–1* (*tyrosylprotein sulfotransferase–1*) seedlings were treated with 1 µM brassinazole (BZ), an inhibitor of BR biosynthesis (Asami *et al.*, 2001), and/or with 1 nM 24–epibrassinolide (BL) and root growth in response to PSK was analyzed (Figure 7). The *tpst–1* mutant lacks the ability for sulfation of the PSK precursor peptides to generate active ligands. *tpst–1* seedlings have smaller shoots and shorter roots than the wt, a phenotype that is partially restored by treatment with 1 µM PSK (Stührwohldt *et al.*, 2011; Figure 7b,c). Moreover, *tpst–1* seedlings have shorter epidermal cells, and treatment of *tpst–1* seedlings with 1 µM PSK fully restored the mature wt cell length in roots (Figure 7a). This finding is in accord with previous reports showing that PSK controls elongation growth (Kutschmar *et al.*, 2009), whereas other sulfated peptides of the RGF growth factor family control meristematic activity in roots (Matsuzaki *et al.*, 2010).

Treatment of wt or *tpst–1* seedlings with 1 nM BL did not significantly alter root length (Figure 7b,c). Treatment with 1 µM BZ on the other hand resulted in shorter roots in both genotypes, indicating that growth inhibition in *tpst–1* was further aggravated in the absence of BR. The addition of

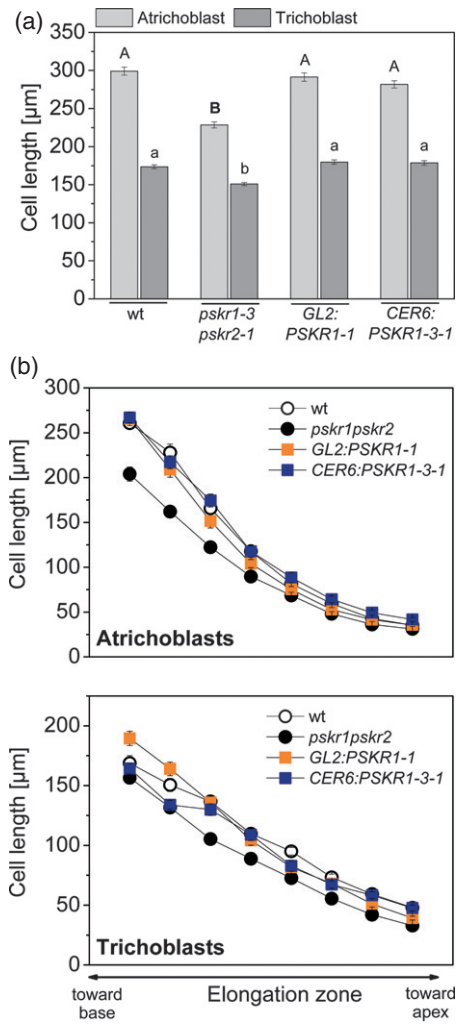

Figure 6. Expression of *PSKR1* in atrichoblasts promotes the elongation of trichoblast cells.

(a) Mature cell lengths of atrichoblasts and trichoblasts were determined separately in 5–day-old light-grown wt, *pskr1–3 pskr2–1*, *GL2:PSKR1–1 pskr1–3 pskr2–1* (*GL2:PSKR1–1*) and *CER6:PSKR1–3–1 pskr1–3 pskr2–1* (*CER6:PSKR1–3–1*) seedlings. Different letters indicate statistically different values. Average (±SE) mature cell lengths of atrichoblasts and trichoblasts were determined for the lines indicated in two independent experiments with $n \geq 94$ cells analyzed per genotype. Different letters indicate significantly different values ($P < 0.001$, ANOVA, Tukey's test).

(b) Average consecutive cell lengths were determined in atrichoblast and trichoblast cell files, starting at the root hair zone and extending towards the root apex for the lines indicated. Results are averages from three independent experiments, with at least 28 cell files from at least 14 plants analyzed per genotype and cell type.

1 nM BL to BZ-treated *tpst–1* seedlings partially restored responsiveness to PSK in the *tpst–1* background (Figure 7b,c). The data thus support the view that PSK signaling of root elongation is mediated through BR signaling. To see whether BR was required for PSK signaling in the epidermis, we analyzed root growth in *CER6:PSKR1–3–1 pskr1–3 pskr2–1* and in the overexpression line *PSKR1ox12* (Figure 7d). Both lines showed comparable root growth that was enhanced in the presence of 1 µM PSK. Treatment with 1 µM BZ strongly inhibited root growth and resulted in unresponsiveness to treatment with 1 µM PSK, suggesting that PSK signaling in the epidermis is dependent on the presence of BR signaling.

As an independent means to verify the involvement of BRs in the PSK signaling of growth we employed mutants that are defective in either BR synthesis or signaling. *det2–1* (*deetiolated2–1*) is a BR biosynthesis mutant (Chory *et al.*, 1991, 1994). DET2 is a steroid 5α–reductase responsible for the conversion of (24*R*)–24–methylcholest-4-En-3-1 to (24*R*)–24–methyl-5α-cholestan-3-1 in the early BR synthetic pathway (Noguchi *et al.*, 1999). The BR receptor mutant *bri1-200A* has a T–DNA insertion 1245 bp downstream of the ATG in the LRR coding region of the BR receptor gene *BRI1* (*BRASSINOSTEROID INSENSITIVE 1*), which leads to the knock-down of *BRI1* gene expression. BZR1 (BRASSINAZOLE-RESISTANT 1) and BES1 (BRI1-EMS SUPPRESSOR 1) are transcription factors that mediate BR responses (Clouse, 2011). *det2–1* seedlings displayed a dwarf phenotype with very short roots similar to *tpst–1* seedlings (Figure 8a,b). Roots of *bzr1–1D*, *bes1–1* and *bri1–200A* seedlings were only slightly shorter than wt roots (Figure 8b). BZR1 and BES1 can act in a redundant fashion such that the knock-out of one gene may not result in a growth phenotype. Treatment with 1 µM PSK promoted root elongation in wt and *tpst–1*, included as controls, in *bes1–1, bzr1–1D* and to a lesser, but significant, extent in *bri1-200A*, which is in accord with the weak phenotype of these BR signaling mutants. By contrast, root growth of *bri1–9* seedlings of the *A. thaliana* ecotype Wassilweskija with a loss-of-function mutation in the BRI1 receptor is not promoted by PSK (Figure 8c). Similarly, knock-out of BR synthesis in *det2–1* abolished responsiveness to PSK (Figure 8b), indicating that BR synthesis and perception are a prerequisite for the PSK signaling of cell elongation.

In order to test whether PSK signaling affects BR synthesis or signaling at the transcriptional level, we analyzed expression of the biosynthetic genes *DET1*, *DWF4* (*DWARF4;* Asami *et al.*, 2001), *CYP85A1 (Cytochrome P450 85A1; BR6ox, BRASSINOSTEROID-6-OXIDASE 1*; Bancos *et al.*, 2002), *SMT2* (*STEROL METHYLTRANSFERASE 2*; Bouvier-Navé *et al.*, 1998) and *CPD* (*CONSTITUTIVE PHOTOMORPHOGENESIS AND DWARFISM*; Bancos *et al.*, 2002), and of the signaling genes *BRI1* (*BRASSINOSTEROID INSENSITIVE 1*; Clouse *et al.*, 1996) and *BAK1* (*BRI1-ASSOCIATED RECEPTOR KINASE 1*; Nam and Li, 2002) in wt, *tpst–1*, *pskr1–3 pskr2–1* and *PSKR1ox* seedlings by qPCR (Figure 9). Expression of all genes was normalized to *Actin2* and *GAPC* (*GLYCERALDEHYDE-3-PHOSPHATE DEHYDROGENASE C*). The results indicated that transcript levels of genes encoding for enzymes of BR synthesis were not significantly changed in PSK signaling and synthesis mutants. *BAK1* transcript levels were unchanged as well.

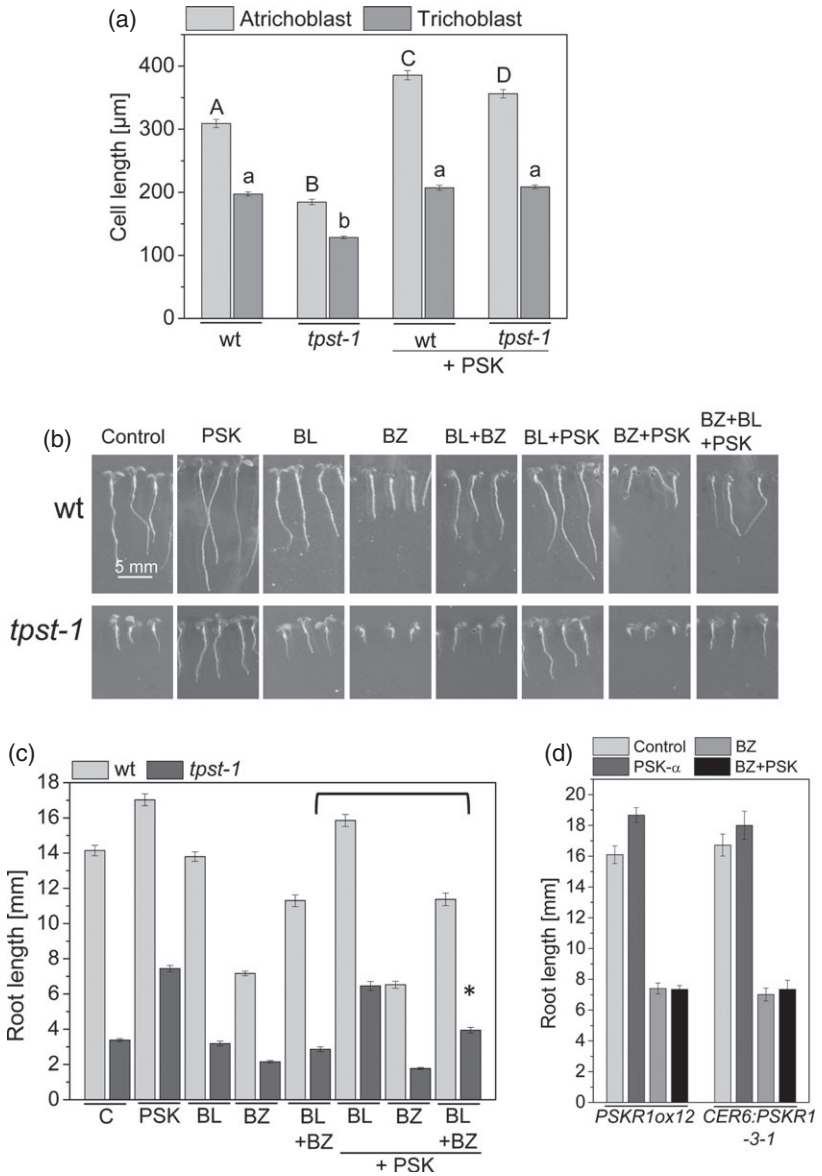

Figure 7. Promotion of root growth by PSK is dependent on BR synthesis.
(a) Average (±SE) mature trichoblast and atrichoblast cell lengths of wt and *tpst–1* seedlings treated with or without 1 µM PSK were determined in two independent experiments, with $n = 96$ cells analyzed per genotype and treatment. Different letters indicate genotype-specific significantly different values for each cell type ($P < 0.05$, ANOVA, Tukey's test).
(b) Phenotypes of wt and *tpst–1* seedlings raised under long-day conditions for 5 days without effector or supplemented with 1 µM PSK in the presence or absence of 1 nM 24–epibrassinolide (BL) and/or 1 µM brassinazole (BZ).
(c) Average root lengths (±SEs) were determined in three independent experiments with $n \geq 70$.
(d) *PSKR1ox12* and *CER6:PSKR1–3–1 pskr1–3 pskr2–1* (*CER6:PSKR1–3–1*) seedlings were raised for 5 days under long-day conditions without effector as a control, or in the presence of 1 µM PSK, 1 µM BZ or combinations of these. Data are averages (±SEs) with $n \geq 17$ seedlings analyzed per genotype.

BRI1 transcript levels were slightly reduced to 0.60–fold and 0.62–fold in *PSKR1ox* and *tpst–1* roots, respectively (Figure 9). Overall, the genetic alteration of PSK signaling did not significantly alter the expression of key BR synthesis genes, indicating that interaction may occur at the protein level, possibly in the BR signaling cascade. Taken together, genetic and pharmacological data indicate that PSK perception in atrichoblasts generates a BR-dependent signal that travels to neighboring trichoblast cells.

DISCUSSION

PSK signaling was shown to control root and shoot growth in Arabidopsis (Matsubayashi *et al.*, 2006; Kutschmar *et al.*, 2009; Stührwohldt *et al.*, 2011). Root elongation was enhanced in Arabidopsis seedlings supplemented with PSK, indicating that growth was limited by ligand availability (Kutschmar *et al.*, 2009). Signaling can likewise be limited by the availability of the respective receptor, which is regulated by synthesis, modification and degradation. In Arabidopsis cells overexpressing *PSKR1*, (^{3}H)PSK binding activity in the microsomal fractions was enhanced (Matsubayashi *et al.*, 2006). Arabidopsis plants overexpressing *PSKR1* showed enlarged leaves and delayed senescence (Matsubayashi *et al.*, 2006). In addition, the overexpression of *PSKR1* or *PSKR2* was shown in this study to promote hypocotyl and root elongation growth, indicating that PSK receptor abundance was limiting seedling and plant growth, and that transcriptional upregulation can overcome this limitation. Taken together, PSK signaling results in growth-promoting activity, whereby the degree of

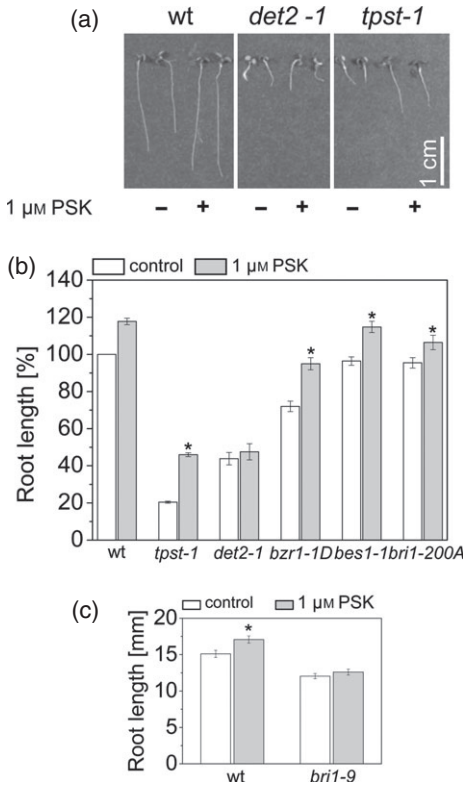

Figure 8. Genetic inhibition of BR synthesis and signaling causes insensitivity towards PSK.
(a) Phenotypes of wt, *det2–1* and *tpst–1* seedlings of Columbia–0 grown for 5 days under long-day conditions with or without 1 µM PSK.
(b) Average root lengths were determined in wt, *tpst–1*, *det2–1*, *bzr1–1D*, *bes1–1* and *bri1-200A* seedlings of ecotype Columbia–0 grown with or without 1 µM PSK. *Significantly different values between treatments for each genotype, as analyzed in three independent experiments ($n \geq 50$; $P < 0.001$).
(c) wt and *bri1–9* seedlings of ecotype Wassilewskija were grown in the presence of 1 µM PSK or left untreated as a control. *bri1–9* is deficient in brassinosteroid perception by BRI1. *Significantly different values between treatments of wt ($n \geq 75$, $P < 0.05$, two independent experiments).

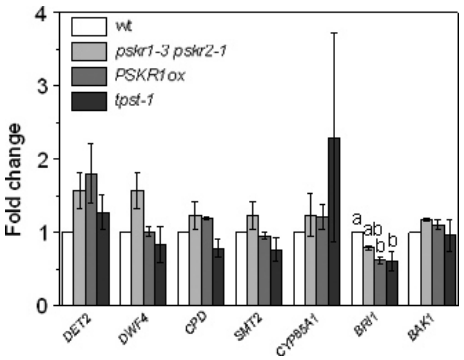

Figure 9. qPCR analysis of BR synthesis and signaling genes in PSK synthesis and signaling mutants. Expression of the BR synthesis genes *DET2* (*DETIOLATED2*), *DWF4 (DWARF4*), *CYP85A1 (Cytochrome P450 85A1; BR6ox* BRASSINOSTEROID-6-OXIDASE 1), *SMT2* (STEROL METHYLTRANSFERASE 2), *CPD (CONSTITUTIVE PHOTOMORPHOGENESIS AND DWARFISM)* and of the signaling genes *BRI1* (*BRASSINOSTEROID INSENSITIVE*) and *BAK1* (*BRI1 ASSOCIATED RECEPTOR KINASE 1)* was analyzed by qPCR. qPCR was performed on roots of 5–day-old de-etiolated seedlings of wt, *pskr1–3 pskr2–1*, *PSKR1ox12* and *tpst–1*. Different letters indicate statistically different values for each of the genes compared between the different genotypes in three independent experiments ($P < 0.05$, ANOVA, Tukey's test; for *CYP85A1* and *BAK1* the *P* value was set to 0.001).

growth promotion can be influenced by regulating the abundance of either ligand or receptor. The abundance of the plasma membrane-bound BR receptor BRI1 was shown to be regulated at the protein level through dephosphorylation catalyzed by PP2A phosphatase. Dephosphorylated BRI1 is degraded, thus terminating BR signaling (Wu *et al.*, 2011). PSK receptor proteins show great structural similarity to BRI1, and it is conceivable that the regulation of PSK receptor abundance likewise takes place at the protein level to modulate the PSK response.

Plant growth is regulated by phytohormones that interact in a signaling network, which includes communication between cell layers (Savaldi-Goldstein and Chory, 2008). Hormones act in a cell or tissue-type specific manner. The epidermis is considered as the cell layer that restricts growth. Stems cut in half curl outwards, indicating that the inner tissues can expand when relieved from strain exerted by the outer tissue layer (Kutschera and Niklas, 2007). Promoters used for tissue-specific expression may be active at very low levels, not detected by common methods employing fluorescent protein or *in situ* hybridization. Nonetheless, preferential expression of *PSKR1* in the epidermis in a PSK receptor null mutant background was sufficient to promote hypocotyl as well as root growth, and to restore the wt growth phenotype.

Brassinosteroids (BRs) are known to regulate cell elongation (Savaldi-Goldstein and Chory, 2008). Subnanomolar levels of brassinolide were shown to promote root growth, whereas concentrations of 1 nM and higher inhibited root growth, as did genetic suppression of BR synthesis, indicating that BRs promote root growth in a dose-dependent manner (Müssig *et al.*, 2003). BR perception specifically in the epidermis was found to be crucial for BR-dependent root growth (Savaldi-Goldstein and Chory, 2008; Hacham *et al.*, 2010). Similarly, BR-dependent shoot growth was shown to be driven by BR perception or brassinolide synthesis in the epidermis (Savaldi-Goldstein *et al.*, 2007). Epidermis-specific expression of the BR receptor *BRI1* or of the key biosynthesis *CPD* gene resulted in a full BR-stimulated growth response, whereas expression in other tissues did not.

The coincident activity of PSK and BR in the epidermis and the fact that both PSK and BR promote cell elongation prompted us to ask if PSK signaling of elongation growth may be mediated by BR signaling. BZ is a specific inhibitor that inhibits the cytochrome P450 monoxygenase DWF4 that acts as steroid 22–hydroxylase within the BR biosynthesis pathway (Asami *et al.*, 2001). Treatment of wt

seedlings with BZ caused a typical BR-deficient phenotype with short hypocotyls and short roots. PSK-deficient *tpst–1* seedlings display severe root growth inhibition, which was further aggravated in the presence of BZ. The addition of the highly active BR 24–epibrassinolide to BZ-treated wt or *tpst–1* seedlings partially reverted root growth inhibition. In *tpst–1* seedlings treated with BZ, responsiveness to PSK was lost but was restored when BR was supplied in addition to BZ, indicating that BR signaling was required for PSK-dependent root growth promotion. The requirement for BR could be direct or indirect. Signaling of growth through the PSK and BR pathways likely occurs in epidermal cells, as PSK responsiveness was also lost in the presence of BZ in *CER6:PSKR1* seedlings that express *PSKR1* preferentially in the epidermis, even though residual activity in other cell layers cannot be excluded. BRs are perceived by the leucine-rich repeat receptor kinase BRI1 at the plasma membrane. Signal transduction occurs through phosphorylations and dephosphorylations, resulting in the activation of the transcription factors BES1 and BZR1 (Clouse, 2011). Genetic disruption of either BR synthesis in *det2–1* or of BR signaling in *bri1–9* rendered seedlings unresponsive to PSK, providing additional evidence that the PSK response is mediated by the BR signaling pathway. Knock-out of either *BES1* or *BZR1* did not compromise PSK-dependent growth, which may be owed to the fact that these transcription factors can act in a redundant fashion (Clouse, 2011).

PSK was described as an autocrine growth factor based on the observation that it promotes the proliferation of suspension-cultured cells kept at a low density (Matsubayashi *et al.*, 1996). Data on the mobility of the PSK peptide or PSK signal *in planta* have so far not been provided. Using atrichoblast-specific *GL2* promoter-driven PSK receptor expression, we showed that localized PSK perception in atrichoblasts caused not only this subpopulation of epidermal cells to elongate, but also trichoblasts that most likely were unable to perceive PSK. PSK signaling of growth thus appears to occur non-cell autonomously. Hence, despite the ubiquitous expression of PSK precursor genes, the PSK peptide does not act as an autocrine growth factor *in planta*. PSK activity is transmitted to neighboring cells and to distant cell layers, such as the cortex and central cylinder in the root, via mobile or possibly mechanical signals. The epidermis limits growth as a result of the constraints imposed on cell expansion by the stiff cell wall. Cells of the inner tissues expand once the epidermis is removed, indicating that they are compressed (Kutschera, 2008). When epidermal cells grow the compression imposed by the epidermis on inner tissue layers is reduced. This altered tissue tension may be perceived as a mechanical signal either at the plasma membrane or in the cell wall of cells in inner tissue layers. Signaling to the protoplast may involve cortical microtubules, which are also known to determine the direction of cell growth through directional deposition of newly synthesized cellulose microfibrils (Paredez *et al.*, 2006). In the context of organogenesis at the shoot apical meristem, Uyttewaal *et al.* (2012) recently described a crucial role for the microtubule-severing katanin in harmonizing the growth rates of adjacent cells. Depending on the degree of mechanical stress, the presence of katanin led to more homogeneous or to more heterogeneous growth within the epidermal tissue. As all cells are directly or indirectly linked to each other via their cell walls, it is easily conceivable that mechanical stress is transmitted not only between cells of one tissue but also between tissue layers to coordinate whole-organ growth.

Although the nature of this coordinating signal remains elusive, the regulation of elongation growth by PSK was shown here to require BR, thus linking PSK peptide signaling with hormone regulation of growth.

EXPERIMENTAL PROCEDURES

Plant material and growth conditions

All experiments were performed with *A. thaliana* ecotype Columbia–0, with the exception of *bri1–9* analysis. *bi1–9* is a loss-of-function mutant of BRI1 of *A. thaliana* ecotype Wassilewskija (Jin *et al.*, 2007). The *pskr1–3*, *pskr2–1* and *tpst–1* insertion lines used in this study have been described previously (Matsubayashi *et al.*, 2006; Amano *et al.*, 2008; Kutschmar *et al.*, 2009; Stührwohldt *et al.*, 2011). In *pskr1–3*, a T–DNA is inserted in the kinase domain of PSK receptor 1 and *pskr2–1* has a T–DNA in the 11th LRR domain of PSK receptor 2. *tpst–1* has a T–DNA inserted in the fifth exon. Two *CER6:GUS* lines were obtained from Dr Shauna Somerville (Department of Plant and Microbial Biology, Berkeley, CA, USA). We further used homozygous *det2–1* (N6159), *bzr1–1D* (N65987), *bes1–1* (N651123) and *bri1–200A* (N678032) mutants obtained from the Nottingham Arabidopsis Stock Centre (NASC, University of Nottingham, Nottingham, UK). *det2–1* and *bzr1–1D* have been previously described (Chory *et al.*, 1991, 1994). *bes1–1* has a T–DNA insertion very close to the stop codon and *bri1-200A* in the LRR coding region of the BR receptor *BRI1*. The *bri1–9* mutant of Arabidopsis ecotype Wassilewskija has a point mutation in the BR binding site, causing a $Ser^{662} \rightarrow$ Phe exchange and BR insensitivity (Jin *et al.*, 2007). Seeds of *bri1–9* and wt Arabidopsis ecotype *Wassilewskija* were kindly provided by Birgit Kemmerling (University of Tübingen, Germany).

Plants were grown in a 2:3 sand:humus mixture that was frozen at –80°C for 2 days to avoid insect contamination and then watered regularly with tap water. Seeds were stratified at 4°C in the dark for 2 days and then transferred to a growth chamber, where they were grown under long-day conditions with 16 h of light (70 μM ol photons m^{-2} s^{-1}) at 22°C. For growth experiments on sterile plates, Arabidopsis seeds were surface sterilized for 20 min in 1 ml 2% (w/v) sodium hypochlorite, washed five times with autoclaved water and laid out under sterile conditions on square plates containing half-concentrated MS media (Murashige and Skoog, 1962) and 1.5% (w/v) sucrose solidified with 0.38% (w/v) gelrite (Duchefa, http://www.duchefabiochemie.nl). The media were supplemented with 1 μM PSK (NeoMPS, http://www.neomps.com), 1 nM 24–epibrassinolide (Duchefa) or 1 μM BZ (TCI Europe, http://www.tcichemicals.com), as indicated.

Plasmid constructs, transformation and histochemical GUS detection

For the *CER6* promoter-driven epidermis-specific *PSKR1* (*At2g02220*) expression, a 1.2–kb genomic fragment upstream of the *CER6* (*At1g68530*) coding region was amplified by PCR using the forward primer 5′–TTTATTCGAGCTCCTTCGATATCGGTTGTTG AC–3′ and the reverse primer 5′–AAATTTGGACTAGTCGTCGGAG AGTTTTAATGT–3′. For the *GLABRA2* (*GL2*) promoter-driven atrichoblast-specific *PSKR1* expression, a 2.1–kb genomic fragment upstream of the *GL2* (*At1g79840*) coding region was amplified by PCR using the forward primer 5′–TTTATTCGAGCTC GTTTCCTTCACTATACGTC–3′ and the reverse primer 5′–CCAC-TAGTCTGTCCCTAGCTAGCTTC–3′. The fragments were cloned into the vector pB7WG2.0 (VIB, http://www.vib.be) by replacing the CaMV *35S* promoter. Point mutations were introduced within the *Spe*I site of the *CER6* and of the *GL2* promoter PCR fragments by overlap extension PCR (Horton *et al.*, 1989), using primers 5′–CCAACAAAATCAAGTTTTTGCTAAAAATAGTTT–3′ and 5′–ACCC GCAAATAAACTATTTTTAGCA–3′ for *CER6*, and primers 5′–TACTG CTACGTACATACCCCTACTATAATAGTCAG–3′ and 5′–CCCAAT CGAATCTAATACACTGACTATTATAGT–3′ for *GL2*. The 3.1–kb coding sequences of the intronless *PSKR1* and *PSKR2* genes were amplified by PCR from genomic DNA using primers 5′–ACGC GTCGACATGCGTGTTCATCGTTTTTGTGTGATCG–3′ and 5′–TACC GGATATCCTAGACATCATCAAGCCAAGAGAC–3′ for *PSKR1* and primers 5′–AAATTTGTCGACATGGTGATCATTCTCC–3′ and 5′–ATA-GTTTAGCGGCCGCTCATTGTTGTTGAACAGAC–3′ for *PSKR2*. The *PSKR1* and *PSKR2* PCR fragments were cloned into the vector pB7WG2.0 downstream of the *CER6, GL2* or CaMV *35S* promoter using the Gateway cloning system (Invitrogen, http://www.invitrogen.com). For *CER6* and *GL2* promoter-driven *PSKR1* expression, the *PSKR1* coding sequence was cloned into the vector pB7WG2.0 downstream of the *CER6* or *GL2* promoter, respectively.

Arabidopsis plants were transformed with *Agrobacterium tumefaciens* (GV3101) using the floral-dip method (Clough and Bent, 1998). Selection of transformed plants was performed by spraying with 200 μM BASTA (AgrEvo, http://www.agrevo.de). Homozygous plants were identified by BASTA selection. β–Glucuronidase (GUS) assays were performed as described by Kutschmar *et al.* (2009). Overview pictures were taken with an Olympus BX 41 microscope (with a Color-View II camera and CELL A software) or with an Olympus zoom stereo microscope SZ 61 (with a CMOS color SC 100 camera and ANALYSIS® GETIT! software; Olympus, http://www.olympus.com). For cell type-specific analysis of GUS expression, roots or hypocotyls were embedded in Technovit 7100 according to the manufacturers' instructions (Heraeus Kulzer, http://heraeus-dental.com). Sections of 15–25 μm thick were cut with a Leica RM 2255 microtome and analyzed using an Olympus BX 41 microscope. Images were taken with a Color-View II camera and CELL A software (Olympus).

RT-PCR and qPCR analysis

RT-PCR expression analysis of *PSKR1* and *PSKR2* was performed on 5–day-old seedlings and on 14–day-old plants using total RNA reverse transcribed with an oligo dT primer. The cDNA was amplified with the forward primer 5′–CAAAGACCAGCTCTTCCATCG–3′ and the reverse primer 5′–CTGTGAACGATTCCTGGACCT–3′ for *Actin2*, which was used as a control, with primers 5′–GAG CGTTGCAATACAATCAG–3′ and 5′–CAGTACTTACATGCGTCTCGT–3′ for *PSKR1*, and with primers 5′–CTCTTCAAGGCTACTGCAAG CATG–3′ and 5′–CATTGT TGTTGAACAGACTCCATAG–3′ for *PSKR2* cDNA. PCR amplifications were performed for 29 cycles for *Actin2* and 37 cycles for *PSKR1* and *PSKR2*, as described by Kutschmar *et al.* (2009).

Quantitative reverse transcription polymerase chain reaction (qRT-PCR) was performed with the QuantiTect SYBR Green RT-PCR Kit (Qiagen, http://www.qiagen.com), according to the manufacturer's instructions. The reverse transcription products were amplified using gene-specific primers 5′–TTTGGAGAGGC GATTGAGTG–3′ and 5′–CTCTTCCTTGAACTTGGCAATG–3′ for *DET2*, 5′–CAGAGGATGAAGCAGAGATGAG–3′ and 5′–TGAGATC GAGAATTTGCTCCG–3′ for *DWF4*, 5′–CCAAAAGAAATCGAAA CCGCC–3′ and 5′–CCAAAAGAAATCGAAACCGCC–3′ for *SMT2*, 5′–ACAGAGCAGAAAACAGAGTGAG–3′ and 5′–GAAGGAGAGCGG AACAGAG–3′ for *CYP85A1*, 5′–CCCAAACCACTTCAAAGATGCT–3′ and 5′–GGGCCTGTCGTTACCGAGTT–3′ for *CPD*, 5′–CCAAAGTTTC AGGTGTTCAAC–3′ and 5′–CTCCAAAATCCGGTGAATCCG–3′ for *BRI1*, 5′–GAAGAAGTGGAGCAGCTAATC–3′ and 5′–CAGCTAAACC ATCTCCTTCAAG–3′ for *BAK1*, and 5′–ATCAAGGAGGAATCC GAAGG–3′ and 5′–AAGTCGACCACACGGGAAT–3′ for *GAPC* and 5′–CAAAGACCAGCTCTTCCATCG–3′ and 5′–GTTGTCTCGTGGATT CCAGCA–3′ for *Actin2*, which were used as controls for standardization. Reactions were performed with a 7300 real-time PCR-system (Life Technologies, http://www.lifetechnologies.com). All data were normalized to *GAPC* and *Actin2* and analyzed using the $2^{-\Delta\Delta ct}$ method (Livak and Schmittgen, 2001). Three independent biological repeats were performed and statistical analysis was performed as described below.

Growth measurements and statistical analysis

Hypocotyl and root lengths were determined from photographs using IMAGEJ (National Institutes of Health, http://rsb.info.nih.gov/ij). Epidermal cell lengths were determined on intact roots using an Olympus microscope BX41 and an Olympus Color-View II camera, with a 20-fold magnification and image software CELL A (Olympus). Statistical analysis was performed with MINITAB (Minitab Inc., http://www.minitab.com). An ANOVA (Tukey's test) or a two-sample Stiden'ts *t*–test was performed to test the statistical significance of means. Before statistical analysis, constant variance and normal distribution of data were verified and the *P* value was set to $P < 0.001$ if one of these conditions was not achieved. *P* values for the Pearson product moment correlation are indicated in the figure legends.

ACKNOWLEDGEMENT

We gratefully thank Dr Shauna Somerville (Department of Plant and Microbial Biology, Berkeley, CA, USA) for supplying homozygous *CER6:GUS* seeds and Dr Birgit Kemmerling (University of Tübingen, Germany) for providing seeds of wt Arabidopsis ecotype Wassilewskija and *bri1–9*.

SUPPORTING INFORMATION

Additional Supporting Information may be found in the online version of this article.

Figure S1. Overexpression of *PSKR2* promotes root and hypocotyl growth.

REFERENCES

Amano, Y., Tsubouchi, H., Shinohara, H., Ogawa, M. and Matsubayashi, Y. (2007) Tyrosine-sulfated glycopeptide involved in cellular proliferation and expansion in Arabidopsis. *Proc. Natl Acad. Sci. USA* **104**, 18333–18338.

Asami, T., Mizutani, M., Fujioka, S. *et al.* (2001) Selective interaction of triazole derivatives with DWF4, a cytochrome P450 monooxygenase of the brassinosteroid biosynthetic pathway, correlates with brassinosteroid deficiency in planta. *J. Biol. Chem.* **276**, 25687–25691.

Bancos, S., Nomura, T., Molnár, G., Boshop, G.J., Koncz, C., Yokota, T., Nagy, F. and Szekeres, M. (2002) Regulation of transcript levels of the Arabidopsis cytochrome p450 genes involved in brassinosteroid biosynthesis. *Plant Physiol.* **130**, 504–513.

Bemis, S.M. and Torii, K.U. (2007) Autonomy of cell proliferation and developmental programs during Arabidopsis aboveground organ morphogenesis. *Dev. Biol.* **304**, 367–381.

Bouvier-Navé, P., Husselstein, T. and Benveniste, P. (1998) Two families of sterol methyltransferases are involved in the first and the second methylation steps of plant sterol biosynthesis. *Eur. J. Biochem.* **256**, 88–96.

Chory, J., Nagpal, P. and Peto, C.A. (1991) Phenotypic and genetic analysis of det2, a new mutant that affects light-regulated seedling development in Arabidopsis. *Plant Cell*, **3**, 445–459.

Chory, J., Reinecke, D., Sim, S., Washburn, T. and Brenner, M. (1994) A role for cytokinins in de-etiolation in Arabidopsis (det mutants have an altered response to cytokinins). *Plant Physiol.* **104**, 339–347.

Clough, S.J. and Bent, A.F. (1998) Floral dip: a simplified method for Agrobacterium-mediated transformation of *Arabidopsis thaliana*. *Plant J.* **16**, 735–743.

Clouse, S.D. (2011) Brassinosteroid signal transduction: from receptor kinase activation to transcriptional networks regulating plant development. *Plant Cell*, **23**, 1219–1230.

Clouse, S.D., Langford, M. and McMorris, T.C. (1996) A brassinosteroid-insensitive mutant in *Arabidopsis thaliana* exhibits multiple defects in growth and development. *Plant Physiol.* **111**, 671–678.

Hacham, Y., Holland, N., Butterfield, C., Ubeda-Tomas, S., Bennett, M.J., Chory, J. and Savaldi-Goldstein, S. (2010) Brassinosteroid perception in the epidermis controls root meristem size. *Development*, **138**, 839–848.

Hanai, H., Matsuno, T., Yamamoto, M., Matsubayashi, Y., Kobayashi, T., Kamada, H. and Sakagami, Y. (2000) A secreted peptide growth factor, phytosulfokine, acting as a stimulatory factor of carrot somatic embryo formation. *Plant Cell Physiol.* **41**, 27–32.

Hooker, T.S., Millar, A.A. and Kunst, L. (2002) Significance of the expression of the CER6 condensing enzyme for cuticular wax production in Arabidopsis. *Plant Physiol.* **129**, 1568–1580.

Horton, R.M., Hunt, H.D., Ho, S.N., Pullen, J.K. and Pease, L.R. (1989) Engineering hybrid genes without the use of restriction enzymes: gene splicing by overlap extension. *Gene*, **77**, 61–68.

Hung, C.Y., Lin, Y., Zhang, M., Pollock, S., Marks, M.D. and Schiefelbein, J. (1998) A common position-dependent mechanism controls cell-type patterning and GLABRA2 regulation in the root and hypocotyl epidermis of Arabidopsis. *Plant Physiol.* **117**, 73–84.

Jin, H., Yan, Z., Nam, K.H. and Li, J. (2007) Allele-specific suppression of a defective brassinosteroid receptor reveals a physiological role of UGGT in ER quality control. *Mol. Cell*, **26**, 821–830.

Komori, R., Amano, Y., Ogawa-Ohnishi, M. and Matsubayashi, Y. (2009) Identification of tyrosylprotein sulfotransferase in Arabidopsis. *Proc. Natl Acad. Sci. USA*, **106**, 15067–15072.

Kutschera, U. (1992) The role of the epidermis in the control of elongation growth in stems and coleoptiles. *Bot. Acta.* **105**, 246–252.

Kutschera, U. (2008) The growing outer epidermal wall: design and physiological role of a composite structure. *Ann. Bot.* **101**, 615–621.

Kutschera, U. and Niklas, K.J. (2007) The epidermal-growth-control theory of stem elongation: an old and a new perspective. *J. Plant Growth Regul.* **164**, 1395–1409.

Kutschmar, A., Rzewuski, G., Stührwohldt, N., Beemster, G.T.S., Inzé, D. and Sauter, M. (2009) PSK-α promotes root growth in Arabidopsis. *New Phytol.* **181**, 820–831.

Lin, Y. and Schiefelbein, J. (2001) Embryonic control of epidermal cell patterning in the root and hypocotyl of Arabidopsis. *Development*, **128**, 3697–3705.

Livak, K.J. and Schmittgen, T.D. (2001) Analysis of relative gene expression data using real-time quantitative PCR and the 2(-Delta Delta C(T)) method. *Methods*, **25**, 402–408.

Marcotrigiano, M. (2001) Genetic mosaics and the analysis of leaf development. *Int. J. Plant Sci.* **162**, 513–525.

Matsubayashi, Y., Ogawa, M., Morita, M. and Sakagami, Y. (1997) Phytosulfokine, sulfated peptides that induce the proliferation of single mesophyll cells of *Asparagus officinalis* L. *Proc. Natl Acad. Sci. USA*, **93**, 7623–7627.

Matsubayashi, Y., Ogawa, M., Morita, M. and Sakagami, Y. (2002) An LRR receptor kinase involved in perception of a peptide plant hormone, phytosulfokine. *Science*, **296**, 1470–1472.

Matsubayashi, Y., Ogawa, M., Kihara, H., Niwa, M. and Sakagami, Y. (2006) Disruption and overexpression of Arabidopsis phytosulfokine receptor gene affects cellular longevity and potential for growth. *Plant Physiol.* **142**, 45–53.

Matsuzaki, Y., Ogawa-Ohnishi, M., Mori, A. and Matsubayashi, Y. (2010) Secreted peptide signals required for maintenance of root stem cell niche in Arabidopsis. *Science*, **329**, 1065–1067.

Millar, A.A., Clemens, S., Zachgo, S., Giblin, E.M., Taylor, D.C. and Kunst, L. (1999) *CUT1*, an Arabidopsis gene required for cuticular wax biosynthesis and pollen fertility, encodes a very-long-chain fatty acid condensing enzyme. *Plant Cell*, **11**, 825–838.

Murashige, T. and Skoog, F. (1962) A revised medium for rapid growth and bioassays with tobacco cultures. *Plant Physiol.* **15**, 473–497.

Müssig, C., Shin, G.H. and Altmann, T. (2003) Brassinosteroids promote root growth in Arabidopsis. *Plant Physiol.* **133**, 1261–1271.

Nam, K.H. and Li, J. (2002) BRI1/BAK1, a receptor kinase pair mediating brassinosteroid signaling. *Cell*, **110**, 203–212.

Niklas, K. and Paolillo, D. (1997) The role of the epidermis as a stiffening agent in Tulipa (Liliaceae) stems. *Am. J. Bot.* **84**, 735.

Noguchi, T., Fujioka, S., Takatsuto, S., Sakurai, A., Yoshida, S., Li, J. and Chory, J. (1999) Arabidopsis det2 is defective in the conversion of (24R)-24-methylcholest-4-En-3-1 to (24R)-24-methyl-5alpha-cholestan-3-1 in brassinosteroid biosynthesis. *Plant Physiol.* **20**, 833–840.

Paredez, A.R., Somerville, C.R. and Ehrhardt, D.W. (2006) Visualization of cellulose synthase demonstrates functional association with microtubules. *Science*, **312**, 1491–1495.

Peters, W.S. and Tomos, A.D. (1996) The history of tissue tension. *Ann. Bot.* **77**, 657–665.

Savaldi-Goldstein, S. and Chory, J. (2008) Growth coordination and the shoot epidermis. *Curr. Opin. Plant Biol.* **11**, 42–48.

Savaldi-Goldstein, S., Peto, C. and Chory, J. (2007) The epidermis both drives and restricts plant shoot growth. *Nature*, **446**, 199–202.

Serralbo, O., Pérez-Pérez, J.M., Heidstra, R. and Scheres, B. (2006) Non-cell-autonomous rescue of anaphase-promoting complex function revealed by mosaic analysis of HOBBIT, an Arabidopsis CDC27 homolog. *Proc. Natl Acad. Sci. USA*, **103**, 13250–13255.

Srivastava, R., Liu, J.X. and Howell, S. (2008) Proteolytic processing of a precursor protein for a growth-promoting peptide by a subtilisin serine protease in Arabidopsis. *Plant J.* **56**, 219–227.

Stahl, Y. and Simon, R. (2010) Plant primary meristems: shared functions and regulatory mechanisms. *Curr. Opin. Plant Biol.* **13**, 53–58.

Stewart, R.N. and Burk, L.G. (1970) Independence of tissues derived from apical layers in ontogeny of the tobacco leaf and ovary. *Am. J. Bot.* **57**, 1010–1016.

Stührwohldt, N., Dahlke, R.I., Steffens, B., Johnson, A. and Sauter, M. (2011) Phytosulfokine-α controls hypocotyl length and cell expansion in *Arabidopsis thaliana* through phytosulfokine receptor 1. *PLoS ONE*, **6**, e21054.

Szymkowiak, E.J. and Sussex, I.M. (1996) What chimeras can tell us about plant development. *Annu. Rev. Plant Physiol. Plant Mol. Biol.* **47**, 351–376.

Uyttewaal, M., Burian, A., Alim, K. *et al.* (2012) Mechanical stress acts via katanin to amplify differences in growth rate between adjacent cells in Arabidopsis. *Cell*, **149**, 439–451.

Winter, D., Vinegar, V., Nahal, H., Ammar, R., Wilson, G.V. and Provart, N.J. (2007) An ''Electronic Fluorescent Pictograph'' browser for eexploring and analyzing large-scale biological data sets. *PLoS ONE*, **8**, e718.

Wu, G., Wang, X., Li, X., Kamiya, Y., Otegui, M.S. and Chory, J. (2011) Methylation of a phosphatase specifies dephosphorylation and degradation of activated brassinosteroid receptors. *Sci. Signal.* **172**, ra29.

Yang, H., Matsubayashi, Y., Hagani, H. and Sakagami, Y. (2000) Phytosulfokine-a, a peptide growth factor found in higher plants: its structure, functions and receptors. *Plant Cell Physiol.* **41**, 825–830.

Yang, H., Matsubayashi, Y., Hagani, H., Nakamura, K. and Sakagami, Y. (2001) Diversity of Arabidopsis genes encoding precursors for phytosulfokine, a peptide growth factor. *Plant Physiol.* **127**, 842–851.

Supplementary Figure S1

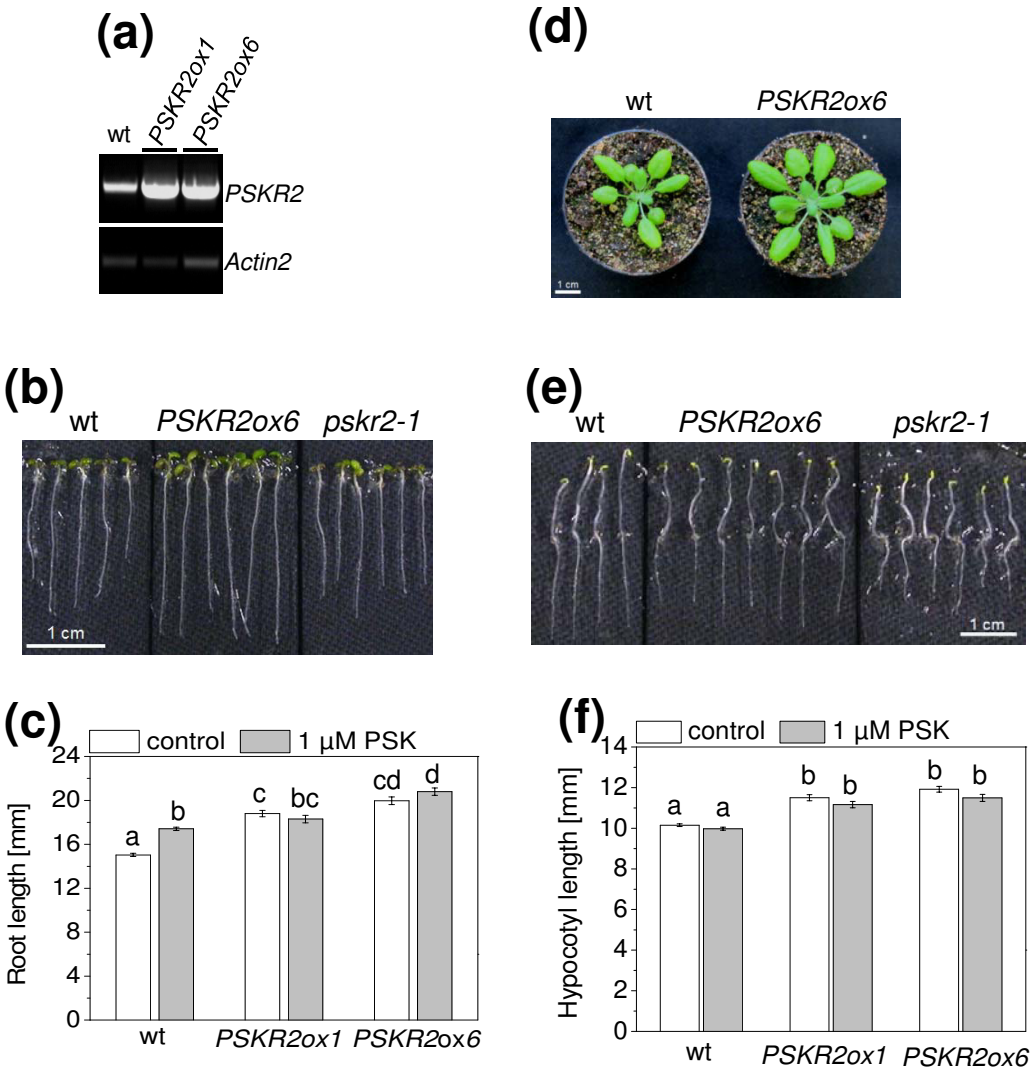

Supplemental Figure S2

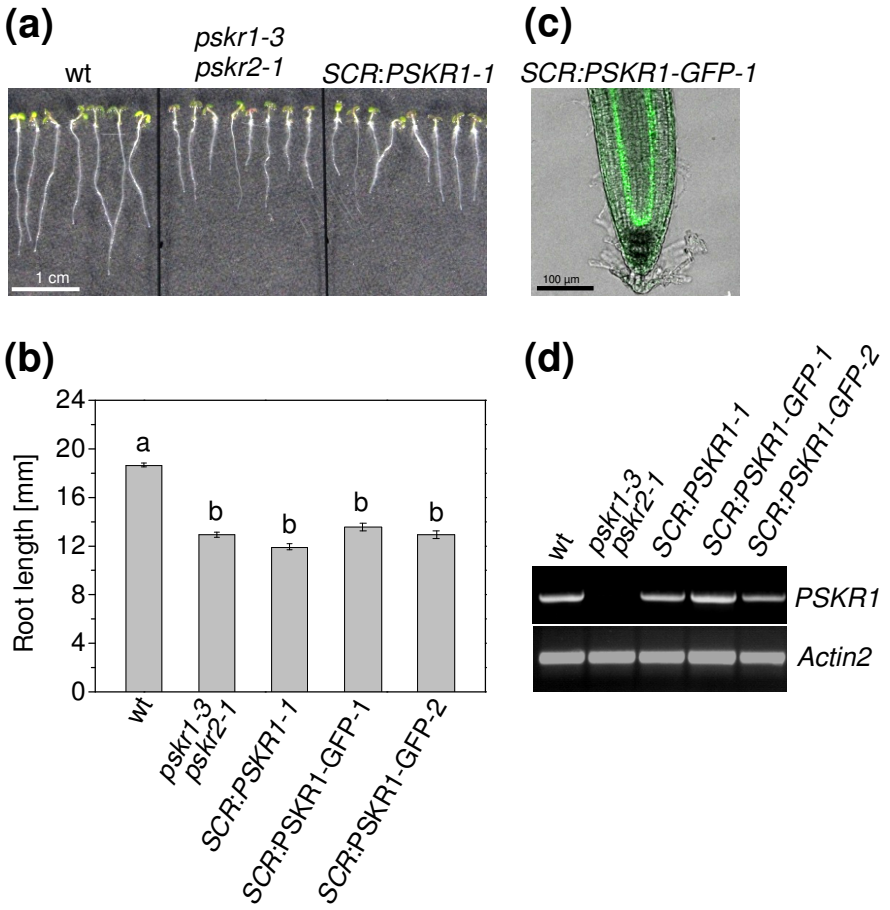

LEGEND FOR SUPPORTING INFORMATION

Supplemental Figure S1. Overexpression of *PSKR2* promotes root and hypocotyl growth. (A) RT-PCR analysis of *PSKR2* expression in leaves of 14-day-old wt, *PSKR2ox1* and *PSKR2ox6* plants. *Actin2* cDNA was amplified as a control for RNA input. (B) Phenotypes of 5-day-old de-etiolated wt, *PSKR2ox6* and *pskr2-1* seedlings. (C) Average (± SE) root lengths of 5-day-old de-etiolated wt, *PSKR2ox1* and *PSKR2ox6* seedlings raised with or without 1 µM PSK were determined in two independent experiments with n ≥61 seedlings analyzed per genotype and treatment. (D) Phenotypes of 4-week old soil-grown wt and *PSKR2ox6* plants. (E) Phenotypes of 5-day-old etiolated wt, *PSKR2ox6* and *pskr2-1* seedlings. (F) Average (± SE) hypocotyl lengths of 5-day-old etiolated wt, *PSKR2ox1* and *PSKR2ox6* seedlings raised with or without 1 µM PSK determined in two experiments with n≥47 seedlings. (C, F) Different letters indicate significantly different values (P<0.001, ANOVA, Tukey test).

Supplemental Figure S2. PSK perception in the endodermis is not sufficient to promote root growth. (a) Phenotypes of 5-day-old de-etiolated seedlings from wt, *pskr1-3 pskr2-1* (*r1r2*) and the complementation line *r1r2 SCR*:*PSKR1-1*. (b) Average (± SE) root lengths were determined for the lines indicated in three independent experiments with at least 46 seedlings analyzed per genotype. Different letters indicate significantly different values (P<0.001, ANOVA, Tukey test). (c) PSKR1-GFP was detected in the endodermis of 5-day-old de-etiolated *SCR:PSKR1-GFP-1* seedlings by confocal laser scanning microscopy. Scale bar = 100 µm. (d) Expression of PSKR1 was analyzed by RT-PCR in 5-day-old seedlings from wildtype (wt), *r1r2*, *SCR*:*PSKR1-1*, *SCR:PSKR1-GFP-1* and *SCR:PSKR1-GFP-2* in the *r1r2* background. Actin2 cDNA was amplified as a control for RNA input.

Kapitel 2

Kinase activity and calmodulin binding are essential for growth signaling by the phytosulfokine receptor PSKR1

Die in diesem Kapitel enthaltenen Arbeiten, mit Ausnahme der in Kooperation mit der Arbeitsgruppe von Prof. Dietrich (Universität Erlangen) durchgeführten BiFC-Analyse, wurden im Rahmen dieser Doktorarbeit von mir angefertigt.

the plant journal

SEB Society for Experimental Biology

The Plant Journal (2014) **78,** 192–202 doi: 10.1111/tpj.12460

Kinase activity and calmodulin binding are essential for growth signaling by the phytosulfokine receptor PSKR1

Jens Hartmann[1], Cornelia Fischer[2], Petra Dietrich[2] and Margret Sauter[1,*]

[1]Entwicklungsbiologie und Physiologie der Pflanzen, Universität Kiel, Am Botanischen Garten 5, Kiel 24118, Germany, and [2]Molekulare Pflanzenphysiologie, Friedrich-Alexander-Universität Erlangen-Nürnberg, Staudtstrasse 5, Erlangen 91058, Germany

Received 2 December 2013; revised 16 January 2014; accepted 22 January 2014; published online 4 February 2014.
*For correspondence (e-mail msauter@bot.uni-kiel.de).

SUMMARY

The cell growth-promoting peptide phytosulfokine (PSK) is perceived by leucine-rich repeat (LRR) receptor kinases. To elucidate PSK receptor function we analyzed PSKR1 kinase activity and binding to Ca^{2+} sensors and evaluated the contribution of these activities to growth control *in planta*. Ectopically expressed PSKR1 was capable of auto- and transphosphorylation. Replacement of a conserved lysine within the ATP-binding region by a glutamate resulted in the inhibition of auto- and transphosphorylation kinase activities. Expression of the kinase-inactive PSKR1(K762E) receptor in the *pskr* null background did not restore root or shoot growth. Instead, the mutant phenotype was enhanced suggesting that the inactive receptor protein exerts growth-inhibitory activity. Bioinformatic analysis predicted a putative calmodulin (CaM)-binding site within PSKR1 kinase subdomain VIa. Bimolecular fluorescence complementation analysis demonstrated that PSKR1 binds to all isoforms of CaM, more weakly to the CaM-like protein CML8 but apparently not to CML9. Mutation of a conserved tryptophan (W831S) within the predicted CaM-binding site strongly reduced CaM binding. Expression of PSKR1(W831S) in the *pskr* null background resulted in growth inhibition that was similar to that of the kinase-inactive receptor. We conclude that PSK signaling requires Ca^{2+}/CaM binding and kinase activity of PSKR1 *in planta*. We further propose that the inactivated kinase interferes with other growth-promoting signaling pathway(s).

Keywords: phytosulfokine, calmodulin, calcium, *Arabidopsis thaliana*, kinase activity, LRR receptor kinase, root growth.

INTRODUCTION

Peptide signaling has been recognized as a key mechanism for the control of growth and development in plants. CLAVATA3/EMBRYO SURROUNDING REGION (ESR)-related (CLE) peptides play a central role in regulating the activities and organization of shoot and root apical meristems (Kondo *et al.*, 2006; Ohyama *et al.*, 2009; Matsuzaki *et al.*, 2010; Meng *et al.*, 2012; Stahl *et al.*, 2013). Sulfonylation at tyrosine residues is required for the function of the peptides PSY1 and phytosulfokine (PSK) (Komori *et al.*, 2009). PSY1 is a tyrosine-sulfonylated and glycosylated peptide (Amano *et al.*, 2007). PSK is a dityrosine-sulfonylated pentapeptide with the amino acid backbone YIYTQ (Matsubayashi and Sakagami, 1996). Both peptides promote growth through enhanced cell elongation (Amano *et al.*, 2007; Stührwohldt *et al.*, 2011; Hartmann *et al.*, 2013) and have been implicated in the response to pathogens (Loivamäki *et al.*, 2010; Mosher *et al.*, 2013; Shen and Diener, 2013).

Phytosulfokine is perceived by receptor proteins that belong to the receptor-like kinase family (Matsubayashi *et al.*, 2002; Gish and Clark, 2011). The leucine-rich repeat (LRR) PSK receptor kinase is encoded by two genes in *Arabidopsis thaliana*. PSKR1 and PSKR2 have been assigned to subfamily LRRX of the LRR receptor kinase family (Osakabe *et al.*, 2013). They are closely related to the brassinosteroid receptor BRASSINOSTEROID INSENSITIVE 1 (BRI1) and to the CLV3 receptor CLAVATA1 (CLV1). PSK receptors possess a predicted extracellular N-terminal domain with 21 LRRs each consisting of 24 amino acids (Matsubayashi *et al.*, 2002). LRR 18 is interrupted by an island domain that was shown to bind the ligand PSK (Shinohara *et al.*, 2007). Binding of PSK to its receptor was shown for carrot (*Daucus carota*) and Arabidopsis (Matsubayashi *et al.*, 2002, 2006).

The PSK receptor protein has a single helical transmembrane domain which ankers it in the plasma membrane.

The cytoplasmic region of PSK receptors is a predicted serine/threonine kinase based on the 12 subdomains typically found in this class of kinases (Hanks *et al.*, 1988; Lindberg *et al.*, 1992; Matsubayashi *et al.*, 2002) (Figure S1).

Kinases are characterized by highly conserved domains (Li and Chory, 1997). In particular the residues that are engaged in ATP binding and phosphotransfer have been well characterized. The ATP-binding kinase fold of Ser/Thr protein kinases consists of an N-terminal (N) lobe with 5 β-sheets and one α-helix, and a C lobe. ATP is bound in a cleft between these two lobes that is covered by a highly conserved phosphate binding loop extending between the first two β-sheets of the N lobe. A conserved Lys residue within the ATP-binding cleft of subdomain II (K911 in BRI1) is engaged in positioning the α- and β-phosphate groups for ATP hydrolysis (Huse and Kuriyan, 2002). Stability and proper positioning of this Lys is achieved through the interaction with a conserved Glu in subdomain III in the α-helix of the N lobe. Mutation of the Lys to Glu (K911E) abolished kinase activity of BRI1 *in vitro* (Oh *et al.*, 2000). The so-called activation loop in subdomain VIII interacts with the α-helix of the N lobe and prevents either substrate binding and/or lowers the rate of phosphotransfer to the substrate in the kinase-off state (Huse and Kuriyan, 2002; Adams, 2003). Phosphorylation of the activation loop results in a conformational change that strongly promotes kinase activity (Adams, 2003).

The ectopically expressed soluble PSKR1 receptor kinase domain of Arabidopsis possesses kinase activity *in vitro* (Kwezi *et al.*, 2011). Interestingly, PSKR1 also exhibits guanylate cyclase (GC) activity *in vitro* and a GC center was identified within subdomain IX of the kinase (Kwezi *et al.*, 2011; Wong and Gehring, 2013) (Figure S1). Ectopically expressed soluble protein was shown to generate cGMP from GTP *in vitro*. Hence the intracellular domain of PSK receptor PSKR1 can act as a kinase and as a GC *in vitro* (Kwezi *et al.*, 2011; Wong and Gehring, 2013) indicative of multiple signal outputs. The role of either the kinase activity or the GC activity for *in planta* PSK signaling has not been described.

Calmodulins (CaM) are Ca^{2+}-binding proteins that alter their affinity to target proteins upon Ca^{2+} binding and regulate their activity (McCormack *et al.*, 2005; Dodd *et al.*, 2010). CaMs translate changes in local Ca^{2+} concentrations into a specific physiological response. In Arabidopsis, four CaM isoforms are encoded by seven genes: CaM1/CaM4, CaM2/CaM3/CaM5, CaM6 and CaM7 (DeFalco *et al.*, 2009). CaM-binding protein domains are overall little conserved in their primary sequences but share a conserved amphipathic α-helix with the hydrophobic face binding to CaM. The receptor kinases SRK from *Brassica oleracea* (Vanoosthuyse *et al.*, 2003), RLK4, CLV1 (Charpenteau *et al.*, 2004) and BRI1 (Oh *et al.*, 2012) from Arabidopsis were shown to bind CaM.

The CaM-binding domain mapped in BRI1 is conserved in PSKR1 and PSKR2 suggesting that PSK receptor activity may be modulated by Ca^{2+} signaling. In this study we functionally characterized two biochemical activities of PSKR1, kinase activity and CaM binding. We identified a CaM-binding site for PSKR1 and show binding of CaM to PSKR1 *in vivo*. We further studied the contribution of phosphorylation and CaM binding to receptor function *in planta* by expressing site-mutated PSKR1 variants in the receptor null background. This approach led us to conclude that kinase activity and CaM binding of PSKR1 are essential for growth signaling through PSKR1 *in planta*.

RESULTS

PSKR1 acts as an auto- and transphosphorylating kinase

Phytosulfokine receptors belong to the LRR family of receptor kinases (Figure 1a). Alignment of the cytoplasmic carboxyl termini of the PSK receptors PSKR1 and PSKR2 with related protein kinases suggests that the PSKR1 kinase domain with its 12 subdomains extends from amino acid 733–1003 (Figure S1). The juxtamembrane domain thus extends from amino acid 681–732. Localized within the kinase subdomains I and II is the ATP-binding site that is highly conserved in all kinases including the closely related LRR receptor kinases SERK1, BRI1, BAK1 and CLV1 (Figure 1b). From studies using single and double gene knock out lines, PSKR1 rather than PSKR2 was shown to regulate growth signaling in Arabidopsis roots and shoots (Kutschmar *et al.*, 2009). We therefore chose PSKR1 to elucidate PSK receptor function. To study PSKR1 kinase activity *in vitro*, we ectopically expressed the kinase domain of PSKR1 from amino acid 686–1008 as a fusion protein with an N-terminal H_6-tag to generate H_6-PSKR1-KD. Affinity-purified H_6-PSKR1-KD protein autophosphorylated when incubated with [γ-^{32}P]ATP (Figure 1c). The ability of H_6-PSKR1-KD to phosphorylate other proteins was shown with the common substrate myelin basic protein (MBP), the phosphorylated protein with a size of about 21.5 kDa corresponds to monomeric MBP with a typical retained migration on the gel (Cheifetz and Moscarello, 1985). The phosphorylated proteins with a size of about 24 kDa and 40 kDa could correspond to the multimeric complexes of MBP that were reported previously (Määttä *et al.*, 1997). An invariant Lys residue in subdomain II is directly involved in the phosphotransfer reaction of kinases (Kamps and Sefton, 1986) (Figures S1 and 1a, b). To test if the PSKR1 kinase was likewise functionally conserved we generated a mutant kinase in which Glu replaced this Lys residue (Figure 1a). The H_6-PSKR1-K762E protein had no auto- or transphosphorylation activity *in vitro* (Figure 1c).

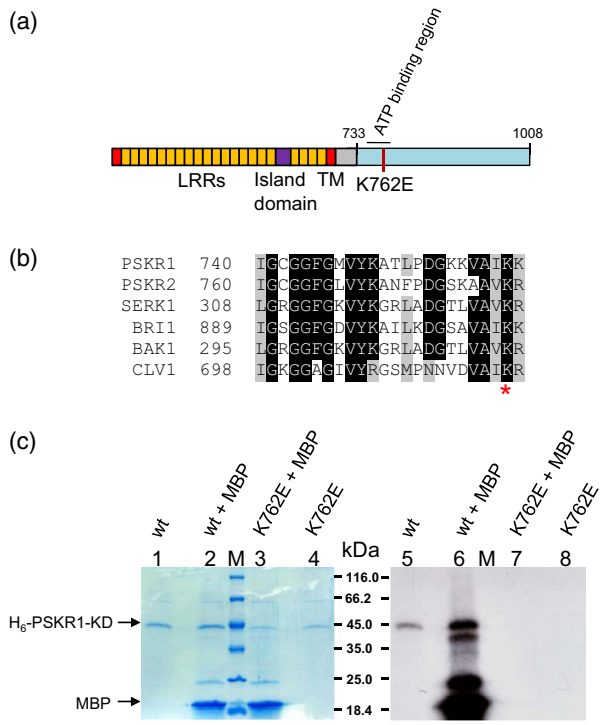

Figure 1. A conserved lysine residue in the PSKR1 ATP-binding site is essential for PSKR1 kinase activity *in vitro*.
(a) Model of PSKR1 (not drawn to scale) indicating from left to right the N-terminal signal peptide (red), the extracellular leucine-rich repeats (LRRs) (yellow) intersected by an island domain (purple), a transmembrane domain (TM, red), the intracellular juxtamembrane domain (gray) and the intracellular kinase region (light blue). Within the cytoplasmic Ser/Thr kinase region a bar indicates the ATP-binding site of 24 amino acids. A point mutation that results in the exchange of Lys 762 for a Glu residue is indicated by a red line.
(b) Sequence alignment of the 24 amino acid-long ATP-binding site of the related LRR receptors PSKR1, PSKR2, SERK1, BRI1, BAK1 and CLV1 from Arabidopsis. The conserved Lys that is also shown in (a) is marked by an asterisk. Amino acid sequences were aligned using ClustalW.
(c) Auto- and transphosphorylation activity analysis of recombinant PSKR1-KD (KD = kinase domain). The left side shows a Coomassie blue-stained gel with affinity-purified H_6–PSKR1–KD (lanes 1 and 2) or the mutant H_6–PSKR1–K762E (lanes 3 and 4) with (lanes 2 and 3) or without (lanes 1 and 4) myelin basic protein (MBP). To the right, an autoradiograph is shown. Affinity-purified H_6–PSKR1–KD (lanes 5, 6) or the mutant H_6–PSKR1–K762E (lanes 7 and 8) were incubated with 20 μCi [γ-^{32}P]ATP in kinase buffer for 1 h at room temperature and separated by SDS-PAGE (same as to the left). The radiolabel was visualized with a phosphor imager. To test for transphosphorylation activity, H_6–PSKR1–KD (lane 6) or the mutant H_6–PSKR1–K762E (lane 7) were incubated with MBP at the same conditions. Molecular masses of marker proteins are indicated in between blots.

Kinase activity of PSKR1 is essential for growth signaling *in planta*

To analyze if the kinase activity of PSKR1 was required for growth regulation *in planta* we generated a point-mutated K762E full-length *PSKR1* sequence. The mutant variant was placed under the control of the 35S cauliflower mosaic virus promoter as well as under the control of the endogenous *PSKR1* promoter (Kutschmar *et al.*, 2009). The *35S:PSKR1(K762E)* and the *PSKR1:PSKR1(K762E)* constructs were transformed into the receptor null *pskr1-3 pskr2-1* (subsequently abbreviated as *r1r2*) background. At least four independent transformant lines were identified and analyzed. The representative lines *35S:PSKR1(K762E)-1* and *PSKR1:PSKR1(K762E)-1* had transgene transcript levels that were comparable to or slightly higher than *PSKR1* mRNA levels in the wild-type (Figure 2a). The null background line *r1r2* had no detectable *PSKR1* mRNA.

The role of PSKR1 kinase activity for growth promotion in roots was analyzed in 5-day-old seedlings (Figure 2b,c). Compared to the wild type, *r1r2* seedlings were characterized by a short-root phenotype. Expression of *PSKR1-GFP* in *r1r2* under the control of the 35S promoter restored root growth. PSKR1-GFP fluorescence was observed at the periphery of the epidermal cells, indicating the expression and plasma membrane localization of the PSKR1-GFP protein (Figure 2d). By contrast, *r1r2* seedlings expressing the PSKR1(K762E) receptor variant ubiquitously (*35S:PSKR1(K762E)-1)* or under control of the PSKR1 promoter (*PSKR1:PSKR1(K762E)-1)* developed roots that were significantly shorter by 47 and 44% than wild-type roots and that were significantly shorter than roots of *r1r2* seedlings which are kinase-deficient. These data showed that the kinase activity is essential for PSKR1 growth signaling and in addition suggested a dominant-negative effect of the PSKR1(K762E) receptor variant.

A role for PSK signaling in shoot growth was also observed. Rosettes of 4-week-old soil-grown *r1r2* plants were smaller than rosettes of wild-type plants or of complemented *r1r2 35S:PSKR1-GFP-1* plants (Figure 3a,b). Likewise, rosettes of *r1r2 PSKR1(K762E)* plants were smaller than rosettes of wild-type plants and were similar in diameter to the genetic background line *r1r2*. A growth phenotype was also evident at the cellular level (Figure 3c–f). Epidermal cells of the first rosette leaf of 4-week-old soil-grown plants of *r1r2* and of *r1r2 35S:PSKR1(K762E)-1* appeared smaller than wild-type cells or cells of *r1r2 35S:PSKR1-GFP-1*. Taken together, abolishing PSKR1 kinase activity through a targeted point mutation resulted in root and shoot growth retardation.

Calmodulin binding to PSKR1 is required for growth promotion

Analysis of the PSKR1 sequence by algorithms that predict CaM-binding domains (http://calcium.uhnres.utoronto.ca/ctdb/ctdb/home.html, Yap *et al.*, 2000) revealed a putative calmodulin (CaM) binding site within the PSKR1 kinase subdomain VIa (Figures S1 and 4a). This site is highly conserved in distinct LRR-RKs including PSKR2, SERK1, BRI1, BAK1 and CLV1 suggesting that these may be subject to regulation by Ca^{2+}/CaM signaling. The predicted CaM-binding site is structured as an amphipathic α-helix (Figure 4b, c).

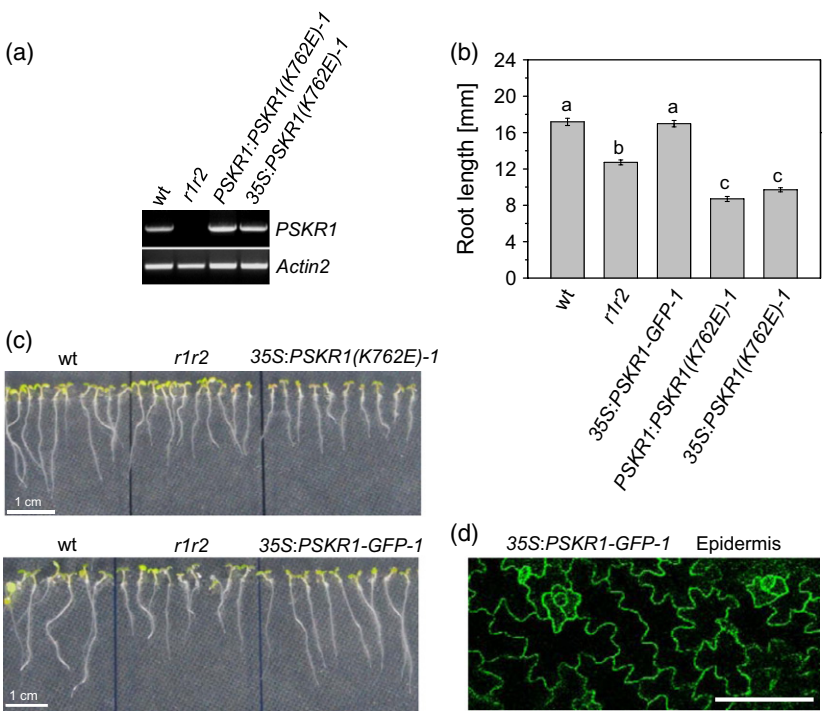

Figure 2. PSKR1 kinase activity is essential for growth regulation through PSKR1 *in planta*.
(a) Expression of *PSKR1* was analyzed by RT-PCR in 5-day-old seedlings from wild type (wt), *r1r2*, *r1r2 PSKR1:PSKR1(K762E)* (*PSKR1:PSKR1 (K762E)-1*), and *r1r2 35S:PSKR1(K762E)* (*35S: PSKR1(K762E)-1*). *Actin2* cDNA was amplified as a control for RNA input.
(b) Average (±standard error (SE)) root lengths were determined in two independent experiments with at least 32 seedlings analyzed per genotype. $^{a-c}$Different letters indicate significantly different values ($P < 0.001$, ANOVA, Tukey test).
(c) Phenotypes of 5-day-old de-etiolated seedlings from wt, *r1r2*, and the complementation lines *35S:PSKR1(K762E)-1* and *35S:PSKR1-GFP* in the *r1r2* background.
(d) PSKR1-GFP localization was analyzed by confocal laser scanning microscopy in the epidermis of cotyledons of 5-day-old de-etiolated *35S:PSKR1-GFP-1* seedlings. The receptor protein is expressed and localized at the plasma membrane. Scale bar = 100 μm.

To test for an interaction between CaM and PSKR1 we performed bimolecular fluorescence complementation (BiFC) analysis. The N-terminal half of the Venus fluorophor (VN) was fused C-terminally of PSKR1, while the C-terminal half of the Venus protein (VC) was added to the N-terminus of the variant CaM proteins from Arabidopsis, CaM2, CaM4, CaM6 and CaM7, as well as to the two CaM-like proteins CML8 and CML9. Interactions were studied in tobacco epidermal cells following co-expression of the fusion proteins. Fluorescence complementation was observed for all VC-CaM fusion proteins in the presence of PSKR1-VN (Figure 5a,c,e,g,m). The BiFC signal was observed at the periphery of the epidermal cells, indicating interaction of PSKR1 with calmodulin at the plasma membrane. Weaker signals were observed in case of the CaM-like protein CML8 and no signals above background levels were detected in case of CML9 (Figure 5i,k). A conserved tryptophan residue at the hydrophobic face of the amphipathic α-helix was previously shown to be critical for CaM binding to CaMKI (Matsushita and Nairn, 1998). To test if CaM binding occurred at this predicted site and hence to verify specificity of the *in planta* CaM-PSKR1 interaction the Trp at position 831 was replaced by a Ser residue. When VC-CaMs were co-expressed with $PSKR1_{W831S}$-VN, the fluorescence complementation was strongly reduced for any VC-CaM variant, and VC-CML8 (Figure 5b,d,f,h,j,m). Similar to the wild-type receptor no interaction was observed between $PSKR1_{W831S}$-VN and VC-CML9 (Figure 5l,m). The data showed that the interaction of PSKR1 with CaMs was specific and occurred at the predicted binding site.

We next asked if a functional CaM-binding site was required for growth regulation through PSKR1 *in planta*. $PSKR1_{W831S}$ was therefore expressed in the receptor null background *r1r2*, under the control of the 35S promoter. Four independent *35S:PSKR1(W831S)* lines with expression levels comparable with or higher than those of the wild-type receptor were identified (Figure 6a). Root lengths were determined in seedlings after a 5 day growth period in the light (Figure 6b,c). For comparison, seedlings of the wild-type, the *r1r2* null mutant, and of the complementation line *r1r2 35S:PSKR1-GFP-1* were analyzed. The short-root phenotype of *r1r2* was complemented by *35S: PSKR1-GFP* expression as shown above (Figures 2b,c and 6c). By contrast, expression of the PSKR1(W831S) receptor variant did not restore seedling root growth indicating that growth signaling was prevented when the CaM-binding site was defective. More so, seedlings of all four *r1r2 35S: PSKR1(W831S)* lines displayed significantly shorter roots than those of the genetic background *r1r2*. Roots of *r1r2* seedlings were about 25% shorter than wild-type roots while roots of *r1r2 35S:PSKR1(W831S)* lines were about 40-45% shorter. These results may indicate a dominant-negative effect of the PSKR1(W831S) receptor protein as may be the case for the kinase-inactive receptor variant (Figure 2).

Growth retardation was also observed during vegetative development. Rosettes of 4-week-old *r1r2 35S:PSKR1 (W831S)* plants were smaller than those of wild-type or of *r1r2 35S:PSKR1-GFP* plants (Figure 6d,e). Reduced shoot size was accompanied by smaller leaf epidermal cells as shown for the *r1r2 35S:PSKR1(W831S)-2* line (Figure 6i).

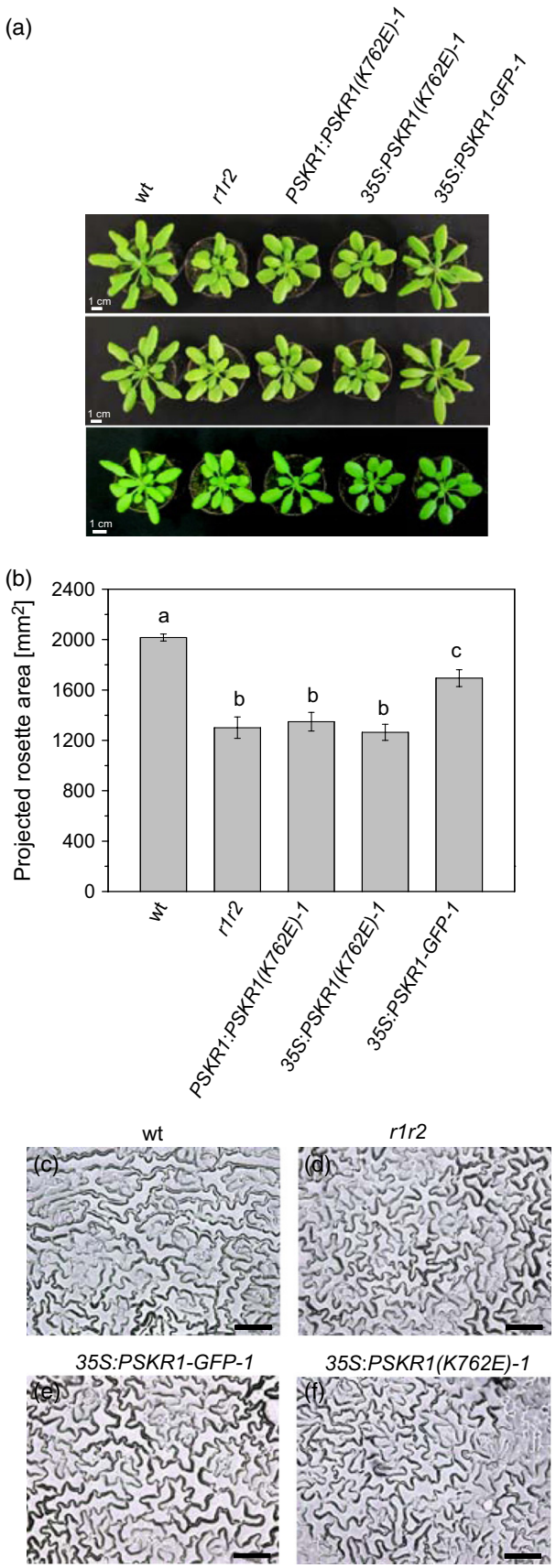

CaM binding to PSKR1 thus appears to contribute to the regulation of cell expansion via PSKR1 signaling.

DISCUSSION

PSKR1 is a functional kinase and phosphorylation is an essential signaling event

The kinase domain of PSKR1 was shown in this study to have both auto- and transphosphorylation activity *in vitro* in agreement with a previous report (Kwezi *et al.*, 2011). Mutation of a conserved lysine to glutamate in the ATP-binding site resulted in loss of PSKR1 kinase activity. As the mutation of the corresponding residue in BRI1 also abolished its kinase activity (Oh *et al.*, 2000) the findings underline the conservation of the kinase domain structure and function in these receptor-like proteins. We furthermore demonstrated the contribution of PSKR1 kinase activity to growth promotion *in planta*. While expression of a PSKR1-GFP fusion protein restored the wild-type growth phenotype in the PSK receptor null mutant, the kinase-dead version of PSKR1 further enhanced the retardation of root growth compared with *r1r2* plants. This growth-inhibitory effect may be explained by an interaction of the kinase-dead receptor with another growth-regulating protein. Dominant-negative effects have been described for other mutated plant RLKs (Diévart and Clark, 2003; Morillo and Tax, 2006) and for kinase-dead variants of BAK1, CLV1 and BRI1 (Li *et al.*, 2002; Diévart *et al.*, 2003; Wang *et al.*, 2005).

Phytosulfokine signaling was previously shown to promote root and shoot growth primarily through cell expansion. In addition, PSK signaling via PSKR1 helps maintain the low proliferation rate of quiescent center cells in the root apical meristem (Heyman *et al.*, 2013). The abundance of either PSK ligand or receptor modulates the growth rate (Matsubayashi *et al.*, 2006; Kutschmar *et al.*, 2009; Stührwohldt *et al.*, 2011; Hartmann *et al.*, 2013). Interestingly, QC cell division activity is increased by brassinosteroid signaling via BRI1 through the transcription factor ERF115 which in turn activates the PSK precursor gene PSK4 (Heyman *et al.*, 2013) thus providing a molecular link between BR and PSK signaling. Our results show that PSKR1 kinase activity essentially contributes to growth promotion via PSKR1 signaling and that PSKR1 likely interacts with one or more proteins. The data support the idea

Figure 3. PSKR1 kinase activity promotes shoot growth.
(a) Phenotypes of 4-week-old soil-grown wt, *r1r2*, *PSKR1:PSKR1(K762E)-1*, *35S:PSKR1(K762E)-1* and *35S:PSKR1-GFP-1* plants each in the null background.
(b) The average projected rosette area (±standard error (SE), $n = 3$) was calculated using the program Rosette Tracker (De Vylder *et al.*, 2012). $^{a-c}$Different letters indicate significantly different values ($P < 0.05$, ANOVA, Tukey test).
(c–f) Epidermis cells of the first rosette leaf from 4-week-old soil-grown wt (c), *r1r2* (d), *35S:PSKR1-GFP-1* (e), and *35S:PSKR1(K762E)-1* (f) plants. Scale bar = 100 μm.

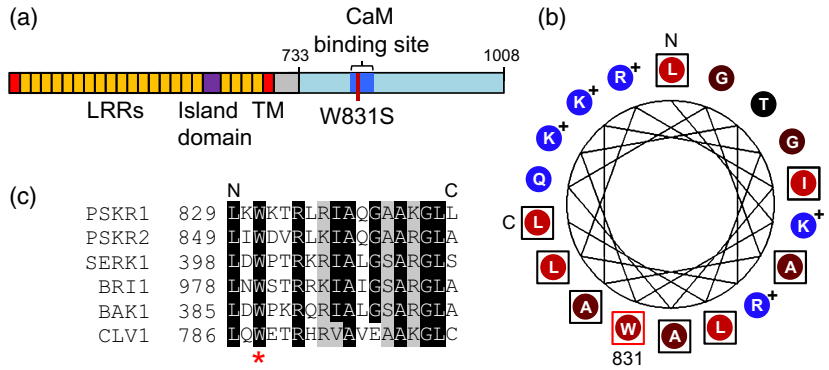

Figure 4. PSKR1 has a predicted calmodulin binding site.
(a) Model of PSKR1 showing a predicted 18-amino acid CaM-binding site (dark blue) within the cytoplasmic Ser/Thr kinase region. A point mutation (W831S) is indicated that results in the exchange of the hydrophobic Trp 831 for a hydrophilic Ser.
(b) Helical wheel projection of amino acids 829–846 representing the predicted PSKR1 CaM-binding site. Positively charged residues are marked by a plus, whereas hydrophobic residues are boxed. Hydrophobic W831 is marked by a red box. Amino acids 829–846 are predicted to form a secondary structure that is typical for CaM-binding: an amphiphilic α-helix with a positively charged face on one side and a predominantly hydrophobic face on the other side.
(c) Sequence alignment of predicted CaM-binding site of the LRR receptors PSKR1, PSKR2, SERK1, BRI1, BAK1 and CLV1 from Arabidopsis. The conserved hydrophobic Trp is marked by an asterisk. Amino acid sequences were aligned with ClustalW. (b, c) The first amino acid of the predicted PSKR1 CaM-binding site is marked by an 'N' and a 'C' indicates the last amino acid.

that PSKR1 shares signaling components with other growth-promoting signaling pathways such as the BR pathway. The BRI1-associated kinase 1 (BAK1) might be a candidate for a PSKR1 binding protein. BAK1 is a promiscuous LRR-RK that interacts with BRI1 and other receptor kinases (Chinchilla *et al.*, 2009). Interaction of BAK1 with BRI1 increases BRI1 kinase activity. Brassinosteroid signaling via BRI1 promotes cell expansion. Interference with brassinosteroid signaling by binding BAK1 to inactive PSK receptor might therefore result in growth retardation. Recently, Halter *et al.* (2014) showed that interaction of BAK1 with the small receptor-like kinase BIR2 prevents binding of BAK1 to the ligand-free flagellin receptor FLS2, and differentially affects BAK-dependent responses. Interacting proteins and the targets of the PSKR1 kinase are not known, and the impact of autophosphorylation and transphosphorylation on protein interactions, ligand binding, receptor activity, and possibly receptor abundance have yet to be elucidated. This study sets the stage for future detailed analyses.

PSK signaling involves binding of calmodulin to the receptor

We identified a CaM-binding domain in PSKR1 based on sequence similarity to BRI1. The soluble BRI1 kinase domain and CaM7 were co-expressed as tagged proteins in *Escherichia coli* and shown to interact in a Ca^{2+}-dependent manner by affinity chromatography pull-down assays (Oh *et al.*, 2012). Analysis of truncated BRI proteins localized the binding in the kinase domain. Interaction of CaM with the corresponding peptide was shown to occur *in vitro*. CaM binding reduced both auto- and transphosphorylation activity of BRI1 *in vitro* when both proteins were ectopically co-expressed in *E. coli* (Oh *et al.*, 2012). The CaM-binding site of BRI1 is conserved in related LRR-RKs including PSKRs. The role of CaM binding for signalling of growth or other responses *in planta* has not been elucidated for any of these LRR-RKs. Here, we provide evidence that PSKR1 binds to different CaM isoforms and that CaM binding is essential for PSKR1 activity *in planta*.

The CaM-binding domain of CaM-binding proteins is commonly restricted to a short region of 14–26 residues that tends to form a basic amphiphilic α-helix (O'Neil and DeGrado, 1990; Ishida and Vogel, 2006; Rainaldi *et al.*, 2007). The basic residues of the α-helix of the predicted PSKR1 CaM-binding domain likewise form a hydrophobic face with a tryptophan as the most hydrophobic residue. Hydrophobic residues such as Trp, Phe, Leu, Val or Ile are localized preferentially at the ends of the sequence that interacts with the N- and C-terminal domains of CaM (Rhoads and Friedberg, 1997; Yap *et al.*, 2000; Yamniuk and Vogel, 2004). The N-terminal Trp residue interacts more strongly with the C-terminal domain of CaM determining the relative orientation of the target within the channel formed by the CaM globular domains (Ikura *et al.*, 1992; Meador *et al.*, 1993; Yamauchi *et al.*, 2003). For CaMKI, the N-terminal Trp of the CaM-binding domain points outward so that its side chain displays high solvent exposure resulting in a high probability that the Trp is the site for the primary interaction with CaM (Goldberg *et al.*, 1996). The importance of hydrophobic residues near the ends of the CaM-binding domains of MLCK, CaMKII and NtMKP1 that act as anchor residues

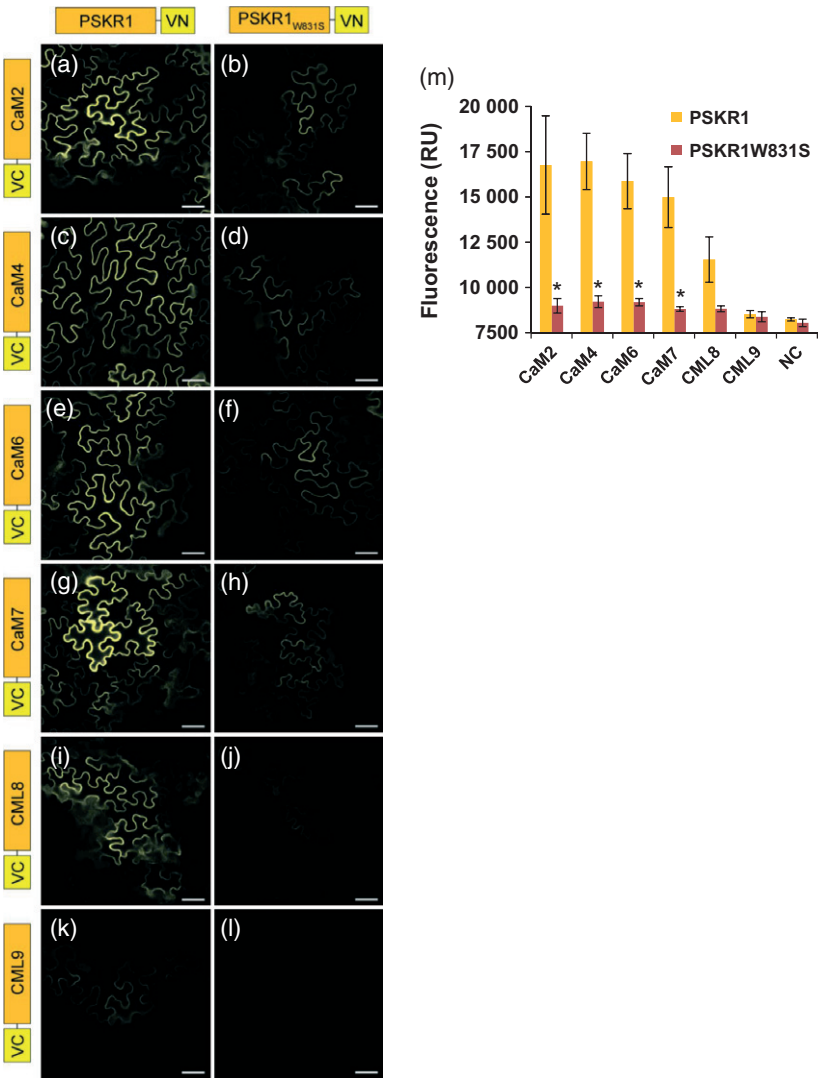

Figure 5. The PSK receptor PSKR1 interacts with calmodulins.
(a–l) Images of BiFC signals in tobacco epidermal cells after co-expression of wild-type PSKR1 (left column) or PSKR1(W831S) (right column) fused to the N-terminal part of Venus (VN) and CaMs/CMLs fused to the C-terminal part of Venus (VC). CaMs/CMLs co-expression partners for each experiment are depicted on the left. For comparison of the BiFC signal intensities all images were taken with the same laser intensities, photomultiplier settings and magnification, and were equally processed. Bars represent 50 μm.
(m) Fluorescence signal intensities (RU) of BiFC experiments were determined from complete leaf discs using a fluorescence reader. As a negative control a vector that contained VC only was used as co-expression partner for PSKR1-VN and PSKR1W831S-VN (NC). $n = 6$ for interaction with CaM2, CaM4 and CaM6; $n = 5$ for interaction with CaM7, CML8 and CaM9; $n = 3$ and 4 for interactions with VC. Asterisks indicate significantly different values of the wild type (wt) and mutated receptor with the CaM indicated ($P < 0.05$).

for CaM binding was documented in several studies (Ikura *et al.*, 1992; Meador *et al.*, 1992, 1993; Findlay *et al.*, 1995; Yamakawa *et al.*, 2004). Truncated peptides of the CaM-binding domain of a Ca^{2+}-ATPase of human erythrocytes that lack one of the terminal hydrophobic residues were shown to bind to CaM with reduced affinity (Kataoka *et al.*, 1991).

The exchange of the N-terminal hydrophobic anchor residue Trp 831 in the PSKR1 CaM-binding site for a hydrophilic serine strongly reduced the interaction with all CaM isoforms. This is in agreement with the view that the hydrophilic serine disturbs the hydrophobic face of the $PSKR1_{W831S}$ CaM-binding site resulting in a lowered hydrophobic moment (Heliquest calculation, Gautier *et al.*, 2008). The residual CaM interaction observed for $PSKR1_{W831S}$ may be attributed to remaining electrostatic interactions of the $PSKR1_{W831S}$ CaM-binding domain and the N- and/or C-terminal lobe of CaM.

Role of CaM binding for PSK receptor function *in vivo*

Expression of CaM-binding-deficient $PSKR1_{W831S}$ in a PSK receptor null mutant background did not restore growth indicating that CaM binding to the receptor is required for growth signaling. Binding of different CaM isoforms to the Ca^{2+}/CaM-binding kinases NtCBK2, NtCaMK1, AtCRK1, AtCRCK1 and AtCRLK1 was shown to stimulate enzyme activities to different degrees (Hua *et al.*, 2003; Ma *et al.*, 2004; Wang *et al.*, 2004; Yang *et al.*, 2004, 2010). Similar to PSKR1, BRI1 exhibited different affinities to the CaM isoforms of Arabidopsis, and its kinase activity was inhibited to different degrees (Oh *et al.*, 2012). It was however not analyzed whether CaM binding to BRI1 affects growth stimulation by brassinosteroids. In this study we showed that plants that express $PSKR1_{W831S}$ were growth-retarded and had a dominant-negative phenotype as also observed in plants that express the kinase-dead PSKR1(K762E) variant.

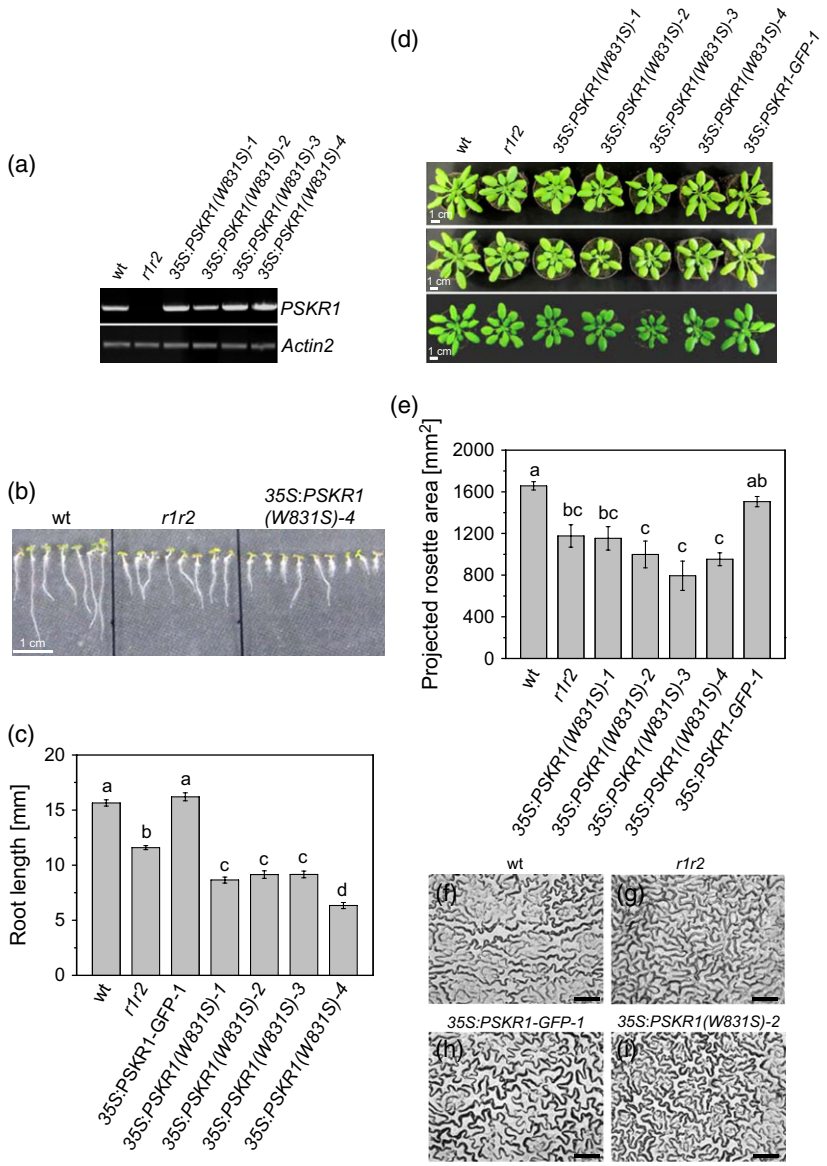

Figure 6. Inhibition of CaM binding to PSKR1 through site-directed mutagenesis impairs growth signaling *in planta*.

(a) Expression of *PSKR1* was analyzed in 5-day-old seedlings by RT-PCR in wt, *r1r2,* and the complementation lines *35S:PSKR1(W831S)-1*, *35S:PSKR1(W831S)-2*, *35S:PSKR1(W831S)-3* and *35S:PSKR1(W831S)-4* in the *r1r2* background. *Actin2* cDNA was amplified as a control for RNA input.

(b) Phenotypes of 5-day-old de-etiolated wt, *r1r2* and *35S:PSKR1(W831S)-4* seedlings.

(c) Average (±standard error (SE)) root lengths were determined for the lines indicated in two independent experiments with at least 46 seedlings analyzed per genotype. $^{a–d}$Different letters indicate significantly different values ($P < 0.001$, ANOVA, Tukey test).

(d) Phenotypes of 4-week-old soil-grown wt, *r1r2*, *35S:PSKR1(W831S)-1,2,3,4* and *35S:PSKR1-GFP-1* plants each in the null background.

(e) The average projected rosette area (±SE, $n = 3$) was calculated with Rosette Tracker (De Vylder *et al.*, 2012). $^{a–c}$Different letters indicate significantly different values ($P < 0.05$, ANOVA, Tukey test).

(f–i) Epidermis cells of the first rosette leaf of 4-week-old soil-grown (f) wt, (g) *r1r2*, (h) *35S:PSKR1-GFP-1*, and (i) *35S:PSKR1(W831S)-2* plants. Scale bar = 100 μm.

In contrast with the inhibiting effect on BRI1, CaM binding to PSKR1 may promote PSKR1 kinase activity. However, phosphorylation activity of the recombinant wild-type PSKR1 kinase was observed in the absence of exogenous CaM, and *E. coli* lacks this calcium sensor. These observations suggest that the auto- and transphosphorylation activities may be modulated by CaM in a more specific manner. For instance, the tyrosine kinase activity of BRI1 was more sensitive to CaM compared with the serine/threonine kinase activity (Oh *et al.*, 2012). It will be challenging to identify how the proposed CaM-induced modulations of the phosphorylation pattern affect downstream growth signaling. Based on our current results we propose that PSK perception at the cell surface triggers a phosphorelay that is subject to control by Ca^{2+}/CaM binding to the receptor.

EXPERIMENTAL PROCEDURES

Plant material, growth conditions and transformation

All experiments were performed with *Arabidopsis thaliana* ecotype Columbia-0. The *r1r2* insertion line used in this study was described previously (Stührwohldt *et al.*, 2011; Hartmann *et al.*, 2013). The T-DNA is inserted in the kinase domain in *pskr1-3* and in the 11th LRR domain in *pskr2-1*. For simplicity the receptor null background will be abbreviated *r1r2* in this study. Plants were grown in a 2:3 sand:humus mixture and watered with tap water. To avoid insect contamination, the soil was frozen at −80°C for 2 days prior to use. For growth experiments on sterile plates, Arabidopsis seeds were surface-sterilized for 20 min in 1 ml 2% (w/v) sodium hypochlorite, washed five times with autoclaved water and laid out under sterile conditions on square plates that contained half-strength Murashige and Skoog medium (Murashige and Skoog, 1962) and 1.5% (w/v) sucrose solidified with 0.38% (w/v) gelrite (Duchefa, Harlem, The Netherlands). Arabidopsis seeds were

stratified at 4°C in the dark for 2 days to break dormancy before being transferred to a growth chamber where they were grown at 22°C at long-day conditions with 16 h light (70 μmol photons m^{-2} sec^{-1}). For the transformation of Arabidopsis plants with *Agrobacterium tumefaciens* (GV3101), the floral dip method was used (Clough and Bent, 1998). Transformed plants and homozygous plants were screened for by selection with 200 μM BASTA (AgroEvo, Berlin, Germany).

Cloning of constructs

The PSKR1-KD encoding the cytoplasmic protein portion of *PSKR1* (*At2 g02220*) from amino acid 686–1008 was amplified by PCR using the forward primer 5′-AAACGCGTCGACTCAGGAGAAGTTGATC-3′ and the reverse primer 5′-AACGCTCCTAGGCTAGACATCATCAAGC-3′. As a template the vector pB7WG2.0 (VIB, Gent, Belgium) that contained the entire 3.1 kb coding sequence of *PSKR1* (Hartmann *et al.*, 2013) was used. The PCR product was cloned into pETDuet-1 (Novagen, Darmstadt, Germany) which resulted in a His_6 N-terminal fusion with PSKR1-KD. To generate the mutant kinase H_6–PSKR1–K762E, the invariant Lys at position 762 in subdomain II was substituted with Glu, which is predicted to eliminate kinase activity (Hanks *et al.*, 1988). *In vitro* mutagenesis was performed by overlap extension PCR (Horton *et al.*, 1989) using primers 5′-GTTGCGATCGAGAAGTTATCCGGTG-3′ and 5′-C ACCGGATAACTTCTCGA TCGCAAC-3′.

To study PSKR1 kinase activity and CaM binding we performed site-directed mutagenesis of the full-length *PSKR1* coding sequence by overlap extension PCR using primers 5′-GTTGC GATCGAGAAGTTATCCGGTG-3′ and 5′-CACCGGATAACTTCTCGA TCGCAAC-3′ to generate *PSKR1(K762E)* and primers 5′-CCAGCG TTGTTGAAGTCTAAAACACGTCTTAG-3′ and 5′-CTAAGACGTGT TTTAGACTTCAACAACGCTGG-3′ to clone *PSKR1(W831S)*. As a template for both constructs the above described vector pB7WG2.0 that contained the full-length *PSKR1* coding sequence, was used. For *PSKR1* promoter-driven *PSKR1* expression, a 2 kb genomic fragment upstream of the *PSKR1* coding region was amplified by PCR using the forward primer 5′-TTTAAA GGGGTACCATCTTAACTTTTCCAC GTAAA-3′ and the reverse primer 5′-TTAAAATTTTGCGGCCGCTTCAAGAACAGAGGAAG-3′. The fragment was cloned into pB7WG2.0 by replacing the CaMV 35S promoter. The *PSKR1(K762E)* and *PSKR1(W831S)* PCR fragments were cloned into the vector pB7WG2.0 downstream of the CaMV 35S or *PSKR1* promoter using the Gateway cloning system (Invitrogen, Darmstadt, Germany). A C-terminal GFP fusion with PSKR1 was obtained using the entry vector pENTR 1A Dual Selection (pENTR 1A DS) (Invitrogen). The GFP coding sequence was amplified by PCR using the forward primer 5′-ATAAG AATGCGGCCGCTATGGTGAGCA AGGGCGAGG-3′, the reverse primer 5′-TTTAACCGCTCGAGTTACTTGTACAGCTCGTCC ATG-3′ and the vector pBGWFS7.0 (VIB, Gent, Belgium) as a template. The fragment was cloned into pENTR 1A DS resulting in pENTR 1A DS-GFP. To generate PSKR1-GFP, the full-length *PSKR1* coding sequence without a stop codon was amplified by PCR using the forward primer 5′-ACGCGT CGACATGCGTGTTCATCGTTTTTGTGT GATCG-3′, the reverse primer 5′-ATAGTTTAG CGGCCGCGACATC ATCAAGCCAAGAGAC-3′ and the above described vector pB7WG2.0 that contained the full-length *PSKR1* coding sequence as a template. The fragment was cloned into pENTR 1A DS-GFP and subsequently into the vector pB7WG2.0 downstream of the CaMV 35S promoter using LR clonase (Invitrogen).

For BiFC analysis *PSKR1* and *PSKR1(W831S)* were amplified using primers 5′-CACCATGCGTGTTCATCGTTTTTG-3′ and 5′-GAC-ATCATCAAGCCAAGAGAC-3′ and ligated into pENTR/D-TOPO (Invitrogen). Recombination of the resulting vectors and CaM4, 6, 7 into respective BiFC expression vectors was performed as described previously (Fischer *et al.*, 2013).

Recombinant protein expression and purification

For the expression of the recombinant H_6-PSKR1-KD and H_6-PSKR1-K762E proteins, the appropriate constructs were transformed into BL21 (DE3) *Escherichia coli* cells (Invitrogen) and induced by adding 1 mM isopropyl-β-D-thiogalactopyranoside (Sigma-Aldrich, St. Louis, MO, USA) and grown for 16 h at 18°C. Soluble proteins were purified under native conditions on a TALON column (Clontech, Saint-Germain-en-Laye, France) following the manufacturer's instructions and purified recombinant proteins were stored at −20°C.

In vitro kinase assay

Autophosphorylation reactions contained 50 mM HEPES, pH 7.4, 10 mM $MnCl_2$, 1 mM dithiothreitol, 0.2 mM unlabeled ATP, 20 μCi of [γ-^{32}P]ATP, 2 μg of affinity-purified H_6–PSKR1–KD or H_6–PSKR1–K762E and double deionized H_2O in a final volume of 30 μl. Transphosphorylation reactions additionally contained 4 μg MBP. Both auto- and transphosphorylation assays were incubated at room temperature for 1 h. Reactions were terminated by the addition of 10 μl of 4× SDS (sodium dodecyl sulphate) loading buffer, followed by 12.5% (w/v) SDS-PAGE and autoradiography.

RT-PCR analysis

RT-PCR expression analysis of *PSKR1* was performed on 5-day-old seedlings. Total RNA was reverse transcribed with an oligodT primer and the cDNA was amplified with the forward primer 5′-CAAAGACCAGCTCTTCCATCG-3′ and the reverse primer 5′-CTGTGAACGATTCCTGGACCT-3′ for *Actin2* which was used as a control. For *PSKR1* RT-PCR expression analysis the cDNA was amplified with primers 5′-GAGCGTTGCAATACAATCAG-3′ and 5′-CAGTACTTACATGCGTCTCGT-3′. Polymerase chain reaction (PCR) amplifications were performed for 29 cycles for *Actin2* and 37 cycles for *PSKR1* as described (Kutschmar *et al.*, 2009; Hartmann *et al.*, 2013).

Bimolecular fluorescence complementation

BiFC assays were performed as described previously (Fischer *et al.*, 2013). For confocal microscopy octadecafluorodecahydronaphthalene was added to the samples to displace the air from the leaf tissue to avoid air rising up during the scans. To quantify the BiFC signals 6 mm leaf discs were cut out of the infiltrated areas and put into a black 96-well plate. Fluorescence intensities of leaf discs were measured in a TECAN infinite F200 plate reader (Tecan, Austria) using a 485 ± 20 nm excitation and a 535 ± 25 nm emission filter.

Growth measurements and statistical analysis

Root lengths were determined from photographs using Image J (National Institute of Health, Bethesda, MD, USA). Projected rosette areas were determined from photographs using the open source program Rosette Tracker (De Vylder *et al.*, 2012). Epidermis cells were visualized by spreading varnish on the first rosette leaf of 4-week-old soil-grown plants. The air-dried pieces of varnish were drawn-off by forceps and placed on slides. Statistical analysis was performed with Minitab (Minitab Inc., Friedrichsdorf, Germany). An analysis of variance (ANOVA) (Tukey test) or a

two-sample *t*-test was performed to test statistical significance of means. Prior to statistical analysis constant variance and normal distribution of data were verified and the *P*-value was set to $P < 0.001$ if one of these conditions was not achieved. *P*-values for the Pearson product moment correlation are indicated in figure legends.

ACKNOWLEDGEMENTS

Financial support by the Deutsche Forschungsgemeinschaft through grants FOR964 (PD) and SA 495/13-1 (MS) is gratefully acknowledged.

CONFLICT OF INTEREST STATEMENT

Authors have no conflict of interest to declare.

SUPPORTING INFORMATION

Additional Supporting Information may be found in the online version of this article.

Figure S1. PSKR1 belongs to the LRR family of receptor kinases.

REFERENCES

Adams, J.A. (2003) Activation loop phosphorylation and catalysis in protein kinases: is there functional evidence for the autoinhibitor model? *Biochemistry*, **42**, 601–607.

Amano, Y., Tsubouchi, H., Shinohara, H., Ogawa, M. and Matsubayashi, Y. (2007) Tyrosine-sulfated glycopeptide involved in cellular proliferation and expansion in Arabidopsis. *Proc. Natl Acad. Sci. USA*, **104**, 18333–18338.

Charpenteau, M., Jaworski, K., Ramirez, B.C., Tretyn, A., Ranjeva, R. and Ranty, B. (2004) A receptor-like kinase from *Arabidopsis thaliana* is a calmodulin-binding protein. *Biochem J.* **379**, 841–848.

Cheifetz, S. and Moscarello, M.A. (1985) Effect of bovine basic protein charge microheterogeneity on protein-induced aggregation of unilamellar vesicles containing a mixture of acidic and neutral phospholipids. *Biochemistry*, **24**, 1909–1914.

Chinchilla, D., Shan, L., He, P., de Vries, S. and Kemmerling, B. (2009) One for all: the receptor-associated kinase BAK1. *Trends Plant Sci.* **14**, 535–541.

Clough, S.J. and Bent, A.F. (1998) Floral dip: a simplified method for *Agrobacterium*-mediated transformation of *Arabidopsis thaliana*. *Plant J.* **16**, 735–743.

De Vylder, J., Vandenbussche, F., Hu, Y., Philips, W. and Van Der Straeten, D. (2012) Rosette tracker: an open source image analysis tool for automatic quantification of genotype effects. *Plant Physiol.* **160**, 1149–1159.

DeFalco, T.A., Bender, K.W. and Snedden, W.A. (2009) Breaking the code: Ca^{2+} sensors in plant signalling. *Biochem J.* **425**, 27–40.

Diévart, A. and Clark, S.E. (2003) Using mutant alleles to determine the structure and function of leucine-rich repeat receptor-like kinases. *Curr. Opin. Plant Biol.* **6**, 507–516.

Diévart, A., Dalal, M., Tax, F.E., Lacey, A.D., Huttly, A., Li, J. and Clark, S.E. (2003) CLAVATA1 dominant-negative alleles reveal functional overlap between multiple receptor kinases that regulate meristem and organ development. *Plant Cell*, **15**, 1198–1211.

Dodd, A.N., Kudla, J. and Sanders, D. (2010) The language of calcium signaling. *Annu. Rev. Plant Biol.* **61**, 593–620.

Findlay, W.A., Martin, S.R., Beckingham, K. and Bayley, P.M. (1995) Recovery of native structure by calcium binding site mutants of calmodulin upon binding of sk-MLCK target peptides. *Biochemistry*, **34**, 2087–2094.

Fischer, C., Kugler, A., Hoth, S. and Dietrich, P. (2013) An IQ domain mediates the interaction with calmodulin in a plant cyclic nucleotide-gated channel. *Plant Cell Physiol.* **54**, 573–584.

Gautier, R., Douguet, D., Antonny, B. and Drin, G. (2008) HELIQUEST: a web server to screen sequences with specific alpha-helical properties. *Bioinformatics*, **24**, 2101–2102.

Gish, L.A. and Clark, S.E. (2011) The RLK/Pelle family of kinases. *Plant J.* **66**, 117–127.

Goldberg, J., Nairn, A.C. and Kuriyan, J. (1996) Structural basis for the autoinhibition of calcium/calmodulin-dependent protein kinase I. *Cell*, **84**, 875–887.

Halter, T., Imkampe, J., Mazzotta, S. *et al.* (2014) The leucine-rich repeat receptor kinase BIR2 is a negative regulator of BAK1 in plant immunity. *Curr. Biol.* **24**, 134–143.

Hanks, S.K., Quinn, A.M. and Hunter, T. (1988) The protein kinase family: conserved features and deduced phylogeny of the catalytic domains. *Science*, **241**, 42–52.

Hartmann, J., Stührwohldt, N., Dahlke, R.I. and Sauter, M. (2013) Phytosulfokine control of growth occurs in the epidermis, is likely to be non-cell autonomous and is dependent on brassinosteroids. *Plant J.* **73**, 579–590.

Heyman, J., Cools, T., Vandenbussche, F. *et al.* (2013) ERF115 controls root quiescent center cell division and stem cell replenishment. *Science*, **342**, 860–863.

Horton, R.M., Hunt, H.D., Ho, S.N., Pullen, J.K. and Pease, L.R. (1989) Engineering hybrid genes without the use of restriction enzymes: gene splicing by overlap extension. *Gene*, **77**, 61–68.

Hua, W., Liang, S. and Lu, Y.T. (2003) A tobacco (*Nicotiana tabacum*) calmodulin-binding protein kinase, NtCBK2, is regulated differentially by calmodulin isoforms. *Biochem J.* **376**, 291–302.

Huse, M. and Kuriyan, J. (2002) The conformational plasticity of protein kinases. *Cell*, **109**, 275–282.

Ikura, M., Clore, G.M., Gronenborn, A.M., Zhu, G., Klee, C.B. and Bax, A. (1992) Solution structure of a calmodulin-target peptide complex by multidimensional NMR. *Science*, **256**, 632–638.

Ishida, H. and Vogel, H.J. (2006) Protein-peptide interaction studies demonstrate the versatility of calmodulin target protein binding. *Protein Pept. Lett.* **13**, 455–465.

Kamps, M.P. and Sefton, B.M. (1986) Neither arginine nor histidine can carry out the function of lysine-295 in the ATP-binding site of p60src. *Mol. Cell. Biol.* **6**, 751–757.

Kataoka, M., Head, J.F., Vorherr, T., Krebs, J. and Carafoli, E. (1991) Small-angle X-ray scattering study of calmodulin bound to two peptides corresponding to parts of the calmodulin-binding domain of the plasma membrane Ca^{2+} pump. *Biochemistry*, **30**, 6247–6251.

Komori, R., Amano, Y., Ogawa-Ohnishi, M. and Matsubayashi, Y. (2009) Identification of tyrosylprotein sulfotransferase in Arabidopsis. *Proc. Natl Acad. Sci. USA* **106**, 15067–15072.

Kondo, T., Sawa, S., Kinoshita, A., Mizuno, S., Kakimoto, T., Fukuda, H. and Sakagami, Y. (2006) A plant peptide encoded by CLV3 identified by *in situ* MALDI-TOF MS analysis. *Science*, **313**, 845–848.

Kutschmar, A., Rzewuski, G., Stührwohldt, N., Beemster, G.T.S., Inzé, D. and Sauter, M. (2009) PSK-α promotes root growth in Arabidopsis. *New Phytol.* **181**, 820–831.

Kwezi, L., Ruzvidzo, O., Wheeler, J.I., Govender, K., Iacuone, S., Thopson, P.E., Gehring, C. and Irving, H.R. (2011) The phytosulfokine (PSK) receptor is capable of guanylate cyclase activity and enabling cyclic GMP-dependent signalling in plants. *J. Biol. Chem.* **286**, 22580–22588.

Li, J. and Chory, J. (1997) A putative leucine-rich repeat receptor kinase involved in brassinosteroid signal transduction. *Cell*, **90**, 929–938.

Li, J., Wen, J., Lease, K.A., Doke, J.T., Tax, F.E. and Walker, J.C. (2002) BAK1, an Arabidopsis LRR receptor-like protein kinase, interacts with BRI1 and modulates brassinosteroid signalling. *Cell*, **110**, 213–222.

Lindberg, R.A., Quinn, A.M. and Hunter, T. (1992) Dual-specificity protein kinases: will any hydroxyl do? *Trends Biochem. Sci.* **17**, 114–119.

Loivamäki, M., Stührwohldt, N., Deeken, R., Steffens, B., Roitsch, T., Hedrich, R. and Sauter, M. (2010) A role for PSK signaling in wounding and microbial interactions in Arabidopsis. *Physiol. Plant.* **139**, 348–357.

Ma, L., Liang, S., Jones, R.L. and Lu, Y.T. (2004) Characterization of a novel calcium/calmodulin-dependent protein kinase from tobacco. *Plant Physiol.* **135**, 1280–1293.

Määttä, J.A., Coffey, E.T., Hermonen, J.A., Salmi, A.A. and Hinkkanen, A.E. (1997) Detection of myelin basic protein isoforms by organic concentration. *Biochem. Biophys. Res. Commun.* **238**, 498–502.

Matsubayashi, Y. and Sakagami, Y. (1996) Phytosulfokine, sulfated peptides that induce the proliferation of single mesophyll cells of *Asparagus officinalis* L. *Proc. Natl Acad. Sci. USA* **93**, 7623–7627.

Matsubayashi, Y., Ogawa, M., Morita, M. and Sakagami, Y. (2002) An LRR receptor kinase involved in perception of a peptide plant hormone, phytosulfokine. *Science*, **296**, 1470–1472.

Matsubayashi, Y., Ogawa, M., Kihara, H., Niwa, M. and Sakagami, Y. (2006) Disruption and overexpression of Arabidopsis phytosulfokine receptor gene affects cellular longevity and potential for growth. *Plant Physiol.* **142**, 45–53.

Matsushita, M. and Nairn, A.C. (1998) Characterization of the mechanism of regulation of Ca^{2+}/calmodulin-dependent protein kinase I by calmodulin and by Ca^{2+}/calmodulin-dependent protein kinase kinase. *J. Biol. Chem.* **273**, 21473–21481.

Matsuzaki, Y., Ogawa-Ohnishi, M., Mori, A. and Matsubayashi, Y. (2010) Secreted peptide signals required for maintenance of root stem cell niche in Arabidopsis. *Science*, **329**, 1065–1067.

McCormack, E., Tsai, Y.C. and Braam, J. (2005) Handling calcium signaling: Arabidopsis CaMs and CMLs. *Trends Plant Sci.* **10**, 383–389.

Meador, W.E., Means, A.R. and Quiocho, F.A. (1992) Target enzyme recognition by calmodulin: 2.4 A structure of a calmodulin-peptide complex. *Science*, **257**, 1251–1255.

Meador, W.E., Means, A.R. and Quiocho, F.A. (1993) Modulation of calmodulin plasticity in molecular recognition on the basis of X-ray structures. *Science*, **262**, 1718–1721.

Meng, L., Buchanan, B.B., Feldman, L.J. and Luan, S. (2012) CLE-like (CLEL) peptides control the pattern of root growth and lateral root development in Arabidopsis. *Proc. Natl Acad. Sci. USA* **109**, 1760–1765.

Morillo, S.A. and Tax, F.E. (2006) Functional analysis of receptor-like kinases in monocots and dicots. *Curr. Opin. Plant Biol.* **9**, 460–469.

Mosher, S., Seybold, H., Rodriguez, P. *et al.* (2013) The tyrosine-sulfated peptide receptors PSKR1 and PSY1R modify the immunity of Arabidopsis to biotrophic and necrotrophic pathogens in an antagonistic manner. *Plant J.* **73**, 469–482.

Murashige, T. and Skoog, F. (1962) A revised medium for rapid growth and bioassays with tobacco cultures. *Plant Physiol.* **15**, 473–497.

Oh, M.H., Ray, W.K., Huber, S.C., Asara, J.M., Gage, D.A. and Clouse, S.D. (2000) Recombinant brassinosteroid insensitive 1 receptor-like kinase autophosphorylates on serine and threonine residues and phosphorylates a conserved peptide motif *in vitro*. *Plant Physiol.* **124**, 751–766.

Oh, M.H., Kim, H.S., Wu, X., Clouse, S.D., Zielinski, R.E. and Huber, S.C. (2012) Calcium/calmodulin inhibition of the Arabidopsis BRASSINOSTEROID-INSENSITIVE 1 receptor kinase provides a possible link between calcium and brassinosteroid signalling. *Biochem J.* **443**, 515–523.

Ohyama, K., Shinohara, H., Ogawa-Ohnishi, M., Matsubayashi, Y., Kakimoto, T., Fukuda, H. and Sakagami, Y. (2009) A glycopeptide regulating stem cell fate in *Arabidopsis thaliana*. *Nat. Chem. Biol.* **5**, 578–580.

O'Neil, K.T. and DeGrado, W.F. (1990) How calmodulin binds its targets: sequence independent recognition of amphiphilic alpha-helices. *Trends Biochem. Sci.* **15**, 59–64.

Osakabe, Y., Yamaguchi-Shinozaki, K., Shinozaki, K. and Tran, L.S. (2013) Sensing the environment: key roles of membrane-localized kinases in plant perception and response to abiotic stress. *J. Exp. Bot.* **64**, 445–458.

Rainaldi, M., Yamniuk, A.P., Murase, T. and Vogel, H.J. (2007) Calcium-dependent and -independent binding of soybean calmodulin isoforms to the calmodulin binding domain of tobacco MAPK phosphatase-1. *J. Biol. Chem.* **282**, 6031–6042.

Rhoads, A.R. and Friedberg, F. (1997) Sequence motifs for calmodulin recognition. *FASEB J.* **11**, 331–340.

Shen, Y. and Diener, A.C. (2013) *Arabidopsis thaliana* resistance to *fusarium oxysporum* 2 implicates tyrosine-sulfated peptide signaling in susceptibility and resistance to root infection. *PLoS Genet.* **9**, e1003525.

Shinohara, H., Ogawa, M., Sakagami, Y. and Matsubayashi, Y. (2007) Identification of ligand binding site of phytosulfokine receptor by on-column photoaffinity labeling. *J. Biol. Chem.* **282**, 124–131.

Stahl, Y., Grabowski, S., Bleckmann, A. ***et al.*** (2013) Moderation of Arabidopsis root stemness by CLAVATA1 and ARABIDOPSIS CRINKLY4 receptor kinase complexes. *Curr. Biol.* **23**, 362–371.

Stührwohldt, N., Dahlke, R.I., Steffens, B., Johnson, A. and Sauter, M. (2011) Phytosulfokine-α controls hypocotyl length and cell expansion in *Arabidopsis thaliana* through phytosulfokine receptor 1. *PLoS ONE* **6**, e21054.

Vanoosthuyse, V., Tichtinsky, G., Dumas, C., Gaude, T. and Cock, J.M. (2003) Interaction of calmodulin, a sorting nexin and kinase-associated protein phosphatase with the *Brassica oleracea* S locus receptor kinase. *Plant Physiol.* **133**, 919–929.

Wang, Y., Liang, S., Xie, Q.G. and Lu, Y.T. (2004) Characterization of a calmodulin-regulated Ca2 + -dependent-protein-kinase-related protein kinase, AtCRK1, from Arabidopsis. *Biochem J.* **383**, 73–81.

Wang, X., Goshe, M.B., Soderblom, E.J., Phinney, B.S., Kuchar, J.A., Li, J., Asami, T., Yoshida, S., Huber, S.C. and Clouse, S.D. (2005) Identification and functional analysis of *in vivo* phosphorylation sites of the Arabidopsis BRASSINOSTEROID-INSENSITIVE1 receptor kinase. *Plant Cell*, **17**, 1685–1703.

Wong, A. and Gehring, C. (2013) The *Arabidopsis thaliana* proteome harbors undiscovered multi-domain molecules with functional guanylyl cyclase catalytic centers. *Cell Commun. Signal.* **11**, 48.

Yamakawa, H., Katou, S., Seo, S., Mitsuhara, I., Kamada, H. and Ohashi, Y. (2004) Plant MAPK phosphatase interacts with calmodulins. *J. Biol. Chem.* **279**, 928–936.

Yamauchi, E., Nakatsu, T., Matsubara, M., Kato, H. and Taniguchi, H. (2003) Crystal structure of a MARCKS peptide containing the calmodulin-binding domain in complex with Ca2 + -calmodulin. *Nat. Struct. Biol.* **10**, 226–231.

Yamniuk, A.P. and Vogel, H.J. (2004) Calmodulin's flexibility allows for promiscuity in its interactions with target proteins and peptides. *Mol. Biotechnol.* **27**, 33–57.

Yang, T., Chaudhuri, S., Yang, L., Chen, Y. and Poovaiah, B.W. (2004) Calcium/calmodulin up-regulates a cytoplasmic receptor-like kinase in plants. *J. Biol. Chem.* **279**, 42552–42559.

Yang, T., Chaudhuri, S., Yang, L., Du, L. and Poovaiah, B.W. (2010) A calcium/calmodulin-regulated member of the receptor-like kinase family confers cold tolerance in plants. *J. Biol. Chem.* **285**, 7119–7126.

Yap, K.L., Kim, J., Truong, K., Sherman, M., Yuan, T. and Ikura, M. (2000) Calmodulin target database. *J. Struct. Funct. Genomics*, **1**, 8–14.

Supplemental Figure S1

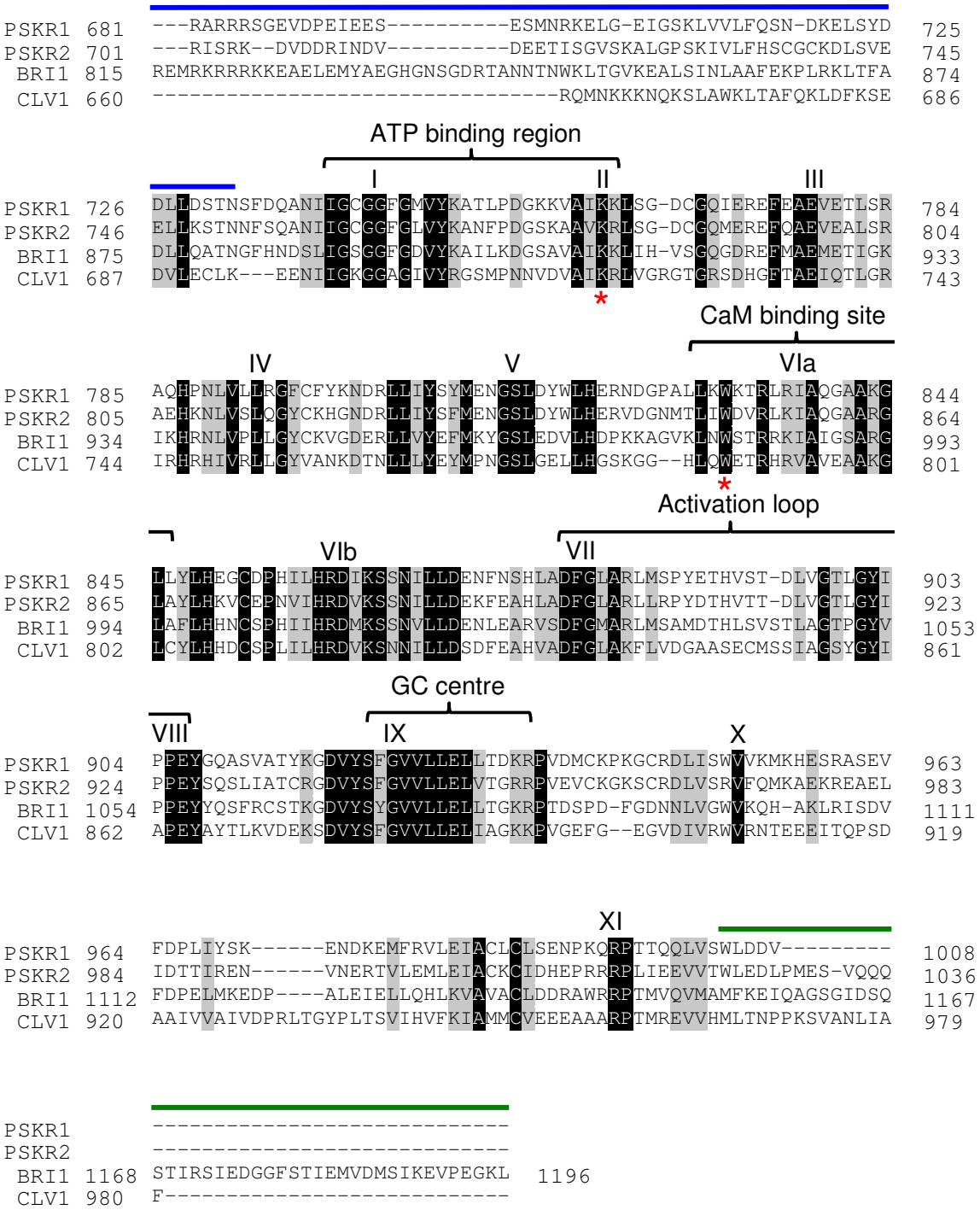

LEGEND FOR SUPPORTING INFORMATION

Supplemental Figure S1. PSKR1 belongs to the LRR family of receptor kinases. ClustalW alignment of the cytoplasmic domains of the PSK receptors PSKR1 and PSKR2 with the related protein kinases BRI1 and CLV1 from Arabidopsis. The juxtamembrane domain of PSKR1 extends from amino acid 681 to 732 and is marked with a blue line. The PSKR1 kinase domain with its 12 subdomains extends from amino acid 733 to 1003 (for a definition of the PSKR1 kinase subdomains, see Hanks et al., 1988; Lindberg et al., 1992). The C-terminal region of PSKR1 starts at amino acid 1004 and is designated by a green line. The site-mutated conserved amino acids in the ATP binding site (K762) in subdomain II and in the CaM binding site (W831) in subdomain VIa are indicated by asterisks.

Kapitel 3

Phosphosite mapping of the phytosulfokine receptor PSKR1 and functional analysis of activation loop phosphorylation sites

Die in diesem Manuskript enthaltenen Arbeiten, mit Ausnahme der in Kooperation mit der Arbeitsgruppe von Prof. Tholey (Universität Kiel) durchgeführten MS-Analysen, wurden im Rahmen dieser Doktorarbeit von mir angefertigt.

Phosphosite mapping of the phytosulfokine receptor PSKR1 and functional analysis of activation loop phosphorylation sites

Jens Hartmann[1], Dennis Linke[2], Andreas Tholey[2], Margret Sauter[1]

[1]Entwicklungsbiologie und Physiologie der Pflanzen, Universität Kiel, Am Botanischen Garten 5, 24118 Kiel, Germany

[2]Systematische Proteomics und Bioanalytik, Universität Kiel, Niemannsweg 11, 24105 Kiel, Germany

Corresponding author:

Entwicklungsbiologie und Physiologie der Pflanzen, Universität Kiel, Am Botanischen Garten 5, 24118 Kiel, Germany
E-mail: msauter@bot.uni-kiel.de
Phone: +49 431 8804210

Running title:

Identification and functional analysis of PSKR1 phosphorylation sites

SUMMARY

The disulfated pentapeptide phytosulfokine (PSK) promotes plant growth through elevated cell expansion and requires active leucine-rich repeat (LRR) receptor kinases for perception and subsequent signal transduction. To elucidate early events in PSK signaling, we performed phosphopeptide mapping of PSKR1. Immunoprecipitation of epitope-tagged PSKR1 protein from *Arabidopsis thaliana* followed by liquid chromatography-tandem mass spectrometry (LC/MS/MS) identified S696 and S698 in the PSKR1 juxtamembrane (JM) region as true *in planta* phosphorylation sites. MS analysis also provided evidence that an additional three residues in the activation loop of PSKR1 kinase subdomain VII/VIII were phosphorylated *in planta*. We also identified S717 in the JM region, S733, S783, S911, S949 and S958 in the kinase domain and two residues close to the C-terminal (CT) domain as *in vitro* PSKR1 autophosphorylation sites using LC/MS/MS. Additionally, the obtained MS/MS product ion spectra provided support that at least one and possibly up to four sites (T890, S893, T894 and T899) in the activation loop of PSKR1 were likely to be phosphorylated *in vitro*. To study functional relevance of PSKR1 activation loop phosphorylation and to resolve ambiguities concerning specific *in planta* and *in vitro* phosphorylation sites in this region, site-directed mutagenesis was performed. The four conserved activation loop residues T890, S893, T894 and T899 were shown to be essential for *in vitro* PSKR1 kinase activity, with respect to both auto- and transphosphorylation. Expression of the quadruply mutated PSKR1(TSTT-A) receptor variant in the *pskr* null background resulted in the most severe growth inhibition. More detailed complementation studies with the doubly or singly mutated PSKR1(S/T893/4A) and PSKR1(T890A) variants also revealed significant impacts on growth. We conclude that phosphorylation of PSKR1 Thr 890 and Ser/Thr 893/4 is required for activation and *in planta* receptor function. We further hypothesize that phosphorylation of Ser residues in the PSKR1 JM domain or of Ser/Thr residues close to the CT domain is not required for general kinase activation but might confer PSKR1-specific signaling properties which still has to be elucidated.

KEYWORDS

phytosulfokine, signal transduction, *Arabidopsis thaliana*, phosphopeptide mapping, LC/MS/MS, PSKR1 activation loop

INTRODUCTION

The pentapeptide phytosulfokine (PSK) with the amino acid backbone YIYTQ has been described as a factor that promotes plant growth through elevated cell expansion. Furthermore, its involvement in the response to pathogens has been reported (Matsubayashi and Sakagami, 1996; Amano et al., 2007; Stührwohldt et al., 2011; Hartmann et al., 2013; Loivamäki et al., 2010; Mosher et al., 2013; Shen and Diener, 2013). Peptide activity depends on posttranslational sulfation of the two tyrosine residues which is catalyzed by the enzyme tyrosylprotein sulfotransferase in the *trans*-Golgi network (Komori et al., 2009).

Perception and transduction of the PSK signal requires a membrane-localized receptor protein. PSK is the natural ligand for the PSK receptor kinases PSKR1 and PSKR2 in *Arabidopsis thaliana*. PSKR1 and PSKR2 belong to a large monophyletic gene family of Arabidopsis leucine-rich repeat receptor-like kinases (LRR RLKs) (Matsubayashi et al., 2002; Shiu et al., 2004; Gish and Clark, 2011). LRR RLKs are characterized by a defined organization of functional domains: LRRs with an extracellular ligand binding domain, a single transmembrane domain and a cytoplasmic protein portion consisting of a catalytic kinase domain (KD) flanked by two regulatory sequences, the juxtamembrane (JM) region and a carboxy terminal (CT) domain. PSKR1 shares this organization of functional domains. PSKR1 possesses a predicted extracellular domain with 21 LRRs. Between the 17th and 18th LRR of PSKR1 a 36-amino-acid island domain is located that was shown to bind PSK (Matsubayashi et al., 2002; Matsubayashi et al., 2006; Shinohara et al., 2007). A single helical 21-amino-acid transmembrane domain spans the plasma membrane followed by a JM region, a serine/threonine KD with its 12 conserved subdomains and a short CT domain (Hanks et al., 1988; Lindberg et al., 1992; Matsubayashi et al., 2002) (Figure 1a; Figure 4a).

The downstream signaling processes that are initiated by PSK binding to PSK receptors have not been elucidated. PSK perception at the cell surface possibly triggers a cellular auto- and transphosphorylation cascade. It has been shown that PSKR1 kinase activity is essential for growth promotion via PSKR1 signaling, although the targets that are recognized and phosphorylated by the activated PSKR1 *in planta* are not known (Hartmann et al., 2014). Furthermore, Hartmann et al. (2014) demonstrated that CaM binding to PSKR1 is required for PSK signaling *in planta*.

PSK binding to PSK receptors possibly triggers a phosphorelay that may depend on Ca^{2+}/CaM binding to PSKR1.

Ligand-induced receptor dimerization followed by autophosphorylation of the cytoplasmic domain is a conserved mechanism of receptor kinase action in plants, as shown for the brassinosteroid receptor BRASSINOSTEROID INSENSITIVE 1 (BRI1) that is closely related to PSK receptors (Kim and Wang, 2010; Clouse, 2011; Wang et al., 2012). Phosphorylation of the cytoplasmic domain of receptor kinases can occur on multiple sites in the JM region, KD and CT domain (Huse and Kuriyan, 2002). The structure of serine/threonine protein kinase domains is highly conserved. The protein structure can be separated into two domains, a small N-terminal ATP binding domain consisting of five β-sheets and one α-helix (αC) and a larger C-terminal substrate binding domain that is predominantly helical (Huse and Kuriyan, 2002; Adams 2003). A conserved activation segment, the so-called activation loop is located in the larger C-terminal domain. The activation loop starts at the highly conserved DFG motif in kinase subdomain VII and most often terminates with the sequence APE in subdomain VIII (Hanks et al., 1988; Lindberg et al., 1992). Phosphorylation of one to three residues in the activation loop results in a conformational change accompanied by kinase activation. In some cases it also affects binding of kinase substrates (Johnson et al., 1996; Adams 2003). A conserved Glu residue is located within the αC-helix of the β-sheet-rich N-terminal kinase domain and interacts with a conserved Lys residue of the ATP binding cleft that coordinates the α and β phosphates of ATP for hydrolysis (Huse and Kuriyan, 2002). The N-terminal region of the activation loop was shown to make contact to the αC-helix. Phosphorylation of the activation loop can cause significant movements in αC. In the dephosphorylated state the Glu-Lys ion pair is disrupted probably resulting in impaired ATP binding and lowered rates of phosphotransfer to the substrate (Huse and Kuriyan, 2002; Adams 2003). Hence, dependent on the phosphorylation state, the activation loop is characterized by defined conformational changes representing a switch that determines whether the kinase is inactive or active (Johnson et al., 1996).

Compared to the activation loop, the JM regions and CT domains show less sequence conservation among receptor kinases but important functions for phosphorylation in these two regions of the LRR RLK BRI1 was demonstrated (Wang et al., 2005; Wang et al., 2008). Dependent on the phosphorylation state it has been

shown that the noncatalytic JM and CT regions of the cytoplasmic BRI1 domain are important not only for specifically modulating kinase activity but also for creating substrate binding sites. Hence, it is possible that the JM region and CT domain of PSKR1 are likewise involved in regulating kinase activity and in the interaction with currently unknown PSKR1 substrates. The role of phosphorylation of either the PSKR1 activation loop, JM region or the CT domain and its role for *in planta* PSK signaling has not been described.

To elucidate PSKR1 function, it is essential to understand early molecular events of PSKR1 signaling such as receptor dimerization and phosphorylation. In this study we used LC/MS/MS analysis of the recombinant PSKR1 kinase domain to show that the cytoplasmic protein portion of the receptor is phosphorylated on specific Ser and Thr residues *in vitro*. Furthermore, phosphopeptide mapping of Ser and Thr residues was used to identify phosphorylation sites of immunoprecipitated PSKR1-GFP protein *in planta*. We further studied the functional role of identified phosphorylation sites in the PSKR1 activation loop with respect to *in vitro* kinase activity. Additionally, the contribution of phosphorylation of specific PSKR1 activation loop residues to receptor function *in planta* was assessed by overexpressing site-mutated PSKR1 variants in the receptor null background. Our data support the view that site-directed, phospho-ablative mutagenesis of specific PSKR1 activation loop residues abolishes PSKR1 kinase activity *in vitro* and that phosphorylation of these Ser and Thr residues is required for growth signaling through PSKR1 *in planta*.

RESULTS

Identification of in vitro PSKR1 autophosphorylation sites by LC/MS/MS

PSK receptors belong to the large family of Arabidopsis LRR RLKs and more precisely to the class of so-called RD kinases. Ligand-induced kinase activation often necessitates phosphorylation of one to three residues in the activation loop. An invariant Asp residue in subdomain VIb (D860 in PSKR1) is required for catalytic activity and can be found in all kinases. In RD kinases this Asp is preceded by a positively charged Arg (R859 in PSKR1) (Figure 1a). This residue probably interacts with phosphorylated, negatively charged amino acids of the activation loop resulting in charge neutralization and substrate access to the catalytic Asp (Johnson et al., 1996).

The organization of the JM region, serine/threonine KD and CT domain of PSKR was derived by an alignment of the cytoplasmic domains of PSKR1 and PSKR2 with related LRR RLKs as shown recently (Hartmann et al., 2014). The activation loop is localized within the PSK receptor kinase subdomains VII and VIII and is highly conserved in the closely related LRR RLKs BRI1 and CLV1 (Figure 1a).

In RD LRR RLKs there is a high degree of sequence conservation of specific Ser or Thr activation loop residues that also in the case of PSKR1 probably have to be phosphorylated for kinase activation (Figure 1a). It has been shown that the ectopically expressed kinase domain of PSKR1 from amino acid 686 to 1008 is capable of auto- and transphosphorylation (Hartmann et al., 2014). To identify specific phosphorylated Ser or Thr residues and to examine activation loop phosphorylation of PSKR1, H_6-PSKR1-KD protein was autophosphorylated *in vitro*, subjected to SDS-PAGE followed by in-gel digestions with four different enzymes. The digested peptides were extracted and subjected to ion trap LC/MS/MS analysis, with or without TiO_2 enrichment of phosphopeptides.

The sequence coverage of H_6-PSKR1-KD was 84-100% which resulted in eight unambiguously determined phosphorylation sites including S717 in the juxtamembrane domain, as well as S733, S783, S911, S949, S958, T998 and S1003 in the kinase domain (Figure 1a; Figure 4a). The obtained MS/MS product ion spectra provided support that the sites T752 and S864 in the PSKR1 kinase domain

are likely to be phosphorylated. Moreover, based on manual inspection of the data, at least one and possibly up to four sites (T890, S893, T894 and T899) in the activation loop of PSKR1 subdomain VII/VIII, spanning residues 878-906, are likely to be phosphorylated. The presence of five Ser and Thr residues in this short region makes a correct assignment of specific phosphorylation sites difficult. The utilization of four different enzymes and TiO_2 enrichment of phosphopeptides prior to LC/MS/MS analysis did not increase the likelihood for the unambiguous PSKR1 activation loop phosphosite mapping.

The next step was to verify that the identified amino acids were indeed targets for phosphorylations by the active PSKR1 kinase. As a negative control affinity-purified, inactive H_6-PSKR1-K762E protein (Hartmann et al., 2014) was subjected to a phosphorylation assay as described above for H_6-PSKR1-KD and analyzed by LC/MS/MS. In this mutant kinase an invariant Lys in subdomain II is replaced by Glu resulting in a loss of kinase activity (Kamps and Sefton, 1986). The sequence coverage of H_6-PSKR1-K762E was 100%, one phosphorylation site was determined that belongs to the phospho-group T890, S893, T894 and T899 (Figure 4a). Due to the high number of Ser, Thr and Tyr residues present in this region, the unambiguous assignment was difficult and could not be improved even by utilization of four enzymes and TiO_2 enrichment of phosphopeptides.

Identification of in planta PSKR1 phosphorylation sites by LC/MS/MS

To identify PSKR1 protein and *in planta* PSKR1 phosphorylation sites, a C-terminally GFP tagged full-length *PSKR1* sequence was generated, placed under control of the 35S promoter and stably expressed in wild-type plants. PSKR1-GFP fluorescence was observed in mesophyll protoplasts derived from 4-week-old *35S:PSKR1-GFP* plants. The PSKR1-GFP protein was localized to the plasma membrane as shown for PSKR1-GFP in the *r1r2* receptor null background (Hartmann et al., 2014) (Figure 2c). Roots of 5-day-old, de-etiolated *35S:PSKR1-GFP* seedlings were significantly longer than wild-type roots indicating that the GFP fusion did not impair *in planta* receptor function (Figure 2a, b). Total protein was extracted from 14-day-old *35S:PSKR1-GFP* and from wild-type seedlings followed by immunoprecipitation with anti-GFP antibody. After immunoprecipitation a band with a size of about 188 kDa was detected in protein samples of the transgenic line only and not in the sample from

wild-type seedlings (Figure 2d). This protein band corresponds to the PSKR1-GFP fusion protein as verified by western blot analysis with anti-GFP antibody. The amount of immunoprecipitated PSKR1-GFP protein correlated with the anti-GFP antibody concentration that was used for immunoprecipitation.

To identify *in planta* PSKR1 phosphorylation sites, the PSKR1-GFP bands were excised, in-gel digested with trypsin or elastase and subjected to ion trap LC/MS/MS analysis, with or without TiO_2 enrichment of phosphopeptides. The compilation of all MS/MS data covered >65% of the PSKR1-GFP sequence and unambiguously identified S696 and S698 in the juxtamembrane region as true *in planta* phosphorylation sites (Figure 1a; Figure 4a). Additionally, the MS/MS product ion spectra provided evidence that S886, S893 and T894 might also be phosphorylated but the specific phosphorylation sites could not be unambiguously assigned.

Site-directed mutagenesis of specific PSKR1 activation loop residues abolishes in vitro PSKR1 kinase activity

To test for a functional role of the phosphorylation sites in the PSKR1 activation loop with respect to kinase activity, site-directed mutagenesis of specific Ser or Thr residues to Ala was performed (Figure 3a). Ala prevents phosphorylation at the specific sites. Mutant PSKR1 kinases (T890A, T899A, S/T893/4A and the simultaneous mutation of all four potential phosphorylation sites, subsequently abbreviated as TSTT-A) from amino acid 686 to 1008 were ectopically expressed as fusion proteins with an N-terminal H_6-tag. The effect of mutagenesis on autophosphorylation of the PSKR1 cytoplasmic domain as well as on transphosphorylation of the common substrate myelin basic protein (MBP) was tested in an *in vitro* kinase assay. As a negative control affinity-purified, inactive H_6-PSKR1-K762E protein was analyzed for *in vitro* auto- and transphosphorylation activity. The H_6-PSKR1-K762E protein had no or only basal auto- or transphosphorylation activity *in vitro* as shown (Hartmann et al., 2014) (Figure 3b, c). Likewise, the mutations T890A, T899A, S/T893/4A and TSTT-A abolished *in vitro* kinase activity, with respect to both auto- and transphosphorylation. By contrast, the unmutated H_6-PSKR1-KD protein was capable of *in vitro* auto- and transphosphorylation. Phosphorylated, monomeric MBP has a size of about 21.5 kDa

and was detected whereas the protein with a size of about 24 kDa could represent a phosphorylated, multimeric complex of MBP (Figure 3b).

Specific Ser and Thr activation loop residues are required for PSKR1 growth signaling in planta

We next analyzed if phosphorylation of specific Ser and Thr activation loop residues is required for growth regulation through PSKR1 *in planta*. Point-mutated T890A, T899A, S/T893/4A and TSTT-A full-length *PSKR1* sequences were generated. Expression of the PSKR1 variants was driven by the 35S cauliflower mosaic virus promoter in the receptor null background. Expression analysis of *PSKR1* in 5-day-old seedlings by RT-PCR revealed that the complementation line *35S:PSKR1-GFP-1* had a *PSKR1* mRNA level that was slightly higher than the one of the wild-type (Figure 5a). The independent lines *35S:PSKR1(T890A)-1*,*2*,*3*, *35S:PSKR1(T899A)-1*,*2*,*3*, *35S:PSKR1(S/T893/4A)-1*,*2*,*3*, and *35S:PSKR1(TSTT-A)-1*,*2*,*3* overall showed *PSKR1* transcript levels that were similar to, slightly higher or slightly lower than those of the wild-type. In the null background line *pskr1-3 pskr2-1* (subsequently abbreviated as *r1r2*) no *PSKR1* mRNA was detected.

The receptor variants were tested for their ability to restore the short-root phenotype of PSK receptor knock out seedlings. Root lengths of 5-day-old de-etiolated wild-type, *r1r2*, *r1r2 35S:PSKR1-GFP-1*, *r1r2 35S:PSKR1(T890A)*, *r1r2 35S:PSKR1(T899A)*, *r1r2 35S:PSKR1(S/T893/4A)* and *r1r2 35S:PSKR1(TSTT-A)* seedlings were compared (Figure 5b). *r1r2* seedlings developed roots that were significantly shorter by 33% than wild-type roots. Expression of wild-type PSKR1 in *r1r2 35S:PSKR1-GFP-1* seedlings complemented the short-root phenotype of *r1r2* and resulted in roots that were similar to the wild-type.

By contrast, mutations in the PSKR1 activation loop affected the ability to restore the short-root phenotype of *r1r2* to different degrees. Seedlings of all three independent lines *r1r2 35S:PSKR1(T890A)-1*,*2*,*3* developed roots that were considerably shorter by 18-29% than wild-type roots (Figure 5b, c). Furthermore, roots of *r1r2 35S:PSKR1(T890A)-1*,*2* seedlings did not significantly differ from those of *r1r2* and thus these two lines failed to complement the short-root phenotype of the receptor null background. The slightly longer roots of *r1r2 35S:PSKR1(T890A)-3* seedlings may be attributed to the slightly lower expression level in this line (Figure 5a).

Expression of the PSKR1(T899A) and PSKR1(S/T893/4A) receptor variants in *r1r2 35S:PSKR1(T899A)-1*,*2*,*3* and *r1r2 35S:PSKR1(S/T893/4A)-1*,*2*,*3* seedlings resulted in roots that showed significant variability in length. Roots of *r1r2 35S:PSKR1(T899A)-3* seedlings were clearly shorter by 35% compared to the wild-type whereas *r1r2 35S:PSKR1(T899A)-1*,*2* seedlings developed roots that were shorter by 18% or by only 6% than wild-type roots. *r1r2 35S:PSKR1(S/T893/4A)-3* seedlings showing the highest expression level of all three independent lines developed roots that were distinctly shorter by 41% than wild-type roots. Roots of this line were even significantly shorter by 19% than *r1r2* roots suggesting a dominant-negative effect. By contrast, seedlings of the independent lines *r1r2 35S:PSKR1(S/T893/4A)-1*,*2* showed a root phenotype that was intermediate between *r1r2* and the wild-type.

Expression of the PSKR1(TSTT-A) receptor variant in *r1r2 35S:PSKR1(TSTT-A)-1*,*2*,*3* seedlings most obviously affected the ability to restore the short-root phenotype of *r1r2*. Independent of the expression level, seedlings of all three lines displayed roots that were even significantly shorter by 15-31% than *r1r2* roots suggesting a dominant-negative effect of this receptor variant.

Analysis of 4-week-old, soil-grown plants revealed that the rosette size of *r1r2 35S:PSKR1(T899A)-3* plants was similar to wild-type plants (Figure 6a, b; Figure S1). Hence, the results for this line indicate contrary roles of the PSKR1(T899A) receptor variant for PSK signaling in shoot development and in root growth of seedlings respectively. Expression of wild-type PSKR1 in *r1r2 35S:PSKR1-GFP-1* plants complemented the smaller rosette size phenotype of *r1r2* and resulted in rosettes that were slightly bigger than those of wild-type plants consistent with the results obtained for the root lengths of seedlings.

By contrast, shoots of *r1r2 35S:PSKR1(T890A)-3* and *r1r2 35S:PSKR1(S/T893/4A)-2* plants were as small as those of *r1r2* plants and thus these two lines failed to complement the smaller rosette size phenotype of the receptor null background. Furthermore, rosettes of *r1r2 35S:PSKR1(S/T893/4A)-3* plants were significantly smaller than those of *r1r2* suggesting a dominant-negative effect of the PSKR1(S/T893/4A) activation loop variant in this line.

Consistent with the clear impairment of root growth in seedlings, rosettes of *r1r2 35S:PSKR1(TSTT-A)-2*,*3* plants were distinctly smaller than wild-type rosettes and did not significantly differ from those of *r1r2*. Hence, the simultaneous phospho-

ablative mutation of the four most conserved PSKR1 activation loop Ser/Thr residues representing potential phosphorylation sites resulted in incapability of the mutated PSKR1(TSTT-A) receptor variant to restore the short-root and smaller rosette size phenotype of *r1r2*.

The observed shoot growth phenotype was studied in more detail at the cellular level. Epidermis cells of the first rosette leaf of 4-week-old plants were analyzed and showed no significant difference between *r1r2 35S:PSKR1-GFP-1*, *r1r2 35S*:*PSKR1(T899A)-3* and wild-type plants (Figure 7a, c, f, h). By contrast, epidermis cells of *r1r2*, *r1r2 35S:PSKR1(T890A)-3*, *r1r2 35S*:*PSKR1(S/T893/4A)-2* and *r1r2 35S:PSKR1(TSTT-A)-3* plants were distinctly smaller than those of wild-type or *r1r2 35S:PSKR1-GFP-1* plants (Figure 7a-h).

DISCUSSION

To understand phosphorylation-dependent signaling mechanisms of PSKR1, one aim of this study was to identify phosphorylation sites in the cytoplasmic protein portion of the receptor by using mass spectrometry analysis. Ectopically expressed H_6-PSKR1-KD protein was shown to be capable of auto- and transphosphorylation *in vitro* as previously described (Hartmann et al., 2014). Phosphoamino acid analysis of autophosphorylated H_6-PSKR1-KD identified eight unambiguous *in vitro* phosphorylation sites located in the PSKR1 JM domain, the KD and close to the CT domain. This phosphorylation pattern is common for receptor kinases (Johnson et al., 1996; Huse and Kuriyan, 2002). The MS data also supported the presence of two additional *in vitro* phosphorylation sites located in the KD but an assignment to specific amino acid residues was not possible. Manual inspection of MS data revealed that at least one and possibly up to four sites in the activation loop of PSKR1 are likely to be phosphorylated. To verify the results obtained for the H_6-PSKR1-KD protein, kinase-inactive H_6-PSKR1-K762E protein (Hartmann et al., 2014) was also analyzed by LC/MS/MS as a negative control. For this mutant protein, one *in vitro* phosphorylation site was determined belonging to the phospho-group T890, S893, T894 and T899 located in the PSKR1 activation loop. An unambiguous assignment was not possible due to the high number of Ser, Thr and Tyr residues present in this region. The identification of this phosphorylation site indicates that the kinase-inactive H_6-PSKR1-K762E protein possibly is a suitable substrate for an as

yet unknown bacterial kinase. Probably, phosphorylation takes place during ectopic expression of the mutant protein in *E. coli*. It is unlikely that the phosphorylation event originates from any kinase activity of the mutant H_6-PSKR1-K762E protein since a replacement of the invariant Lys in subdomain II by Glu results in a loss of kinase-mediated phosphotransfer (Kamps and Sefton, 1986). Consistently, the kinase-inactive H_6-PSKR1-K762E protein showed no or only basal auto- and transphosphorylation activity *in vitro*. Hence, the remaining *in vitro* auto- and transphosphorylation activity observed reflects activity of the wild-type H_6-PSKR1-KD protein rather than bacterial kinase activity.

To identify *in planta* PSKR1 phosphorylation sites, epitope-tagged PSKR1 protein was immunoprecipitated from transgenic Arabidopsis plants followed by LC/MS/MS analysis. A relatively high level of sequence coverage was achieved resulting in the unambiguous identification of two *in planta* phosphorylation sites located in the PSKR1 JM region. Moreover, MS/MS product ion spectra indicated that at least one and possibly up to three sites in the activation loop of PSKR1 are likely to be phosphorylated, consistent with the above described MS data obtained from the H_6-PSKR1-KD protein.

Taken together, the MS analyses identified only phosphorylation of Ser/Thr residues consistent with the fact that PSKR1 displays a predicted Ser/Thr kinase catalytic domain based on the 12 subdomains that are characteristic of this class of kinases (Hanks et al., 1988; Lindberg et al., 1992; Matsubayashi et al., 2002). Furthermore, a preference for Ser over Thr residues was observed which has also been shown for the LRR RLKs BRI1 and CLV1 (Williams et al., 1997; Stone et al., 1998; Oh et al., 2000). Interestingly, a recent study reported on the finding that BRI1, BAK1 and BKK1 are also phosphorylated at Tyr residues indicating that they are dual-specificity kinases (Oh et al., 2009). Bojar et al. (2014) report conservation of the conformation of the activation loop and of core phosphorylation sites among different plant RLKs (Oh et al., 2009; Oh et al., 2010; Klaus-Heisen et al., 2011; Yan et al., 2012). It is hence conceivable that also PSKR1 could exhibit dual-specificity although no phosphorylation of Tyr residues was detected in this study.

In total three phosphorylation sites in the PSKR1 JM domain and two phosphorylation sites close to the CT domain were identified *in vitro* or *in planta* by MS analysis. The role of phosphorylation of the PSKR1 JM or CT domain for *in planta* PSK signaling has not been described but mutational analysis may provide a

clue. Most of the JM or CT domain residues show no conservation among receptor kinases suggesting that phosphorylation at these sites possibly confers PSKR1-specific signaling properties rather than displaying a more general response of kinase activation. It is conceivable that upon phosphorylation specific PSKR1 substrate binding sites are created. Since LRR RLKs function in many diverse physiological processes, phosphorylation of JM and CT regions is one way to overcome this functional diversity and to achieve specificity. It has been shown that deletion of the BRI1 JM domain abolished the signaling function of the receptor whereas phosphorylation of the JM domain activated BRI1 (Wang et al., 2005b; Wang et al., 2008). By contrast, deletion of the BRI1 CT domain has been reported to increase the kinase activity of BRI1 *in vitro* and *in planta* suggesting that the CT domain auto-inhibits BRI1 kinase activity which can be moderated by phosphorylation (Wang et al., 2005b). Also for some receptor tyrosine kinases it has been demonstrated that the C-terminal tail negatively controls tyrosine kinase activation (Shewchuk et al., 2000; Niu et al., 2002; Chiara et al., 2004).

To resolve the ambiguities concerning specific *in vitro* phosphorylation sites in the activation loop of PSKR1 and to test for a functional role of these phosphorylation sites with respect to kinase activity, site-directed mutagenesis was performed. Each of the Ser or Thr residues in question was replaced by Ala to prevent phosphorylation at the specific sites. Single mutations of Thr 890, Ser/Thr 893/4 and Thr 899 abolished *in vitro* kinase activity, with respect to both auto- and transphosphorylation. Likewise, several studies have described an important role of phosphorylation in the activation loop for the kinase activity of BRI1 and BAK1 (Wang et al., 2005a; Wang et al., 2008; Oh et al., 2009; Yun et al., 2009). It has been shown that mutation of the conserved BRI1 and BAK1 activation loop residue corresponding to PSKR1 Thr 899 abolished the kinase activities of both receptors. Mutations of BRI1 activation loop residues corresponding to PSKR1 Thr 890 and Ser 893 had a more moderate effect on BRI1 kinase activity and it has been shown that BAK1 is autophosphorylated *in vitro* on the two equivalent residues. Interestingly, single mutation of BAK1 activation loop residues corresponding to PSKR1 Thr 890, Ser 893 and Thr 894 had little effect on BAK1 kinase activity whereas a replacement of all three Thr residues by Ala abolished the kinase activity. In the present study the simultaneous mutation of all four potential phosphorylation sites in the PSKR1(TSTT-A) receptor variant was shown to have the most severe effect on *in planta* signaling with respect to root

growth of seedlings. The PSKR1(T899A) receptor variant was shown to have only little effect on plant growth which is inconsistent with the above described *in vitro* observation. It has been shown that the BRI1 activation loop residue corresponding to PSKR1 Thr 899 can be differentially phosphorylated *in planta*, thereby probably controlling specificity towards different substrates (Wang et al., 2005a; Wang et al., 2008). By contrast, mutations of PSKR1 Thr 890 or Ser/Thr 893/4 resulted in significantly shorter seedling roots and plants with a smaller rosette area, consistent with the *in vitro* results. Interestingly, BRI1 and SERK1 activation loop residues corresponding to PSKR1 Thr 890 and Ser 893 have been shown to affect substrate phosphorylation more than autophosphorylation *in vitro* (Shah et al., 2001; Wang et al., 2005a). Hence, it is conceivable that one or both of these PSKR1 activation loop residues might be true *in planta* phosphorylation sites. In line with this and based on the crystal structure of the BRI1 kinase domain, Bojar et al. (2014) recently found the BRI1 activation loop residues corresponding to PSKR1 Thr 890 and Ser 893 to be phosphorylated. Bojar et al. (2014) reported that these two residues are surface-oriented and probably contribute to the stabilization of the conformation of the activation loop by interacting with a third residue equivalent to PSKR1 His 891. Hence, phosphorylation of PSKR1 Thr 890 and Ser 893 possibly affects the orientation of the activation loop and with this has an impact on PSKR1 kinase activity and on substrate binding. The severe effect of mutating PSKR1 Thr 890 or Ser/Thr 893/4 on *in vitro* auto- and transphosphorylation and *in planta* signaling suggests that phosphorylation of at least two of these activation loop residues is essential for PSKR1 kinase function. Moreover, one PSKR1(S/T893/4A) line and three PSKR1(TSTT-A) lines showed significantly shorter root phenotypes than untransformed *r1r2* seedlings suggesting a dominant-negative effect similar to that observed when a kinase-inactive PSKR1 was overexpressed in the null background (Hartmann et al., 2014). Interestingly, Diévart et al. (2003) have shown that site-directed mutagenesis of two different CLV1 activation loop residues resulted in an intermediate dominant-negative phenotype.

Based on our current *in vitro* and *in planta* data we propose that phosphorylation of PSKR1 Thr 890 and Ser/Thr 893/4 is required for activation and *in planta* receptor function. Furthermore, based on MS analyses we could show that phosphorylation of Ser residues in the PSKR1 JM domain or of Ser/Thr residues close to the CT domain takes place. We hypothesize that these phosphorylations are

not required for general kinase activation but might confer PSKR1-specific signaling properties which still has to be elucidated.

EXPERIMENTAL PROCEDURES

Plant material, growth conditions and transformation

All experiments were carried out with *Arabidopsis thaliana* (L.) Heynh. ecotype Columbia (Col-0). A 2:3 sand:humus mixture was frozen at -80°C for 2 d to avoid insect contamination before plants were grown in the pretreated soil. Plants were regularly watered with tap water. The *r1r2* T-DNA insertion line was described previously (Stührwohldt et al., 2011; Hartmann et al., 2013). All experiments carried out in this study were performed with homozygous seeds as tested by spraying with 200 µM BASTA (AgroEvo, Berlin, Germany). Surface-sterilization for 20 min in 1 ml 2% (w/v) sodium hypochlorite followed by five washing steps with autoclaved water was carried out prior to growth experiments. After sterilization, seeds were laid out under sterile conditions on square plates containing half-concentrated modified Murashige and Skoog media (Murashige and Skoog, 1962) and 1.5% (w/v) sucrose. The media were solidified with 0.38% (w/v) gelrite (Duchefa, Harlem, The Netherlands). Prior to germination, Arabidopsis seeds were stratified at 4°C in the dark for 2 d. Seedlings were grown at 22°C at long-day conditions with 16 h light (70 µMol photons m^{-2} s^{-1}) in a growth chamber. Arabidopsis plants were transformed with *Agrobacterium tumefaciens* (GV3101) by using the floral dip method (Clough and Bent, 1998). Transformed plants were selected by spraying with 200 µM BASTA.

Site-directed mutagenesis of the PSKR1 full-length and cytoplasmic domain coding sequence and cloning of constructs

To test for a functional role of the potential phosphorylation sites in the PSKR1 activation loop with respect to kinase activity, site-directed mutagenesis of the *PSKR1* cytoplasmic domain coding sequence was performed by overlap extension PCR (Horton *et al.*, 1989). Four individual constructs with

the following substitutions were generated: T890A, T899A, S/T893/4A and TSTT-A. Each construct consists of the cytoplasmic protein portion of PSKR1 from amino acid 686 to 1008. To substitute each specific Ser or Thr with Ala by SOE-PCR, primers 5'-GTCCTTACGAGG CTCATGTAAGTAC-3' and 5'-GTACTTACATGAGCCTCGTAAGGAC-3' for T890A, primers 5'-CTGATTTGGTTGGAGCTTTAGGTTAC-3' and 5'-GTAACCTAAAGCTC CAACCAAATCAG-3' for T899A, primers 5'-ACGCATGTAGCT GCTGATTTGGTTG-3' and 5'-CAACCAAATCAGCAGCTACATGCGT-3' for S/T893/4A and primers 5'-CGAGGCTCATGTAGCTGCTGATTTGGTTGGAGCTTTAG-3' and 5'-CTAAAG CTCCAACCAAATCAGCAGCTACATGAGCCTCG-3' for TSTT-A were used for i*n vitro* mutagenesis reactions. The previously described vector *35S*:*PSKR1* was used as a template containing the entire 3.1 kb coding sequence of *PSKR1* (Hartmann et al., 2013). Subsequently, the PCR products were cloned into pETDuet-1 (Merck, Darmstadt, Germany) resulting in His_6 N-terminal fusions with the four mutant PSKR1 kinases.

Point-mutated T890A, T899A, S/T893/4A and TSTT-A full-length *PSKR1* sequences were generated by overlap extension PCR using the above described primers and template vector. The PCR fragments were cloned into the vector pB7WG2.0 downstream of the CaMV 35S promoter using the Gateway cloning system (Life Technologies, Darmstadt, Germany). All constructs were sequenced to verify the specific mutations and to exclude unwanted mutations. The C-terminal in frame fusion of GFP with PSKR1 and cloning of the PSKR1-GFP construct into the vector pB7WG2.0 downstream of the CaMV 35S promoter were performed as described previously (Hartmann et al., 2014).

Recombinant protein expression, purification and in vitro kinase assay

Constructs of the four mutant PSKR1 kinases T890A, T899A, S/T893/4A and TSTT-A were transformed into BL21 (DE3) *Escherichia coli* cells (Life Technologies, Darmstadt, Germany). Protein expression was induced by adding 1 mM isopropyl-β-D-thiogalactopyranoside (Sigma-Aldrich, St. Louis, USA) followed by incubation of bacterial cultures for 16 h at 18°C. Subsequently, soluble proteins were purified under native conditions on a TALON column (Takara Bio Europe SAS, Saint-Germain-en-Laye, France) as described in the manufacturer's instructions. Purified

recombinant proteins were stored at -20°C.

In vitro kinase assays were conducted as described previously (Hartmann et al., 2014). Incubation of auto- and transphosphorylation assays was carried out at room temperature for 1 h followed by the addition of 10 µl of 4x SDS loading buffer to stop reactions. After *in vitro* phosphorylation assays an aliquot of each reaction was separated by 12.5% (w/v) SDS-PAGE, the gel was stained, dried and autoradiographed. Subsequently, autoradiographs were analyzed using the Advanced Image Data Analyzer Software (AIDA, Raytest, Straubenhardt, Germany) to quantify incorporation of ^{32}P into PSKR1 kinase protein or MBP.

Immunoprecipitation and immunoblot analysis

For immunoprecipitations total protein extracts were prepared from 14-day-old de-etiolated *35S:PSKR1-GFP* and wild-type seedlings. The plant material was collected, ground in liquid nitrogen and subsequently thawed in extraction buffer containing 50 mM Tris-HCl, pH 7.5, 150 mM NaCl and 1% (v/v) Igepal CA 630 (Sigma-Aldrich, St. Louis, USA). After incubation of protein samples on ice for 1 h, suspensions were centrifuged at 300 g for 3 min at 4°C. The protein concentration was determined by bradford method using Roti®-Quant (Carl Roth, Karlsruhe, Germany). Following protein extraction, 10 ml of total plant protein extract (1 mg/ml) in extraction buffer was incubated with 100 µl of 50% (v/v) protein A Sepharose CL-4B beads slurry (GE Healthcare, Chalfont St Giles, UK) in 50 mM Tris-HCl, pH 7.5 and 150 mM NaCl. The samples were centrifuged at 300 g for 3 min at 4°C and the supernatant from the wild-type sample was incubated with 3 µg of anti-GFP antibody (Life Technologies, Darmstadt, Germany). Supernatants from *35S:PSKR1-GFP* samples were incubated with 3 µg, 6 µg and 9 µg of anti-GFP antibody. The incubations were carried out for 1 h at 4°C with gentle mixing of samples followed by the addition of 200 µl of fresh 50% (v/v) protein A beads and overnight incubation. The samples were centrifuged at 300 g for 3 min to pellet protein A beads, the supernatants were removed and the beads were washed four times with 1 ml of washing buffer containing 50 mM Tris-HCl, pH 7.5 and 150 mM NaCl. Proteins were eluted from protein A beads by the addition of SDS loading buffer and boiling at 95°C for 5 min.

Immunoprecipitated PSKR1-GFP protein was detected by immunoblot analysis on PVDF membranes with anti-GFP antibody (Life Technologies, Darmstadt,

Germany) at a dilution of 1:2500. Subsequently, the primary anti-GFP antibody was detected by a horseradish peroxidase–linked secondary antibody. The western blots were developed using the ECL chemiluminesence detection system (GE Healthcare, Chalfont St Giles, UK).

In-gel enzyme digestions

For mass spectrometry analysis, protein bands were cut out of the protein gels and the gel pieces were washed by addition of 500 µl H_2O with shaking for 15 min to remove contaminations. Subsequently, two de-staining steps with 800 µl of de-staining buffer (70% (v/v) H_2O, 30% (v/v) Acetonitril (ACN)) for 30 min and with 500 µl of incubation buffer for 10 min were performed. The supernatant was removed and the gel pieces were dried in a speedvac (Eppendorf, Hamburg, Germany) for 30 min at room temperature. For reduction of disulfide-bonds, 116 µl of reducing solution (1.5 M DTT) were added to the gel pieces and the samples were incubated at 56°C for 30 min. A cool down period of 10 min at 4°C and a washing step with 150 µl of incubation buffer for 10 min were appended. The alkylation reaction was performed in the dark for 20 min by addition of 100 µl of 40 mM iodacetamid followed by a quenching step with 75 µl of reducing solution for 10 min and an additional washing step with 150 µl of incubation buffer for 15 min. To remove reducing and alkylation contaminations, the samples were washed again with 150 µl of incubation buffer for 5 min and 150 µl of pure ACN were added to initiate gel shrinking. The samples were shaken for 15 min before the supernatant was removed and subsequently the samples were dried in a speedvac for 30 min at room temperature before digestion.

For digestion, the enzymes chymotrypsin (250 ng), elastase (250 ng), gluc (250 ng) and trypsin (125 ng) were solubilized in digestion buffer (50 mM NH_4HCO_3, 5% (v/v) ACN) and 10 µl of the enzyme solutions were spotted directly on the gel pieces followed by an incubation step for 15 min to ensure a complete absorption of the enzyme solutions by the gel pieces. To hydrate the gel pieces further, 90 µl of digestion buffer were added and the digestions were carried out overnight at 37°C with gentle agitation. To extract the digested proteins, the supernatant of each enzyme digestion was transferred to a new tube followed by two incubation steps with 150 µl of extraction buffer I (60% (v/v) ACN, 0.5% (v/v) trifluoroacetic acid (TFA)) and with 150 µl of pure ACN for 15 min. The three extracts were combined,

speedvaced to dryness at room temperature, filled up to 10 µl with loading buffer A and stored at -20°C prior to mass spectrometry analysis.

Enrichment of phosphopeptides using TiO_2

Peptide samples were enriched for phosphopeptides using TiO_2 beads. Firstly, 240 µg of TiO_2 beads were washed twice with 20 µl of loading buffer (80% (v/v) ACN, 15% (v/v) H_2O, 5% (v/v) TFA, 1 M glycolic acid) for 15 min with shaking. The supernatant was discarded followed by peptide dilution in 50 µl of loading buffer. Diluted peptides were transferred und incubated with the TiO_2 beads for 15 min while shaking. By centrifugal force, the beads were pelleted and the supernatant (= NB fraction) was transferred to a new tube. 50 µl of washing buffer I (80% (v/v) ACN, 19% (v/v) H_2O, 1% (v/v) TFA) were added and samples were shaken for 15 min. Again, the beads were pelleted by centrifugation and a second washing step with washing buffer II (20% (v/v) ACN, 79.8% (v/v) H_2O, 0.2% (v/v) TFA) was appended. The supernatants of both washing steps were combined and transferred to a new tube. Prior to elution of bound phosphopeptides, the beads were speedvaced to dryness at room temperature for 30 min. Elution was performed twice using 50 µl and 100 µl of elution solution (1% NH_4OH in H_2O). The supernatants were acidified with 5 µl of pure TFA and dried in a speedvac. Prior to to mass spectrometry analysis, each sample (= phosphopeptide fraction) was diluted in 16.5 µl of eluent A (0.05% (v/v) formic acid (FA) in water).

LC-ESI MS/MS analysis

The samples were separated and analyzed by reversed-phase (RP) liquid chromatography (LC) using UltiMate 3000 nano-HPLC system (Dionex, Germering, Germany) coupled online to electrospray mass spectrometry (nano-LC-MS/MS, further on denoted as LC-MS). Solvents used for LC were: Solvent A (0.05% (v/v) FA in water) and solvent B (80% (v/v) ACN, 0.04% (v/v) FA in water). For sample loading, a solution of 3% (v/v) ACN and 0.1% (v/v) TFA was used. 2.5-10 µl of the non-enriched samples, 5 µl of the NB fraction and 5+10 µl of the phosphopeptide fraction were separated on an Acclaim PepMap 100 C_{18} analytical column (3 µm, 75 µm x 150 mm, Dionex, Sunnyvale, CA, USA). The following gradient at a flow rate of

300 nl/min using eluent A and eluent B (0.1% (v/v) FA, 80% (v/v) ACN in water) was applied: 0-4 min, 5% B; 4-5 min, 10% B; 5-85 min, 50% B; 85-95 min, 95% B; 95-100 min, 95% B; 100-101 min, 5% B; 101-139 min, 5% B.

Eluted peptides were analyzed on a LTQ Orbitrap Velos mass spectrometer (Thermo Scientific, Bremen, Germany) equipped with a nano-electrospray ion source. MS data acquisition utilized a dual fragmentation method with collision induced dissociation (CID) (IonTrap analyzer) and higher collision induced dissociation (HCD) (Orbitrap analyzer) which was manually set up. For the MS survey scan (Orbitrap mass analyzer), a resolution of 60.000 was chosen. The preview mode was enabled to start the CID fragmentation already during MS acquisition. For fragmentation, the top five most intense peaks were chosen. Dynamic exclusion was set to 0.5 min, with a repeat count of 3 within 20 sec. The exclusion mass window was set to 1.5. For CID, one scan was used with a normalized collision energy (NCE) of 35%. The remaining settings were default. For HCD, an activation energy of 45% NCE was applied and the precursor isolation window was set to m/z 3. The fragment ions were recorded in Orbitrap mass analyzer with a resolution of 7.500.

Database search and peptide identification

For database search, Proteome Discoverer 1.4 was used and the complete reference proteome set of Arabidopsis was downloaded and imported. The search algorithm SEQUEST HT in combination with PhosphorRS 3.0 to automatically validate and score the phosphorylation sites and with Percolator to improve identifications by semi-supervised machine learning algorithm were chosen. The Scan Event Filter was activated to split data in CID and HCD. As static modifications, carbmidomethyl (C) was used. For the variable modifications oxidation (M), deamidation (N,Q) and phosphorylation (S, T, Y) were activated. For database search, the following settings were chosen: Enzyme-specifity: “no enzyme”; fragment ions: b and y ions; fragment ion mass accuracy: 0.02 Da for HCD and 0.3 Da for CID; Precursor Mass Window: 10 ppm. The data were searched in a MudPIT (Multidimensional Protein Identification Technology) approach. For data export, only peptides with a FDR < 1% were chosen and exports were performed on grouped protein level, grouped peptide level and on Peptide-Spectrum-Match (PSM) level. The exported peptide hits were searched

manually for phosphorylation events and ranked according to the scores with manual validation.

Growth measurements and statistical analysis

The software Image J (National Institute of Health, Bethesda, MD, USA) was used to determine root lengths from photographs. The open source program Rosette Tracker (De Vylder et al., 2012) was used to determine projected rosette areas from photographs. For visualization of epidermis cells varnish was spread on the first rosette leaf of 4-week-old soil-grown plants. The air-dried pieces of varnish were drawn off by forceps, placed on slides and analyzed using an Olympus microscope BX41 and the image software Cell A (Olympus, Hamburg, Germany). The program Minitab (Minitab Inc.) was used for statistical analysis. Statistical significance of means was tested by an ANOVA (Tukey test) or a 2-sample *t*-test. Constant variance and normal distribution of data were verified prior to statistical analysis. If one of these conditions was not achieved, the *P* value was set to $P<0.001$. *P* values for the Pearson product moment correlation are indicated in figure legends.

ACKNOWLEDGMENT

Financial support by the Deutsche Forschungsgemeinschaft through grant SA 495/13-1 (MS) is gratefully acknowledged.

REFERENCES

Adams, J.A. (2003) Activation loop phosphorylation and catalysis in protein kinases: is there functional evidence for the autoinhibitor model? *Biochemistry*, **42**, 601-607.

Amano, Y., Tsubouchi, H., Shinohara, H., Ogawa, M., Matsubayashi, Y. (2007) Tyrosine-sulfated glycopeptide involved in cellular proliferation and expansion in Arabidopsis. *Proc. Natl Acad. Sci. USA*, **104**, 18333-18338.

Bojar, D., Martinez, J., Santiago, J., Rybin, V., Bayliss, R., Hothorn, M. (2014) Crystal structures of the phosphorylated BRI1 kinase domain and implications for brassinosteroid signal initiation. *Plant J*, doi: 10.1111/tpj.12445.

Chiara, F., Bishayee, S., Heldin, C.H., Demoulin, J.B. (2004) Autoinhibition of the platelet-derived growth factor beta-receptor tyrosine kinase by its C-terminal tail. *J Biol Chem*, **279**, 19732-19738.

Clough, S.J. and Bent, A.F. (1998) Floral dip: a simplified method for Agrobacterium-mediated transformation of *Arabidopsis thaliana*. *Plant J,* **16**, 735-743.

Clouse, S.D. (2011) Brassinosteroid signal transduction: from receptor kinase activation to transcriptional networks regulating plant development. *Plant Cell*, **23***,* 1219-1230.

De Vylder, J., Vandenbussche, F., Hu, Y., Philips, W., Van Der Straeten, D. (2012) Rosette tracker: an open source image analysis tool for automatic quantification of genotype effects. *Plant Physiol*, **160**, 1149-1159.

Diévart, A., Dalal, M., Tax, F.E., Lacey, A.D., Huttly, A., Li, J., Clark, S.E. (2003) CLAVATA1 dominant-negative alleles reveal functional overlap between multiple receptor kinases that regulate meristem and organ development. *Plant Cell*, **15**, 1198-1211.

Gish, L.A. and Clark, S.E. (2011) The RLK/Pelle family of kinases. *Plant J*, **66***,* 117-127.

Hanks, S.K., Quinn, A.M., Hunter, T. (1988) The protein kinase family: conserved features and deduced phylogeny of the catalytic domains. *Science*, **241**, 42-52.

Hartmann, J., Stührwohldt, N., Dahlke, R.I., Sauter, M. (2013) Phytosulfokine control of growth occurs in the epidermis, is likely to be non-cell autonomous and is dependent on brassinosteroids. *Plant J*, **73***,* 579-590.

Hartmann, J., Fischer, C., Dietrich, P., Sauter, M. (2014) Kinase activity and calmodulin binding are essential for growth signaling by the phytosulfokine receptor PSKR1. *Plant J*, doi: 10.1111/tpj.12460.

Horton, R.M., Hunt, H.D., Ho, S.N., Pullen, J.K. and Pease, L.R. (1989) Engineering hybrid genes without the use of restriction enzymes: gene splicing by overlap extension. *Gene,* **77**, 61-68.

Huse, M. and Kuriyan, J. (2002) The conformational plasticity of protein kinases. *Cell*, **109**, 275-282.

Johnson, L.N., Noble, M.E., Owen, D.J. (1996) Active and inactive protein kinases: structural basis for regulation. *Cell*, **85**, 149-158.

Kamps, M.P. and Sefton, B.M. (1986) Neither arginine nor histidine can carry out the function of lysine-295 in the ATP-binding site of p60src. *Mol Cell Biol*, **6**, 751-757.

Kim, T.W. and Wang, Z.Y. (2010) Brassinosteroid signal transduction from receptor kinases to transcription factors. *Annu Rev Plant Biol*, **61**, 681-704.

Klaus-Heisen, D., Nurisso, A., Pietraszewska-Bogiel, A., Mbengue, M., Camut, S., Timmers, T., Pichereaux, C., Rossignol, M., Gadella, T.W., Imberty, A., Lefebvre, B., Cullimore, J.V. (2011) Structure-function similarities between a plant receptor-like kinase and the human interleukin-1 receptor-associated kinase-4. *J Biol Chem*, **286**, 11202-11210.

Komori, R., Amano, Y., Ogawa-Ohnishi, M., Matsubayashi, Y. (2009) Identification of tyrosylprotein sulfotransferase in Arabidopsis. *Proc. Natl Acad. Sci. USA*, **106**, 15067-15072.

Lindberg, R.A., Quinn, A.M., Hunter, T. (1992) Dual-specificity protein kinases: will any hydroxyl do? *Trends Biochem Sci*, **17**, 114-119.

Loivamäki, M., Stührwohldt, N., Deeken, R., Steffens, B., Roitsch, T., Hedrich, R., Sauter, M. (2010) A role for PSK signaling in wounding and microbial interactions in Arabidopsis. *Physiol Plant*, **139**, 348-357.

Matsubayashi, Y., Sakagami, Y. (1996) Phytosulfokine, sulfated peptides that induce the proliferation of single mesophyll cells of *Asparagus officinalis* L. *Proc. Natl Acad. Sci. USA*, **93**, 7623-7627.

Matsubayashi, Y., Ogawa, M., Morita, M. and Sakagami, Y. (2002) An LRR receptor kinase involved in perception of a peptide plant hormone, phytosulfokine. *Science*, **296**, 1470-1472.

Matsubayashi, Y., Ogawa, M., Kihara, H., Niwa, M. and Sakagami, Y. (2006) Disruption and overexpression of Arabidopsis phytosulfokine receptor gene affects cellular longevity and potential for growth. *Plant Physiol*, **142**, 45-53.

Mosher, S., Seybold, H., Rodriguez, P., Stahl, M., Davies, K.A., Dayaratne, S., Morillo, S.A., Wierzba, M., Favery, B., Keller, H., Tax, F.E., Kemmerling, B. (2013) The tyrosine-sulfated peptide receptors PSKR1 and PSY1R modify the immunity of Arabidopsis to biotrophic and necrotrophic pathogens in an antagonistic manner. *Plant J*, **73***,* 469-482.

Murashige, T. and Skoog, F. (1962) A revised medium for rapid growth and bioassays with tobacco cultures. *Plant Physiol*, **15**, 473-497.

Niu, X.L., Peters, K.G., Kontos, C.D. (2002) Deletion of the carboxyl terminus of Tie2 enhances kinase activity, signaling, and function. Evidence for an autoinhibitory mechanism. *J Biol Chem*, **277**, 31768-31773.

Oh, M.H., Ray, W.K., Huber, S.C., Asara, J.M., Gage, D.A., Clouse, S.D. (2000) Recombinant brassinosteroid insensitive 1 receptor-like kinase autophosphorylates on serine and threonine residues and phosphorylates a conserved peptide motif in vitro. *Plant Physiol*, **124**, 751-766.

Oh, M.H., Wang, X., Kota, U., Goshe, M.B., Clouse, S.D., Huber, S.C. (2009) Tyrosine phosphorylation of the BRI1 receptor kinase emerges as a component of brassinosteroid signaling in Arabidopsis. *Proc. Natl Acad. Sci. USA*, **106**, 658-663.

Oh, M.H., Wang, X., Wu, X., Zhao, Y., Clouse, S.D., Huber, S.C. (2010) Autophosphorylation of Tyr-610 in the receptor kinase BAK1 plays a role in brassinosteroid signaling and basal defense gene expression. *Proc. Natl Acad. Sci. USA*, **107**, 17827-17832.

Shah, K., Vervoort, J., de Vries S.C. (2001) Role of threonines in the *Arabidopsis thaliana* somatic embryogenesis receptor kinase 1 activation loop in phosphorylation. *J Biol Chem*, **276**, 41263-41269.

Shen, Y. and Diener, A.C. (2013) *Arabidopsis thaliana* resistance to *fusarium oxysporum* 2 implicates tyrosine-sulfated peptide signaling in susceptibility and resistance to root infection. *PLoS Genet*, **9**, e1003525.

Shewchuk, L.M., Hassell, A.M., Ellis, B., Holmes, W.D., Davis, R., Horne, E.L., Kadwell, S.H., McKee, D.D., Moore, J.T. (2000) Structure of the Tie2 RTK domain: self-inhibition by the nucleotide binding loop, activation loop, and C-terminal tail. *Structure*, **8**, 1105-1113.

Shinohara, H., Ogawa, M., Sakagami, Y. and Matsubayashi, Y. (2007) Identification of ligand binding site of phytosulfokine receptor by on-column photoaffinity labeling. *J Biol Chem*, **282**, 124-131.

Shiu, S.H., Karlowski, W.M., Pan, R., Tzeng, Y.H., Mayer, K.F., Li, W.H. (2004) Comparative analysis of the receptor-like kinase family in Arabidopsis and rice. *Plant Cell*, **16**, 1220-1234.

Stone, J.M., Trotochaud, A.E., Walker, J.C., Clark, S.E. (1998) Control of meristem development by CLAVATA1 receptor kinase and kinase-associated protein phosphatase interactions. *Plant Physiol*, **117**, 1217-1225.

Stührwohldt, N., Dahlke, R.I., Steffens, B., Johnson, A. and Sauter, M. (2011) Phytosulfokine-α controls hypocotyl length and cell expansion in *Arabidopsis thaliana* through phytosulfokine receptor 1. *PLoS ONE,* **6**, e21054.

Wang, X., Goshe, M.B., Soderblom, E.J., Phinney, B.S., Kuchar, J.A., Li, J., Asami, T., Yoshida, S., Huber, S.C., Clouse, S.D. (2005a) Identification and functional analysis of *in vivo* phosphorylation sites of the Arabidopsis BRASSINOSTEROID-INSENSITIVE1 receptor kinase. *Plant Cell*, **17**, 1685-1703.

Wang, X., Li, X., Meisenhelder, J., Hunter, T., Yoshida, S., Asami, T., Chory, J. (2005b) Autoregulation and homodimerization are involved in the activation of the plant steroid receptor BRI1. *Dev Cell*, **8**, 855-865.

Wang, X., Kota, U., He, K., Blackburn, K., Li, J., Goshe, M.B., Huber, S.C., Clouse, S.D. (2008) Sequential transphosphorylation of the BRI1/BAK1 receptor kinase complex impacts early events in brassinosteroid signaling. *Dev Cell*, **15**, 220-235.

Wang, Z.Y., Bai, M.Y., Oh, E., Zhu, J.Y. (2012) Brassinosteroid signaling network and regulation of photomorphogenesis. *Annu Rev Genet*, **46**, 701-724.

Williams, R., Wilson, J., Meyerowitz, E. (1997) A possible role for kinase-associated protein phosphatase in the Arabidopsis CLAVATA1 signaling pathway. *Proc. Natl Acad. Sci. USA*, **94**, 10467-10472.

Yan, L., Ma, Y., Liu, D., Wei, X., Sun, Y., Chen, X., Zhao, H., Zhou, J., Wang, Z., Shui, W., Lou, Z. (2012) Structural basis for the impact of phosphorylation on the activation of plant receptor-like kinase BAK1. *Cell Res*, **22**, 1304-1308.

Yun, H.S., Bae, Y.H., Lee, Y.J., Chang, S.C., Kim, S.K., Li, J., Nam, K.H. (2009) Analysis of phosphorylation of the BRI1/BAK1 complex in arabidopsis reveals amino acid residues critical for receptor formation and activation of BR signaling. *Mol Cells*, **27**, 183-190.

FIGURE LEGENDS

Figure 1. PSKR1 is a member of the family of Arabidopsis LRR RLKs and phosphorylation within the cytoplasmic protein portion can be detected. (a) PSK receptors belong to the class of RD kinases. A ClustalW alignment of the cytoplasmic domains of PSKR1 and PSKR2 with the related RD kinases BRI1 and CLV1 from Arabidopsis is shown. The amino acids 681 and 732 border the juxtamembrane domain of PSKR1 marked with a blue line. The PSKR1 kinase domain with its 12 subdomains starts at Ser 733 and ends at Ser 1003 (for a definition of the PSKR1 kinase subdomains, see Hanks et al., 1988; Lindberg et al., 1992). The C-terminal region of PSKR1 starts at amino acid 1004 and is designated by a green line. The invariant Asp 860 and Arg 859 in PSKR1 subdomain VIb are marked with a red box. The invariant Lys 762 in the ATP binding site located in PSKR1 subdomain II is indicated by an red asterisk. The four most conserved PSKR1 activation loop sites Thr 890, Ser 893, Thr 894 and Thr 899 are designated by red asterisks. The confirmed PSKR1 phosphorylation sites are marked with squares and putative phosphorylation sites are marked with circles containing the letter “P”. *In vitro* PSKR1 autophosphorylation sites are represented by red squares or circles whereas *in planta* phosphorylation sites are designated by green squares/circles. Putative phosphorylation sites found *in planta* as well as *in vitro* are marked with half green and half red circles.

Figure 2. Overexpression of *PSKR1-GFP* in the wild-type background promotes root growth and the fusion protein can be successfully immunoprecipitated. (a) Phenotypes of 5-day-old de-etiolated seedlings from wt and *35S:PSKR1-GFP* in the wild-type background. (b) Average (± SE) root lengths were determined in two independent experiments with at least 46 seedlings analyzed per genotype. The asterisk indicates significantly different values between wt and *35S:PSKR1-GFP* ($P<0.05$, 2-sample *t*-test). (c) PSKR1-GFP localization was analyzed by confocal laser scanning microscopy in mesophyll protoplasts of 4-week-old soil-grown *35S:PSKR1-GFP* plants in the wild-type background. The receptor protein is expressed and localized at the plasma membrane. Scale bar = 5 µm. (d) Total protein extracts from wt seedlings and PSKR1-GFP transformed wt seedlings were immunoprecipitated with anti-GFP antibody at the concentrations indicated. The

immunoprecipitation products from wt and PSKR1-GFP seedlings were separated on a 10% SDS-PAGE gel. The blot was incubated with anti-GFP antibody. Molecular masses of marker proteins are indicated to the left of the Coomassie Blue-stained gel and the immunoblot.

Figure 3. Site-directed mutagenesis of specific PSKR1 activation loop residues abolishes PSKR1 kinase activity *in vitro*. (a) Scheme of PSKR1 (not drawn to scale) showing from left to right the signal peptide region (red), the extracellular leucine-rich repeats (yellow) interjected by an island domain (purple), a single helical transmembrane domain (TM, red), the intracellular juxtamembrane domain (grey) and the intracellular kinase domain (light blue). The activation loop located within the catalytic Ser/Thr kinase region is marked with a bar. The point mutations T890A, S/T893/4A, and T899A are indicated by red lines. (b) Auto- and transphosphorylation activity analysis of recombinant PSKR1-KD (KD=kinase domain). To the right, a Coomassie Blue-stained gel with affinity-purified H_6-PSKR1-KD (lane 1), the mutant H_6-PSKR1-K762E (lane 2), H_6-PSKR1-T890A (lane 3), H_6-PSKR1-T899A (lane 4), H_6-PSKR1-S/T893/4A (lane 5) and H_6-PSKR1-TSTT-A (lane 6) with myelin basic protein (MBP) as a substrate is shown. On the left, the respective autoradiograph is shown. Molecular masses of marker proteins are indicated in between autoradiograph and Coomassie Blue-stained gel. The six samples were incubated with 20 µCi [γ-^{32}P]ATP in kinase buffer for 1 h at room temperature and separated by SDS-PAGE (same as above). The radiolabel was visualized with a phosphor imager. (c) Radioactivity was expressed as photo-stimulated luminescence (PSL).

Figure 4. Schematic structure of PSKR1 with confirmed and putative phosphorylation sites. (a) PSKR1 is composed of a signal peptide region (SP), 21 leucine-rich repeats (LRR) and a 36-amino-acid island domain (ID), a single helical 21-amino-acid transmembrane domain (TM), a juxtamembrane region (JM), a kinase domain (KD) and a carboxy terminal domain (CT). The PSKR1 activation loop is designated “AL”. The designations for confirmed and putative PSKR1 phosphorylation sites are the same as in Figure 1a. The one putative phosphorylation site Thr 890 found in the negative control with *in vitro* autophosphorylated H_6-PSKR1-K762E protein (Hartmann et al., 2014) is written in turquoise.

Figure 5. Inhibition of phosphorylation of specific PSKR1 activation loop residues through site-directed mutagenesis impairs growth signaling *in planta*. (a) Expression of *PSKR1* was analyzed by RT-PCR in 5-day-old seedlings from wild-type (wt), *r1r2*, *35S:PSKR1(T890A)-1*,*2*,*3*, *35S:PSKR1(T899A)-1*,*2*,*3*, *35S:PSKR1(S/T893/4A)-1*,*2*,*3* and *35S:PSKR1(TSTT-A)-1*,*2*,*3* each in the *r1r2* background. *Actin2* cDNA was amplified as a control for RNA input. (b) Average (± SE) root lengths were determined in three independent experiments with at least 32 seedlings analyzed per genotype. Asterisks indicate significantly different values between *r1r2* and the other genotypes ($P<0.001$, 2-sample *t*-test). (c) Phenotypes of 5-day-old de-etiolated seedlings from wt, *r1r2* and the complementation line *35S:PSKR1(T890A)-3* in the *r1r2* background. (d) Phenotypes of 5-day-old de-etiolated seedlings from wt, *r1r2* and *35S:PSKR1(TSTT-A)-3* in the *r1r2* background.

Figure 6. Phosphorylation of specific Ser and Thr residues in the activation loop of PSKR1 is required for shoot growth. (a) Representative phenotypes of 4-week-old soil-grown wt, *r1r2*, *35S:PSKR1(T890A)-3*, *35S:PSKR1(S/T893/4A)-2*,*3*, *35S:PSKR1(T899A)-3*, *35S:PSKR1(TSTT-A)-2*,*3* and *35S:PSKR1-GFP-1* plants each in the null background. (b) The average projected rosette area from plants shown in Supplemental Figure S1 (± SE, n=8-9) was calculated using the program Rosette Tracker (De Vylder et al., 2012). Asterisks indicate significantly different values between *r1r2* and the other genotypes ($P<0.05$, 2-sample *t*-test).

Figure 7. Mutation of specific Ser and Thr PSKR1 activation loop residues impairs epidermal cell expansion. (a-g) Epidermis cells of the first rosette leaf from 4-week-old soil-grown wt (a), *r1r2* (b), *35S:PSKR1-GFP-1* (c), *35S:PSKR1(T890A)-3* (d), *35S:PSKR1(S/T893/4A)-2* (e), *35S:PSKR1(T899A)-3* (f) and *35S:PSKR1(TSTT-A)-3* (g) plants each in the null background. Scale bar = 100 µm. (h) The average (± SE, n=3) epidermal cell size [μm^2] was determined for wt, *r1r2*, *35S:PSKR1(T890A)-3*, *35S:PSKR1(S/T893/4A)-2*, *35S:PSKR1(T899A)-3*, *35S:PSKR1(TSTT-A)-3* and *35S:PSKR1-GFP-1*. Different letters indicate significantly different values ($P<0.05$, ANOVA, Tukey test).

Figure 1

(a)

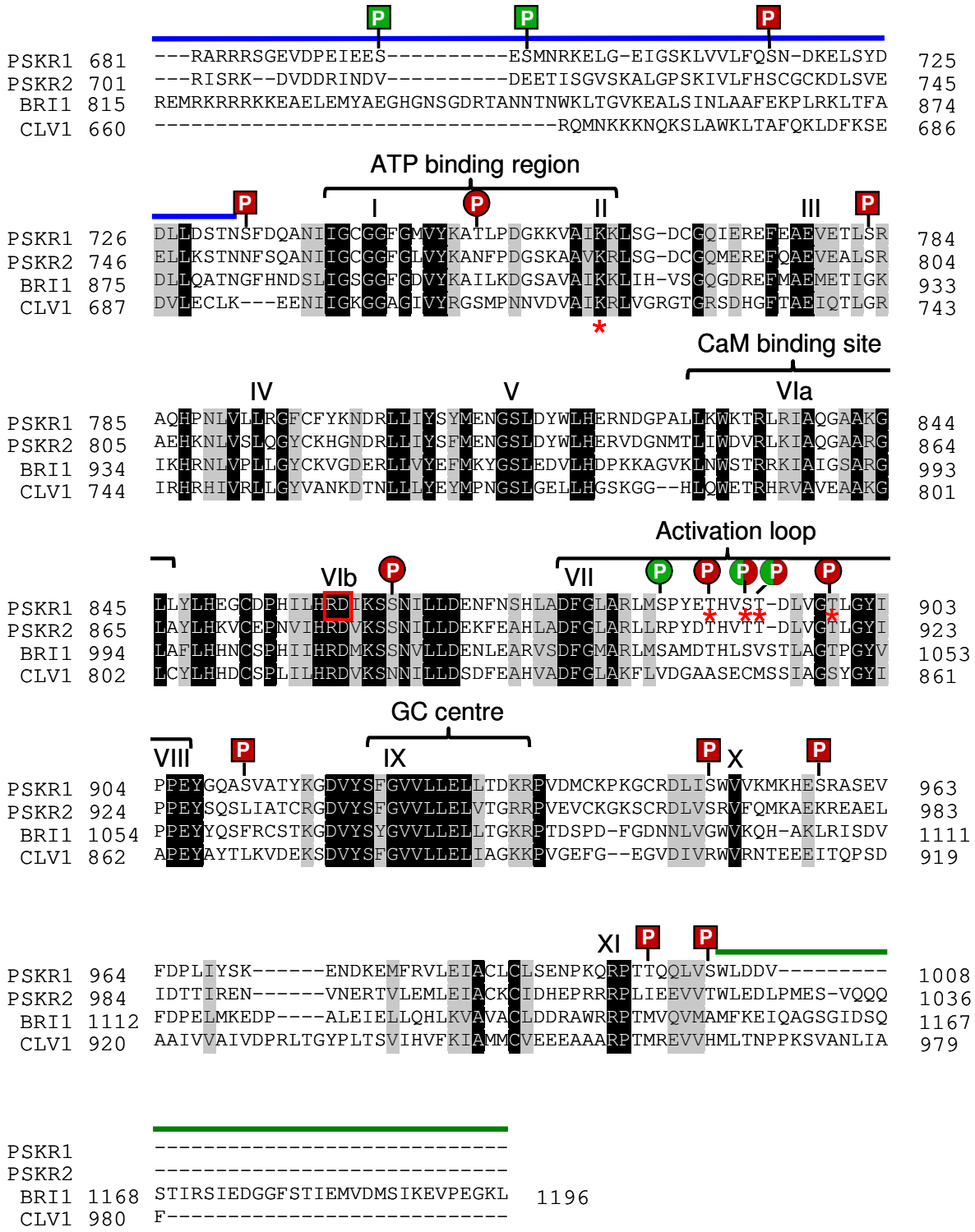
ATP binding region
I
II
III
CaM binding site
IV
V
VIa
Activation loop
VIb
VII
GC centre
VIII
IX
X
XI
PSKR1 681 ---RARRRSGEVDPEIEES----------ESMNRKELG-EIGSKLVVLFQSN-DKELSYD 725
PSKR2 701 ---RISRK--DVDDRINDV----------DEETISGVSKALGPSKIVLFHSCGCKDLSVE 745
BRI1 815 REMRKRRRKKEAELEMYAEGHGNSGDRTANNTNWKLTGVKEALSINLAAFEKPLRKLTFA 874
CLV1 660 ----------RQMNKKKNQKSLAWKLTAFQKLDFKSE 686
PSKR1 726 DLLDSTNSFDQANIIGCGGFGMVYKATLPDGKKVAIKKLSG-DCGQIEREFEAEVETLSR 784
PSKR2 746 ELLKSTNNFSQANIIGCGGFGLVYKANFPDGSKAAVKRLSG-DCGQMEREFQAEVEALSR 804
BRI1 875 DLLQATNGFHNDSLIGSGGFGDVYKAILKDGSAVAIKKLIH-VSGQGDREFMAEMETIGK 933
CLV1 687 DVLECLK---EENIIGKGGAGIVYRGSMPNNVDVAIKRLVGRGTGRSDHGFTAEIQTLGR 743
PSKR1 785 AQHPNLVLLRGFCFYKNDRLLIYSYMENGSLDYWLHERNDGPALLKWKTRLRIAQGAAKG 844
PSKR2 805 AEHKNLVSLQGYCKHGNDRLLIYSFMENGSLDYWLHERVDGNMTLIWDVRLKIAQGAARG 864
BRI1 934 IKHRNLVPLLGYCKVGDERLLVYEFMKYGSLEDVLHDPKKAGVKLNWSTRRKIAIGSARG 993
CLV1 744 IRHRHIVRLLGYVANKDTNLLLYEYMPNGSLGELLHGSKGG--HLQWETRHRVAVEAAKG 801
PSKR1 845 LLYLHEGCDPHILHRDIKSSNILLDENFNSHLADFGLARLMSPYETHVST-DLVGTLGYI 903
PSKR2 865 LAYLHKVCEPNVIHRDVKSSNILLDEKFEAHLADFGLARLLRPYDTHVTT-DLVGTLGYI 923
BRI1 994 LAFLHHNCSPHIIHRDMKSSNVLLDENLEARVSDFGMARLMSAMDTHLSVSTLAGTPGYV 1053
CLV1 802 LCYLHHDCSPLILHRDVKSNNILLDSDFEAHVADFGLAKFLVDGAASECMSSIAGSYGYI 861
PSKR1 904 PPEYGQASVATYKGDVYSFGVVLLELLTDKRPVDMCKPKGCRDLISWVVKMKHESRASEV 963
PSKR2 924 PPEYSQSLIATCRGDVYSFGVVLLELVTGRRPVEVCKGKSCRDLVSRVFQMKAEKREAEL 983
BRI1 1054 PPEYYQSFRCSTKGDVYSYGVVLLELLTGKRPTDSPD-FGDNNLVGWVKQH-AKLRISDV 1111
CLV1 862 APEYAYTLKVDEKSDVYSFGVVLLELIAGKKPVGEFG--EGVDIVRWVRNTEEEITQPSD 919
PSKR1 964 FDPLIYSK------ENDKEMFRVLEIACLCLSENPKQRPTTQQLVSWLDDV--------- 1008
PSKR2 984 IDTTIREN------VNERTVLEMLEIACKCIDHEPRRRPLIEEVVTWLEDLPMES-VQQQ 1036
BRI1 1112 FDPELMKEDP----ALEIELLQHLKVAVACLDDRAWRRPTMVQVMAMFKEIQAGSGIDSQ 1167
CLV1 920 AAIVVAIVDPRLTGYPLTSVIHVFKIAMMCVEEEAAARPTMREVVHMLTNPPKSVANLIA 979
PSKR1 ----------
PSKR2 ----------
BRI1 1168 STIRSIEDGGFSTIEMVDMSIKEVPEGKL 1196
CLV1 980 F----------

Figure 2

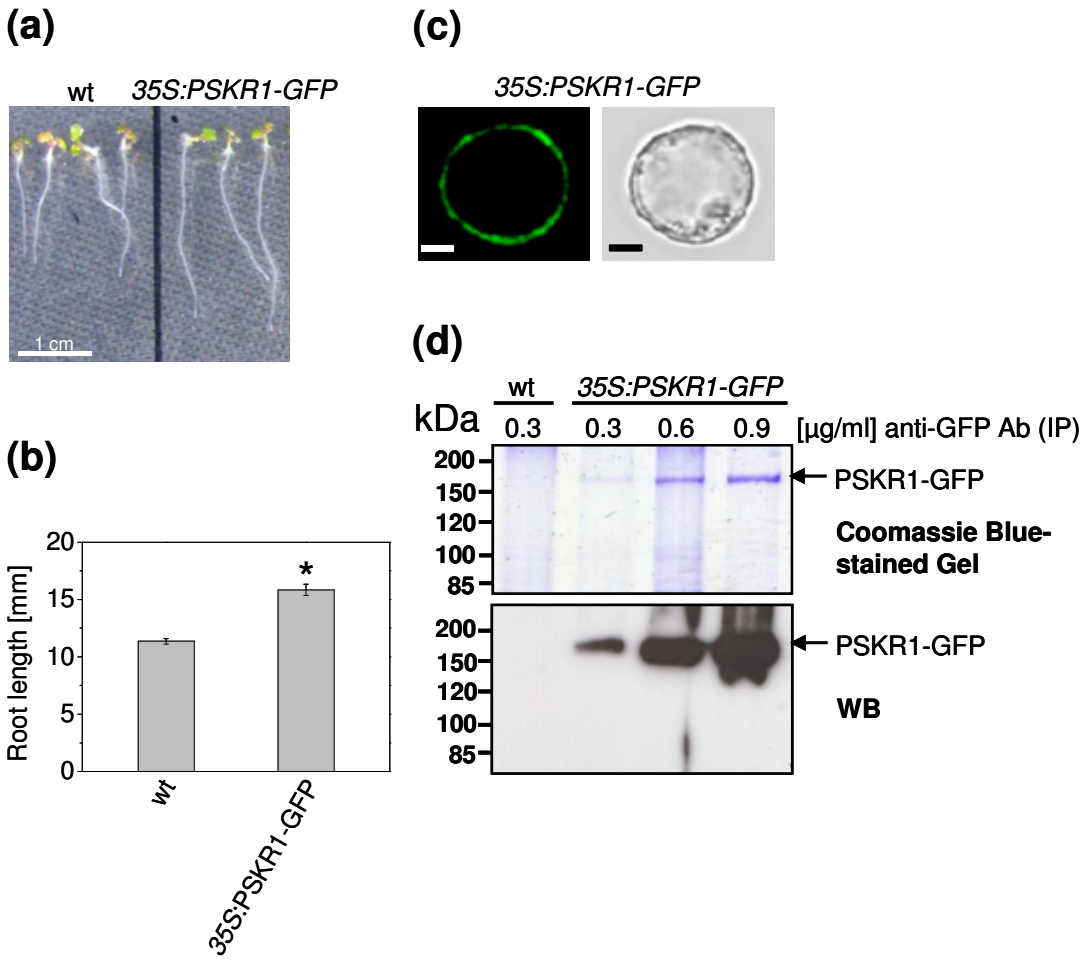
(a)
wt
35S:PSKR1-GFP
1 cm
(b)
Root length [mm]
20
15
10
5
0
*
wt
35S:PSKR1-GFP
(c)
35S:PSKR1-GFP
(d)
wt
35S:PSKR1-GFP
kDa
0.3
0.3
0.6
0.9
[µg/ml] anti-GFP Ab (IP)
200
150
120
100
85
PSKR1-GFP
Coomassie Blue-stained Gel
200
150
120
100
85
PSKR1-GFP
WB

Figure 3

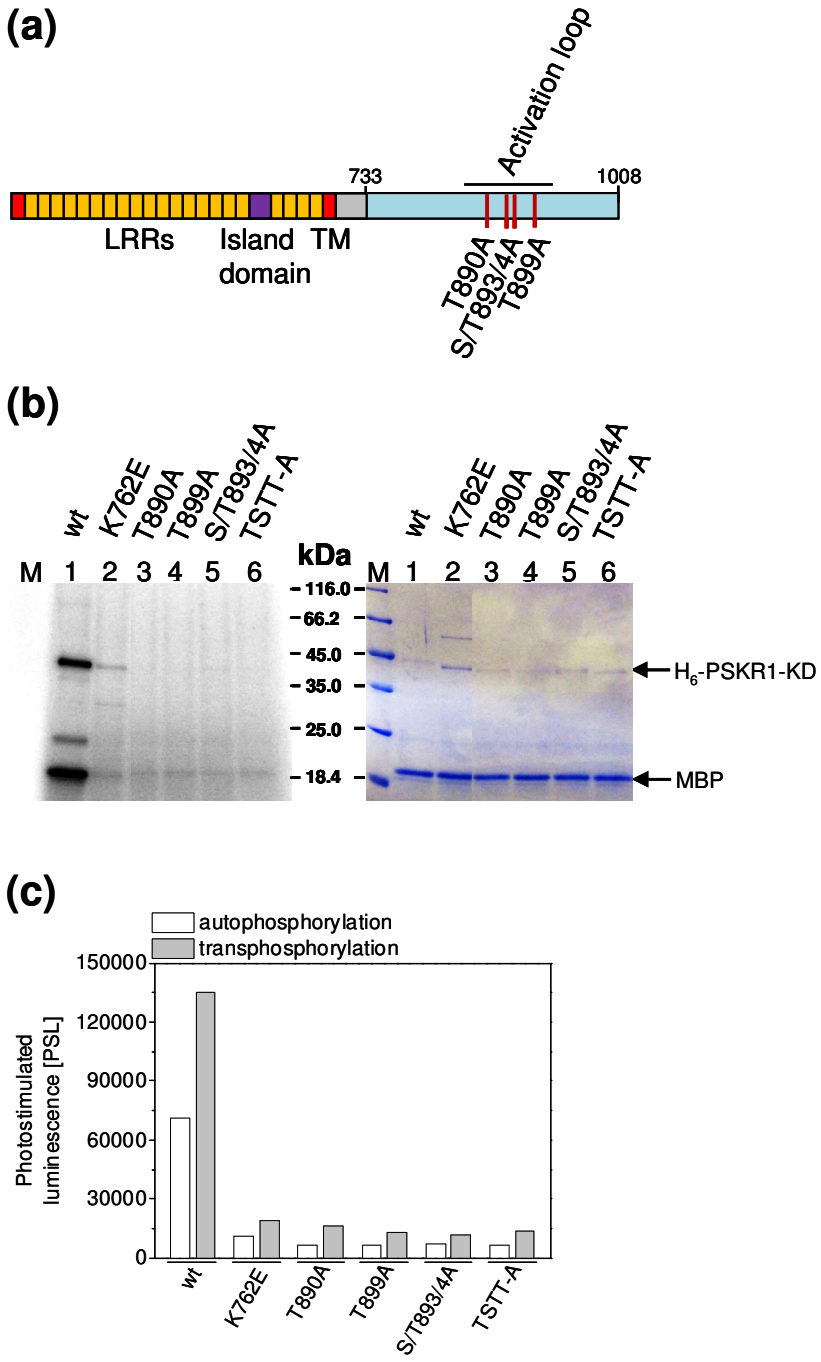
(a)
Activation loop
733
1008
LRRs
Island domain
TM
T890A
S/T893/4A
T899A
(b)
wt
K762E
T890A
T899A
S/T893/4A
TSTT-A
M 1 2 3 4 5 6
kDa
116.0
66.2
45.0
35.0
25.0
18.4
H6-PSKR1-KD
MBP
(c)
autophosphorylation
transphosphorylation
Photostimulated luminescence [PSL]
150000
120000
90000
60000
30000
0
wt
K762E
T890A
T899A
S/T893/4A
TSTT-A

Figure 4

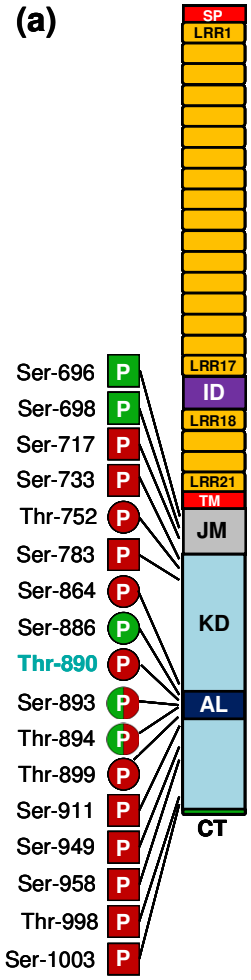
(a)
SP
LRR1
LRR17
ID
LRR18
LRR21
TM
JM
KD
AL
CT
Ser-696
Ser-698
Ser-717
Ser-733
Thr-752
Ser-783
Ser-864
Ser-886
Thr-890
Ser-893
Thr-894
Thr-899
Ser-911
Ser-949
Ser-958
Thr-998
Ser-1003
P

Figure 5

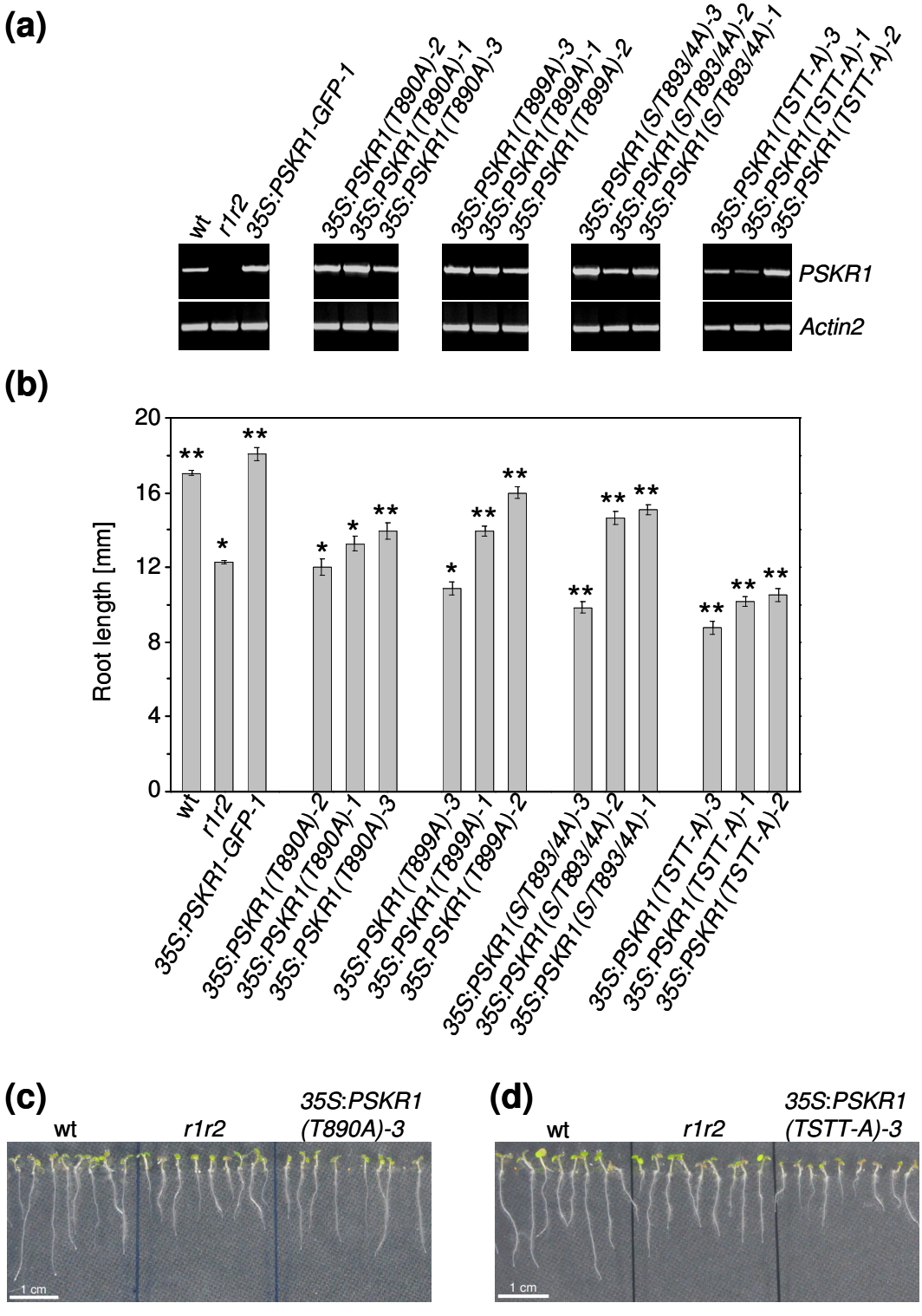
(a)
wt
r1r2
35S:PSKR1-GFP-1
35S:PSKR1(T890A)-2
35S:PSKR1(T890A)-1
35S:PSKR1(T890A)-3
35S:PSKR1(T899A)-3
35S:PSKR1(T899A)-1
35S:PSKR1(T899A)-2
35S:PSKR1(S/T893/4A)-3
35S:PSKR1(S/T893/4A)-2
35S:PSKR1(S/T893/4A)-1
35S:PSKR1(TSTT-A)-3
35S:PSKR1(TSTT-A)-1
35S:PSKR1(TSTT-A)-2
PSKR1
Actin2
(b)
Root length [mm]
0
4
8
12
16
20
(c)
wt
r1r2
35S:PSKR1 (T890A)-3
1 cm
(d)
wt
r1r2
35S:PSKR1 (TSTT-A)-3
1 cm

Figure 6

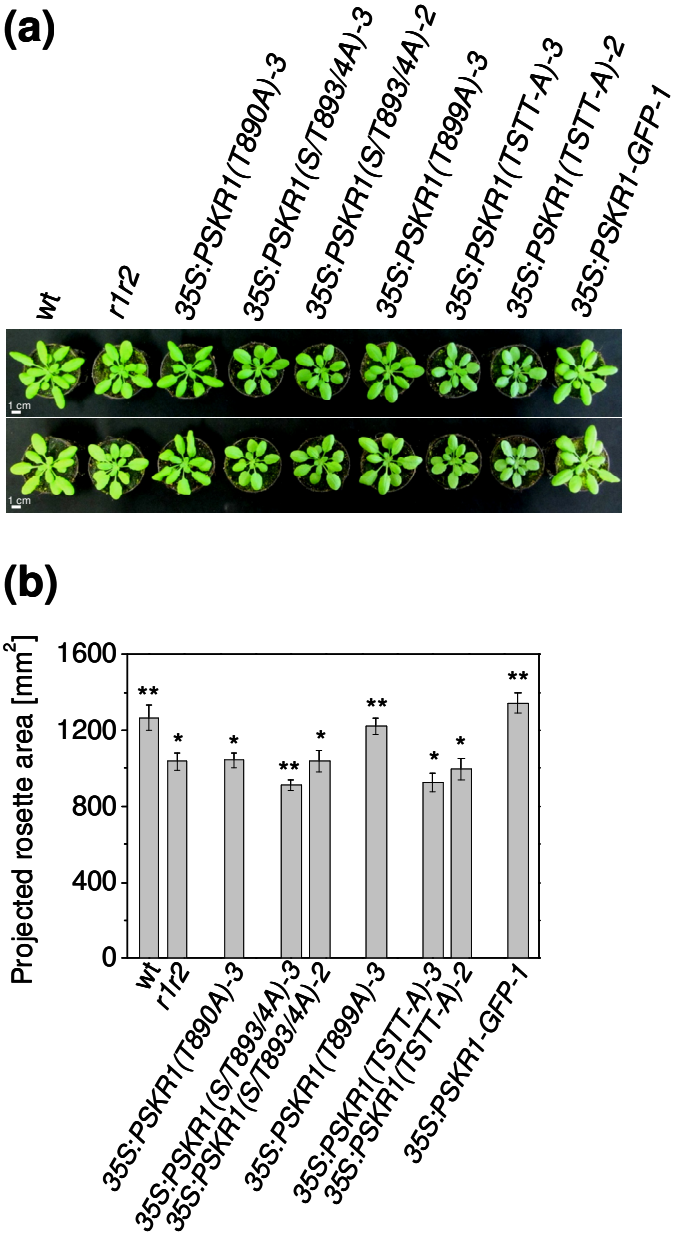
(a)
wt
r1r2
35S:PSKR1(T890A)-3
35S:PSKR1(S/T893/4A)-3
35S:PSKR1(S/T893/4A)-2
35S:PSKR1(T899A)-3
35S:PSKR1(TSTT-A)-3
35S:PSKR1(TSTT-A)-2
35S:PSKR1-GFP-1
1 cm
(b)
Projected rosette area [mm²]
1600
1200
800
400
0
**
*
wt
r1r2
35S:PSKR1(T890A)-3
35S:PSKR1(S/T893/4A)-3
35S:PSKR1(S/T893/4A)-2
35S:PSKR1(T899A)-3
35S:PSKR1(TSTT-A)-3
35S:PSKR1(TSTT-A)-2
35S:PSKR1-GFP-1

Figure 7

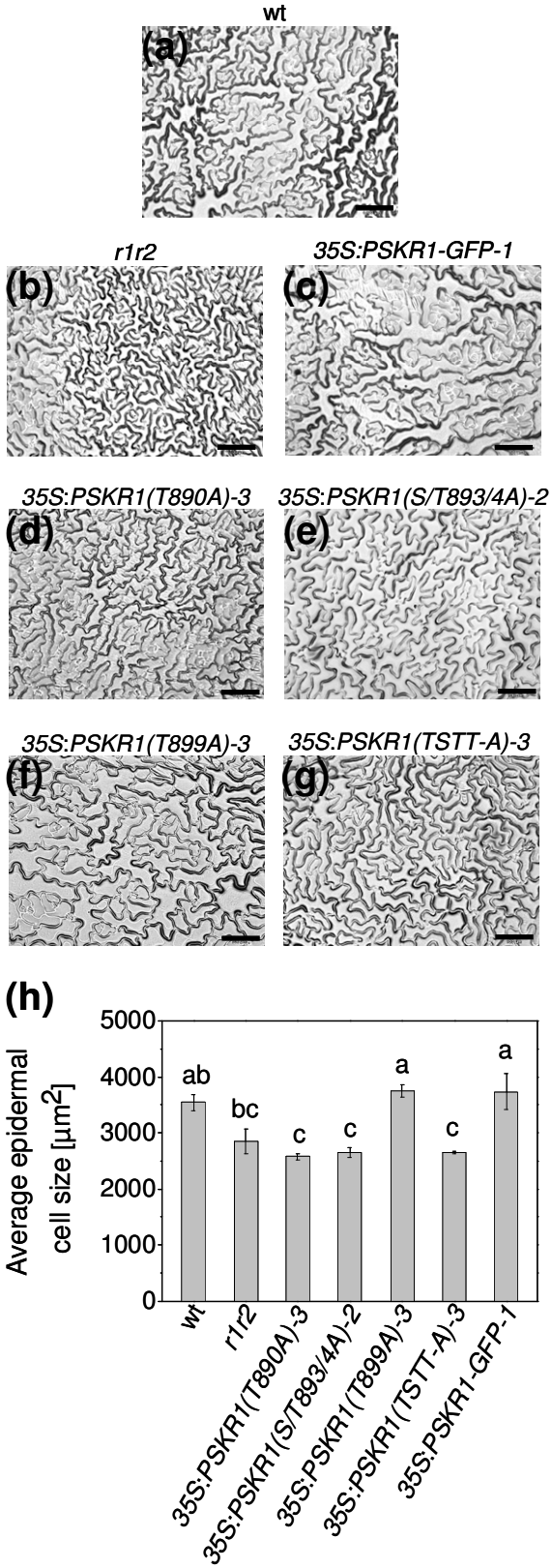
wt
(a)
r1r2
(b)
35S:PSKR1-GFP-1
(c)
35S:PSKR1(T890A)-3
(d)
35S:PSKR1(S/T893/4A)-2
(e)
35S:PSKR1(T899A)-3
(f)
35S:PSKR1(TSTT-A)-3
(g)
(h)
Average epidermal cell size [µm2]
5000
4000
3000
2000
1000
0
ab
bc
c
c
a
c
a
wt
r1r2
35S:PSKR1(T890A)-3
35S:PSKR1(S/T893/4A)-2
35S:PSKR1(T899A)-3
35S:PSKR1(TSTT-A)-3
35S:PSKR1-GFP-1

Supplemental Figure S1

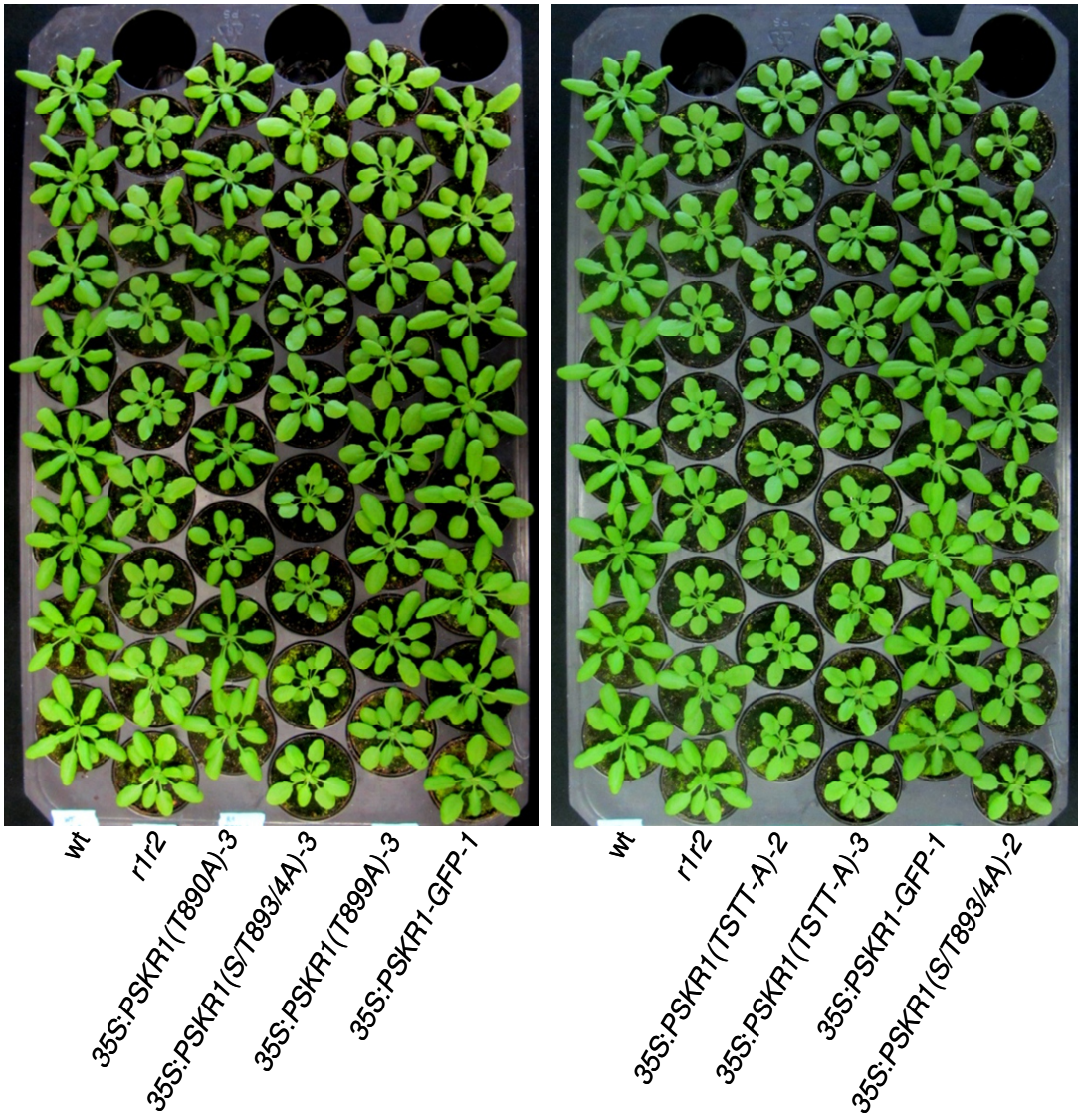

Supplemental Figure S1. Site-directed mutagenesis of specific PSKR1 activation loop residues impairs growth signaling *in planta*. Phenotypes of 4-week-old soil-grown wt, *r1r2*, *35S:PSKR1(T890A)-3*, *35S:PSKR1(S/T893/4A)-2,3*, *35S:PSKR1(T899A)-3*, *35S:PSKR1(TSTT-A)-2,3* and *35S:PSKR1-GFP-1* plants each in the *r1r2* background.

Abschließende Diskussion

Der PSK-Signalweg in Arabidopsis reguliert das Wurzel-, Hypokotyl- und Sprosswachstum (Matsubayashi et al., 2006; Kutschmar et al., 2009; Stührwohldt et al., 2011). Dies ist vorrangig auf eine Förderung der Zellexpansion zurückzuführen. Die Zugabe von PSK zu Arabidopsis-Keimlingen bewirkt eine Steigerung des Wurzelwachstums (Kutschmar et al., 2009). Eine Überexpression des Präproproteins PSK4 resultiert in Keimlingen mit längeren Wurzeln (Matsubayashi et al., 2006). Dies waren Hinweise darauf, dass die Konzentration des Liganden PSK das durch den PSK-Signalweg geförderte Wurzelwachstum begrenzt. In Kapitel 1 dieser Arbeit wurde gezeigt, dass der PSK-Signalweg in Arabidopsis auch durch die Menge an verfügbaren PSK-Rezeptoren eingeschränkt sein kann. Eine Überexpression von *PSKR1* beziehungsweise *PSKR2* in Wildtyp-Keimlingen führte in beiden Fällen zu einer signifikanten Steigerung des Wurzel- und Hypokotylwachstums im Vergleich zum Wildtyp. Die Zugabe von 1 µM PSK resultierte in einem nochmals gesteigerten Wurzelwachstum. Daraus kann geschlossen werden, dass PSK-abhängiges Wurzelwachstum sowohl durch die Konzentration des Liganden, als auch durch die verfügbare Rezeptormenge begrenzt wird. Entsprechend zeigen *DcPSKR1*-überexprimierende Karottenzellen nach der Zugabe von PSK eine gesteigerte Teilungsrate (Matsubayashi et al., 2002). Darüber hinaus ist in mikrosomalen Fraktionen von *AtPSKR1*-überexprimierenden Arabidopsiszellen die Bindungsaktivität für Tritium-markiertes PSK erhöht (Matsubayashi et al., 2006). Durch eine Analyse von *pskr2-1 Knockout*-Keimlingen war vor dieser Arbeit gezeigt worden, dass PSKR2 nur einen geringen Einfluss auf das Wurzelwachstum hat (Kutschmar et al., 2009). Die Ergebnisse in Kapitel 1 weisen darauf hin, dass PSKR2 ebenfalls das durch den PSK-Signalweg geförderte Wurzelwachstum begrenzt.

Die Regulation eines Rezeptors kann über seine Synthese, Modifikation oder den Abbau erfolgen. Die Abundanz des Plasmamembran-lokalisierten Brassinosteroid-Rezeptors BRI1 wird durch eine von der Phosphatase PP2A katalysierte Dephosphorylierung reguliert (Wu et al., 2011). Nach der Dephosphorylierung wird BRI1 abgebaut und damit der BR-Signalweg ausgeschaltet. Die Endozytose stellt eine weitere Möglichkeit für die Regulation an verfügbarem Rezeptor dar. So führt die Endozytose von aktiviertem BRI1 zu einer Abschwächung des nachgeschalteten Signalwegs, eine Inhibierung der BRI1-Endozytose dagegen zu einer gesteigerten

Signalweiterleitung (Irani et al., 2012). Es besteht eine hohe strukturelle Ähnlichkeit zwischen BRI1 und den PSK-Rezeptoren. Um die PSK-Antwort anzupassen, ist eine über vergleichbare Mechanismen ablaufende Regulation der verfügbaren Menge an PSKR1 und PSKR2 denkbar.

Wachstum wird durch PSK in einer nicht-zellautonomen Weise gefördert

PSKR1 wird ubiquitär in Wurzeln, Hypokotylen, Blättern, Stängeln und Blüten exprimiert (Matsubayashi et al., 2006; Kutschmar et al., 2009; Stührwohldt et al., 2011). Ein entsprechendes ubiquitäres Expressionsmuster wurde auch für die PSK Präproproteine nachgewiesen (Yang et al., 2001; Matsubayashi et al., 2006; Kutschmar et al., 2009; Stührwohldt et al., 2011). Promotor-GUS Analysen zeigten in der Wurzel eine Aktivität des *PSKR1*-Promotors in allen Zellschichten der Wachstumsregion. Epidermiszellen, die mit zwei darunterliegenden Cortexzellen Kontakt haben, differenzieren zu spezialisierten Trichoblasten, welche Wurzelhaare ausbilden (Kuppusamy et al., 2009). Im Gegensatz dazu bilden Atrichoblasten keine Wurzelhaare aus. Diese Zellen stehen mit nur einer Cortexzelle in Kontakt.
Das Expressionsmuster von *PSKR1* beziehungsweise der PSK Präproproteine ließ vermuten, dass sowohl der Rezeptor als auch der Ligand *in planta* ubiquitär gebildet werden. Es stellte sich die Frage, ob PSK *in planta* als autokriner Wachstumsfaktor fungiert. Peters und Tomos (1996) berichteten, dass Sachs bereits 1875 die Hypothese aufgestellt hatte, nach der die äußeren Zellschichten passiv den expandierenden inneren Zellschichten folgen. In neueren Studien wurde diese Hypothese dahingehend weiterentwickelt, dass die durch dicke Zellwände charakterisierte Epidermisschicht die Wachstumsrate von Stängeln und Hypokotylen bestimmt (Niklas und Paolillo, 1997; Kutschera und Niklas, 2007; Kutschera, 2008; Savaldi-Goldstein et al., 2007).
In dieser Arbeit wurde gezeigt, dass PSK-Signale *in planta* mobil sind und PSK daher als nicht-zellautonomer Wachstumsfaktor fungiert (Hartmann et al., 2013). Eine Expression von *PSKR1* unter der Kontrolle des *CER6*-Promotors in der Epidermis der Doppelmutante *pskr1-3 pskr2-1* (abgekürzt *r1r2*) war ausreichend für eine PSK-vermittelte Wachstumsförderung von Wurzeln und Hypokotylen. In einem weiteren Komplementationsversuch wurde der Atrichoblasten-spezifische *GLABRA2* (*GL2*)-Promotor verwendet. Dabei zeigte sich, dass die in Atrichoblasten lokalisierte PSK-Perzeption nicht nur bei diesen spezialisierten Epidermiszellen eine Zellexpansion

hervorrief. Auch bei Trichoblasten ohne *PSKR1*-Expression wurde Wachstum angeregt. Die Komplementation mit dem Endodermis-spezifischen *SCR*-Promotor führte nicht zu Wurzelwachstum, was darauf hindeutete, dass der PSK-Signalweg nicht über die Endodermis das Wurzelwachstum reguliert. Diese Ergebnisse lassen darauf schließen, dass eine PSK-Perzeption in der Epidermisschicht ausreicht, um das Wachstum nicht nur der äußeren, sondern auch der inneren Zellschichten anzuregen. Es ist denkbar, dass ein mobiles oder möglicherweise mechanisches Signal von PSK-perzipierenden Atrichoblasten zu benachbarten Trichoblasten und zu weiter entfernt liegenden inneren Zellschichten weitergeleitet wird.

Die für die Aufrechterhaltung von Stammzellen im Spross- und Wurzelapikalmeristem verantwortlichen Rezeptorkinasen CLV1 und ACR4 reichern sich bevorzugt an Plasmodesmen an (Stahl et al., 2013). Stahl und Simon (2013) schlugen ein Modell vor, nach dem ein bislang unbekannter mobiler Stammzellfaktor von Zellen des ruhenden Zentrums durch Plasmodesmen zu benachbarten Zellschichten wandern kann. Die interzelluläre Bewegung von Transkriptionsfaktoren durch Plasmodesmen stellt bei der epidermalen Zelldifferenzierung eine Kommunikation zwischen Zellschichten dar (Kurata et al., 2005). Auch für andere Signalwegskomponenten wurde gezeigt, dass sie sich über Plasmodesmen zwischen angrenzenden Zellen bewegen (Sevilem et al., 2013).

Es ist denkbar, dass mobile PSK-Signale durch Plasmodesmen von Atrichoblasten zu Trichoblasten und anderen Zellschichten wandern, um Wachstum anzuregen. Darüber hinaus besteht die Möglichkeit, dass PSKR1 von Atrichoblasten entlang der Plasmamembran über Plasmodesmen zu benachbarten Trichoblasten wandert, um auch dort eine PSK-Perzeption zu ermöglichen. Das unbekannte mobile PSK-Signal ist möglicherweise auch mit der durch Phytohormone vermittelten Wachstumsförderung in Verbindung zu bringen. Das Hypokotylwachstum von Arabidopsis-Keimlingen wird durch verschiedene Phytohormone kontrolliert (Vandenbussche et al., 2005). Das pflanzliche Hormon Gibberellinsäure fördert über eine erhöhte Zellstreckung das Hypokotylwachstum (Cowling und Harberd, 1999). Gibberellinsäure ist auch bei der Kontrolle der Zellstreckungsrichtung und der Zellteilung beteiligt (Achard et al., 2009; Ubeda-Tomás et al., 2008). Auxin spielt eine Rolle sowohl bei der Förderung des Hypokotylwachstums, als auch bei der Ethylen-vermittelten Hemmung der Hypokotylstreckung (Vandenbussche et al., 2005). Das Hypokotyl von Höheren Pflanzen setzt sich von außen nach innen aus den

Zellschichten Epidermis, Cortex, Endodermis und dem Leitgewebe zusammen. Es wurde gezeigt, dass die Epidermis stärker auf Auxin reagiert als die inneren Zellschichten (Kutschera, 1992). Dies war ein Hinweis darauf, dass die Epidermis das bevorzugte Ziel einer Auxinwirkung darstellt. Neben der Förderung des zellulären Streckungswachstums spielt Auxin auch eine Rolle bei der Organbildung (Vanneste und Friml, 2009).

Anders als Auxin regulieren Brassinosteroide (BRs), wie auch das PSK, vorwiegend die Zellstreckung (Kim und Wang, 2010). BRs fördern das Wurzel- und Hypokotylwachstum (Müssig et al., 2003; Srivastava et al., 2009). *Knockout*-Mutanten wie *bri1* und *bak1* sind BR-insensitiv, beziehungsweise weisen eine geringere Sensitivität gegenüber BRs auf (Clouse et al., 1996; Kauschmann et al., 1996; Li et al., 1996, 2002). Die Phänotypen dieser *Knockout*-Mutanten lassen sich auf Defekte in der Zellstreckung zurückführen. Savaldi-Goldstein et al. (2007) zeigten, dass eine BR-Perzeption beziehungsweise eine BR-Synthese in der Epidermis für die Wachstumsförderung des gesamten Hypokotyls ausreichend ist. BRs regulieren nicht über innere Zellschichten, sondern über die Epidermis das Wachstum (Savaldi-Goldstein et al., 2007). Möglicherweise ist eine interzelluläre Bewegung von BR-Signalwegskomponenten zwischen der Epidermis und den inneren Zellschichten durch Plasmodesmen an diesem Prozess beteiligt (Savaldi-Goldstein et al., 2007). Des Weiteren ist eine interzelluläre Kommunikation zwischen der Epidermis und inneren meristematischen Zellen in die BRI1-vermittelte Kontrolle der Wurzelmeristemgröße involviert (Hacham et al., 2011).

Die vorgestellten Ergebnisse zeigen, dass sowohl PSK, als auch BRs das Wachstum des gesamten Organs über seine äußerste Zellschicht, die Epidermis, kontrollieren. Es stellten sich somit die Fragen, ob sich die beiden Signalwege überschneiden und ob die PSK-vermittelte Wachstumsförderung BR-abhängig ist. Brassinazol (BZ) bindet spezifisch an die Steroid 22-Hydroxylase *DWARF4* (DWF4) und inhibiert dadurch die Hydroxylierung an der C-22 Position der Seitenkette von BRs und damit die BR-Synthese (Asami et al., 2001). BZ-behandelte *tpst-1* Keimlinge waren PSK-insensitiv, reagierten aber bei einer gleichzeitigen Applikation von BZ mit dem hochaktiven Brassinosteroid 24-Epibrassinolid (BL) wieder auf PSK (Hartmann et al., 2013). In Arabidopsis wandelt *DE-ETIOLATED2* (DET2) in dem zweiten Schritt der BR-Synthese Campesterol in Campestanol um (Fujioka et al., 1997). Das Ausschalten der BR-Synthese in *det2-1* Keimlingen machte diese insensitiv

gegenüber PSK. Eine Herunterregulierung von BRI1 in *bri1-200A* Keimlingen führte ebenfalls zu einem reduzierten PSK-vermittelten Wurzelwachstum (Hartmann et al., 2013). Nach der BR-Perzeption durch BRI1 an der Plasmamembran wird eine Signaltransduktionskette mit Phosphorylierungen und Dephosphorylierungen in Gang gesetzt, welche in der Aktivierung der Transkriptionsfaktoren BES1 und BZR1 resultiert (Clouse, 2011). In *bzr1-1D* und *bes1-1 Knockout*-Keimlingen wurde das PSK-vermittelte Wurzelwachstum nicht beeinträchtigt (Hartmann et al., 2013). Dies ist möglicherweise auf eine redundante Funktionsweise dieser Transkriptionsfaktoren zurückzuführen (Clouse, 2011). Zusammengefasst deuten diese Ergebnisse darauf hin, dass der BR-Signalweg für die PSK-vermittelte Förderung des Wurzelwachstums benötigt wird.

Die Kinaseaktivität von PSKR1 ist essentiell für die wachstumsfördernde Wirkung *in planta*

Kinasen zeichnen sich durch hochkonservierte Domänen aus (Li und Chory, 1997). Der Aufbau einer Kinase kann in zwei funktionale Bereiche eingeteilt werden, wobei der kleinere für die ATP- und der größere für die Substratbindung zuständig ist (Huse und Kuriyan, 2002; Adams, 2003). In einer Spalte zwischen dem kleineren und dem größeren Bereich befindet sich die ATP-Binderegion von PSKR1, welche die Subdomänen I und II umfasst (Hartmann et al., 2014). Hier ist ein invariantes Lysin (Lys) der Subdomäne II an der Positionierung der α- und β-Phosphatgruppen des ATPs beteiligt, um eine Hydrolyse zu ermöglichen (Huse und Kuriyan, 2002). Ein Austausch dieses Lys gegen ein Glutamat (Glu) in PSKR1 bewirkt den Verlust der *in vitro* Kinaseaktivität von PSKR1 (Hartmann et al., 2014). Eine Überexpression der Kinase-inaktiven Variante von PSKR1 in *r1r2* führte zu einer nochmals gesteigerten Hemmung des Wurzelwachstums im Vergleich zu *r1r2*-Keimlingen. Dieser wachstumshemmende Effekt lässt sich möglicherweise auf eine Interaktion des Kinase-inaktiven PSKR1 mit einem anderen, bisher unbekannten wachstumsfördernden Protein zurückführen. Entsprechende wachstumshemmende Effekte konnten auch für Kinase-inaktive Varianten von BAK1, CLV1 und BRI1 gezeigt werden (Li et al., 2002; Diévart et al., 2003; Wang et al., 2005b). Wie bereits erwähnt, fördert der PSK-Signalweg die Zellexpansion. Nach Heyman et al. (2013) ist PSK zudem in der Aufrechterhaltung einer geringen Teilungsrate von Zellen des ruhenden Zentrums im Wurzelapikalmeristem beteiligt. Der BR-Signalweg steigert die

Teilungsrate von Zellen des ruhenden Zentrums über den Transkriptionsfaktor ERF115. Dabei aktiviert ERF115 wiederum das Präproprotein PSK5, was auf eine direkte Verbindung zwischen PSK und dem BR-Signalweg hindeutet (Heyman et al., 2013). Es ist denkbar, dass PSKR1 Signalwegskomponenten mit anderen wachstumsfördernden Signalwegen wie beispielsweise dem des BR teilt. Der BRI1-Korezeptor BAK1, der auch als Korezeptor für einige andere Liganden-bindende RLKs wie beispielsweise FLS2 fungiert, ist ein möglicher Kandidat (Chinchilla et al., 2007, 2009; Li, 2010; Halter et al., 2014). Die Interaktion von BAK1 mit BRI1 steigert die BRI1-Kinaseaktivität und die BR-abhängige Zellexpansion. Der wachstums-hemmende Effekt vom Kinase-inaktiven PSKR1 könnte auf die Interaktion mit BAK1 und eine daraus resultierende Beeinträchtigung des BR-Signalwegs zurückgehen.

Funktionale Analysen von kartierten Phosphorylierungsstellen in PSKR1

Es ist nicht bekannt, wie das PSK-Signal nach der Perzeption des Liganden durch die PSK-Rezeptoren übertragen wird. Die ektopisch exprimierte Kinasedomäne von PSKR1 besitzt *in vitro* eine Kinaseaktivität (Kwezi et al., 2011). Darüber hinaus wurde innerhalb der PSKR1 Subdomäne IX ein Guanylatzyklase-Zentrum identifiziert (Kwezi et al., 2011; Wong und Gehring, 2013). Die ektopisch exprimierte cytoplasmatische Domäne von PSKR1 bildet *in vitro* den zellulären Botenstoff cGMP aus GTP. PSKR1 kann daher *in vitro* mehrere Signale aussenden. Die *in vitro* Kinaseaktivität von PSKR1 wurde in dieser Arbeit bestätigt (Hartmann et al., 2014). Durch massenspektrometrische Analysen wurden *in vitro* Autophosphorylierungs-stellen in der Domäne hinter dem Transmembransegment (*Juxtamembrane* (JM)-Domäne), in der Kinasedomäne und nahe dem C-Terminus (CT) von PSKR1 identifiziert. Es stellte sich die Frage, ob die PSK-Perzeption an der Zelloberfläche durch PSKR1 *in planta* eine intrazelluläre Auto- und Transphosphorylierungs-Kaskade auslöst. Hinweise darauf lieferten weitere massenspektrometrische Analysen, die *in planta* Phosphorylierungsstellen in der JM Domäne und der Kinasedomäne von PSKR1 identifizierten. Außerdem wurden *in planta* mindestens eine und bis zu drei putative Phosphorylierungsstellen in der Aktivierungsschleife der PSKR1-Subdomäne VII/VIII identifiziert. Alle Massen-spektrometrieanalysen von PSKR1 zeigten, dass *in vitro* und *in planta* vorrangig Serine (Ser) phosphoryliert wurden. Dies wurde zuvor ebenfalls für die LRR RLKs BRI1 und CLV1 gezeigt (Williams et al., 1997; Stone et al., 1998; Oh et al., 2000). In einer

phosphoproteomischen Analyse von Membranproteinen aus Arabidopsis wurde gezeigt, dass bei über fünfzig RLKs mehr als 75% der identifizierten *in planta* Phosphorylierungsstellen in der JM- und CT-Domäne vorkamen. Die restlichen Phosphorylierungsstellen wurden in der Kinasedomäne identifiziert (Nühse et al., 2004). Es ist bisher nicht bekannt, ob und wie Phosphorylierungen in der JM Domäne die Aktivität von PSKR1 regulieren. Die meisten Aminosäuren in der JM Domäne sind zwischen LRR RLKs nicht konserviert. Bei der RLK ACR4 gibt es eine intramolekulare Interaktion zwischen der JM- und Kinasedomäne, welche die ACR4-Kinaseaktivität reguliert (Meyer et al., 2013). Bei der PDGF- und Eph-Rezeptorfamilie hält die JM Domäne im nicht phosphorylierten Zustand die Kinase in einer inaktiven Konformation (Griffith et al., 2004; Wiesner et al., 2006; Walter et al., 2007; Davis et al., 2008). Die Entfernung der JM Domäne von BRI1 führt zu einem Verlust der Signalfunktion des Rezeptors (Wang et al., 2005c; Wang et al., 2008).

Die massenspektrometrischen Analysen deuteten an, dass mindestens eine und möglicherweise bis zu vier Aminosäuren (Threonin (T) 890, S893, T894 und T899) in der Aktivierungsschleife von PSKR1 phosphoryliert werden. Eine zielgerichtete phosphoablative Mutagenese dieser putativen Phosphorylierungsstellen resultierte jeweils in einem Verlust der *in vitro* Kinaseaktivität des Rezeptors. Phosphorylierungen von einer bis drei Aminosäuren in der Aktivierungsschleife führen zu einer Konformationsänderung, welche die Substratbindung begünstigt und die Kinaseaktivität anschaltet (Johnson et al., 1996; Adams 2003). Phosphoablative Mutationen von Phosphorylierungsstellen innerhalb der Aktivierungsschleifen von BRI1 und BAK1 führen ebenfalls zu einem Verlust der Kinaseaktivität dieser Rezeptoren (Wang et al., 2005b; Wang et al., 2008; Oh et al., 2009; Yun et al., 2009). Mutationen der möglichen Phosphorylierungsstellen in der Aktivierungsschleife von PSKR1 führten *in planta* zu einer differenziellen Hemmung des Wachstums. Die Überexpression einer phosphoablativen PSKR1-Variante in *r1r2*, bei der alle vier potenziellen Phosphorylierungsstellen mutiert wurden, resultierte in der deutlichsten Wachstumshemmung. Der wachstumshemmende Effekt war vergleichbar mit dem des Kinase-inaktiven PSKR1. Das lässt darauf schließen, dass die vierfache phosphoablative Mutagenese innerhalb der Aktivierungsschleife bei dieser PSKR1-Variante eine Aktivierung des Rezeptors unterbindet. Dadurch kann zum einen der PSK-Signalweg nicht angeschaltet werden, zum anderen könnten weitere wachstumsfördernde Signalwege mit beeinträchtigt sein. Detailliertere

Komplementationsversuche mit der zweifach mutierten PSKR1(S/T893/4A)- und der einfach mutierten PSKR1(T890A)-Variante führten zu ebenfalls signifikanten Beeinträchtigungen des Wachstums. Mutationen von Aminosäuren in den Aktivierungsschleifen von BRI1 und SERK1, welche dem Thr 890 und Ser 893 von PSKR1 entsprechen, führen *in vitro* zu einer größeren Beeinträchtigung der Substrat- als der Autophosphorylierung (Shah et al., 2001; Wang et al., 2005b). Bei BRI1 wurden in der Aktivierungsschleife Phosphorylierungen von Aminosäuren nachgewiesen, die dem Thr 890 und Ser 893 von PSKR1 entsprechen (Bojar et al., 2014). Nach Bojar et al. (2014) sind die beiden entsprechenden Aminosäuren zur Oberfläche von BRI1 gerichtet und wirken möglicherweise an der Stabilisierung der Konformation der Aktivierungsschleife mit. Demnach könnten beim PSKR1 das Thr 890 allein oder Thr 890 und Ser 893 zusammen echte *in planta* Phosphorylierungsstellen darstellen.

Die Bindung von Calmodulin an PSKR1 wird für die Wachstumsförderung *in planta* benötigt

Für PSKR1 wurde bisher eine Kinaseaktivität nachgewiesen, die essentiell für die *in planta* Wachstumsförderung ist (Hartmann et al., 2014). Des Weiteren besitzt PSKR1 *in vitro* eine Guanylatzyklase-Aktivität (Kwezi et al., 2011). In dieser Arbeit wurden darüber hinaus Ergebnisse für eine Bindung des Kalziumsensors Calmodulin (CaM) an PSKR1 gezeigt (Hartmann et al., 2014). CaMs sind Ca^{2+}-bindende Proteine, welche durch die Bindung an Kalzium ihre Konformation und damit ihre Affinität gegenüber Zielproteinen ändern. Dadurch wird die Aktivität dieser Zielproteine reguliert (McCormack et al., 2005; Dodd et al., 2010). CaMs perzipieren lokale Ca^{2+}-Konzentrationen und vermitteln eine spezifische physiologische Antwort. Für die *S LOCUS RECEPTOR KINASE* (SRK) aus *Brassica oleracea* sowie für RLK4, CLV1 und BRI1 aus Arabidopsis wurde *in vitro* eine Bindung an CaM gezeigt (Vanoosthuyse et al., 2003; Charpenteau et al., 2004; Oh et al., 2012). Über eine bioinformatische Analyse wurde eine 18 Aminosäuren lange CaM-Bindungsdomäne (CaMBD) innerhalb der Subdomäne VI der PSKR1-Kinasedomäne identifiziert. Durch eine Bimolekulare Fluoreszenzkomplementations (BiFC)-Analyse wurde gezeigt, dass *in planta* alle CaM-Isoformen aus Arabidopsis an PSKR1 binden. In geringerem Umfang interagierte das CaM-ähnliche (CML) Protein CML8, wohingegen CML9 keine detektierbare Bindung an PSKR1 zeigte. CaMBDs weisen insgesamt eine

geringe Konservierung auf der Aminosäureebene auf. Die Gemeinsamkeit von CaMBDs besteht in einer konservierten Sekundärstruktur, der amphipathischen α-Helix (Rainaldi et al., 2007).

Der Austausch der N-terminalen hydrophoben Anker-Aminosäure Tryptophan in der CaMBD von PSKR1 gegen ein hydrophiles Serin resultierte in einer starken Reduzierung der Bindung aller CaM-Isoformen an den Rezeptor (Hartmann et al., 2014). Das Ergebnis der Berechnung der physikochemischen Eigenschaften der mutierten CaMBD von PSKR1 nach Gautier et al. (2008) mittels “Heliquest“ ließ darauf schließen, dass das hydrophile Serin die hydrophobe Oberfläche der α-Helix stört. Der unvollständige Verlust der CaM-Bindung an den CaMBD-mutierten PSKR1 geht möglicherweise auf noch vorhandene elektrostatische Interaktionen zwischen der CaMBD und den N- beziehungsweise C-terminalen Domänen der CaMs zurück. Die Überexpression der CaMBD-mutierten Variante von PSKR1 in *r1r2* führte zu einer Wachstumshemmung, ähnlich wie bei der Überexpression des Kinase-inaktiven Rezeptors. Daraus lässt sich schließen, dass die CaM-Bindung an PSKR1 *in planta* für eine PSK-vermittelte Wachstumsförderung benötigt wird. Die CaM-Bindung an NtCBK2, NtCaMK1, AtCRK1, AtCRCK1 und AtCRLK1 förderte die jeweiligen Enzymaktivitäten dieser Zielproteine in verschiedenem Ausmaß (Hua et al., 2003a; Ma et al., 2004; Wang et al., 2004; Yang et al., 2004). Ähnlich wie PSKR1 zeigte BRI1 unterschiedliche Affinitäten gegenüber den vier CaM-Isoformen aus Arabidopsis (Oh et al., 2012). Die *in vitro* Kinaseaktivität von BRI1 wurde durch die Bindung der CaM-Isoformen AtCaM6 und AtCaM7 sowie des AtCML8 negativ reguliert. Es ist denkbar, dass die Kinaseaktivität von PSKR1 durch die Bindung bestimmter CaM-Isoformen ebenfalls reguliert wird. Aufgrund der beschriebenen *in planta* Ergebnisse ist eine Hemmung der Kinaseaktivität von PSKR1 unwahrscheinlich. Möglicherweise wird die von PSKR1 ausgelöste Phosphorylierungskaskade durch eine Bindung von CaM spezifisch reguliert.

Du und Poovaiah (2005) wiesen auch *in planta* eine Verbindung zwischen der Ca^{2+}- und BR-Signalwirkung nach. Das BR-Biosyntheseprotein *DWARF1* (DWF1) bindet spezifisch CaMs, was essentiell für die *in planta* Funktion von DWF1 ist (Du und Poovaiah, 2005). In Arabidopsis wandelt DWF1 24-Methylencholesterin in Campesterol um (Choe et al., 1999). Die BR-Perzeption durch BRI1 bewirkt einen Anstieg der cytoplasmatischen Ca^{2+}-Konzentration, was eine Ca^{2+}-Signalkaskade auslöst (Zhao et al., 2013). Die BR-abhängige Ca^{2+}-Signalkaskade fungiert

unabhängig von der BRI1-Phosphorylierungskaskade (Zhao et al., 2013). In diesem Zusammenhang wurde gezeigt, dass die LRR RLK *PLANT ELICITOR PEPTIDE RECEPTOR1* (PEPR1), wie PSKR1 und BRI, *in vitro* cGMP generiert (Qi et al., 2010). Dieses durch PEPR1 gebildete cGMP aktiviert während des PEP-Signalwegs *in planta* den *CYCLIC NUCLEOTIDE-GATED CHANNEL 2* (CNGC2), der Ca^{2+}-Ionen in die Zelle passieren lässt (Ma et al., 2013). Der CNGC-vermittelte Anstieg der cytoplasmatischen Ca^{2+}-Konzentration wird durch die Bindung von CaM an den Kanal unterbunden (Hua et al., 2003b). Qi et al. (2010) spekulierten, dass ein cGMP-produzierender PEPR1 und ein durch das cGMP aktivierter CNGC2 in der Plasmamembran einen Proteinkomplex bilden. Demnach könnten die Konzentrationen des zellulären Botenstoffs cGMP in der Umgebung des CNGC2 erhöht sein. Dadurch könnte der Kanal dort aktiviert werden und nachfolgend einen Anstieg der cytoplasmatischen Ca^{2+}-Konzentration bewirken. Ein entsprechender Proteinkomplex könnte eine Erklärung dafür liefern, wie PSKR1, ein Ca^{2+}-durchlässiger CNGC und CaM zusammenarbeiten, um eine genau abgestimmte PSK-abhängige Signalkaskade auszulösen.

Literaturverzeichnis

Achard, P., Gusti, A., Cheminant, S., Alioua, M., Dhondt, S., Coppens, F., Beemster, G.T., Genschik, P. (2009) Gibberellin signaling controls cell proliferation rate in Arabidopsis. Current Biology 19: 1188–1193.

Adams, J. A. (2003) Current Topics Activation Loop Phosphorylation and Catalysis in Protein Kinases: Is There Functional Evidence for the Autoinhibitor Model? Biochemistry 42: 601–607.

Aida, M., Beis, D., Heidstra, R., Willemsen, V., Blilou, I., Galinha, C., Nussaume, L., Noh, Y.S., Amasino, R., Scheres, B. (2004) The PLETHORA Genes Mediate Patterning of the Arabidopsis Root Stem Cell Niche. Cell 119: 109–120.

Albrecht, C., Russinova, E., Kemmerling, B., Kwaaitaal, M., de Vries, S.C. (2008) Arabidopsis SOMATIC EMBRYOGENESIS RECEPTOR KINASE proteins serve brassinosteroid-dependent and -independent signaling pathways. Plant Physiology 148: 611–619.

Albrecht, C., Boutrot, F., Segonzac, C., Schwessinger, B., Gimenez-Ibanez, S., Chinchilla, D., Rathjen, J.P., de Vries, S.C., Zipfel, C. (2012) Brassinosteroids inhibit pathogen-associated molecular pattern-triggered immune signaling independent of the receptor kinase BAK1. Proceedings of the National Academy of Sciences of the United States of America 109: 303–308.

Amano, Y., Tsubouchi, H., Shinohara, H., Ogawa, M., Matsubayashi, Y. (2007) Tyrosine-sulfated glycopeptide involved in cellular proliferation and expansion in Arabidopsis. Proceedings of the National Academy of Sciences of the United States of America 104: 18333–18338.

Asami, T., Mizutani, M., Fujioka, S., Goda, H., Min, Y.K., Shimada, Y., Nakano, T., Takatsuto, S., Matsuyama, T., Nagata, N., Sakata, K., Yoshida, S. (2001) Selective interaction of triazole derivatives with DWF4, a cytochrome P450 monooxygenase of the brassinosteroid biosynthetic pathway, correlates with brassinosteroid deficiency in planta. The Journal of Biological Chemistry 276: 25687–25691.

Barr, P.J. (1991) Mammalian Subtilisins : The Long-Sought Dibasic Processing Endoproteases. Cell 66: 3–5.

Bedinger, P.A., Pearce, G., Covey, P.A. (2010) RALFs: Peptide regulators of plant growth. Plant Signaling & Behavior 5: 1342–1346.

Beisswanger, R., Corbeil, D., Vannier, C., Thiele, C., Dohrmann, U., Kellner, R., Ashman, K., Niehrs, C., Huttner, W.B. (1998) Existence of distinct tyrosylprotein sulfotransferase genes: molecular characterization of tyrosylprotein sulfotransferase-2. Proceedings of the National Academy of Sciences of the United States of America 95: 11134–11139.

Belkhadir, Y., Jaillais, Y., Epple, P., Balsemão-Pires, E., Dangl, J.L., Chory, J. (2012) Brassinosteroids modulate the efficiency of plant immune responses to microbe-associated molecular patterns. Proceedings of the National Academy of Sciences of the United States of America 109: 297–302.

Bellincampi, D., Morpurgo, G. (1987) Conditioning factor affecting growth in plant cells in culture. Plant Science 51: 83–91.

Bemis, S.M., Torii, K.U. (2007) Autonomy of cell proliferation and developmental programs during Arabidopsis aboveground organ morphogenesis. Developmental Biology 304: 367–381.

Berger, F., Haseloff, J., Schiefelbein, J., Dolan, L. (1998) Positional information in root epidermis is defined during embryogenesis and acts in domains with strict boundaries. Current Biology 8: 421–430.

Bergonci, T., Ribeiro, B., Ceciliato, P.H.O., Guerrero-Abad, J.C., Silva-Filho, M.C., Moura, D.S. (2014) Arabidopsis thaliana RALF1 opposes brassinosteroid effects on root cell elongation and lateral root formation. Journal of Experimental Botany: doi:10.1093/jxb/eru099

Birnberg, P.R., Somers, D.A., Brenner, M.L. (1988) Characterization of Conditioning Factors that Increase Colony Formation from «Black Mexican Sweet Corn» Protoplasts. Journal of Plant Physiology 132: 316–321.

Bleckmann, A., Weidtkamp-Peters, S., Seidel, C.A.M., Simon, R. (2010) Stem cell signaling in Arabidopsis requires CRN to localize CLV2 to the plasma membrane. Plant Physiology 152: 166–176.

Bojar, D., Martinez, J., Santiago, J., Rybin, V., Bayliss, R., Hothorn, M. (2014) Crystal structures of the phosphorylated BRI1 kinase domain and implications for brassinosteroid signal initiation. The Plant Journal 78: 31–43.

Boonburapong, B., Buaboocha, T. (2007) Genome-wide identification and analyses of the rice calmodulin and related potential calcium sensor proteins. BMC Plant Biology 7: 4.

Bouché, N., Yellin, A., Snedden, W.A., Fromm, H. (2005) Plant-specific calmodulin-binding proteins. Annual Review of Plant Biology 56: 435–466.

Brand, U., Fletcher, J.C., Hobe, M., Meyerowitz, E.M., Simon, R. (2000) Dependence of Stem Cell Fate in Arabidopsis on a Feedback Loop Regulated by CLV3 Activity. Science 289: 617–619.

Busch, W., Benfey, P.N. (2010) Information processing without brains--the power of intercellular regulators in plants. Development 137: 1215–1226.

Butenko, M.A., Vie, A.K., Brembu, T., Aalen, R.B., Bones, A.M. (2009) Plant peptides in signalling: looking for new partners. Trends in Plant Science 14: 255–263.

Caesar, K., Elgass, K., Chen, Z., Huppenberger, P., Witthöft, J., Schleifenbaum, F., Blatt, M.R., Oecking, C., Harter, K. (2011) A fast brassinolide-regulated response pathway in the plasma membrane of Arabidopsis thaliana. The Plant Journal 66: 528–540.

Caño-Delgado, A., Yin, Y., Yu, C., Vafeados, D., Mora-García, S., Cheng, J.-C., Nam, K.H., Li, J., Chory, J. (2004) BRL1 and BRL3 are novel brassinosteroid receptors that function in vascular differentiation in Arabidopsis. Development 131: 5341–5351.

Cao, J., Shi, F. (2012) Evolution of the RALF Gene Family in Plants: Gene Duplication and Selection Patterns. Evolutionary Bioinformatics Online 8: 271–292.

Charpenteau, M., Jaworski, K., Ramirez, B.C., Tretyn, A., Ranjeva, R., Ranty, B. (2004) A receptor-like kinase from Arabidopsis thaliana is a calmodulin-binding protein. The Biochemical Journal 379: 841–848.

Chen, X., Chang, M., Wang, B., Wu, B. (1997) Cloning of a Ca(2+)-ATPase gene and the role of cytosolic Ca2+ in the gibberellin-dependent signaling pathway in aleurone cells. The Plant Journal 11: 363–371.

Chen, Y.F., Matsubayashi, Y., Sakagami, Y. (2000) Peptide growth factor phytosulfokine-alpha contributes to the pollen population effect. Planta 211: 752-755.

Chin, D., Means, A.R. (2000) Calmodulin: a prototypical calcium sensor. Trends in Cell Biology 10: 322–328.

Chinchilla, D., Zipfel, C., Robatzek, S., Kemmerling, B., Nürnberger, T., Jones, J.D.G., Felix, G., Boller, T. (2007) A flagellin-induced complex of the receptor FLS2 and BAK1 initiates plant defence. Nature 448: 497–500.

Chinchilla, D., Shan, L., He, P., de Vries, S., Kemmerling, B. (2009) One for all: the receptor-associated kinase BAK1. Trends in Plant Science 14: 535–541.

Choe, S., Dilkes, B.P., Gregory, B.D., Ross, A.S., Yuan, H., Noguchi, T., Fujioka, S., Takatsuto, S., Tanaka, A., Yoshida, S., Tax, F.E., Feldmann, K.A. (1999) The Arabidopsis dwarf1 mutant is defective in the conversion of 24-methylenecholesterol to campesterol in brassinosteroid biosynthesis. Plant Physiology 119: 897–907.

Chono, M., Honda, I., Zeniya, H., Yoneyama, K., Saisho, D., Takeda, K., Takatsuto, S., Hoshino, T., Watanabe, Y. (2003) A Semidwarf Phenotype of Barley uzu Results from a Nucleotide Substitution in the Gene Encoding a Putative Brassinosteroid Receptor. Plant Physiology 133: 1209-1219.

Clapham, D.E. (2007) Calcium signaling. Cell 131: 1047–1058.

Clark, S.E., Williams, R.W., Meyerowitz, E.M. (1997) The CLAVATA1 gene encodes a putative receptor kinase that controls shoot and floral meristem size in Arabidopsis. Cell 89: 575–585.

Clouse, S.D. (2011) Brassinosteroid signal transduction: from receptor kinase activation to transcriptional networks regulating plant development. The Plant Cell 23: 1219–1230.

Clouse, S.D., Langford, M., McMorris, T.C. (1996) A brassinosteroid-insensitive mutant in Arabidopsis thaliana exhibits multiple defects in growth and development. Plant Physiology 111: 671–678.

Covey, P.A, Subbaiah, C.C., Parsons, R.L., Pearce, G., Lay, F.T., Anderson, M.A., Ryan, C.A., Bedinger, P.A. (2010) A pollen-specific RALF from tomato that regulates pollen tube elongation. Plant Physiology 153: 703–715.

Cowling, R.J., Harberd, N.P. (1999) Gibberellins control Arabidopsis hypocotyl growth via regulation of cellular elongation. Journal of Experimental Botany 50: 1351–1357.

Crouch, T.H., Klee, C.B. (1980) Positive cooperative binding of calcium to bovine brain calmodulin. Biochemistry 19: 3692–3698.

Dardick, C., Ronald, P. (2006) Plant and animal pathogen recognition receptors signal through non-RD kinases. PLoS Pathogens 2: e2. doi:10.1371/journal.ppat.0020002.

Davis, T.L., Walker, J.R., Loppnau, P., Butler-Cole, C., Allali-Hassani, A., Dhe-Paganon, S. (2008) Autoregulation by the juxtamembrane region of the human ephrin receptor tyrosine kinase A3 (EphA3). Structure 16: 873–884.

Day, I.S., Reddy, V.S., Shad Ali, G., Reddy, A.S.N. (2002) Analysis of EF-hand-containing proteins in Arabidopsis. Genome Biology 3: RESEARCH0056.

De Smet, I., Jürgens, G. (2007) Patterning the axis in plants--auxin in control. Current Opinion in Genetics & Development 17: 337–343.

De Smet, I., Vassileva, V., De Rybel, B., Levesque, M.P., Grunewald, W., Van Damme, D., Van Noorden, G., Naudts, M., Van Isterdael, G., De Clercq, R., Wang, J.Y., Meuli, N., Vanneste, S., Friml, J., Hilson, P., Jürgens, G., Ingram, G.C., Inzé, D., Benfey, P.N., Beeckman, T. (2008) Receptor-Like Kinase ACR4 Restricts Formative Cell Divisions in the Arabidopsis Root. Science 322: 594-597.

De Smet, I., Voss, U., Jürgens, G., Beeckman, T. (2009) Receptor-like kinases shape the plant. Nature Cell Biology 11: 1166–1173.

DeFalco, T.A, Bender, K.W., Snedden, W.A. (2010) Breaking the code: Ca2+ sensors in plant signalling. The Biochemical Journal 425: 27–40.

Diévart, A., Clark, S.E. (2003) Using mutant alleles to determine the structure and function of leucine-rich repeat receptor-like kinases. Current Opinion in Plant Biology 6: 507–516.

Diévart, A., Dalal, M., Tax, F.E., Lacey, A.D., Huttly, A., Li, J., Clark, S.E. (2003) CLAVATA1 Dominant-Negative Alleles Reveal Functional Overlap between Multiple Receptor Kinases That Regulate Meristem and Organ Development. The Plant Cell 15: 1198–1211.

Dodd, A.N., Kudla, J., Sanders, D. (2010) The language of calcium signaling. Annual Review of Plant Biology 61: 593–620.

Du, L., Poovaiah, B.W. (2005) Ca2+/calmodulin is critical for brassinosteroid biosynthesis and plant growth. Nature 437: 741–745.

Fletcher, J.C., Brand, U., Running, M.P., Simon, R., Meyerowitz, E.M. (1999) Signaling of Cell Fate Decisions by CLAVATA3 in Arabidopsis Shoot Meristems. Science 283: 1911–1914.

Fletcher, J.C., Meyerowitz, E.M. (2000) Cell signaling within the shoot meristem. Current Opinion in Plant Biology 3: 23–30.

Friedrichsen, D.M., Joazeiro, C.A., Li, J., Hunter, T., Chory, J. (2000) Brassinosteroid-insensitive-1 is a ubiquitously expressed leucine-rich repeat receptor serine/threonine kinase. Plant Physiology 123: 1247–1256.

Fujioka, S., Li, J., Choi, Yong-Hwa, Seto, H., Takatsuto, S., Noguchi, T., Watanabe, T., Kuriyama, H., Yokota, T., Chory, J., Sakurai, A. (1997) The Arabidopsis deetiolated2 mutant is blocked early in brassinosteroid biosynthesis. The Plant Cell 9: 1951-1962.

Galinha, C., Hofhuis, H., Luijten, M., Willemsen, V., Blilou, I., Heidstra, R., Scheres, B. (2007) PLETHORA proteins as dose-dependent master regulators of Arabidopsis root development. Nature 449: 1053–1057.

Gallagher, K.L., Benfey, P.N. (2005) Not just another hole in the wall: understanding intercellular protein trafficking. Genes & Development 19: 189–195.

Gampala, S.S., Kim, T., He, J., Tang, W., Deng, Z., Guan, S., Lalonde, S., Sun, Y., Gendron, J.M., Chen, H., Shibagaki, N., Ferl, R.J., Ehrhardt, D., Chong, K., Burlingame, A.L., Wang, Z.Y. (2007) An Essential Role for 14-3-3 Proteins in Brassinosteroid Signal Transduction in Arabidopsis. Developmental Cell 13: 177–189.

Gautier, R., Douguet, D., Antonny, B., Drin, G. (2008) HELIQUEST: a web server to screen sequences with specific alpha-helical properties. Bioinformatics 24: 2101–2102.

Goldberg, J., Nairn, A.C., Kuriyan, J. (1996) Structural basis for the autoinhibition of calcium/calmodulin-dependent protein kinase I. Cell 84: 875–887.

Gómez-Gómez, L., Boller, T. (2000) FLS2: an LRR receptor-like kinase involved in the perception of the bacterial elicitor flagellin in Arabidopsis. Molecular Cell 5: 1003–1011.

Gonzalez, N., De Bodt, S., Sulpice, R., Jikumaru, Y., Chae, E., Dhondt, S., Van Daele, T., De Milde, L., Weigel, D., Kamiya, Y., Stitt, M., Beemster G.T.S., Inzé, D. (2010) Increased leaf size: different means to an end. Plant Physiology 153: 1261–1279.

González-García, M.-P., Vilarrasa-Blasi, J., Zhiponova, M., Divol, F., Mora-García, S., Russinova, E., Caño-Delgado, A.I. (2011) Brassinosteroids control meristem size by promoting cell cycle progression in Arabidopsis roots. Development 138: 849–859.

Griffith, J., Black, J., Faerman, C., Swenson, L., Wynn, M., Lu, F., Lippke, J., Saxena, K. (2004) The structural basis for autoinhibition of FLT3 by the juxtamembrane domain. Molecular Cell 13: 169–178.

Guo, Y., Han, L., Hymes, M., Denver, R., Clark, S.E. (2010) CLAVATA2 forms a distinct CLE-binding receptor complex regulating Arabidopsis stem cell specification. The Plant Journal 63: 889–900.

Hacham, Y., Holland, N., Butterfield, C., Ubeda-Tomas, S., Bennett, M.J., Chory, J., Savaldi-Goldstein, S. (2011) Brassinosteroid perception in the epidermis controls root meristem size. Development 138: 839–848.

Haecker, A., Gross-Hardt, R., Geiges, B., Sarkar, A., Breuninger, H., Herrmann, M., Laux, T. (2004) Expression dynamics of WOX genes mark cell fate decisions during early embryonic patterning in Arabidopsis thaliana. Development 131: 657–668.

Hahm, S.H., Saunders, M.J. (1991) Cytokinin increases intracellular Ca2+ in Funaria: detection with Indo-1. Cell Calcium 12: 675–681.

Halter, T., Imkampe, J., Mazzotta, S., Wierzba, M., Postel, S., Bücherl, C., Kiefer, C., Stahl, M., Chinchilla, D., Wang, X., Nürnberger, T., Zipfel, C., Clouse, S., Borst, J.W., Boeren, S., de Vries, S.C., Tax, F., Kemmerling, B. (2014) The leucine-rich repeat receptor kinase BIR2 is a negative regulator of BAK1 in plant immunity. Current Biology 24: 134-143.

Han, J., Tan, J., Tu, L., Zhang, X. (2014) A peptide hormone gene, GhPSK promotes fibre elongation and contributes to longer and finer cotton fibre. The Plant Biotechnology Journal: doi: 10.1111/pbi.12187.

Hanai, H., Nakayama, D., Yang, H., Matsubayashi, Y., Hirota, Y., Sakagami, Y. (2000a) Existence of a plant tyrosylprotein sulfotransferase: novel plant enzyme catalyzing tyrosine O-sulfation of preprophytosulfokine variants in vitro. FEBS Letters 470: 97–101.

Hanai, H., Matsuno, T., Yamamoto, M., Matsubayashi, Y., Kobayashi, T., Kamada, H., Sakagami, Y. (2000b) A secreted peptide growth factor, phytosulfokine, acting as a stimulatory factor of carrot somatic embryo formation. Plant & Cell Physiology 41: 27–32.

Hartmann, J., Stührwohldt, N., Dahlke, R.I., Sauter, M. (2013) Phytosulfokine control of growth occurs in the epidermis, is likely to be non-cell autonomous and is dependent on brassinosteroids. The Plant Journal 73: 579–590.

Hartmann, J., Fischer, C., Dietrich, P., Sauter, M. (2014) Kinase activity and calmodulin binding are essential for growth signaling by the phytosulfokine receptor PSKR1. The Plant Journal 78: 192–202.

Haruta, M., Monshausen, G., Gilroy, S., Sussman, M.R. (2008) A cytoplasmic Ca2+ functional assay for identifying and purifying endogenous cell signaling peptides in Arabidopsis seedlings: identification of AtRALF1 peptide. Biochemistry 47: 6311–6321.

He, J.X., Gendron, J.M., Sun, Y., Gampala, S.S.L., Gendron, N., Sun, C.Q., Wang, Z.Y. (2005) BZR1 is a transcriptional repressor with dual roles in brassinosteroid homeostasis and growth responses. Science 307: 1634–1638.

He, K., Gou, X., Yuan, T., Lin, H., Asami, T., Yoshida, S., Russell, S.D., Li, J. (2007) BAK1 and BKK1 regulate brassinosteroid-dependent growth and brassinosteroid-independent cell-death pathways. Current Biology 17: 1109–1115.

He, J., Gendron, J.M., Sun, Y., Gampala, S.S.L., Sun, C.Q., Wang, Z.Y. (2010) BZR1 is a transcriptional repressor with dual roles in brassinosteroid homeostasis and growth responses. Science 307: 1634-1638.

Hepler, P.K. (2005) Calcium: a central regulator of plant growth and development. The Plant Cell 17: 2142–2155.

Heyman, J., Cools, T., Vandenbussche, F., Heyndrickx, K.S., Van Leene, J., Vercauteren, I., Vanderauwera, S., Vandepoele, K., De Jaeger, G., Van Der Straeten, D., De Veylder, L. (2013) ERF115 controls root quiescent center cell division and stem cell replenishment. Science 342: 860–863.

Hirakawa, Y., Shinohara, H., Kondo, Y., Inoue, A., Nakanomyo, I., Ogawa, M., Sawa, S., Ohashi-Ito, K., Matsubayashi, Y., Fukuda, H. (2008) Non-cell-autonomous control of vascular stem cell fate by a CLE peptide/receptor system. Proceedings of the National Academy of Sciences of the United States of America 105: 15208–15213.

Hobe, M., Müller, R., Grünewald, M., Brand, U., Simon, R. (2003) Loss of CLE40, a protein functionally equivalent to the stem cell restricting signal CLV3, enhances root waving in Arabidopsis. Development Genes and Evolution 213: 371–381.

Hothorn, M., Belkhadir, Y., Dreux, M., Dabi, T., Noel, J.P., Wilson, I.A., Chory, J. (2011) Structural basis of steroid hormone perception by the receptor kinase BRI1. Nature 474: 467-471.

Hothorn, M., Belkhadir, Y., Dreux, M., Dabi, T., Joseph, P., Wilson, I.A., Chory, J. (2012) Structural basis of steroid hormone perception by the receptor kinase BRI1. Nature 474: 467-471.

Hua, W., Liang, S., Lu, Y.-T. (2003a) A tobacco (Nicotiana tabaccum) calmodulin-binding protein kinase, NtCBK2, is regulated differentially by calmodulin isoforms. The Biochemical Journal 376: 291–302.

Hua, B., Mercier, R.W., Zielinski, R.E., Berkowitz, G.A. (2003b) Functional interaction of calmodulin with a plant cyclic nucleotide gated cation channel. Plant Physiology and Biochemistry 41: 945–954.

Huse, M., Kuriyan, J. (2002) The conformational plasticity of protein kinases. Cell 109: 275–282.

Huttner, W.B. (1982) Sulphation of tyrosine residues-a widespread modification of proteins. Nature 299: 273-276.

Igarashi, D., Tsuda, K., Katagiri, F. (2012) The peptide growth factor, phytosulfokine, attenuates pattern-triggered immunity. The Plant Journal 71: 194–204.

Igasaki, T., Akashi, N., Ujino-Ihara, T., Matsubayashi, Y., Sakagami, Y., Shinohara, K. (2003) Phytosulfokine stimulates somatic embryogenesis in Cryptomeria japonica. Plant & Cell Physiology 44: 1412–1416.

Ikura, M., Clore, G.M., Gronenborn, A.M., Zhu, G., Klee, C.B., Bax, A. (1992) Solution structure of a calmodulin-target peptide complex by multidimensional NMR. Science 256: 632–638.

Irani, N.G., Di Rubbo, S., Mylle, E., Van den Begin, J., Schneider-Pizoń, J., Hniliková, J., Šíša, M., Buyst, D., Vilarrasa-Blasi, J., Szatmári, A.M., Van Damme, D., Mishev, K., Codreanu, M.C., Kohout, L., Strnad, M., Caño-Delgado, A., Friml, J., Madder, A., Russinova, E. (2012) Fluorescent castasterone reveals BRI1 signaling from the plasma membrane. Nature Chemical Biology 8: 583–589.

Ishida, H., Vogel, H.J. (2006) Protein-peptide interaction studies demonstrate the versatility of calmodulin target protein binding. Protein & Peptide Letters 13: 455-465.

Jaillais, Y., Hothorn, M., Belkhadir, Y., Dabi, T., Nimchuk, Z.L., Meyerowitz, E.M., Chory, J. (2011) Tyrosine phosphorylation controls brassinosteroid receptor activation by triggering membrane release of its kinase inhibitor. Genes & Development 25: 232–237.

Jeong, S., Trotochaud, A.E., Clark, S.E. (1999) The Arabidopsis CLAVATA2 gene encodes a receptor-like protein required for the stability of the CLAVATA1 receptor-like kinase. The Plant Cell 11: 1925–1934.

Johnson, L.N., Noble, M.E., Owen, D.J. (1996) Active and inactive protein kinases: structural basis for regulation. Cell 85: 149–158.

Jun, J., Fiume, E., Roeder, A.H.K., Meng, L., Sharma, V.K., Osmont, K.S., Baker, C., Man Ha, C., Meyerowitz, E.M., Feldman, L.J., Fletcher, J.C. (2010) Comprehensive analysis of CLE polypeptide signaling gene expression and overexpression activity in Arabidopsis. Plant Physiology 154: 1721–1736.

Kataoka, M. (1991) Small-angle X-ray scattering study of calmodulin bound to two peptides corresponding to parts of the calmodulin-binding domain of the plasma membrane Ca2+ pump. Biochemistry 30: 6247-6251.

Katsir, L., Davies, K.A., Bergmann, D.C., Laux, T. (2011) Peptide signaling in plant development. Current Biology 21: 356–364.

Kauschmann, A., Jessop, A., Koncz, C., Szekeres, M., Willmitzer, L., Altmann, T. (1996) Genetic evidence for an essential role of brassinosteroids in plant development. The Plant Journal 9: 701–713.

Kim, T.W., Wang, Z.Y. (2010) Brassinosteroid signal transduction from receptor kinases to transcription factors. Annual Review of Plant Biology 61: 681–704.

Kinoshita, T., Caño-Delgado, A., Seto, H., Hiranuma, S., Fujioka, S., Yoshida, S., Chory, J. (2005) Binding of brassinosteroids to the extracellular domain of plant receptor kinase BRI1. Nature 433: 167-171.

Kinoshita, A., Betsuyaku, S., Osakabe, Y., Mizuno, S., Nagawa, S., Stahl, Y., Simon, R., Yamaguchi-Shinozaki, K., Fukuda, H., Sawa, S. (2010) RPK2 is an essential receptor-like kinase that transmits the CLV3 signal in Arabidopsis. Development 137: 4327–4327.

Klein, M., Papenbrock, J. (2004) The multi-protein family of Arabidopsis sulphotransferases and their relatives in other plant species. Journal of Experimental Botany 55: 1809–1820.

Klein, M., Reichelt, M., Gershenzon, J., Papenbrock, J. (2006) The three desulfoglucosinolate sulfotransferase proteins in Arabidopsis have different substrate specificities and are differentially expressed. The FEBS Journal 273: 122–136.

Kobayashi, T., Eun, C.H., Hanai, H., Matsubayashi, Y., Sakagami, Y., Kamada, H. (1999) Phytosulphokine-α , a peptidyl plant growth factor, stimulates somatic embryogenesis in carrot. Journal of Experimental Botany 50: 1123–1128.

Kobe, B., Kajava, A.V. (2001) The leucine-rich repeat as a protein recognition motif. Current Opinion in Structural Biology 11: 725–732.

Koka, C.V, Cerny, R.E., Gardner, R.G., Noguchi, T., Fujioka, S., Takatsuto, S., Yoshida, S., Clouse, S.D. (2000) A putative role for the tomato genes DUMPY and CURL-3 in brassinosteroid biosynthesis and response. Plant Physiology 122: 85–98.

Komori, R., Amano, Y., Ogawa-Ohnishi, M., Matsubayashi, Y. (2009) Identification of tyrosylprotein sulfotransferase in Arabidopsis. Proceedings of the National Academy of Sciences of the United States of America 106: 15067–15072.

Kondo, T., Sawa, S., Kinoshita, A., Mizuno, S., Kakimoto, T., Fukuda, H., Sakagami, Y. (2006) A plant peptide encoded by CLV3 identified by in situ MALDI-TOF MS analysis. Science 313: 845–848.

Krupa, A., Abhinandan, K.R., Srinivasan, N. (2004) KinG: a database of protein kinases in genomes. Nucleic Acids Research 32: 153–155.

Kuppusamy, K.T., Chen, A.Y., Nemhauser, J.L. (2009) Steroids are required for epidermal cell fate establishment in Arabidopsis roots. Proceedings of the National Academy of Sciences of the United States of America 106: 8073–8076.

Kurata, T., Ishida, T., Kawabata-Awai, C., Noguchi, M., Hattori, S., Sano, R., Nagasaka, R., Tominaga, R., Koshino-Kimura, Y., Kato, T., Sato, S., Tabata, S., Okada, K., Wada, T. (2005) Cell-to-cell movement of the CAPRICE protein in Arabidopsis root epidermal cell differentiation. Development 132: 5387–5398.

Kutschera, U. (1992) The Role of the Epidermis in the Control of Elongation Growth in Stems and Coleoptiles. Plant Biology 105: 246–252.

Kutschera, U. (2008) The growing outer epidermal wall: design and physiological role of a composite structure. Annals of Botany 101: 615–621.

Kutschera, U., Niklas, K.J. (2007) The epidermal-growth-control theory of stem elongation: an old and a new perspective. Journal of Plant Physiology 164: 1395–1409.

Kutschmar, A., Rzewuski, G., Stührwohldt, N., Beemster, G.T.S., Inzé, D., Sauter, M. (2009) PSK-α promotes root growth in Arabidopsis. The New Phytologist 181: 820–831.

Kwezi, L., Ruzvidzo, O., Wheeler, J.I., Govender, K., Iacuone, S., Thompson, P.E., Gehring, C., Irving, H.R. (2011) The phytosulfokine (PSK) receptor is capable of guanylate cyclase activity and enabling cyclic GMP-dependent signaling in plants. The Journal of Biological Chemistry 286: 22580–22588.

Lau, S., Jürgens, G., De Smet, I. (2008) The evolving complexity of the auxin pathway. The Plant Cell 20: 1738–1746.

Laux, T., Mayer, K.F., Berger, J., Jürgens, G. (1996) The WUSCHEL gene is required for shoot and floral meristem integrity in Arabidopsis. Development 122: 87–96.

Li, J. (2010) Multi-tasking of somatic embryogenesis receptor-like protein kinases. Current Opinion in Plant Biology 13: 509–514.

Li, J., Chory, J. (1997) A putative leucine-rich repeat receptor kinase involved in brassinosteroid signal transduction. Cell 90: 929–938.

Li, J., Nagpal, P., Vitart, V., McMorris, T.C., Chory, J. (1996) A role for brassinosteroids in light-dependent development of Arabidopsis. Science 272: 398–401.

Li, J., Wen, J., Lease, K.A., Doke, J.T., Tax, F.E., Walker, J. C. (2002) BAK1, an Arabidopsis LRR Receptor-like Protein Kinase, Interacts with BRI1 and Modulates Brassinosteroid Signaling. Cell 110: 213–222.

Lorbiecke, L., Sauter, M. (2002) Comparative analysis of PSK peptide growth factor precursor homologs. Plant Science 163: 321-332.

Luan, S. (2009) The CBL-CIPK network in plant calcium signaling. Trends in Plant Science 14: 37–42.

Ma, L., Liang, S., Jones, R.L., Lu, Y.T. (2004) Characterization of a novel calcium/calmodulin-dependent protein kinase from tobacco. Plant Physiology 135: 1280-1293.

Ma, Y., Zhao, Y., Walker, R.K., Berkowitz, G.A. (2013) Molecular steps in the immune signaling pathway evoked by plant elicitor peptides: Ca2+-dependent protein kinases, nitric oxide, and reactive oxygen species are downstream from the early Ca2+ signal. Plant Physiology 163: 1459–1471.

Marcotrigiano, M. (2001) Genetic mosaics and the analysis of leaf development. International Journal of Plant Sciences 162: 513-525.

Matos, J.L., Fiori, C.S., Silva-Filho, M.C., Moura, D.S. (2008) A conserved dibasic site is essential for correct processing of the peptide hormone AtRALF1 in Arabidopsis thaliana. FEBS Letters 582: 3343–3347.

Matsubayashi, Y. (2000) 120- and 160-kDa Receptors for Endogenous Mitogenic Peptide, Phytosulfokine-alpha , in Rice Plasma Membranes. Journal of Biological Chemistry 275: 15520–15525.

Matsubayashi, Y. (2011) Post-translational modifications in secreted peptide hormones in plants. Plant & Cell Physiology 52: 5–13.

Matsubayashi, Y. (2012) MBSJ MCC Young Scientist Award 2010. Recent progress in research on small post-translationally modified peptide signals in plants. Genes to Cells: 17: 1–10.

Matsubayashi, Y., Sakagami, Y. (1996) Phytosulfokine, sulfated peptides that induce the proliferation of single mesophyll cells of Asparagus officinalis L. Proceedings of the National Academy of Sciences of the United States of America 93: 7623–7627.

Matsubayashi, Y., Sakagami, Y. (1999) Characterization of specific binding sites for a mitogenic sulfated peptide, phytosulfokine-alpha, in the plasma-membrane fraction derived from Oryza sativa L. European Journal of Biochemistry 262: 666–671.

Matsubayashi, Y., Sakagami, Y. (2006) Peptide hormones in plants. Annual Review of Plant Biology 57: 649–674.

Matsubayashi, Y., Hanai, H., Hara, O., Sakagami, Y. (1996) Active Fragments and Analogs of the Plant Growth Factor, Phytosulfokine: Structure–Activity Relationships. BIOCHEMICAL AND BIOPHYSICAL RESEARCH COMMUNICATIONS 225: 209–214.

Matsubayashi, Y., Takagi, L., Sakagami, Y. (1997) Phytosulfokine-alpha, a sulfated pentapeptide, stimulates the proliferation of rice cells by means of specific high- and low-affinity binding sites. Proceedings of the National Academy of Sciences of the United States of America 94: 13357–13362.

Matsubayashi, Y., Takagi, L., Omura, N., Morita, A., Sakagami, Y. (1999) The endogenous sulfated pentapeptide phytosulfokine-alpha stimulates tracheary element differentiation of isolated mesophyll cells of zinnia. Plant Physiology 120: 1043–1048.

Matsubayashi, Y., Ogawa, M., Morita, A., Sakagami, Y. (2002) An LRR receptor kinase involved in perception of a peptide plant hormone, phytosulfokine. Science 296: 1470–1472.

Matsubayashi, Y., Ogawa, M., Kihara, H., Niwa, M., Sakagami, Y. (2006). Disruption and overexpression of Arabidopsis phytosulfokine receptor gene affects cellular longevity and potential for growth. Plant Physiology 142: 45–53.

Matsushita, M., Nairn, A.C. (1998) Characterization of the mechanism of regulation of Ca2+/ calmodulin-dependent protein kinase I by calmodulin and by Ca2+/calmodulin-dependent protein kinase kinase. The Journal of Biological Chemistry 273: 21473-21481.

Matsuzaki, Y., Ogawa-Ohnishi, M., Mori, A., Matsubayashi, Y. (2010) Secreted peptide signals required for maintenance of root stem cell niche in Arabidopsis. Science 329: 1065–1067.

Mayer, K.F., Schoof, H., Haecker, A., Lenhard, M., Jürgens, G., Laux, T. (1998) Role of WUSCHEL in regulating stem cell fate in the Arabidopsis shoot meristem. Cell 95: 805–815.

McAinsh, M.R., Pittman, J.K. (2009) Shaping the calcium signature. The New Phytologist 181: 275-294.

McCormack, E., Braam, J. (2003) Calmodulins and related potential calcium sensors of Arabidopsis. The New Phytologist 159: 585–598.

McCormack, E., Tsai, Y.C., Braam, J. (2005) Handling calcium signaling: Arabidopsis CaMs and CMLs. Trends in Plant Science 10: 383–389.

Meador, W.E., Means, A.R., Quiocho, F.A. (1992) Target enzyme recognition by calmodulin: 2.4 A structure of a calmodulin-peptide complex. Science 257: 1251–1255.

Meador, W.E., Means, A.R., Quiocho, F.A. (1993) Modulation of calmodulin plasticity in molecular recognition on the basis of x-ray structures. Science 262: 1718–1721.

Meindl, T., Boller, T., Felix, G. (1998) The plant wound hormone systemin binds with the N-terminal part to its receptor but needs the C-terminal part to activate it. The Plant Cell 10: 1561–1570.

Meng, L., Buchanan, B.B., Feldman, L.J., Luan, S. (2012) CLE-like (CLEL) peptides control the pattern of root growth and lateral root development in Arabidopsis. Proceedings of the National Academy of Sciences of the United States of America 109: 1760–1765.

Meyer, M.R., Shah, S., Rao, A.G. (2013) Insights into molecular interactions between the juxtamembrane and kinase subdomains of the Arabidopsis Crinkly-4 receptor-like kinase. Archives of Biochemistry and Biophysics 535: 101–110.

Montoya, T., Nomura, T., Farrar, K., Kaneta, T., Yokota, T., Bishop, G.J. (2002) Cloning the Tomato Curl3 Gene Highlights the Putative Dual Role of the Leucine-Rich Repeat Receptor Kinase tBRI1 / SR160 in Plant Steroid Hormone and Peptide Hormone Signaling. The Plant Cell 14: 3163-3176.

Moore, K.L. (2003) The biology and enzymology of protein tyrosine O-sulfation. The Journal of Biological Chemistry 278: 24243–24246.

Mora-García, S., Vert, G., Yin, Y., Caño-Delgado, A., Cheong, H., Chory, J. (2004) Nuclear protein phosphatases with Kelch-repeat domains modulate the response to brassinosteroids in Arabidopsis. Genes & Development 18: 448–460.

Mosher, S., Seybold, H., Rodriguez, P., Stahl, M., Davies, K.A., Dayaratne, S., Morillo, S.A., Wierzba, M., Favery, B., Keller, H., Tax, F.E., Kemmerling, B. (2013) The tyrosine-sulfated peptide receptors PSKR1 and PSY1R modify the immunity of Arabidopsis to biotrophic and necrotrophic pathogens in an antagonistic manner. The Plant Journal 73: 469–482.

Mu, R., Borghi, L., Kwiatkowska, D., Laufs, P. (2006) Dynamic and Compensatory Responses of Arabidopsis Shoot and Floral Meristems to CLV3 Signaling. The Plant Cell 18: 1188-1198.

Müller, R., Borghi, L., Kwiatkowska, D., Laufs, P., Simon, R. (2006) Dynamic and compensatory responses of Arabidopsis shoot and floral meristems to CLV3 signaling. The Plant Cell 18: 1188-1198.

Müller, R., Bleckmann, A., Simon, R. (2008) The receptor kinase CORYNE of Arabidopsis transmits the stem cell-limiting signal CLAVATA3 independently of CLAVATA1. The Plant Cell 20: 934–946.

Müssig C., Shin, G.H., Altmann, T. (2003) Brassinosteroids Promote Root Growth in Arabidopsis. Plant Physiology 133: 1261–1271.

Murphy, E., Smith, S., De Smet, I. (2012) Small signaling peptides in Arabidopsis development: how cells communicate over a short distance. The Plant Cell 24: 3198–3217.

Muschietti, J., Eyal, Y., McCormick, S. (1998) Pollen tube localization implies a role in pollen-pistil interactions for the tomato receptor-like protein kinases LePRK1 and LePRK2. The Plant Cell 10: 319–330.

Nam, K.H., Li, J. (2002) BRI1/BAK1, a receptor kinase pair mediating brassinosteroid signaling. Cell 110: 203–212.

Ni, J., Clark, S.E. (2006) Evidence for functional conservation, sufficiency, and proteolytic processing of the CLAVATA3 CLE domain. Plant Physiology 140: 726-733.

Ni, J., Guo, Y., Jin, H., Hartsell, J., Clark, S.E. (2011) Characterization of a CLE processing activity. Plant Molecular Biology 75: 67–75.

Niklas, K.J., Paolillo, D.J. (1997) The role of the epidermis as a stiffening agent in Tulipa (Liliaceae) stems. The American Journal of Botany 84: 735–744.

Nimchuk, Z.L., Tarr, P.T., Meyerowitz, E.M. (2011) An evolutionarily conserved pseudokinase mediates stem cell production in plants. The Plant Cell 23: 851–854.

Noguchi, T., Fujioka, S., Choe, S., Takatsuto, S., Yoshida, S., Yuan, H., Feldmann, K.A., Tax, F.E. (1999) Brassinosteroid-insensitive dwarf mutants of Arabidopsis accumulate brassinosteroids. Plant Physiology 121: 743–752.

Nomura, T., Bishop, G.J., Kaneta, T., Reid, J.B., Chory, J., Yokota, T. (2003) The LKA gene is a BRASSINOSTEROID INSENSITIVE 1 homolog of pea. The Plant Journal 36: 291–300.

Nühse, T.S., Stensballe, A., Jensen, O.N., Peck, S.C. (2004) Phosphoproteomics of the Arabidopsis plasma membrane and a new phosphorylation site database. The Plant Cell 16: 2394-2405.

Ogawa, M., Shinohara, H., Sakagami, Y., Matsubayashi, Y. (2008) Arabidopsis CLV3 peptide directly binds CLV1 ectodomain. Science 319: 294.

Oh, M.H., Ray, W.K., Huber, S.C., Asara, J.M., Gage, D.A., Clouse, S.D. (2000) Recombinant brassinosteroid insensitive 1 receptor-like kinase autophosphorylates on serine and threonine residues and phosphorylates a conserved peptide motif in vitro. Plant Physiology 124: 751–766.

Oh, M.H., Wang, X., Kota, U., Goshe, M.B., Clouse, S.D., Huber, S.C. (2009) Tyrosine phosphorylation of the BRI1 receptor kinase emerges as a component of brassinosteroid signaling in Arabidopsis. Proceedings of the National Academy of Sciences of the United States of America 106: 658–663.

Oh, M.H., Kim, H.S., Wu, X., Clouse, S.D., Zielinski, R.E., Huber, S.C. (2012) Calcium/calmodulin inhibition of the Arabidopsis BRASSINOSTEROID-INSENSITIVE 1 receptor kinase provides a possible link between calcium and brassinosteroid signalling. The Biochemical Journal 443: 515–523.

Ohyama, K., Shinohara, H., Ogawa-Ohnishi, M., Matsubayashi, Y. (2009) A glycopeptide regulating stem cell fate in Arabidopsis thaliana. Nature Chemical Biology 5: 578–580.

Olsen, A.N., Mundy, J., Skriver, K. (2002) Peptomics, identification of novel cationic Arabidopsis peptides with conserved sequence motifs. In Silico Biology 2: 441-451

O'Neil, K.T., DeGrado, W.F. (1990) A thermodynamic scale for the helix-forming tendencies of the commonly occurring amino acids. Science 250: 646–651.

Ouyang, Y.B., Lane, W.S., Moore, K.L. (1998) Tyrosylprotein sulfotransferase: purification and molecular cloning of an enzyme that catalyzes tyrosine O-sulfation, a common posttranslational modification of eukaryotic proteins. Proceedings of the National Academy of Sciences of the United States of America 95: 2896–2901.

Pearce, G., Strydom, D., Johnson, S., Ryan, C.A. (1991) A polypeptide from tomato leaves induces wound-inducible proteinase inhibitor proteins. Science 253: 895-897.

Pearce, G., Moura, D.S., Stratmann, J., Ryan, C.A. (2001) RALF, a 5-kDa ubiquitous polypeptide in plants, arrests root growth and development. Proceedings of the National Academy of Sciences of the United States of America 98: 12843-12847.

Peters, W.S., Tomos, A.D. (1996) The history of tissue tension. Annals of Botany 77: 657–665.

Popescu, S.C., Popescu, G.V., Bachan, S., Zhang, Z., Seay, M., Gerstein, M., Snyder, M., Dinesh-Kumar, S.P. (2007) Differential binding of calmodulin-related proteins to their targets revealed through high-density Arabidopsis protein microarrays. Proceedings of the National Academy of Sciences of the United States of America 104: 4730–4735.

Qi, Z., Verma, R., Gehring, C., Yamaguchi, Y., Zhao, Y., Ryan, C.A., Berkowitz, G.A. (2010) Ca2+ signaling by plant Arabidopsis thaliana Pep peptides depends on AtPepR1, a receptor with guanylyl cyclase activity, and cGMP-activated Ca2+ channels. Proceedings of the National Academy of Sciences of the United States of America 107: 21193–21198.

Rainaldi, M., Yamniuk, A.P., Murase, T., Vogel, H.J. (2007) Calcium-dependent and -independent binding of soybean calmodulin isoforms to the calmodulin binding domain of tobacco MAPK phosphatase-1. The Journal of Biological Chemistry 282: 6031–6042.

Rautengarten, C., Steinhauser, D., Büssis, D., Stintzi, A., Schaller, A., Kopka, J., Altmann, T. (2005) Inferring hypotheses on functional relationships of genes: Analysis of the Arabidopsis thaliana subtilase gene family. PLoS Computational Biology 1: e40. doi:10.1371/journal.pcbi.0010040.

Raveh, D., Huberman, E., Galun, E. (1973) In vitro culture of tobacco protoplasts: use of feeder techniques to support division of cells plated at low densities. In Vitro 9: 216-222.

Reddy, A.S.N. (2001) Calcium: silver bullet in signaling. Plant Science 160: 381–404.

Reddy, V.S., Reddy, A.S.N. (2004) Proteomics of calcium-signaling components in plants. Phytochemistry 65: 1745–1776.

Reddy, V.S., Safadi, F., Zielinski, R.E., Reddy, A.S.N. (1999) Interaction of a Kinesin-like Protein with Calmodulin Isoforms from Arabidopsis. The Journal of Biological Chemistry 274: 31727-31733.

Rhoads, A.R., Friedberg, F. (1997) Sequence motifs for calmodulin recognition. FASEB Journal 11: 331–340.

Ryan, C.A. (1974) Assay and Biochemical Properties of the Proteinase Inhibitor-inducing Factor, a Wound Hormone. Plant Physiology 54: 328-332.

Ryan, C.A., Pearce, G. (2003) Systemins: a functionally defined family of peptide signals that regulate defensive genes in Solanaceae species. Proceedings of the National Academy of Sciences of the United States of America 100: 14577–14580.

Ryan, C.A., Pearce, G., Scheer, J., Moura, D.S. (2002) Polypeptide Hormones. The Plant Cell 14: 251–265.

Satina, S., Blakeslee, A.F., Avery, A.G. (1940) Demonstration of the three germ layers in the shoot apex of Datura by means of induced polyploidy in periclinal chimeras. American Journal of Botany 27: 895-905.

Savaldi-Goldstein, S., Peto, C., Chory, J. (2007) The epidermis both drives and restricts plant shoot growth. Nature 446: 199–202.

Schaller, A., Oecking, C. (1999) Modulation of plasma membrane H+-ATPase activity differentially activates wound and pathogen defense responses in tomato plants. The Plant Cell 11: 263–272.

Scheer, J.M., Ryan, C.A. (2002) The systemin receptor SR160 from Lycopersicon peruvianum is a member of the LRR receptor kinase family. Proceedings of the National Academy of Sciences of the United States of America 99: 9585–9590.

Scheres, B. (2007) Stem-cell niches: nursery rhymes across kingdoms. Nature Reviews. Molecular Cell Biology 8: 345–354.

Scheres, B., Benfey, P.N. (1999) Asymmetric Cell Division in Plants. Annual Review of Plant Physiology and Plant Molecular Biology 50: 505–537.

Schoof, H., Lenhard, M., Haecker, A., Mayer, K.F., Jürgens, G., Laux, T. (2000) The stem cell population of Arabidopsis shoot meristems in maintained by a regulatory loop between the CLAVATA and WUSCHEL genes. Cell 100: 635–644.

Schuster, C., Gaillochet, C., Medzihradszky, A., Busch, W., Daum, G., Krebs, M., Kehle, A., Lohmann, J.U. (2014) A regulatory framework for shoot stem cell control integrating metabolic, transcriptional, and phytohormone signals. Developmental Cell 28: 438-449.

Serralbo, O., Pérez-Pérez, J.M., Heidstra, R., Scheres, B. (2006) Non-cell-autonomous rescue of anaphase-promoting complex function revealed by mosaic analysis of HOBBIT, an Arabidopsis CDC27 homolog. Proceedings of the National Academy of Sciences of the United States of America 103: 13250–13255.

Sevilem, I., Miyashima, S., Helariutta, Y. (2013) Cell-to-cell communication via plasmodesmata in vascular plants. Cell Adhesion & Migration 7: 27–32.

Shah, K., Vervoort, J., de Vries, S.C. (2001) Role of threonines in the Arabidopsis thaliana somatic embryogenesis receptor kinase 1 activation loop in phosphorylation. The Journal of Biological Chemistry 276: 41263–41269.

She, J., Han, Z., Kim, T.W., Wang, J., Cheng, W., Chang, J., Shi, S., Wang, J., Yang, M., Wang, Z.Y., Chai, J. (2011) Structural insight into brassinosteroid perception by BRI1. Nature 474: 472-476.

Shen, Y., Diener, A.C. (2013) Arabidopsis thaliana resistance to fusarium oxysporum 2 implicates tyrosine-sulfated peptide signaling in susceptibility and resistance to root infection. PLoS Genetics 9: e1003525. doi:10.1371/journal.pgen.1003525.

Shinohara, H., Ogawa, M., Sakagami, Y., Matsubayashi, Y. (2007) Identification of ligand binding site of phytosulfokine receptor by on-column photoaffinity labeling. The Journal of Biological Chemistry 282: 124–131.

Shiu, S.H., Bleecker, A.B. (2001) Receptor-like kinases from Arabidopsis form a monophyletic gene family related to animal receptor kinases. Proceedings of the National Academy of Sciences of the United States of America 98: 10763–10768.

Shiu, S., Karlowski, W.M., Pan, R., Tzeng, Y.H., Mayer, K.F., Li, W.H. (2004) Comparative Analysis of the Receptor-Like Kinase Family in Arabidopsis and Rice. The Plant Cell 16:1220-1234.

Song, W.H., Wang, G.L., Chen, L.L., Kim, H.S., Pi, L.Y., Holsten, T., Gardner, J., Wang, B., Zhai, W.X., Zhu, L.H., Fauquet, C., Ronald, P. (1995) A receptor kinase-like protein encoded by the rice disease resistance gene, Xa21. Science 270: 1804-1806.

Song, S.K., Lee, M.M., Clark, S.E. (2006) POL and PLL1 phosphatases are CLAVATA1 signaling intermediates required for Arabidopsis shoot and floral stem cells. Development 133: 4691–4698.

Sparks, E., Wachsman, G., Benfey, P.N. (2013) Spatiotemporal signalling in plant development. Nature Reviews Genetics 14: 631-644.

Srivastava, R., Liu, J.X., Howell, S.H. (2008) Proteolytic processing of a precursor protein for a growth-promoting peptide by a subtilisin serine protease in Arabidopsis. The Plant Journal 56: 219–227.

Srivastava, R., Liu, J.X., Guo, H., Yin, Y., Howell, S.H. (2009) Regulation and processing of a plant peptide hormone, AtRALF23, in Arabidopsis. The Plant Journal 59: 930–939.

Stahl, Y., Simon, R. (2009) Is the Arabidopsis root niche protected by sequestration of the CLE40 signal by its putative receptor ACR4? Plant Signaling & Behavior 4: 634–635.

Stahl, Y., Simon, R. (2010) Plant primary meristems: shared functions and regulatory mechanisms. Current Opinion in Plant Biology 13: 53–58.

Stahl, Y., Wink, R.H., Ingram, G.C., Simon, R. (2009) A signaling module controlling the stem cell niche in Arabidopsis root meristems. Current Biology 19: 909-914.

Stahl, Y., Grabowski, S., Bleckmann, A., Kühnemuth, R., Weidtkamp-Peters, S., Pinto, K.G., Kirschner, G.K., Schmid, J.B., Wink, R.H., Hülsewede, A., Felekyan, S., Seidel, C.A.M., Simon, R. (2013) Moderation of Arabidopsis root stemness by CLAVATA1 and ARABIDOPSIS CRINKLY4 receptor kinase complexes. Current Biology 23: 362–371.

Stewart, R.N., Burk, L.G. (1970) Independence of Tissues Derived from Apical Layers in Ontogeny of the Tobacco Leaf and Ovary. American Journal of Botany 55: 354-369.

Stone, J., Trotochaud, A., Walker, J., Clark, S. (1998) Control of meristem development by CLAVATA1 receptor kinase and kinase-associated protein phosphatase interactions. Plant Physiology 117: 1217–1225.

Stührwohldt, N., Dahlke, R.I., Steffens, B., Johnson, A., Sauter, M. (2011) Phytosulfokine-α controls hypocotyl length and cell expansion in Arabidopsis thaliana through phytosulfokine receptor 1. PloS One 6: e21054. doi:10.1371/journal.pone.0021054.

Sun, Y., Fokar, M., Asami, T., Yoshida, S., Allen, R.D. (2004) Characterization of the brassinosteroid insensitive 1 genes of cotton. Plant Molecular Biology 54: 221–232.

Sun, Y., Fan, X.Y., Cao, D.M., He, K., Tang, W., Zhu, J.Y., He, J.X., Bai, M.Y., Zhu, S., Oh, E., Patil, S., Kim, T.W., Ji, H., Wong, W.H., Rhee, S.Y., Wang, Z.Y. (2010) Integration of brassinosteroid signal transduction with the transcription network for plant growth regulation in Arabidopsis. Developmental Cell 19: 765-777.

Szymkowiak, E.J., Sussex, I.M. (1996) WHAT CHIMERAS CAN TELL US ABOUT PLANT DEVELOPMENT. Annual Review of Plant Physiology and Plant Molecular Biology 47: 351-376.

Tang, W., Kim, T., Oses-Prieto, J.A., Sun, Y., Deng, Z., Zhu, S., Wang, R., Burlingame, A.L., Wang, Z.Y. (2008) Brassinosteroid-Signaling Kinases (BSKs) mediate signal transduction from the receptor kinase BRI1 in Arabidopsis. Science 321: 557–560.

Tang, W., Yuan, M., Wang, R., Yang, Y., Wang, C., Oses-Prieto, J.A., Kim, T.W., Zhou, H.W., Deng, Z., Gampala, S.S., Gendron, J.M., Jonassen, E.M., Lillo, C., DeLong, A., Burlingame, A.L., Sun, Y., Wang, Z.Y. (2011) PP2A activates brassinosteroid-responsive gene expression and plant growth by dephosphorylating BZR1. Nature Cell Biology 13: 124–131.

Torii, K.U. (2004) Leucine-rich repeat receptor kinases in plants: structure, function, and signal transduction pathways. International Review of Cytology 234: 1-46.

Torii, K.U., Mitsukawa, N., Oosumi, T., Matsuura, Y., Yokoyama, R., Whittier, R.F., Komeda, Y. (1996) The Arabidopsis ERECTA gene encodes a putative receptor protein kinase with extracellular leucine-rich repeats. The Plant Cell 8: 735–746.

Trotochaud, A.E., Hao, T., Wu, G., Yang, Z., Clark, S.E. (1999) The CLAVATA1 receptor-like kinase requires CLAVATA3 for its assembly into a signaling complex that includes KAPP and a Rho-related protein. The Plant Cell 11: 393–406.

Ubeda-Tomás, S., Swarup, R., Coates, J., Swarup, K., Laplaze, L., Beemster, G.T.S., Hedden, P., Bhalerao, R., Bennett, M.J. (2008) Root growth in Arabidopsis requires gibberellin/DELLA signalling in the endodermis. Nature Cell Biology 10: 625–628.

Vandenbussche, F., Verbelen, J.P., Van Der Straeten, D. (2005) Of light and length: regulation of hypocotyl growth in Arabidopsis. BioEssays 27: 275–284.

Van den Berg, C., Willemsen, V., Hage, W., Weisbeek, P., Scheres, B. (1995) Cell fate in the Arabidopsis root meristem determined by directional signalling. Nature 378: 62–65.

Van den Berg, C., Willemsen, V., Hendriks, G., Scheres, B. (1997) Short-range control of cell differentiation in the Arabidopsis root meristem. Nature 390: 287–289.

Van Norman, J.M., Breakfield, N.W., Benfey, P.N. (2011) Intercellular communication during plant development. The Plant Cell 23: 855–864.

Vanneste, S., Friml, J. (2009) Auxin: a trigger for change in plant development. Cell 136: 1005–1016.

Vanoosthuyse, V., Tichtinsky, G., Dumas, C., Gaude, T., Cock, J.M. (2003) Interaction of Calmodulin, a Sorting Nexin and Kinase-Associated Protein Phosphatase with the Brassica oleracea S Locus Receptor Kinase. Plant Physiology 133: 919-929.

Vogel, H.J. (1994) The Merck Frosst Award Lecture 1994. Calmodulin: a versatile calcium mediator protein. Biochemistry and Cell Biology 72: 357-376.

Walter, M., Lucet, I.S., Patel, O., Broughton, S.E., Bamert, R., Williams, N.K., Fantino, E., Wilks, A.F., Rossjohn, J. (2007) The 2.7 A crystal structure of the autoinhibited human c-Fms kinase domain. Journal of Molecular Biology 367: 839–847.

Wang, Z.Y. (2012) Brassinosteroids modulate plant immunity at multiple levels. Proceedings of the National Academy of Sciences of the United States of America 109: 7–8.

Wang, X., Chory, J. (2006) Brassinosteroids regulate dissociation of BKI1, a negative regulator of BRI1 signaling, from the plasma membrane. Science 313: 1118–1122.

Wang, G., Fiers, M. (2010) CLE peptide signaling during plant development. Protoplasma 240: 33–43.

Wang, Y., Liang, S., Xie, Q.G., Lu, Y.T. (2004) Characterization of a calmodulin-regulated Ca2+-dependent-protein-kinase-related protein kinase, AtCRK1, from Arabidopsis. The Biochemical Journal 383: 73–81.

Wang, J.W., Wang, L.J., Mao, Y.B., Cai, W.J., Xue, H.W., Chen, X.Y. (2005a) Control of root cap formation by MicroRNA-targeted auxin response factors in Arabidopsis. The Plant Cell 17: 2204-2216.

Wang, X., Goshe, M.B., Soderblom, E.J., Phinney, B.S., Kuchar, J.A., Li, J., Asami, T., Yoshida, S., Huber, S.C., Clouse, S.D. (2005b) Identification and functional analysis of in vivo phosphorylation sites of the Arabidopsis BRASSINOSTEROID-INSENSITIVE1 receptor kinase. The Plant Cell 17: 1685-1703.

Wang, X., Li, X., Meisenhelder, J., Hunter, T., Yoshida, S., Asami, T., Chory, J. (2005c) Autoregulation and homodimerization are involved in the activation of the plant steroid receptor BRI1. Developmental Cell 8: 855–865.

Wang, X., Kota, U., He, K., Blackburn, K., Li, J., Goshe, M.B., Huber, S.C., Clouse, S.D. (2008) Sequential transphosphorylation of the BRI1/BAK1 receptor kinase complex impacts early events in brassinosteroid signaling. Developmental Cell 15: 220–235.

Wang, M., Sun, S., Wu, C., Han, T., Wang, Q. (2014) Isolation and Characterization of the Brassinosteroid Receptor Gene (GmBRI1) from Glycine max. International Journal of Molecular Sciences 15: 3871–3888.

Wiesner, S., Wybenga-Groot, L.E., Warner, N., Lin, H., Pawson, T., Forman-Kay, J.D., Sicheri, F. (2006) A change in conformational dynamics underlies the activation of Eph receptor tyrosine kinases. The EMBO Journal 25: 4686–4696.

Williams, R.W., Wilson, J.M., Meyerowitz, E.M. (1997) A possible role for kinase-associated protein phosphatase in the Arabidopsis CLAVATA1 signaling pathway. Proceedings of the National Academy of Sciences of the United States of America 94: 10467–10472.

Witthöft, J., Caesar, K., Elgass, K., Huppenberger, P., Kilian, J., Schleifenbaum, F., Oecking, C., Harter, K. (2011) The activation of the Arabidopsis P-ATPase 1 by the brassinosteroid receptor BRI1 is independent of threonine 948 phosphorylation. Plant Signaling & Behavior 6: 1063–1066.

Wong, A., Gehring, C. (2013) The Arabidopsis thaliana proteome harbors undiscovered multi-domain molecules with functional guanylyl cyclase catalytic centers. Cell Communication and Signaling 11: doi:10.1186/1478-811X-11-48.

Wu, G., Wang, X., Li, X., Kamiya, Y., Otegui, M.S., Chory, J. (2011) Methylation of a phosphatase specifies dephosphorylation and degradation of activated brassinosteroid receptors. Science Signaling 4: ra29. doi: 10.1126/scisignal.2001258.

Yadav, R.K., Perales, M., Gruel, J., Girke, T., Jönsson, H., Reddy, G.V. (2011) WUSCHEL protein movement mediates stem cell homeostasis in the Arabidopsis shoot apex. Genes & Development 25: 2025–2030.

Yamakawa, S., Sakuta, C., Matsubayashi, Y., Sakagami, Y., Kamada, H., Satoh, S. (1998) The Promotive Effects of a Peptidyl Plant Growth Factor, Phytosulfokine-α, on the Formation of Adventitious Roots and Expression of a Gene for a Root-Specific Cystatin in Cucumber Hypocotyls. Journal of Plant Research 111: 453–458.

Yamakawa S., Matsubayashi Y., Sakagami Y., Kamada H., Satoh, S. (1999) Promotive effects of the peptidyl plant growth factor, phytosulfokine-alpha, on the growth and chlorophyll content of Arabidopsis seedlings under high night-time temperature conditions. Bioscience, Biotechnology, and Biochemistry 63: 2240-2243.

Yamakawa, H., Katou, S., Seo, S., Mitsuhara, I., Kamada, H., Ohashi, Y. (2004) Plant MAPK phosphatase interacts with calmodulins. The Journal of Biological Chemistry 279: 928–936.

Yamamuro, C., Ihara, Y., Wu, X., Noguchi, T., Fujioka, S., Takatsuto, S., Ashikari, M., Kitano, H., Matsuoka, M. (2000) Loss of function of a rice brassinosteroid insensitive1 homolog prevents internode elongation and bending of the lamina joint. The Plant Cell 12: 1591–1606.

Yamauchi, E., Nakatsu, T., Matsubara, M., Kato, H., Taniguchi, H. (2003) Crystal structure of a MARCKS peptide containing the calmodulin-binding domain in complex with Ca2+-calmodulin. Nature Structural Biology 10: 226–231.

Yang, T., Poovaiah, B.W. (2000) Molecular and Biochemical Evidence for the Involvement of Calcium/Calmodulin in Auxin Action. Journal of Biological Chemistry 275: 3137–3143.

Yang, H., Matsubayashi, Y., Nakamura, K., Sakagami, Y. (1999) Oryza sativa PSK gene encodes a precursor of phytosulfokine-alpha, a sulfated peptide growth factor found in plants. Proceedings of the National Academy of Sciences of the United States of America 96: 13560-13565.

Yang, H., Matsubayashi, Y., Hanai, H., Sakagami, Y. (2000) Phytosulfokine-alpha, a peptide growth factor found in higher plants: its structure, functions, precursor and receptors. Plant & Cell Physiology 41: 825–830.

Yang, H., Matsubayashi, Y., Nakamura, K., Sakagami, Y. (2001) Diversity of Arabidopsis Genes Encoding Precursors for Phytosulfokine, a Peptide Growth Factor 1. Plant Physiology 127: 842-851.

Yang, T., Chaudhuri, S., Yang, L., Chen, Y., Poovaiah, B.W. (2004) Calcium/calmodulin up-regulates a cytoplasmic receptor-like kinase in plants. The Journal of Biological Chemistry 279: 42552–42559.

Yin, Y., Wu, D., Chory, J. (2002) Plant receptor kinases: systemin receptor identified. Proceedings of the National Academy of Sciences of the United States of America 99: 9090–9092.

Yin, Y., Vafeados, D., Tao, Y., Yoshida, S., Asami, T., Chory, J. (2005) A new class of transcription factors mediates brassinosteroid-regulated gene expression in Arabidopsis. Cell 120: 249–259.

Yu, L.P., Simon, E.J., Trotochaud, A.E., Clark, S.E. (2000) POLTERGEIST functions to regulate meristem development downstream of the CLAVATA loci. Development 127: 1661–1670.

Yu, X., Li, L., Zola, J., Aluru, M., Ye, H., Foudree, A., Guo, H., Anderson, S., Aluru, S., Liu, P., Rodermel, S., Yin, Y. (2011) A brassinosteroid transcriptional network revealed by genome-wide identification of BESI target genes in Arabidopsis thaliana. The Plant Journal 65: 634–646.

Yun, H.S., Bae, Y.H., Lee, Y.J., Chang, S.C., Kim, S.K., Li, J., Nam, K.H. (2009) Analysis of phosphorylation of the BRI1/BAK1 complex in arabidopsis reveals amino acid residues critical for receptor formation and activation of BR signaling. Molecules and Cells 27: 183–190.

Zhang M., Tanaka, T., Ikura, M. (1995) Calcium-induced conformational transition revealed by the solution structure of apo calmodulin. Nature Structural & Molecular Biology 2: 758-767.

Zhang, L., Lu, Y.T. (2003) Calmodulin-binding protein kinases in plants. Trends in Plant Science 8: 123–127.

Zhao, Y., Qi, Z., Berkowitz, G.A. (2013) Teaching an old hormone new tricks: cytosolic Ca2+ elevation involvement in plant brassinosteroid signal transduction cascades. Plant Physiology 163: 555–565.

Zhou, W., Wei, L., Xu, J., Zhai, Q., Jiang, H., Chen, R., Chen, Q., Sun, J., Chu, J., Zhu, L., Liu, C.M., Li, C. (2010) Arabidopsis Tyrosylprotein sulfotransferase acts in the auxin/PLETHORA pathway in regulating postembryonic maintenance of the root stem cell niche. The Plant Cell 22: 3692–3709.

Danksagung

Herzlich danken möchte ich zunächst meiner Doktormutter Frau Prof. Dr. Margret Sauter für die Unterstützung, das mir entgegengebrachte Vertrauen, die konstruktive Kritik sowie die stetige Diskussionsbereitschaft während der Zeit meiner Doktorarbeit.

Des Weiteren danke ich Dr. Bianka Steffens, Dr. Renate Dahlke und Dr. Nils Stührwohldt für die anfängliche Hilfe und die gute Zusammenarbeit. Mein besonderer Dank gilt unserem Technischen Assistenten Timo Staffel, der vor allem bei methodischen Problemen immer mit Rat zur Seite stand und schnell zu einem echten Labor-Kumpanen wurde. Auch bei den anderen Laborkollegen möchte ich mich für die Hilfsbereitschaft und kollegiale Arbeitsatmosphäre bedanken.

Allen Kooperationspartnern danke ich für die kontinuierlich gute Zusammenarbeit und die problemlose Kommunikation.

Schließlich danke ich meiner Familie für die liebevolle Unterstützung und das Verständnis während meiner Promotion. Meiner Freundin Johanna danke ich für ihre Geduld und ihre Fähigkeit, Dinge wieder ins richtige Licht rücken zu können.

Lebenslauf

Persönliche Daten

Name, Vorname:	Hartmann, Jens
Geburtsdatum /-ort:	21.11.1982 in Hannover
Nationalität:	deutsch
Familienstand:	ledig

Ausbildung

Schulbildung

06/2002	Abitur, Gymnasium Ernestinum Rinteln

Studium

10/2003 – 09/2006	Studium der Pflanzenbiotechnologie an der Leibniz Universität Hannover Abschluss Bachelor of Science (B. Sc.)
10/2006 – 09/2008	Studium der Pflanzenbiotechnologie an der Leibniz Universität Hannover Abschluss: Master of Science (M. Sc.)

Promotion

04/2010-03/2014	Promotionsstudium an der Christian-Albrechts-Universität zu Kiel mit Zellbiologie als Hauptfach

Erklärung

Hiermit erkläre ich, dass die vorliegende Arbeit „Funktionale Analyse des Phytosulfokin Rezeptors 1 aus *Arabidopsis thaliana*“, abgesehen von der Beratung durch meine Betreuerin Frau Prof. Dr. Margret Sauter, nach Inhalt und Form meine eigene Arbeit ist. Die vorliegende Arbeit hat zu keinem Teil bereits in einem anderen Prüfungsverfahren vorgelegen und wurde weder ganz noch zum Teil veröffentlicht oder zur Veröffentlichung eingereicht. Die vorliegende Arbeit ist unter Einhaltung der Regeln guter wissenschaftlicher Praxis der Deutschen Forschungsgemeinschaft entstanden.

Teile der Arbeit sind in folgenden Publikationen enthalten:

Hartmann, J., Stührwohldt, N., Dahlke, R.I., Sauter, M. (2013) Phytosulfokine control of growth occurs in the epidermis, is likely to be non-cell autonomous and is dependent on brassinosteroids. The Plant Journal 73: 579–590.

Hartmann, J., Fischer, C., Dietrich, P., Sauter, M. (2014) Kinase activity and calmodulin binding are essential for growth signaling by the phytosulfokine receptor PSKR1. The Plant Journal 78: 192–202.

Kiel, den

Jens Hartmann